Development of New Materials and Design Modifications of Knee Joint Prosthesis to Improve Fatigue Life and Wear

Submitted in
fulfillment of the requirements for the degree of

Doctor of Philosophy

by

Lalit Guglani
ID: 2012RME9029

Under the Supervision of
Dr. T.C. Gupta

DEPARTMENT OF MECHANICAL ENGINEERING
MALAVIYA NATIONAL INSTITUTE OF TECHNOLOGY JAIPUR

May 2019

DECLARATION

I, **Lalit Guglani**, declare that the thesis entitled, "**Development of New Materials and Design Modifications of Knee Joint Prosthesis to Improve Fatigue Life and Wear**", and the work presented in it, are my own. I confirm that:

- This work was done wholly or mainly while in candidature for a research degree at this university.
- Where any part of this thesis has previously been submitted for a degree or any other qualification at this university or any other institution, this has been clearly stated.
- Where I have consulted the published work of others, this is always clearly attributed.
- Where I have quoted from the work of others, the source is always given. With the exception of such quotations, this thesis is entirely my own work.
- I have acknowledged all main sources of help.
- Where the thesis is based on work done by myself, jointly with others. I have made clear exactly what was done by others and what I have contributed myself.

Date :

Lalit Guglani
(2012RME9029)

CERTIFICATE

This is to certify that the thesis entitled "**Development of New Materials and Design Modifications of Knee Joint Prosthesis to Improve Fatigue Life and Wear**" being submitted by **Lalit Guglani (2012RME9029)** is a bonafide research work carried out under my supervision and guidance in fulfillment of the requirement for the award of the degree of **Doctor of Philosophy** in the Department of Mechanical Engineering, Malaviya National Institute of Technology, Jaipur, India. The matter embodied in this thesis is original and has not been submitted to any other University or Institute for the award of any other degree.

Place: Jaipur
Date:

(Dr. T.C. Gupta)
Supervisor
Associate Professor
Department of Mechanical Engineering,
MNIT, Jaipur

ACKNOWLEDGEMENT

First and foremost, I would like to extend my hearty indebtedness to my guide **Dr. T.C. Gupta,** Associate Professor, Mechanical Engineering Department, MNIT, Jaipur for his valuable guidance, constant encouragement and kind help at different stages for the execution of this research work. The completion of the thesis would not have been possible, without his constant support and motivation.

I extend my deep sense of gratitude and respect towards honorable **Prof.** (**Dr.) S. K. Nayak**, Director General, Central Institute of Plastics Engineering & Technology for his continuous inspiration and motivation to carry out this research work.

I am grateful to **Prof. Udaykumar R. Yaragatti**, Director, Malaviya National Institute of Technology, Jaipur, who has been a constant source of encouragement for me. I am also thankful to **Dr. Amar Patnaik**, Professor, Mechanical Engineering Department, MNIT for his continual help and guidance. I would also like to extend my appreciation to DREC members **Dr. Himanshu Choudhary, Dr. Amit Kumar Singh and Dr. Dinesh Kumar** for their valuable suggestions. I appreciate the encouragement from DPGC Convener, faculty members of the department and help from my fellow research scholars.

I extend my gratitude towards **Shri D.R. Mehta**, Founder and Chief Patron, **Dr. M.K. Mathur**, Consultant (R&D) and **Dr. Pooja Mukul**, Technical Consultant, Bhagwan Mahaveer Viklang Sahayata Samiti (BMVSS), Jaipur for providing me the required technical inputs for completing this research work. I am also thankful to **Dr. S.C. Bhaduri**, Director, J.K. Lakshmipat University, Jaipur and **Dr. K V R Rao**, Director, Centre of Converging Technologies, University of Rajasthan, Jaipur for their guidance and help during my research work.

I wish to acknowledge my sincere thanks to my colleagues at CIPET, Jaipur and ARSTPS, Chennai for their scholarly advice at various stages of this research work and help in conducting experimentation.

Finally, I am eternally grateful to my loving family and friends for always being there and providing tremendous amount of inspiration and moral support during my research work. Thanks in particular to my wife Manisha and son Anshul for their continuous support and providing working environment at home.

I would also like to extend my gratitude to all those who have directly or indirectly contributed in the successful accomplishment of this thesis.

Date:

MNIT, Jaipur **Lalit Guglani**

ABSTRACT

The primary objective of this research work is the development of new materials and design modifications of knee joint prosthesis to improve fatigue life and wear. Most individuals in developing countries including India live below the poverty line and cannot afford costly above knee prosthesis devices manufactured by developed countries. These devices can be made affordable by making them from cheaper and low cost materials such as plastics. The research work is divided in two parts. In first part, the new material is developed by preparing the composites of Nylon66-aluminum oxide and Nylon66-titanium dioxide by adding different weight % of the filler. The composites are developed by compounding the material on a twin screw extruder and mechanical & tribological properties investigated. Tests for sliding wear were performed using the pin-on-disk equipment under different loads, sliding velocity and sliding distance combinations to determine the wear rate & coefficient of friction. The images of the worn surfaces were examined using scanning electron microscopy, to understand the wear mechanism. The improved tribological and mechanical properties of Nylon66-Al_2O_3 and Nylon66-TiO_2 composites will enhance the application of plain Nylon 66. Technique for Order of Preference by Similarity to Ideal Solution (TOPSIS), a Multiple Criteria Decision Analysis (MCDA) technique was used to formulate material selection matrix. Composite of Nylon66 with 2 wt.% of aluminum oxide ranked first and was chosen as the material for the knee joint prosthesis. The composite of Nylon66 with 2 wt.% of aluminum oxide exhibited much less wear rate and better mechanical properties compared to oil impregnated nylon material and thus will result in enhanced functional life. The fatigue testing is performed for the composite of Nylon66 with 2 wt.% of aluminum oxide and oil impregnated nylon material to predict their fatigue life.

In the second part, static proof and ultimate stress analysis of the knee joint prosthesis, is conducted by finite element analysis using ANSYS software. By comparing stress distributions with failure criteria for prosthesis, the suitability of proposed design changes were assessed. In these finite element analyses, all the

simulations for static and cyclic stress analysis were conducted by following the ISO 10328 standard protocol. The study is done as per the loading conditions P5 (I & II) of ISO 10328:2006 for static and cyclic tests suitable for an amputee of 100 kg weight. The finite element analysis (FEA) of knee prosthesis revealed failure of some of the components under static and cyclic tests. The total deformation exceeded the prescribed value of 5 mm as per ISO 10328 standard and von Mises stresses are more compared to the yield strength of the material. FEA of existing design with newly developed composite of Nylon 66 filled with 2 wt.% microparticulate of aluminum oxide has shown marginal improvements, yet it failed. Improvements in the design of knee joint prosthesis have been carried out by modifying the geometry of the individual components with an objective to reduce the stresses, total deformation, weight reduction and overcome failure. L9 orthogonal array from Taguchi design of experiments is used to develop new designs. New designs of knee prosthesis were studied by the finite element analysis. The optimized design of knee joint prosthesis meeting all the performance requirements was recommended which complied with the strength and deformation criteria for P5 load level conditions prescribed as per ISO 10328 and components predicted the fatigue life of more than $3x10^6$ cycles in comparison to the fatigue life of $1.93x10^6$ cycles of the existing design. The weight of optimized knee prosthesis is 356 grams compared to the existing design of 372 grams thus reducing the weight by 4.3 %.

Table of Contents

List of Figures

List of Tables

Abbreviations

ASTM	:	American Society for Testing and Materials
ISO	:	International Organization for Standardization
FEM	:	Finite Element Method
FEA	:	Finite Element Analysis
SEM	:	Scanning Electron Microscopy
HRC	:	Rockwell Hardness C Scale
HDT	:	Heat Deflection Temperature
CoR	:	Centre of Rotation
F	:	Force
N	:	Newton
kN	:	kilo Newton
N/mm^2	:	Newton per square millimetre
KJ/m^2	:	Kilo Joules per meter square
Pa	:	Pascal
MPa	:	Mega Pascal
3D	:	Three Dimensional
m	:	meter
mm	:	millimetre
nm	:	nanometer
mm^3	:	cubic millimetre
m/s	:	meter per second
rpm	:	revolution per minute
L/D	:	length to diameter ratio
wt.	:	weight
^0C	:	degree Celsius
wrt	:	with respect to
i.e.	:	that is
sec	:	second
gm	:	grams
kg	:	kilogram
g/mol	:	grams per mole
g/cm^3	:	grams per cubic centimetre
kg/m^3	:	kilograms per cubic meter
%	:	percentage

CHAPTER 1

INTRODUCTION

CHAPTER 1
INTRODUCTION

The Census 2011 of India revealed that, out of the 1.21 billion population, 2.21% of the total population i.e. about 26.8 million persons are ‘disabled’ and 20% of them are having movement disability [1]. Movement disability occurs due to loss of lower limb. The lower limb supports the body structure during standing and transport the body during walking. Lower limb is also required for many other essential activities like walking, standing and driving the vehicles etc. and loss of lower limbs makes amputees unable to perform their daily activities of life. Loss of any limb brings catastrophic change in anyone’s life and the loss of lower limbs is more crucial as they are needed for walking and movement.

1.1 Amputation

Amputation of the lower limb becomes necessary due to several reasons like (i) road accidents, (ii) war injuries, (iii) vascular and diabetic diseases, (iv) growth of tumor and (v) sometimes for the children born with congenitally deformed limbs. Lower limb amputations may be performed at different levels along the lower limb according to the nature and type of the problem:

1) Transtibial
2) Transfemoral
3) Knee disarticulation
4) Hip disarticulation
5) Partial foot
6) Ankle disarticulation

Irrespective of the reason and the type of amputation, the amputee undergoes trauma both in physical and psychological terms.

1.1.1 Transfemoral Amputation

In movement disability, transfemoral amputation also known as an above knee amputation is a most occurring type of the lower limb amputation which happens through the femur bone in the thigh. Two of the most important joints of the

human being i.e. knee and ankle joints are lost by the person due to this type of amputation. To ensure the proper rehabilitation of the amputee, care should be taken during surgery to leave as much residual limb as possible, preserve the adductor muscle, and effectively suture the remaining soft tissue to minimize scarring [2].

Transfemoral amputees faces distinct challenges, such as balance and stability problems, discomfort while sitting and difficulty rising from a seated position and increased energy requirements [3]. Above knee amputees face more challenges ambulating throughout the community. They cannot participate in the sports and other essential activities. Young amputees response is good to the functional need, but aged amputees find it difficult to overcome the energy cost [4].

1.2 Prosthesis

The word “prosthetics" comes from the Ancient Greek, meaning “to place an addition" [5]. In orthopedic field, prosthesis is defined as an artificial device that replaces the amputed limb of the body [6]. Lower limb prostheses were designed to assist the amputees to overcome the above difficulties and improve their lives. The replacement of any lost natural limb, in true sense, is practically impossible by any artificial mechanical system due to the fact that the natural limb is an integrated part of the body which has grown up by natural biological processes with complex articular linkages and neuromuscular control system. However, a well-functioning prosthesis has the ability to return independence to an amputee and may allow him or her to participate in socio-economic activities that would otherwise be impossible. It is a well accepted criterion for the successful prosthetic device that it shall rehabilitate the lower limb amputees with a normal appearing gait. Also, the prosthetic replacement shall be comfortable, safe and amputee uses it without undue physical effort and mental agony. Basically two types of prosthesis (below or above knee) are used to replace the lower limb, depending on the kind of amputation.

1.2.1 Transfemoral Prosthesis / Above Knee Prosthesis

In the case of transfemoral amputation, the replacement limb is called the transfemoral prosthesis or above knee prosthesis and it must allow the amputee to control the knee prosthesis by means of the residual limb and enable walking. There

are two types of transfemoral prosthesis: exoskeletal and endoskeletal as shown in Figure 1.1(a) and 1.1(b). Exoskeletal prosthesis is the primitive design with plastic laminated outer skin or shell of wood and polyurethane foam interiors and endoskeletal prosthesis consists of four major components – socket, knee joint, pylon and foot.

(a) Exoskeletal

(b) Endoskeletal

Figure 1.1 Transfemoral prosthesis

Knee joint is the most important component of the above knee prosthesis and must be able to substitute the functionality of the muscles lost due to amputation, particularly the stability during walking in the stance phase and control during the swing phase [7]. The knee joint is very complex and biggest joint of the human body, lying between hip and ankle joint and is essentially made of four bones – Femur, Tibia, Fibula and Patella (knee cap).

Even though more than 100 different designs of knee joint prosthesis are commercially available in the markets worldwide, but prosthetic knees can be classified as per kinematic function into two types: single-axis and polycentric [8]. Single axis knee is defined as any knee joint in which the shin moves in pure rotation about a fixed centre of rotation which is located at the knee bolt, whereas in the polycentric knee design, the shin moves in a combination of translational and rotational motion. This combined translational and rotational motion is described

mechanically in terms of pure rotational motion. This continuously changing centre of rotation is called instantaneous centre of rotation [9].

In single axis knee prosthesis, the amputee needs to walk over a fully extended i.e. straight knee during the weight-bearing phase which leads to the unnatural appearing gait and contributes to the physiological abnormalities to the above-knee amputee [10]. In comparison to single axis knee, four-bar knee design provides increased stability during the heel strike, through the early stance phase and reduced energy requirement. The overall length of the prosthesis gets shortened during the swing phase and the four bar design provides increased voluntary control of knee flexion in the terminal stance [11-13]. Due to these important features, the four-bar knee prosthesis have gained large acceptance by the amputees.

1.3 Knee Prosthesis Material

The material selection of knee joint is done by considering the strength and weight of the material. The necessary trade off is made between the strength and weight of the prosthesis and decision is taken on the strength to weight ratio so that amputee need not to walk with too much weight. Cost of the prosthesis depends upon material selected. There are many amputees who cannot afford advanced prosthesis due to paucity of funds. Therefore selecting a low cost material can make the prosthetic device much more affordable for many amputees throughout the developing countries.

1.3.1 Knee Prosthesis in the Developed World

The material selection for prosthetic knee joints in the developed countries is primarily based on the mechanical properties, regardless of cost. The selected material shall have high strength combined with low density, high fatigue strength and corrosion resistance properties. Titanium alloys, stainless steel, high strength aluminum alloys and carbon fiber materials are normally used for the knee prosthesis in the developed countries. In some of the knee joints, the composite and copolymer materials are used for the bearing or contact surfaces due to their less coefficient of friction and self lubricating properties. Polymer composite materials offers excellent strength to weight ratio and their development has led to

technological advances in prosthetic devices [14]. The knee joints commonly used by the amputees in developed countries costs thousands of US dollars which is the result of chosen material and the manufacturing processes.

1.3.2 Knee Prosthesis in the Developing World

As most of the amputees in the developing countries live below the poverty line, the material selection for knee joint prosthesis is dependent more on the locally available material having less cost. Thermoplastics are primarily used as the main material due to their relatively less cost, light weight due to less density, low friction and ease of machining. The most commonly used materials include different types of nylon, polyacetal, polypropylene and polyethylene. However, these prosthetic components shall be capable of withstanding the high loads present during mobility and provide sufficient strength complying with the requirements of international standards [15]. The above polymer materials suffer from poor mechanical strength and wear properties compared to the metal & alloys used in prosthetic devices. The wear is caused on some of the components of the knee prosthesis as a result of severe loading developed during the various daily activities. The repetitive action of such loading leads to the failure of some of the prostheses [16]. Thus the need is felt to develop new materials having less wear and better mechanical properties.

1.3.3 ISO 10328

The development of lower limb prostheses took place only on the basis of field use by the amputee, without performing any structural testing, for so many years. As it is recommended to first establish the safety of the product before the commencement of mass production, an International Standard “ISO 10328:2006 Prosthetics - Structural testing of lower limb prostheses - Requirements and test methods”, was developed [16,17]. Thus it is very much essential to develop the knee prosthesis which shall meet the performance criteria of ISO 10328 standard.

1.4 Finite Element Method

The development time for new designs can be accelerated and experimentation cost can be reduced significantly by simulating the tests using the finite element method. Finite element analysis softwares such as ANSYS are utilized for this

purpose. The finite element method revealed the stress distributions induced on prosthetic devices and predicted their fatigue life and the validation results confirm the fidelity of its application [18, 19]. Thus it is concluded that the application of FEM suits well for the design of prosthesis.

With this background knowledge, the present work has been undertaken to develop new materials, study their structural suitability and develop new design of knee joint prosthesis meeting the performance criteria specified in "ISO 10328:2006 standard".

Main purpose of this thesis is to develop new Nylon66 based composite having better mechanical and tribological properties for knee joint prosthesis. The properties of all the developed composites are studied and their performances are compared. The study would help the research community to select the composites for different engineering applications. Further, one of the low cost knee prosthesis used in developing countries is studied for its static strength and fatigue life analysis using finite element method to develop new optimized design.

1.5 Thesis Outline

The remaining part of thesis is structured as below:

Chapter 2: Includes literature review considered to provide an outline of the existing basic knowledge and issues involving the present research interest. It describes the research works on above knee prosthesis, its mechanism, design, types etc. Study of various types of polymer composites of nylon by addition of different fillers. Research on application of FEM in the area of above knee prosthesis conducted by various researchers and design optimization techniques.

Chapter 3: This chapter briefly illustrates the properties and specifications of the selected materials, methodology to develop composites, test procedure for the mechanical characterisation and tribological studies. Material selection process by TOPSIS, a multi criteria design analysis and the methodology of finite element analysis and the requirements of ISO 10328: 2006 standard in detail.

Chapter 4: This chapter covers the results of mechanical and tribological properties of oil impregnated nylon material (Oilon), Nylon66 and composites of Nylon66 material. The interpretation of the results and comparison for various compositions is elaborated in detail. The SEM results of worn out surface of the specimens is also depicted. The result of material selection, based on multi objective design criteria is also covered in detail.

Chapter 5: This chapter covers the finite element analysis of knee joint prosthesis as per the procedure of ISO 10328. The static proof and ultimate strength analysis of the knee joint prosthesis, by finite element method is covered in detail.

Chapter 6: It presents a detailed study on design modifications of the existing design and FEA of knee joint prosthesis. Fatigue testing of the materials and the analysis of optimized design for fatigue life, is also discussed.

Chapter 7: Important findings of this research work are presented in this chapter and explicit conclusions deduced from the investigations are outlined and suggestions for future work are mentioned.

The next chapter briefly discusses the literature review of various research papers on knee joint prosthesis, its mechanism, design, types etc. Study on various types of polymer composites used in prosthesis. Research work involving the application of FEM and ISO 10328 standard in the area of knee joint prosthesis is discussed. The specific objectives of research work are explicitly outlined in the next chapter.

CHAPTER 2

LITERATURE REVIEW

CHAPTER 2
LITERATURE REVIEW

The purpose of the literature review is to gain useful insight and information on the issues to be considered in this thesis and to emphasize the importance and relevance of the present study. This review seeks out to summarize, evaluate and describe the works in the field of above knee prosthesis. The types of knee prosthesis used in developed and developing countries and the materials used for knee prosthesis is studied in detail, particularly the polymer composites. Research work related to the application of FEM, design optimization and ISO 10328 standard in the area of above knee prosthesis is also studied.

This thesis includes various aspects of polymer composites, particularly with a special reference to the mechanical and wear characteristics. The topics included in this literature review are:

2.1 History of Prostheses
2.2 Types of Knee Prosthesis
2.3 Materials used for Prosthesis
2.4 Material Selection methods
2.5 Applications of FEM in Prosthesis
2.6 ISO 10328 applications in knee prosthesis
2.7 Taguchi Technique for Design of Experimentation

Literature survey summary and knowledge gap in the previous research work is given at the end of chapter. The objectives of this research are clearly outlined.

2.1 History of Prostheses

The earliest prosthesis found a mention in Rigveda with reference to the warrior queen Vishpala. We got the evidence from the wooden toe of an individual that the prostheses were in existence from earlier times of Egyptians [20]. In the earlier era, simple stubs of wood prostheses were used by the amputees for balancing while walking. Until the late 18th century, the prosthesis design did not assumed an anthropomorphic (human like) design and before the 20th century, the

prostheses in use were mostly passive [21]. More prosthetic devices were developed by researchers, as the numbers of amputations in war were increased. A pneumatic hand developed in Germany was the first powered prosthesis and since then tremendous improvements have taken place and improved powered prosthetic designs are developed [22]. Presently, highly sophisticated microprocessor controlled prosthetic devices involving state of the art hardware and software which are capable of imitating the natural human gait are available in the developed countries. These advanced high-tech prostheses are not accessible to everyone due to the high cost and still millions of amputees in the developing countries are dependent on passive or semi- passive prostheses.

Prosthesis for individuals with amputations above the knee through femur bone is referred to as transfemoral or the above-knee prosthesis. The amputees with knee disarticulation who have transection between the tibial and femoral condyles, also suffers from the loss of functions of knee, and their prostheses are known as knee disarticulation prostheses. In knee disarticulation, the challenge is to manage the long residual limb. It shall be ensured that the shank and thigh segments are in proportion to the intact limb. Knee joint is required in both the above types of amputees, thus the term transfemoral or above knee prosthesis includes knee disarticulation also.

Transfemoral prosthesis has four main components, a socket and suspension for interfacing and securing the prosthesis to the residual limb, a knee joint, shank or pylon with connectors and a foot component. All of these components are having their own importance and are responsible for a comfortable and well-functioning prosthesis. The comfort, load-bearing capability, proprioception, and control of the prosthetic limb are dependent on the fit of the socket & suspension to the amputee [23]. The knee joint plays a major role for articulating the mobility activities. They are sitting, stair climbing, squatting, kneeling, swing-phase walking and facilitates limited performance, depending upon the design. Knee joint plays a major role in stability during weight-bearing [24, 25]. Stability, comfort, smooth rollover and progression of the shank, are dependent on the foot component of the prosthesis [26-

28]. The successful fitment and use of the above knee prosthesis, is dependent on the setup, alignment and interaction of all the components of the prosthesis.

2.2 Types of Knee Prosthesis

From the literature review, it is revealed that the prosthetic knee joints of following types are in use:

1. Knee with Manual Locking
2. Single Axis Knee with Constant Friction
3. Polycentric Knee
4. Weight Activated Stance Control Knee
5. Knee joint fitted with Outside Hinges

Knee with manual locking gives maximum stability from the above given types, but it does not provide the voluntary control. As seen, outside hinges on knee joint gives the highest voluntary control but has minimum stability of all given designs. Control means ability to influence by the amputee on prosthetic device and stability means influence of the prosthesis on the amputee wearing it. Locking mechanisms of the knee joint are manual and weight activated. K scale or K score is defined by “The Medicare Functional Modifier System” to differentiate knees which ranges from K0 to K4. K0 is for healthy humans and K4 for children, athletes and bilateral amputees. Most of the amputees come under category of K2 and K3, where they have to do many activities in different areas [29]. The different passive knee joint prosthesis are classified on the basis of design aspects such as axes, mechanisms for locking, adjustability, friction, and microprocessor control etc. [30-32]. Single axis and polycentric are the two main types of prosthesis. The knee joints equipped with frictional components can be, hydraulic or pneumatic, with constant or variable friction. Extension aids fitted with the above knee prosthesis are either external or internal. Different types of knee prosthesis designs are made on the basis of Thigh-Knee-Ankle (TKA) weight line and its relation to the instantaneous centre of rotation. Stability and control is dependent on TKA weight line. Stability is high when TKA weight line is anterior with respect to the knee axis and situation is reverse when TKA weight line is posterior to the knee axis [42, 56-59].The design which is suggested also depends upon the stump length of the amputee. The amputee

who has long stump length can have voluntary control and stability. Such amputee needs low stability, high control knee joints. Whereas the amputees with short stump length cannot have voluntary control due to not having enough muscles, so they needs low control and high stability prosthetic knee joints [34].

2.2.1 Passive Prosthesis

The functioning of Passive prostheses depends upon energy which is stored and released during gait, during heel strike the energy is stored and is released during toe off [35]. With the help of springs, the energy storage and release is done in some of the passive prosthesis designs. Due to high energy expenditure while walking, amputees are not able to use the prosthesis as much as needed [36]. With good prosthetic design, the energy expenditure can be reduced. Some of the popular passive prosthetic knee joints are manually locking, polycentric, and weight activated knees for stance control. Because these prosthetic knee designs can function without microprocessor control and allow for simple mechanical or geometric locking. The asymmetric transfemoral prosthesis designed by Sushko et al. was successful in restoring symmetric gait due to its less weight than the conventional prosthetic devices [37].

In the developing world, most of the individuals due to their poor economic conditions tend to use passive knee prostheses, designed purely based on mechanical means. Single axis knee prosthesis is the most common model with no swing phase control and offers the lowest cost and little to no maintenance lifespan [38, 39]. However, this model exhibits stability problems, offers no variance in walking speed and gait problems [39]. Due to these problems, many amputees consequently switch to manually locking single axis knee for more stability over uneven terrain [39, 40]. The ICRC manually locking knee exhibits a low failure rate and offers no in-gait swing or stance control. Weight-activated friction knee was developed by ATLAS to address the absence of control, but it showed unreliable function and high rates of structural failure. The failure problems noted in these prosthetic designs were primarily attributed to the high wear of the braking mechanisms and changes in the friction coefficient due to the factors such as humidity and moisture [40].

The four bar linkage knee mechanism, based on polycentric action is in existence for almost four decades and was designed primarily to offer stance phase stability & swing phase mobility [9]. The four-bar linkage knee prosthesis provides greater toe clearance during the swing phase of walking compared to the single-axis knees and negated the need for a joint lock thereby increasing the functionality & mechanical advantage of the artificial knee joint and consequently increases the efficiency of the prosthesis and decreasing the energy requirement for the amputee patient [60]. The four bar knee prosthesis mechanism is modified adding a fifth link and offers a stance flexion feature to the amputees in early stance and mid-stance phases of the gait [61]. Patil and Chakraborty [62] gave a six bar knee-ankle design. It provides and coordinates motion between knee and ankle joint while walking and squatting. Otto Bock developed Total Knee & 3R60 Knee prosthesis using six-bar mechanism [63]. This study shows us six bar mechanism is better than four-bar mechanism. It can be designed in better way to achieve the desired trajectory of the ankle joint [59].

Due to the development of cheaper and better designs, the usage of knee prosthesis based on four bar mechanism principle are increasing in the developing world [52]. The four-bar knee offers better stability and enables relatively natural gait movement due to its polycentric design but still experiences abrasion wear problems. Bhagwan Mahavir Viklang Sahayta Samiti (BMVSS), Jaipur has developed a low cost prosthesis in collaboration with Stanford University which costs less than 40 dollars and is widely used in the developing countries [33, 41].

Uses of spring can minimize the energy required by mimicking the musculotendonous structures. The energy is stored and released during the gait cycle as per the requirement. Spring is very much efficient and is useful due to its high power/weight ratio [54]. A prototype was developed by Unal et al. [55], which uses a set of springs, coupling knee and joints which can harvest and return energy. This design works on energy distribution which is balanced between the ankle and knee joints in a single stride.

2.2.2 Active Prosthetics

Most of the low cost prostheses currently in use lack technology that assists the amputee during swing-phase of the gait cycle. Swing-phase control knee joints aid to limit heel rise, assist extension, and reduce impact at the end of knee extension for more comfortable, efficient and aesthetic gait [42]. Microprocessors are used in Active prostheses to control and position of the knee and ankle joints which are monitored by the sensors. Other variables tracked are, stride lengths, stride velocity and applied forces [43]. The parameters are tracked to assimilate the movements of the healthy limb. The actuators which are used in these devices are hydraulic or pneumatic, or the electric motors can be used [48]. Pneumatic based designs give enough power and precise control during the work [44]. Hydraulic based designs gives high power to weight ratio and has lesser leakages but it is heavier than pneumatic based devices [45, 46]. Yokogushi et al. made successful design of hydraulic polycentric knee. It performed under different step rates and gives the results similar to that of healthy human limb [47]. The active prostheses adapt to the motion of the wearer and compensate for the lack of muscle control in the residual limb. Significant improvements in the gait and balance were experienced by the transfemoral amputees fitted with active microprocessor controlled prostheses, when compared to the passive prostheses. The major constraints to these designs are high cost, large size and heavy weight.

2.2.3 Problems Experienced by Transfemoral Prosthesis Users

Current models of low-cost prosthetic knee used by amputees in the developing countries offer very little functionality and serve primarily as structural support for the amputee. Inadequately functioning knee joint prosthesis can lead to significant gait deviations compromising on the mobility, independence and morale of the amputee [49]. Transfemoral amputees experience innumerable problems such as gait asymmetry, which affect their quality of life [50]. Socket, which is a component of prosthesis, is fitted on the residual stump of the transfemoral amputee. The sockets are mounted tightly on the residual stump to avoid slipping which causes increased discomfort. The residual stump is affected by the continuous rubbing, friction and sweat resulting in skin sores and other dermatological problems

[51]. The studies also tell us that the amount of residual limb is the main factor deciding the comfort level of the amputee. The main drawback with the active prosthesis is that they are extremely costly, needs portable power source and creates lot of noise. The number of amputees is high in the developing countries who cannot afford the cost and avail the opportunities available in west. Hence, cheaper prosthetic devices are needed so that the less privileged amputees can walk and lead a normal life [53]. A passive knee joint with simple design which can be manufactured using cheaper materials and less costly manufacturing techniques are the need for the amputees belonging to the developing countries.

2.3 Materials used for Prosthesis

The material selection of knee joint is done by considering the strength and weight of the material. The necessary trade off is made between the strength and weight of the prosthesis and decision is taken on the strength to weight ratio so that amputee need not to walk with too much weight. The knee joint material should be selected on the basis of the patient's need and abilities depending on the age and the size of residual limb [64]. The cost of the prosthesis depends on material which is selected. There are many amputees who don't have money to buy advanced prostheses. So to reduce the cost we shall select material which is low in cost and has good mechanical properties and less wear. The material shall be biocompatible and easily available [65]. Different new materials are used like titanium alloys and carbon fiber. There are certain composites and copolymers which can be moulded with less technology. Polymer composite materials offers excellent strength to weight ratio and their development has led to technological advances in the field of prosthetic devices [14]. We shall choose a material which is not costly so that many amputees can afford it. So, material selection is very much important in deciding cost of prosthesis.

2.3.1 Metals

Metals are used for manufacturing components of prosthesis, like knees and ankles etc. Aluminum is preferred over steel as it is lighter. Steel is conventionally used for manufacturing smaller prosthetic components. Now-a-days use of titanium is increasing as it is non-toxic metal and is non-magnetic. It is light and is immune

to corrosion and thus it is best for prosthetic devices [67]. A variety of metals such as aluminum, titanium, magnesium, copper and steel etc. are used for prosthetic devices. Titanium is used in many medical and engineering applications. It has favorable properties and gives good strength, excellent corrosion resistance, low density and is light weight [68]. Titanium is generally alloyed with other metals such as aluminum and vanadium to improve certain properties and enhance its application.

The modulus of elasticity of titanium is similar to that of bone and offers many advantages when used as implant. Titanium being lightweight, strong, resistant to corrosion and biocompatible is an ideal choice for the application of prosthetics.

2.3.2 Plastics

Now-a-days wood, aluminum and leather are replaced by thermoplastics and advanced composites and this has led to advances in this field [69]. The use of thermoplastic as a material for structural components in artificial limbs is increasing as they possess low density, mouldability, corrosion resistant and shock absorbent and fatigue & wear resistant [70]. The usage of thermoplastic materials such as polyethylene and polypropylene became more commonly during 1960's in prosthetics and orthotics. The first important application of thermoplastics in orthotics is the drop foot brace which is perhaps still the most produced orthopedic device made of thermoplastic material [71]. The thermoplastics are commonly used to produce long-leg braces (knee-ankle-foot orthoses) and for the manufacture of spinal orthoses [72]. Polypropylene found its use in developing below knee prosthesis due to its light weight and less energy consumption [73, 74]. The sockets for transfemoral amputees also made of polypropylene material [75]. Since the last five decades, UHMWPE is extensively used as the most popular artificial replacement material in clinical applications [76]. “Ultra-high-molecular-weight polyethylene (UHMWPE)” has been considered as the most suitable material used in arthroplasty applications [77], especially for the artificial knee and hip implants. Nylon impregnated with oil is used as the material to manufacture Jaipur knee joint [41, 82]. The oil filler reduces the friction at the bearing surface in result in longer wear life than unfilled nylons. Also, the moisture absorption is reduced and

eliminates the need for lubrication. However, it suffers from structural stability at elevated temperatures, flammable and exhibits increased wear and friction under high load conditions [187]. Nylon sheaths and stockings are in use since long. Poly-ether-ether-ketone (PEEK) is a polymer that is used for a number of fixed and removable prosthesis in spinal and hip applications and has many potential uses in dentistry [79-81]. Plastic polymer laminate is used in bonding layers of carbon, fiberglass and nylon. Thermosets often used in sockets are made from acrylic, epoxy, and polyester [67].

2.3.3 Carbon fibers

Carbon fibers have good modulus with less density than many other materials used in prostheses [78]. There are some other good properties of carbon fibers. It has high stiffness, tensile strength, chemical resistance, temperature tolerance and low thermal expansion. The elastic modulus of carbon fiber composites is three times higher than steel, magnesium, titanium and aluminum. Normally materials which have high elastic modulus are not very ductile but carbon fiber composites have very high tensile and compressive strengths [65]. Carbon fiber is now routinely used for prostheses, orthoses, corsets and orthopaedic footwear [66]. Also, carbon fibers are very strong for amputee with heavy weight. Due to the high cost, carbon fiber prosthesis usage is limited to developed countries.

2.3.4 Polymer Composite Material

Composites are materials developed when two or more than two chemically different constituents are added on a macro-scale. The basic material for composite can be metal, polymer or ceramic. If the base material is polymer, the composite is known as polymer matrix composite (PMC). The reinforcement materials can be fibrous or particulate [83]. Polymer composites have gained lot of attention of researchers in recent years. When fillers are added, we get composites with better properties. With the addition of fillers mechanical, structural, tribological and other properties of the composite materials get modified [84, 85]. The UHMHDPE is susceptible to aseptic loosening due to debris of wear originating from polyethylene cup and creep deformations. This happens as the glass transition temperature is lower than the body temperature [86]. The effect of adding fillers like alumina,

zirconia to UHMHDPE studied by Juan C. Baena et al. [76] and results showed less stress variations. If 2 to 5% by weight of multiwall carbon nanotubes is added to bone cements based on acrylics, fatigue performance gets improved and SiO_2 is added to PMMA to develop nano-composites in order to optimize properties [87-89]. PEEK is also improved by adding materials like carbon fibers and elastic modulus is increased upto 18 GPa [80]. For example; incorporation of carbon fibers can increase the elastic modulus. To improve the mechanical properties and reduce cost, particulate filled thermoplastic composites are made. Mechanical strength, heat deflection and modulus etc. are improved by mixing inorganic mineral fillers in the plastic resin [90]. These properties are also dependent on the size, shape and filler distribution in the particulate filled polymer composite. It also depends upon the adhesion of the filler at the interface surface.

2.3.4.1 Effect of inorganic fillers Al_2O_3/TiO_2 on the properties of Polymeric material

Nylon [91] is used in packaging, automobile, electrical & electronics, textiles and consumer sectors mostly because of its good mechanical properties. Thus, it founds applications. The nylon has low HDT, hence dimensionally unstable at higher temperatures. It also has high water absorption and thus applications are limited where structural strength is the requirement. Hence, fillers such as titanium oxide, zirconium oxide, aluminum oxide, silicon carbide etc. are added as reinforcing agents to improve the stiffness and strength [92-95].

It is well reported that the 3.0 wt% - 4.0 wt.% Al_2O_3 polyimide nanocomposite gave the lowest loss of wear volume under high load and it also exhibited lower friction coefficient [96]. Yongjui Zhao et al. [97] studied the mechanical properties and thermal conductivity of the Epoxy resin / Al_2O_3 composite and found that heat conducting property increases with the increase in the content of Al_2O_3 and reach to 0.46 W/m.K. at 30% micron Al_2O_3. When the mass fraction of Al_2O_3 is 20%, the mechanical properties of the composite are better, J. Cho et al. [98] found that the tensile strength of Al_2O_3 – Vinyl Ester resin can be improved by reducing the particle size. However, in composite with 3 vol.% nanoparticles the tensile strength was less compared with addition of microparticles. This may be due to poor

dispersion of the nanoparticles at higher loading. Praveen Bhimraj et al. [99] investigated the friction & wear properties of PET filled with alumina nanoparticles and the results revealed that 2% addition of filler resulted in increasing the wear resistance by nearly two times with a 10% decrease in average coefficient of friction over the unfilled polymer. Wear resistance varies independent of crystallinity, whereas coefficient of friction is affected both by crystallinity and nanoparticles. The tribological behaviour of poly phenylene sulphide (PPS) composite made with nanoscale particle of Al_2O_3 was investigated by Christian J. Schwatz et al. [100] and found that the lowest wear was obtained for composite with 2 vol.% filler whereas COF was higher with addition of filler except with 10 vol.% alumina. Flexural strength also reduced with filler %. Another work concluded that the friction coefficient of the PA6/ Al_2O_3 nanocomposites was more than that of monomer casting PA6 but less than that of microcomposite and decreased with load. But the wear rate is lowest for 3% nano Al_2O_3 content and the microcomposites also demonstrated lower wear than pure Nylon 6[101].

The use of TiO_2 nano powder has also increased in past years, because it is chemically inert and non toxic. It has UV resistant properties and antibacterial from its photo irradiation effect. Further, it is corrosion resistant, high refractive index and low cost [102]. Various researchers investigated the effect of adding micro and nanoparticles of TiO_2 to Epoxy, Polypropylene, PEEK, Polystyrene, ABS and Nylon. C. B. Ng et al. [103] found that nanophase TiO_2 particle fillers at 10% weight level increase both the modulus and the strain-to-failure of epoxy whereas micron-size TiO_2 filler increases the epoxy modulus, but decreases the strain-to-failure. Farah. T. Mohammed Noori et al. [104] concluded that the wear rate increases with the load applied and decreases with increasing weight percentage of titanium dioxide in epoxy matrix having the lowest wear rate at nano 5wt% titanium dioxide and nano composites of epoxy / TiO_2 have many advantages over micro composites in terms of wear and hardness tests. The mechanical and morphological properties of polypropylene (PP)/ TiO_2 composites were investigated by Sirirat Wacharawichanant et al. [105] and the results indicated that the mixing conditions can improve the distribution of TiO_2 particles, leading to improved mechanical properties. The

tribological (friction and wear) behaviour of TiO_2 filled ABS polymer was investigated by J. Sudeepan et al. [106] using Taguchi analysis and it is found that normal load has major contribution on tribological properties followed by filler content and speed. Kei Sahibata et al. [107] investigated the tribological behaviour of polyamide66 resin containing rice bran ceramic particles at a wide range of pressure-velocity values under dry conditions and noted low friction coefficients independent of pv values whereas for pure PA66 it increases at higher pv values. The fracture behaviour of PA66 filled with various fractions of TiO_2 (21nm) nanoparticles was studied using an energy partitioned work of fracture method and found that the plastic work of composites was decreased with increasing nanoparticle fractions [108]

2.4 Material Selection Methods

Many a times the material is chosen by trial and error or depending on the past usage. Generally, when two or more materials are suitable, final selection is difficult. There will always be some advantages as well as disadvantages of the available choice of materials [109]. For the selection of material, we require experts from different fields of study such as material science and engineering, mechanical engineering, industrial engineering and others. Chiner suggested five steps for material selection: first is design objectives, second is analysis of the material properties followed by screening of possible material choices, fourth step is the evaluation and decision for finding the optimal solution, and finally validation tests [110]. Farag explained the material selection during the design stage, first is initial screening, secondly comparing the alternatives and finally selecting the optimal material [111]. The “multi-criteria decision making (MCDM)” methods can be divided into two main groups, “multiple objective decision making (MODM)” and “multiple attribute decision making (MADM)” approaches.

2.4.1 Multiple attribute decision making

The choice of materials is not decided considering a single factor but evaluated against multiple criteria in most of the applications. The best material is selected from many materials on the basis of many attributes is known as “multiple attribute decision making (MADM)” method [112]. The variables can be quantitative

such as numbers or qualitative such as poor or good etc. and few others can be described by text and images [113]. “MAUA (Multi-attribute utility analysis)” is mathematical tool by which we can compare & evaluate alternatives in decision making [124]. The MAUA can be used for material selection as an operations research technique by applying subjective probability assessment (SPA) [125]. Sirisalee et al. [126] gave a method which can deal with three objectives in MAUA.

2.4.2 Fuzzy multi-criteria decision-making techniques

The main elements in human thinking are in labels of fuzzy sets and not in numbers and on this premise the Fuzzy set theory was developed. In material and process selection the application of fuzzy logic is quite useful as decisions are based on the preliminary design stages which depend upon uncertain requirements, various parameters, and relationships [114]. Wang and Chang [116] suggested it for the selection of tool steel materials and proposed a fuzzy set multiple criteria decision making approach [117]. The important weights of different criteria and the material adequacy ratings of various alternatives under different criteria were given in linguistic terms.

2.4.3 Technique for Order of Preference by Similarity to Ideal Solution

TOPSIS is a multi-criteria decision analysis method, which was originally developed by Hwang and Yoon[115] in 1981 with further developments by Yoon[118], and Hwang, Lai and Liu [119]. TOPSIS methodology is based on the theory that the chosen option should have the least geometric distance from the positive ideal solution (PIS) and the highest geometric distance from the negative ideal solution (NIS) [120].

In this technique, a set of alternatives are compared by identifying weights for each criteria by compensatory aggregation and normalizing scores for each criteria. The geometric distance between each choice and the ideal choice is then calculated for finding the best score of each criterion. In multi criteria problems, the normalization is generally required as the criteria or parameters are often of inconsistent dimensions [121,122]. TOPSIS is a compensatory method in which trade-off is made between the available criteria’s. The effect of poor result in one

criterion is overcome by the good result in other criteria and provides more rational form of modeling. On the other hand, the non-compensatory methods works on the basis of hard cut-offs, in which the alternative solutions are included or excluded [123].

2.4.4 Computer simulation

The application of computer simulation techniques in material selection were discussed by Goldsberry [127]. The Moldflow software was used to evaluate the available materials of different costs. Flow analysis is the simulation technique in which the ability of various materials is compared by computer simulation rather than by doing the trial and error on the molding machine. Due to the recent advances in finite element methods, the computer simulation is used for optimizing the design of composite structures. According to Aceves et al. [128], the computer simulation is much useful in case where the single objective can be defined and are less useful where the design objectives are conflicting (e.g. minimum weight and cost).

2.4.5 Material Selection Methods used in Biomedical Engineering

Most of material selection studies in the area of biomedical engineering used finite element analysis as a tool for the computer simulation [129]. The MCDM-based techniques have been utilized in the material selection of hip joint prosthesis [130], and few others used compliant-layer methods for selecting the artificial hip joint materials [131]. Even though, various MCDM methods have been developed to solve the material selection problems, still there is a great necessity to use suitable approaches in agreement with the nature of the problem [132]. In this regard Marjan Bahraminasab and Ali Jahan [133] used comprehensive VIKOR method to select the optimum material, and a systematic technique for sensitivity analysis of weights was introduced to find more reliable results. Taahirah Mangera et al. [134] used ELECTRE III ranking procedure and successfully applied to the material selection of a light metal alloy for a pediatric prosthetic knee. Golam Kabira and Afruna Lizub [135] developed a systematic, simple and logical scientific approach to evaluate the appropriate material for the femoral component for total knee replacement (TKR) by integrating Fuzzy Analytical Hierarchy Process (FAHP) with the Preference Ranking Organization Method for Enrichment Evaluations

(PROMETHEE). This decision-making approach was developed by taking the advantage of the synergy between FAHP and PROMETHEE multi-criteria decision making methods wherein their weak and strong points are detected and the ranking is developed by doing the sensitivity analysis and the final selection for the decision maker is facilitated.

2.5 Applications of FEM in Prosthesis

The Finite Element Methods (FEM) has been widely used in the biomechanics to predict stress, strain and deformation in the complicated systems and is identified as an important tool for analyzing the load transfer in prosthesis [136]. In the finite element method, the problem structure is divided (mesh) in the smaller domain areas (finite element) which are connected by nodes, called mesh. For finding the solution to these finite elements (FEs), loads are applied to the structure boundary of each node, as well as the boundary conditions are defined and finally the global solution is arrived by assembling all the elementary solutions. Many specialists consider FEM as one of the most common numerical methods for the structural analysis. Regardless of the type and complexity of the problems, FEM is used in different fields of engineering and science. FEM is increasingly used in medical science and is quite useful in the field of dentistry and all of its specialties [137]. FEM can be used for static and dynamic problems as well. Hasan Saad et al. [138] performed three dimensional Finite Element (FE) modeling of prosthetic lower limb. A modified three dimensional finite element model of socket was developed in workbench of ANSYS 14.0 to find out the stress distribution and deformation pattern under functionally appropriate loading condition during normal gait cycle. This work tried to improve the deflection of the loading of socket, foot, and pylon shank. The contact pressures and ligament forces were analyzed by Reggiani et al. [139] during the passive and stance phase of gait conditions by developing a finite element model of prosthesis.

S. Miharadi et al. [140] evaluated three-dimensional models of above-knee prosthesis using finite element method software ANSYS to determine whether or not the design has fulfilled strength criteria and for static loading simulation, vertical load of 923.4 N representing total body weight of 90 Kg was applied to the

prosthesis model. In another work M.A. Kumbhalkar et al. [141] studied and evaluated the loads and stresses acting on knee joint during different motions such as steady, walking and lifting by applying the calculated loads in the finite element analysis software ANSYS and compared the same with the implant results. The distribution of von-mises stresses, contact pressure and total deformation was studied by Saurabh Samadhiya et al. [142] by assigning it the different combination of biomaterials for femoral and tibial components with load gradually increasing from 600N to 5000N for different biomaterials and used ANSYS 12.0 finite element analysis software. Ashutosh Nayan Nautiyal et al. [143] has done the modeling and finite element analysis of knee joint of the complex femoral and tibial structure in ProE 4.0 and Ansys 15.0 for different loading conditions of standing, walking and stair climbing at various angles ranging from 0^0 to 120^0 for varying person's weights from 50 to 80 kg. It was noted that the von-mises stress increases continuously with increasing loads. In another study, ANSYS 11.0 was used to investigate numerical estimation of contact stresses and the effects of the sagittal radius, flexion angles on stresses in the joint [144].

2.6 ISO 10328 applications in knee prosthesis

ISO 10328 describes the procedures for static and cyclic strength tests on lower limb prostheses in which a single force is applied to produce the effect of compound loadings. The compound loads in the test sample simulate loading which normally occurs at different instants during the stance phase of walking [145]. C. Colombo et al. [146] proposed a valid method to adapt the ISO standard for testing adult prostheses to children. They found a parameter that can be used as a factor of proportionality using data related to dummies and both geometrical characteristics and loads prescribed by the standard are rescaled. For all the performed experimental tests the results were positive, with expected trends of displacements. To check the structural integrity of a four-bar link prosthetic knee, Sittikorn Lapapong et al. [19] showed a process to simulate the static & cyclic strength tests by following the test protocols of ISO 10328: 2006. Simulation of the prosthesis was done using finite element method as the primary computational tool. This is a numerical technique which is used to model any physical system. Strength of prosthesis was determined

by the method of explicit nonlinear transient stress analysis and finally the fatigue life is predicted by finite element model which revealed the stress distributions. In the cyclic test, the prosthesis is subjected to $3x10^6$ cycles of mechanical endurance testing to determine its fatigue strength. Tomaso Villa et al. [188] studied the structural integrity of metal tibial components in terms of fatigue life by means of experimental tests and FEM simulations. FEM models were used to calculate the stress patterns on Cr-Co alloy tibial tray based on ISO standards. B.R. Rawal et al. [189] approached the fatigue phenomena using FEM and estimated the life expectancy of knee prosthesis for various combinations of materials. The proper dimensions of a polycentric prosthetic knee were found by Belkys T. Amador et al. [147] from the structural perspective. Finite element method was used to perform stress analysis under three load conditions. A compressive load equivalent to 100 kg weight of a person and two other loads related with ISO10328 were applied. For the most critical load condition, safety factor of less than 1 was predicted in 5 out of the 9 components of prosthesis and suggested a redesign. In the redesign, diameter of the axes was increased and modifications done in the four links. Suwattanarwong Phanphet et al. [148] carried out the finite element simulations for the structural tests on the knee joint prosthesis with an objective to improve the existing design quality of the knee prosthesis and recommended the optimized knee prosthesis design meeting all the requirements. Structural tests on the knee prosthesis developed as per optimized design, confirmed the results predicted by finite element analysis.

2.7 Taguchi Technique of Design Optimization

Genichi Taguchi developed statistical methods to improve the quality of manufactured goods. It is applied to biotechnology, engineering, marketing and advertising [148-151]. All professional statisticians have welcomed the improvements made by the Taguchi methods, especially in development of designs for studying variation. To design systems that are reliable under uncontrollable conditions were the main objective [152-154]. This method adjusted the design parameters to the optimal levels by which the system response is robust; it is insensitive to noise factors, which otherwise are impossible to control. These techniques are majorly

used in engineering design [155]. To achieve the result for best product quality and a robust process this Taguchi method is used [156-158].

S. Kamaruddin et al. [159] also used this method for manufacturing products in the optimization of injection moulding parameters from the plastic blends. To determine the process conditions for producing synthetic lightweight aggregate, How-Ji Chen et al. [160] used this technique with an orthogonal array L16 (45). Design of monolimb was optimized by using Statistical-based method alongwith computational modeling [161]. So we can conclude that Taguchi method was used to find the importance of various design factors and recommended an optimized design of monolimb which is capable of resisting failure in the normal usage and provide the needed flexibility.

2.8 The Knowledge Gap in Previous Investigations

The literature review on knee joint prosthesis and polymer materials revealed a number of research gaps. Field study was undertaken by visiting a leading organisation in India, which is serving more than twenty thousand new amputees every year, to understand the type of above knee prosthesis being fitted to the amputees and the procedure adopted for the same. It is observed that the organisation is fitting above knee prosthesis with Single axis knee joint and four bar knee joint.

The single axis above-knee prosthesis is indigenously designed and fabricated from locally manufactured high-quality, high-density polyethylene (HDPE) pipes. Above knee prosthesis based on polycentric concept is designed using the four-bar linkage geometry. It is made from oil-impregnated nylon. This design mimics normal human gait by providing stability in stance and easy movement.

Four bar polycentric knee joint was studied in detail and interaction with the officials and feedback of the amputees revealed the following:

- Enlarging of the assembly holes due to wear
- Failure from the fitting portion
- Loosening of the screws

- Not suitable for uneven surfaces- knee buckles
- User not able to sit fully squatting
- Noise produced by the joint as amputee walked
- Poor aesthetics

Based on the literature review and the field study the following research gaps have been identified from this literature review:

1. The static and dynamic analysis studies of low cost four bar knee joint prosthesis used in developing countries are lacking in literature.
2. The studies on structural test analysis of the low cost knee joint prosthesis made of oil impregnated nylon as per ISO 10328 are scarcely available.
3. Studies revealed poor fatigue life and enlargement of assembly holes due to abrasion wear of the knee joint prosthesis made of oil impregnated nylon.
4. Less study was found on the nylon composites applications in prosthetics.
5. Research work to develop cheap nylon composite material having better tribological properties and enhanced mechanical properties have been considered as a challenge in the field of materials and any investigation in this regard would be beneficial for the application in knee joint and other engineering applications.
6. Literature based on addition of microparticulates of alumina and titanium dioxide to Nylon66 are less reported.
7. Studies on material selection based on mechanical and tribolological properties for knee joint application are lacking.
8. The research work involving development of new material, static and fatigue life analysis using FEM as per ISO 10328 and design optimization of knee prosthesis is not available.

2.9 Proposed objectives of the research work

The objectives of this research work are outlined as follows:

1. To develop new grades of materials to improve fatigue life and wear of knee joint prosthesis.
2. Static analysis of the low cost four bar knee joint prosthesis used in developing countries.
3. Design modifications for overcoming the failure problems and to reduce weight.

To achieve the above objectives, following activities were accomplished:

1. Mechanical characterization of Oilon (Nylon6 oil filled) material which is presently being used for knee joint prosthesis.
2. Development of composites of Nylon66 material by adding different weight percentage of titanium dioxide.
3. Development of composites of Nylon66 material by adding different weight percentage of aluminium dioxide.
4. Mechanical characterization of Nylon66 and newly developed composites of Nylon66 with titanium dioxide and aluminium dioxide.
5. Tribological study for wear rate & coefficient of friction of Oilon, Nylon66 and composites of Nylon66 with titanium dioxide and aluminium dioxide.
6. Optimal material selection by implementing Multiple Criteria Decision Analysis method using TOPSIS technique on the basis of the obtained experimental results.
7. Generation of experimental data for stress vs. number of cycles to failure for Oilon and Nylon 66 – 2 wt.% Al_2O_3 composite on fatigue testing machine.
8. Finite element analysis of existing design for static and cyclic loads as per ISO 10328:2006 using ANSYS software.
9. Design modifications to reduce the stresses, total deformation and weight reduction. Developing the optimized design using orthogonal array as per Taguchi design of experiment technique.
10. Fatigue life prediction of the optimized design as per ISO 10328:2006 standard.

This chapter has described:

- An exhaustive literature review of research works on knee joint prosthesis, its types, problems and material used etc.
- The literature review of various aspects of filler and particulate reinforced polymer composites of nylon material investigated by various researchers.
- The literature review of application of FEM and ISO 10328 to solve the problems of knee joint prosthesis.
- The knowledge gap in previous investigations.
- The objectives of the present thesis work.

The next chapter exhibits the materials for the fabrication of composites and methods used for the processing and testing of the composites, the mechanical and tribological characterization. Material selection procedure and the procedure for FEM as per ISO 10328, fatigue testing and design optimisation is briefed.

CHAPTER 3

MATERIALS AND METHODOLOGY

CHAPTER 3

MATERIALS AND METHODOLOGY

This chapter briefly illustrates the properties and specifications of the materials selected for investigation, methodology to develop composites for the research work and injection moulding of test specimens. Methodology adopted for the mechanical characterisation and tribological studies of developed composites are covered in detail. Material selection by multi criteria design analysis technique, TOPSIS is also discussed. Further, the chapter includes the methodology of finite element analysis and the requirements of ISO 10328: 2006 standard in detail.

3.1 Materials Selection, Properties and Specifications

The research work to explore the development of polymer composite material for better properties in terms of mechanical characterization and tribological properties is planned on the basis of research gaps presented and discussed in the Chapter 2. For the above purpose, following materials are chosen for development as listed in Table 3.1

Table 3.1: Materials used for preparing Nylon 66 based composites

Sr. No.	Type of ingredient	Name of element	Grade	Supplier
1.	Resin	Nylon66	Zytel 101L NC 010	M/s E.I. DuPont India Pvt. Ltd., Gurgaon
2.	Filler	Aluminum Oxide	Aluminum oxide active neutral Activity I-II (mesh size 40)	M/s Merck Specialties Pvt. Ltd., Mumbai, India.
3.	Filler	Titanium Dioxide	Titanium(IV) oxide (mesh size 45)	M/s Merck Specialties Pvt. Ltd., Mumbai, India.

3.1.1 Nylon66

Nylon66 is basically a polyamide made by polycondensation of hexamethylenediamine and adipic acid and contains each repeating unit consisting of 12 carbon atoms in each. Nylon 66 consists of a repeating unit with crystalline density of 1.24 g/cm^{3}and molecular weight of 226.32 g/mol. Nylon66 is a semi-crystalline polymeric material and is one of the most widely used material in engineering applications such as packaging and consumer applications, automobiles, textiles, electrical and electronics, because of their excellent properties such as strength, toughness, flexibility and abrasion resistance [162]. It has excellent corrosion resistance, good wear & abrasion resistance and favourable self lubricating property. Nylon66 is also known for its moldability, low coefficient of friction, low creep and resistance to solvents and oils. Nylon is used extensively in the field of prostheses applications such as nylon stockings, prosthetic sheaths, bushings and suction valves etc. [131].

Chemical composition and general specification of Nylon66 material are shown in Figure 3.1 and Table 3.2, respectively.

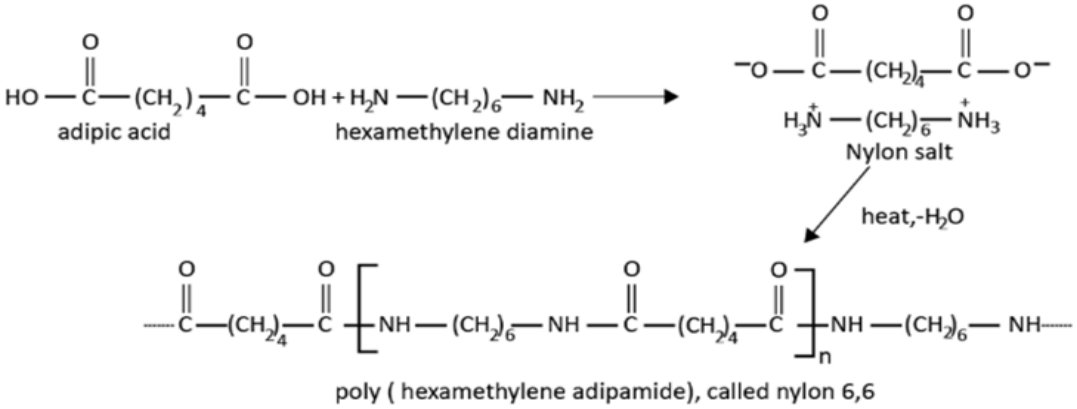

Figure 3.1: Chemical composition of Nylon 66

Table 3.2: General specifications of the Nylon 66

Properties	**Value**
Heat Deflection Temperature under load 0.45 MPa	200^{o}C
Impact Strength (Izod) notched at 23^{0}C	5.5 kJ/m^2
Tensile Strength	82 MPa
Tensile Modulus	3100 MPa
Density	1140 kg/m^3

3.1.2 Aluminium Oxide (Al_2O_3)

An aluminium oxide microparticle, also known as alumina microparticle or micro alumina, exhibits the properties of improving electrical conductivity, ductility and toughness, hardness and strength etc. compared to virgin material. The application of micro alumina is increasing day by day. In periodic table, Aluminium is placed at Period 3 of Block P, while oxygen is placed at Period 2 of the Block P. Alumina particles are spherical and appear as white powder.

Some of the properties of Al_2O_3 particles are given in the following Table 3.3

Table 3.3: Properties of Al_2O_3 particles

Properties	**Metric**
Colour	White
Specific Gravity	4 (Water =1)
Molar mass	101.96 g/mol
Melting point	2072°C

The major applications of alumina includes formation of electrical circuit base-boards, transparent ceramics, moderate pressure sodium lamps, cosmetic fillers, single crystal, sapphire, cutting tools, packaging materials, high-strength aluminium oxide ceramic, winding axle, crucible with high purity, furnace tubes, glass components, polishing materials, metal parts, semiconductor materials and grinding belts, wear-resistant polymer support, better water-proof materials, catalyst and catalyst-carrier, analytical reagents, special glass, fluorescent materials, vapour deposition materials, composite materials etc. In the liquid form, alumina particles are used for the applications like refractory parts, to improve ceramics density and softness, fracture-toughness, thermal fatigue-resistance, creep and wear resistance of plastic parts. [163-165]

3.1.3 Titanium Dioxide (TiO_2)

TiO_2 is generally available in the form of micro or nano crystals having a high surface area. Titanium belongs to Period-4 of Block-D, while oxygen belongs to Period-2 of Block-P, of the periodic table.

Some of the properties of TiO_2 particles are given in the following Table 3.4

Table 3.4: Properties of TiO_2 particles

Properties	**Metric**
Colour	White
Density	4.20 g/cc
Molar mass	79.87 g/mol
Melting point	1,855° C

TiO_2 shows good photo catalytic properties, so it can be used in antibacterial and antiseptic compositions for degrading organic-germs and contaminants. It can also be useful for forming Ultra violet resistant material, formation of self-cleaning ceramics, glass, printing ink, coating, etc. It is also used for improving the opacity of paper in the paper industry. [166-168]

3.2 Procedure for Preparation of Composites based on Nylon66

In the present work, the preparation of composites based on Nylon66 with aluminum oxide and Nylon66 with titanium dioxide was done by mixing of weighted percentage of the filler micro particulate to the granules of Nylon 66 polymer and subsequently compounding the mixture using twin screw extruder of 40 L/D and screw rpm 40 (M/s Lab Tech Engineers Company Ltd., Thailand, Model: TARCT).

Figure 3.2: Twin screw extruder

Feeding zone to metering zone temperature profile was kept at 237°C, 254°C, 256°C & 259°C. Also, the barrel was maintained at temperature profiles of 255°C, 263°C, 266°C, 268°C, 270°C, 272°C and 274°C from hooper to the die.

Eight types of polymer composite granules of cylindrical shape having average size of diameter 1.5mm were prepared by adding 2%, 4%, 6% and 8% weight micro particulate of Al_2O_3 and TiO_2 respectively to the Nylon 66 material.

Figure 3.3: Polymer composite granules of Nylon66 and Al_2O_3

Figure 3.4 Polymer composite granules of Nylon66 and TiO_2

3.3 Preparation of test specimens by injection moulding technique

For doing the mechanical characterisation of the developed composites as per relevant ASTM standards, test specimens need to be prepared. In this case the test specimens were prepared by injection moulding technique by the following procedure:

1. The developed composite granules were fed into hopper of injection moulding of 80 ton capacity from M/S JIT, Philippines.
2. Test specimen moulds were used for preparing the specimens for testing various properties like Izod impact, tensile strength, HDT, compression and flexural strength respectively.
3. The specimens were moulded with the processing temperatures set at 220°C, 268°C and 269°C.
4. Injection moulding machine is shown in Figure 3.5 and test specimen moulds in Figure 3.6. The process parameters are exhibited in Table 3.5.
5. The silicon-spray is used as a releasing agent, to assist easy removal of the specimens from the mould.

Figure 3.5 Injection Moulding Machine

Table 3.5: Process parameters for Injection Moulding

Parameters	**Values**
Melt Temperature	$270^{o}C \pm 15^{o}C$
Mould Temperature	$80^{o}C \pm 10^{o}C$
Injection Pressure	90 ± 10 Bar
Packing Pressure	80 Bar
Shot size	40 mm

(a) Mould for tensile test specimen (b) Mould for flexural test specimen

Figure 3.6: Mould for preparing specimens

Figure 3.7: Test specimens prepared by Injection Moulding

3.3.1 Test Specimens

The test specimens for tensile properties were molded as per ASTM D-638, for flexural properties as per ASTM D 790, for compressive strength as per ASTM D 695, for heat deflection temperature as per ASTM D 648 and for Izod impact as per ASTM D 256. The shape and size of the specimens are as follows:

- Tensile – Dumbbell Shape – $165 \times 12.67 \times 3.2$ mm^3
- Flexural – Strip Shape – $127 \times 12.7 \times 3.2$ mm^3
- Compressive Strength – Rectangular Shape – $25 \times 12.7 \times 12.7$ mm^3
- Heat Deflection Temperature - Strip Shape – $127 \times 12.7 \times 3.2$ mm^3
- Izod Impact – Strip Shape – $63.5 \times 12.7 \times 3.2$ mm^3

3.4 Mechanical Characterisation

Mechanical properties of the plastic materials are investigated in accordance to ASTM standards and procedure which are described below:

3.4.1 Density

By using the density apparatus from Mettler Toledo, Switzerland, the density of the samples was found by following the standard test method ASTM D 792.

Figure 3.8: Density Test Apparatus

3.4.2 Tensile Strength and Modulus

The mechanical properties such as tensile strength, elongation at break and modulus were determined by using the universal testing machine (AG-IS, Shimadzu, Japan) as per standard test method of ASTM D 638. The test was carried out at the speed of 50 mm/minute. The average values of three specimens of each composition were reported.

Figure 3.9: Universal Testing Machine (UTM)

3.4.3 Izod Impact Strength

"Izod Impact Strength can be defined as the kinetic energy required, beginning the fracture and continuing the fracture until the specimen is broken". To prevent the deformation of test specimen during the impact test, the specimens for Izod are prepared with notch. The size of specimen is 63.5×10×3 mm^3 and notch angle of 45±1°. The test specimen is mounted in a fixture with the notched side facing the striking edge of the swinging pendulum. The pendulum is released with the help of lever and allowed to strike through the specimen. The impact strength is measured by using Tinius Olsen Impact tester (model Impact -104) according to ASTM D256.

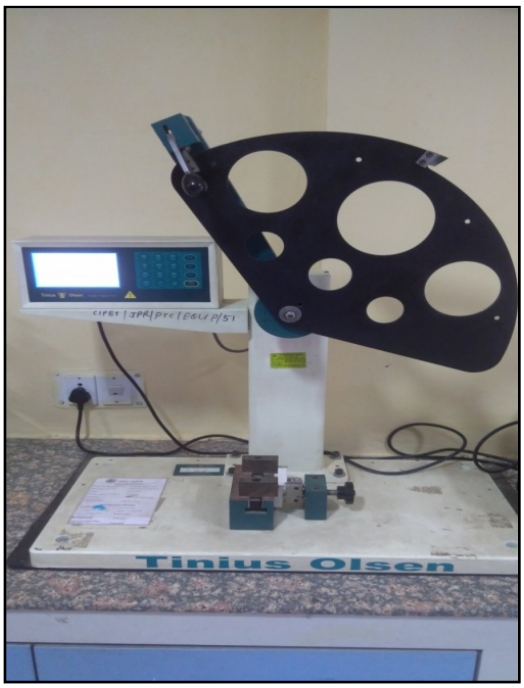

Figure 3.10: Pendulum Impact Tester

3.4.4 Flexural Strength and Modulus

"Flexural strength is a material property, which can be defined as stress in a material just before it yields in a flexure test. Using a three-point flexural test method, the transverse bending test is most frequently employed, in which a specimen having rectangular cross-section is bent until yielding. The flexural strength corresponds to the highest stress experienced within the material at its moment of failure".

In this study, three-point flexural test of specimen of size 127×12.7×3.2 $mm^3$are performed with the help of Universal Testing Machine (Shimadzu, Japan) according to ASTM D790.

3.4.5 Compressive Strength

"Compressive strength of a material is the force per unit area it can withstand during compression. The stress at which the permanent deformation occurs corresponds to compressive yield strength whereas ultimate compressive strength is the stress required to rupture a specimen. For most of the polymer materials that do not rupture, the compressive strength can be reported at a specific deformation such as 1%, 5% or 10% of the test sample's original height". In this study, compressive

strength of specimens with sizes 12.5×12.5×25.5 mm^3 were prepared according to the ASTM D 695 standard. The tests for compressive strength were performed on Universal Testing Machine (UTM) of Shimadzu make.

3.4.6 Heat Deflection Temperature (HDT)

Heat deflection temperature was measured by using heat deflection temperature test apparatus (Gotech, Taiwan, model no. HV-2000A). "In this test, a rectangular bar is tested in the edgewise position as a simple beam with the load applied at its centre to give maximum fiber stresses of 1.82 MPa. The specimen is immersed under the load in a heat transfer medium provided with a means of raising the temperature at 2 ± 0.2 ^{0}C/min. The temperature of the medium is measured when the test bar has deflected 0.25 mm".

Figure 3.11: Heat Deflection Temperature Test Apparatus

3.4.7 Rockwell Hardness

"A Rockwell hardness number is a number derived from the net increase in depth impression as the load on an indenter is increased from a fixed minor load to a major load and then returned to a minor load". Rockwell hardness number is directly relates to the hardness of a plastic material caused due to indentation, higher the reading, harder the material. The Rockwell hardness test was performed using

hardness tester (Arun Industries, model no. AI-RAS) in accordance to the ASTM D 785 standard.

Figure 3.12: Rockwell Hardness Tester

Hardness of three specimens of each composition is taken. The mean-value of five indentations on each specimen is determined.

3.5 Study of Tribological Properties

The Pin on Disc Friction & Wear Test Rig is mainly used for determining the tribological characteristics of wide range of polymeric materials under various conditions of normal loads & temperatures, dry or lubricated conditions under different environmental conditions. In a pin-on-disc wear tester, a pin is loaded against a flat rotating disc specimen such that a circular wear path is generated by the machine. The machine can be used to evaluate wear and friction properties of materials under pure sliding conditions.

The pin-on-disc type wear and friction monitoring test rig of M/s Magnum make conforming to ASTM G 99 standard was used for conducting the sliding wear test. The disc was made of EN31 hardened steel having a track radius of 50 mm and variable speed of 480, 670, 860, 1050 and 1240 rpm. The test specimen of size

12.7x12.7x 25.4 mm^3 was held stationary in the fixture and the disc is rotated while a normal load is applied through a lever mechanism. The sliding wear tests were performed at temperature of 24^0C under different normal loading of 50N, 60N, 70N, 80N, 90N and 100N keeping the sliding velocity of 6.5m/sec and sliding distance of 2000 m. Also, the tests were conducted at variable sliding velocities of 2.5, 3.5, 4.5, 5.5 and 6.5 m/s at constant normal load of 100 N and sliding distance of 2000 m. In another combination the tests were performed for different sliding distances of 500, 1000, 1500 and 2000 m at sliding velocity of 6.5 m/s and normal load of 100N.

Figure 3.13: Pin-on-disc type wear and friction monitoring test rig

The material volume loss from the test specimen during the wear test is measured using precision electronic weighing balance having an accuracy of 0.001 gm. Also, the coefficient of friction is calculated from the experimental results.

3.6 Scanning Electron Microscopy

SEM is employed to characterize the composite morphology and reinforcement dispersion and analyze the failure mechanism in the fractured surface of polymer composites. Scanning Electron Microscope (SEM) has focused beams of electrons to gain information and is most widely used for morphological study of materials. The high-resolution, 3-D images formed by SEM, give invaluable insight to morphological and topographical compositional information and are used

extensively in research applications. The worn out surfaces of the composite specimens after the sliding wear test were subjected to Scanning Electron Microscopy [SEM] examination to understand the wear mechanism and SEM 450 model, Zeiss make (Figure 3.14) was used for SEM images of samples.

Figure 3.14: Scanning Electron Microscope

3.7 Material Selection by Multi Criteria Design Analysis

There are many techniques available to select the optimal material, when more than one choice of material is available or multiple objectives to be fulfilled. In our case we have chosen "TOPSIS (Technique for Order Preference by Similarity to Ideal Solution)" technique which is based on "Multi Criteria Design Analysis (MCDA)" and has wide applicability and is used for solving the ranking problems due to its simple and easy approach. Following steps are undertaken to arrive at the solution:

I. The criteria defining the performance and alternatives of the problem are identified and a decision matrix is created. The decision matrix having an order of M × N is prepared; where the number of alternative is M and the number of performance defining criterion are N.

II. In order to make all the values of the decision matrix comparable, the decision matrix is normalized. The normalized matrix R= [ ], and the normalized value calculated as

$$r_{ij} = \frac{a_{ij}}{\left[\sum_{i=1}^{M}\left(a_{ij}^{2}\right)\right]^{1/2}} \quad \text{…….. (3.1)}$$

III. On the basis of weighted normalized ratings, the positive ideal solution (PIS) and the negative ideal solution (NIS) are determined as given below:

$A^{+}=(r_1^{+}, r_2^{+}, \ldots\ldots r_N^{+})$ and $A^{-}=(r_1^{-}, r_2^{-}, \ldots\ldots r_N^{-})$ …….. (3.2)

where,

$r_j^{+}=\{(\max_i r_{ij}),$ if j is a benefit criteria/ $(\min_i r_{ij}),$ if j is a cost criteria$\}$ and

$r_j^{-}=\{(\min_i r_{ij}),$ if j is a benefit criteria/ $(\max_i r_{ij}),$ if j is a cost criteria$\}$

for j= 1,2,3,….N

IV. The geometric distances between each of the choices and the positive ideal solution and the negative ideal solution are calculated as shown:

$$D_i^{+}=\sqrt{\sum_{j}^{N}(r_i^{+}-r_{ij})^2} \quad \text{and} \quad D_i^{-}=\sqrt{\sum_{j}^{N}(r_{ij}-r_i^{-})2} \quad \text{…….. (3.3)}$$

for i = 1, 2, ….M

V. Finally, the overall preference or closeness index (CI) of the alternatives is calculated. All the alternatives are then rated according to the value of their closeness index. The closeness index (CI) of the alternatives is calculated as:

"Closeness Index = $D_i^{-}/(D_i^{+}+D_i^{-})$" for i = 1,2,….M …….. (3.4)

The experimental values of various mechanical and tribological properties are used for the construction of the decision matrix which is used for finding the optimal selection of the material using TOPSIS analysis.

3.8 Fatigue Testing

A method for determining the behavior of materials under fluctuating loads is known as fatigue testing. An alternating load with a specified mean load are applied to the test specimen and the number of loading cycles required to produce the fatigue failure (fatigue life) is recorded. A fatigue test helps to determine the material's ability to withstand cyclic loading conditions. In design, a material is

selected to meet or exceed service loads that are anticipated in fatigue testing applications. The fatigue testing as per ASTM D7791 is performed for Oilon and the composite material selected by the Multi Criteria Design Analysis (MCDA) procedure as described in 3.7. The sinusoidal loading as shown in Figure 3.15 is used for doing the fatigue testing on INSTRON make, Model 8874, 25 kN fatigue tester. The experimental results obtained are used to generate S-N curves.

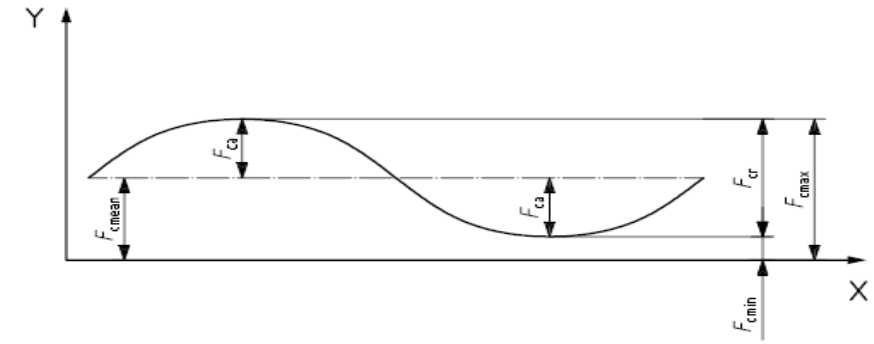

Key

X	time	F_{cr}	cyclic range of test force
Y	test force	F_{ca}	cyclic amplitude of test force
F_{cmax}	maximum test force	F_{cmean}	mean test force
F_{cmin}	minimum test force		

Figure 3.15 Load cycle for fatigue testing

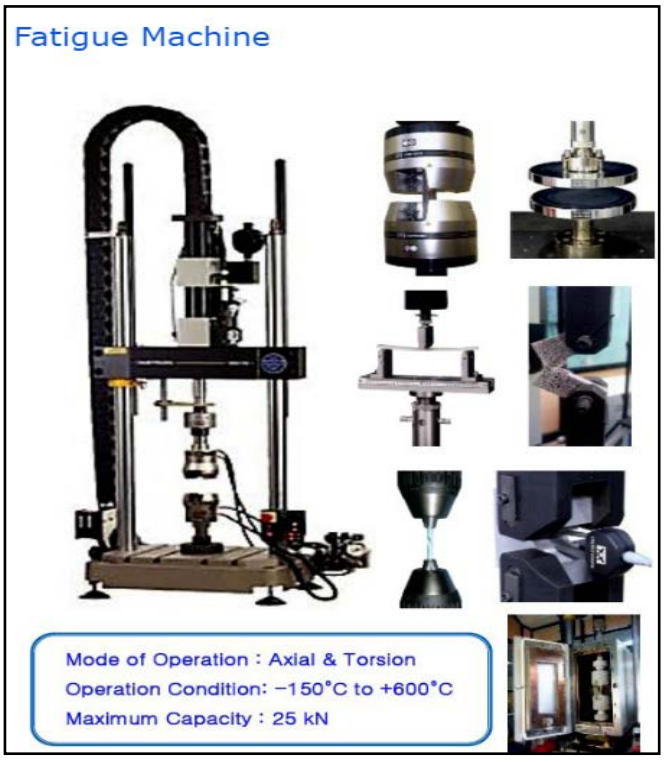

Figure 3.16: Fatigue testing machine

3.9 ISO 10328:2006

Prosthetic knee is one of the most important components of the above knee prosthesis which assists the amputee to regain mobility and improve the quality of life of an above-knee amputee. The safety is one of the most important design considerations in addition to the stability, comfort, appearance, and ease of use of the prosthesis[19].“The International Organization for Standardization (ISO) has developed a standard called ISO 10328:2006 Prosthetics - Structural Testing of Lower-Limb Prostheses - Requirements and Test Methods to outline a procedure to physically conduct the static and cyclic strength tests of the prosthetic devices to ensure the safety of the prosthesis”[145].

The test protocol of ISO 10328:2006 is invariably followed in this research work and is used to conduct static and fatigue stress analysis of the low cost knee joint of above knee prosthesis, used in developing country, by finite element method.

3.9.1 ISO 10328 Coordinate System

“ISO 10328 specifies that each test configuration shall be defined by a three dimensional, rectangular coordinate system which shows the directions of the axes for testing prostheses and has been included below as Figure 3.17. The coordinate system is defined in relation to prosthesis when the device is standing on the ground in an upright position. From the origin, o corresponds to the positive x axis, while u is the positive y-axis, and f is the positive z-axis. The o-u-f coordinate system will be used throughout this study regarding the orientation of force loads, force locations, and points for investigation on the above knee prosthesis”.

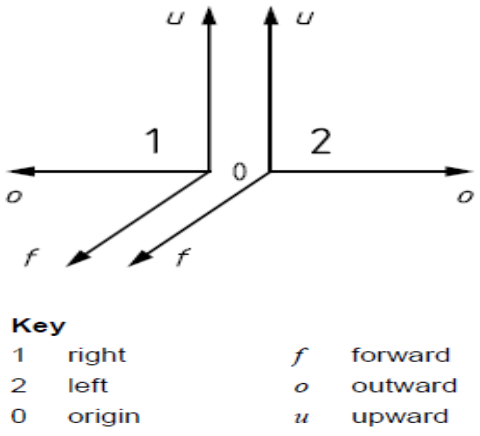

Figure 3.17: ISO 10328 coordinate system

3.9.2 Reference Planes- ISO 10328 Coordinate System

"The reference planes that are used in the modelling lie parallel to each other and perpendicular to the u –axis. Various reference planes are described as follows:

1. Top reference plane: The top reference plane, T, is located at a distance $u = u_T$ from the origin. It contains the top load application point P_T.
1. Knee reference plane: The knee reference plane, K, is located at a distance $u = u_K$ from the origin. It contains the knee load reference point P_K and the effective knee-joint centre.
2. Ankle reference plane: The ankle reference plane, A, is located at a distance $u = u_A$ from the origin. It contains the ankle load reference point P_A and the effective ankle-joint centre.
3. Bottom reference plane: The bottom reference plane, B, is located at a distance $u = u_B$ from the origin. It contains the bottom load application point P_B."

The reference planes as described in ISO 10328 are shown in Figure 3.18. The analysis test set-up is prepared by developing CAD model by using these reference planes.

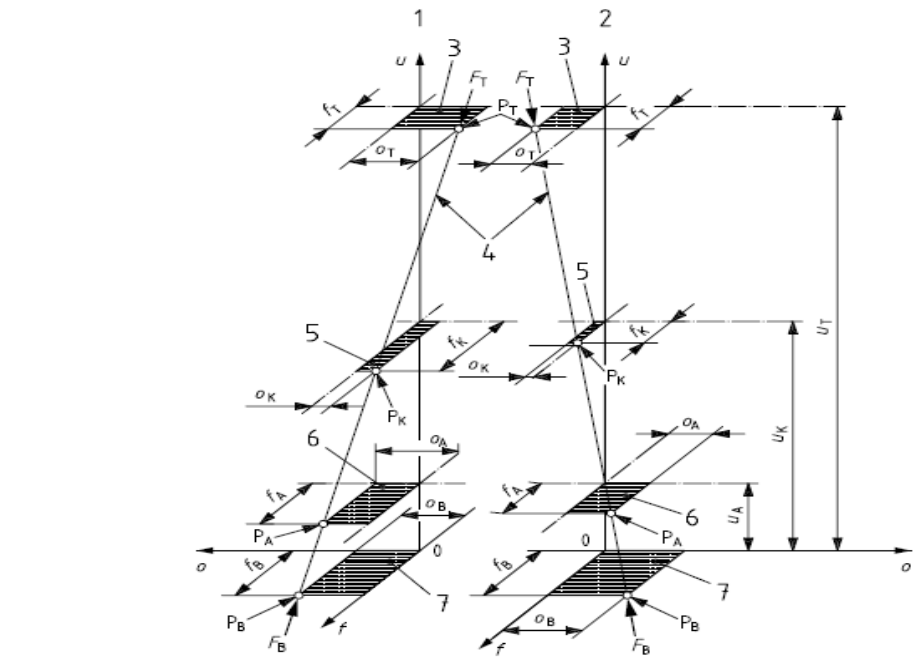

Key

1	right leg	5	knee reference plane, K	P_T	top load application point
2	left leg	6	ankle reference plane, A	P_K	knee load reference point
3	top reference plane, T	7	bottom reference plane, B	P_A	ankle load reference point
4	load line			P_B	bottom load application point

Figure 3.18: Reference planes- ISO 10328 coordinate system

3.9.3 Test Loading Condition

"According to the ISO 10328 standard, a single test force is applied through a specific line of load application which produces axial compression, shear forces, bending moments and/or torque as single components of loading or compound loadings. However, depending upon test conditions and load levels, the magnitude and direction of the test force are varied". Two different test loading conditions, condition I- Heel loading and condition II- Forefoot loading are defined for various test loading levels P3, P4 and P5 suitable for weight of person 60 kg, 80 kg & 100 kg respectively. The value of offset at various reference planes is taken from the ISO standard. The application of a specific test configuration for loading condition II forefoot loading for a left sided sample is shown in Figure 3.19

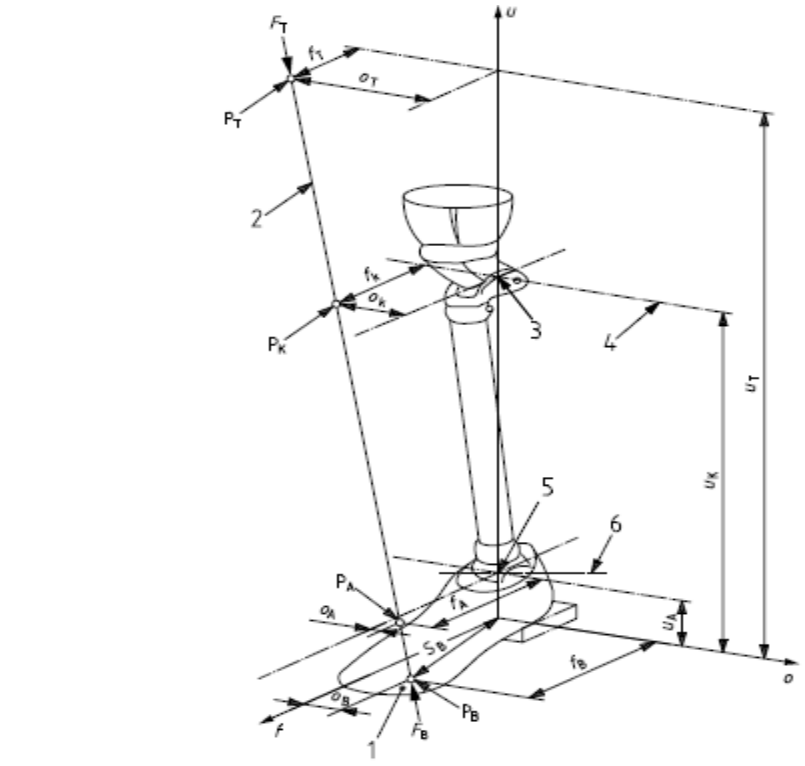

Key

1 left foot
2 load line
3 effective knee-joint centre
4 effective knee-joint centreline
5 effective ankle-joint centre
6 effective ankle-joint centreline
P_K knee load reference point
P_A ankle load reference point
P_B bottom load application point
P_T top load application point

Figure 3.19: Test loading condition for forefoot loading to a left-sided sample

3.9.4 Test Set-up

For the purpose of applying the load as per the load offset values prescribed in the ISO 10328 standard, the CAD model of the knee joint prosthesis is developed by adding load application levers and the total length of the assembly for test set-up is maintained to 650 mm by adding end attachments, and non-prosthetic extension pieces. The load application lever and end attachments material is chosen as that of stainless steel whose mechanical properties are readily available from the literature. Also, the strength of steel is much higher than the polymeric composites under study.

3.10 Finite Element Method

Finite Element Method is a most popular numerical analysis technique for obtaining approximate solutions to a wide variety of engineering problems. This method is based on dividing a complex shape into the finite elements, applying the loading conditions at each node, solving the equilibrium equations for each element, and then applying the element's results to obtain the global solution to the original problem. The success of the method will depend on various factors such as mesh shape, mesh size and the analysis types. Many types of software are available in the market for FEM/FEA and ANSYS 16.0 is used for this research work.

The following step by step process is used for doing the finite element analysis and the procedure consists of three essential stages:

1. Pre-processing: This involves the preparation of the model data. The pre-processor is a program, in which the geometric model of a component is developed by the engineers. This model is used for meshing of the model and finite elements may be generated. Required inputs to the pre-processor include;
    a. Geometric parameters: eg. Type of elements, nodal coordinates, variation of mesh density, etc.
    b. Loading characteristics: eg. Magnitudes, positions and directions of point loads, pressures; thermal loads, centrifugal loads, frequency and dependent forces, etc.
    c. Boundary conditions: eg. Positions and directions of nodal fixities, rotational axes and frictional resistances, etc.

d. Material properties: eg. Young's Modulus, Poisson ratio, density, coefficient of friction, coefficient of expansion, etc. as per the type of analysis.

2. Analyzing the model: After the preparation of the model data, the analysis is executed to get the result.

3. Post-processing: With the post-processor program, the results of the model are analysed. The output of the analyzed results from the post-processor may be either in the form of data or graphical display.

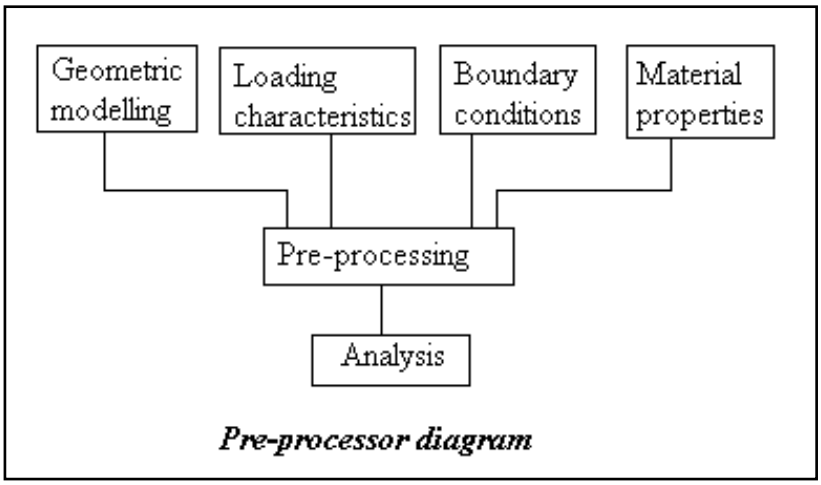

Figure 3.20: Pre- processing step of FEA

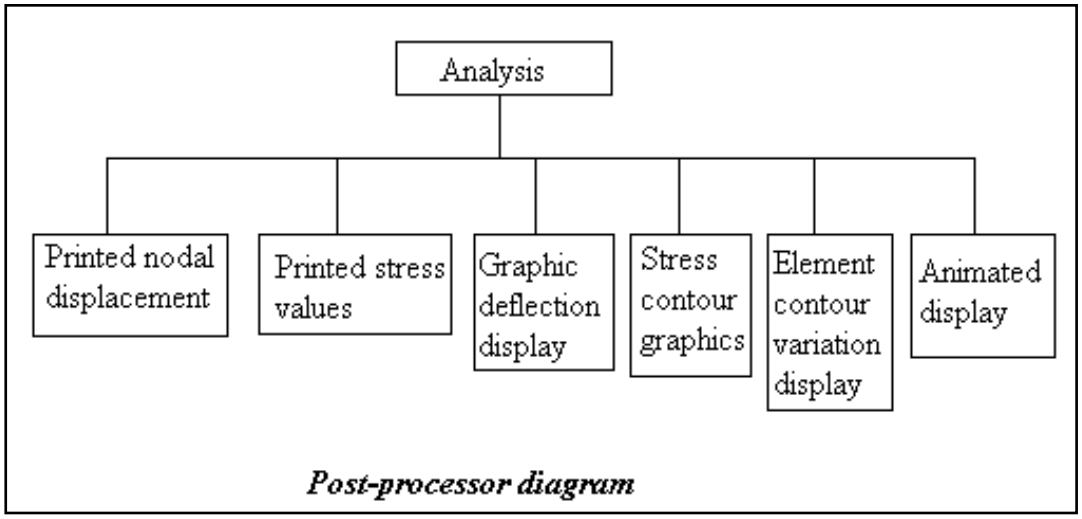

Figure 3.21: Post- processing step of FEA

3.10.1 Geometric Modelling

Creo3.0 CAD modeling software was used to develop three dimensional solid models of the individual components and assembly of knee joint of above knee prosthesis. Creo3.0 is a Parametric, reliable, easy to use, 3d modeling tool that accelerate the product design process as like other CAD software. It utilizes a constant feature-based approach and is a Para solid-based solid creator, to form models and assemblies. Creo3.0 creates products more efficiently & cost effectively, without sacrificing innovation or quality and offers the most scalable range of 3D CAD product development packages & tools. Its variety of specific features, capabilities, & tools help to imagine, design, & create better above knee prosthesis by modifying the design from the parametric data of existing knee joint.

3.10.2 Factors for Finite Element Analysis

The finite element analysis of above knee prosthesis is done by deciding the input for the following factors:

1. Type of analysis.
2. The material type.
3. Mesh size and type of meshing
4. The element shape and type.
5. The number of nodes.
6. The degrees of freedom at each node.
7. The external loads.
8. The boundary conditions.
9. Interpretation of the results.

3.10.2.1 Type of Analysis

Structural analysis is probably the most common application of the finite element method. Various types of structural analyses are possible with the ANSYS software such as static, modal, harmonic and fatigue etc. Prosthesis is subjected to a series of load actions while performing varying daily activities like standing, walking, running, stair climbing, squatting, kneeling etc. In our study we have followed the protocol of ISO 10328:2006 standard and it specifies static and cyclic strength tests. The static tests relate to the worst loads generated in any activity

while the cyclic tests relate to normal walking activities where loads occur regularly with each step. The following type of analysis is performed to ascertain the safety of the above knee prosthesis:

1. Analysis for proof strength under static load representing an occasional severe event, which can be sustained by the prosthetic device/structure and still allow it to function as intended.
2. Analysis for ultimate strength under static load representing a gross single event, which can be sustained by the prosthetic device/structure but which could render it thereafter unusable.
3. Analysis for fatigue strength under cyclic load which can be sustained by the prosthetic device/structure for a given number of cycles.

3.10.2.2 Material Properties

The mechanical properties of the material of the intended product for analysis are assigned to the CAD model. The value of properties is either chosen or assigned from the Materials Library available in the Toolbox or it can be added to the library. Essential properties like density, yield strength, Poison's ratio etc. are added to the library for the materials under study.

3.10.2.3 Loading for FEA

As the above knee prosthesis is widely utilized by people of developing countries, making it appropriate to test for the highest realistic loading condition, the loading values associated with the level P5 have been applied to the models to be analysed. The test loading level P5 corresponds to the amputees of body mass 100 kg. According to ISO 10328 7.2.3 Note 1, field experience has shown that there is a need for lower limb prostheses which can sustain the loads more than the loading level P5 for the structural testing of such prostheses, test loading level P6 suitable for 120 kg amputee weight has been developed. As per ISO 10328 standard loading level P3 and P4 corresponds to the amputees of body weight 60 kg and 80 kg respectively.

3.10.2.4 Mesh Generation

Meshing is defined as the process of dividing the whole component into number of elements so that whenever the load is applied on the component it distributes the load uniformly called as meshing. Meshing is nothing but discretization of continuous body into finite number of elements which refers to the generation of nodal coordinates and elements. Meshing reduces the degree of freedom from infinite to finite.

The selection of mesh depends on:

1. Geometry shape and size
2. Type of analysis
3. Computational time

The geometry can be categorized as 1D, 2D, or 3D based on the dominant dimensions and then the type of mesh element is selected accordingly.

1D Element - Line

Used for geometries having one of the dimensions that is very large in comparison to the other two.

2D Element - Quad, Tria

Used when two of the dimensions are very large in comparison to third one.

3D Element - Tetra, Hex, Prism, Pyramid

Used when all three dimensions are comparable. These four elements can be used, in various combinations, to mesh any 3D solid model.

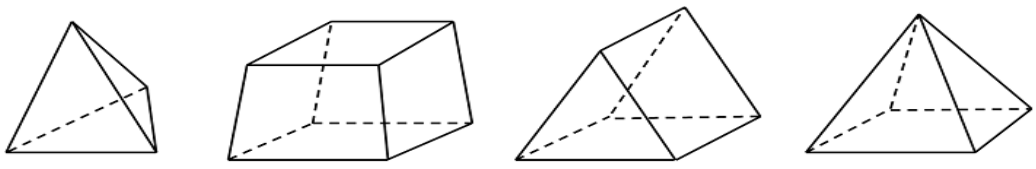

Tetra Hex Prism Pyramid

Figure 3.22: 3D mesh element

Mesh convergence test is carried out to decide upon the mesh size. As the mesh size is reduced, the number of element increases which in turn increases the computational time. The stress level is calculated for different mesh sizes and the mesh size is chosen when there are no further significant changes in the value of stresses.

Mesh generation is of two types in CAD/CAM software.

1. Manual meshing: In manual mesh generation the analyst discretizes the simplified geometry of the object to be studied that is the geometric model of the object, into nodes and elements. Nodes are defined by specifying their coordinates, while element connectivity defines the elements. Manual meshing is inefficient; error prone, meshing data can grow rapidly and become confusing for complex objects especially for three-dimensional ones.
2. Automatic meshing: It refers to the automatic creation and numbering of nodes and elements based on a minimal amount of user supplied data. Automatic mesh generation reduces errors, and saves a great deal of user time, therefore reducing the FEA cost.

3.10.2.5 Boundary Conditions and Type of Interface

All models require boundary conditions for doing the finite element analysis. Proper boundary conditions can save modelling and solution time and result in more accurate analyses. The boundary conditions to be applied depend on the type of analysis to be performed. Boundary conditions are often called "loads" or "supports". They constrain or act upon the model by exerting forces or rotations or by fixing the model in such a way that it cannot deform. The data on loading can be input by using one of the following options.

- Constant – Supported.
- Tabular (Time Varying) – Supported.
- Tabular (Spatially Varying) - Not Supported for Explicit Dynamics.
- Function (Time Varying) - Not Supported for Explicit Dynamics.
- Function (Spatially Varying) - Not Supported for Explicit Dynamics.
- Free – Supported.

It is necessary to define the type of interface between various components of an assembly. The type of interface will depend on the analysis to be performed and shall be chosen from the following options:
Bonded, No separation, Frictionless, Rough and Frictional.

3.10.2.6 Interpretation of Results

The type of result is selected from the solution palette for the CAD model under study. The nodal solution and von Mises stress was selected; total deformation with stress magnitude was generated and recorded. Equivalent stress (also called von Mises stress) is generally used in design work because it allows any arbitrary three-dimensional stress state to be represented as a single positive stress value. Equivalent stress is part of the maximum equivalent stress failure theory used to predict yielding in a ductile material. The von Mises stress is calculated and compared with the yield stress of the material.

3.11 Design Improvement of the Knee Joint Prosthesis

The finite element analysis results of the existing design are analyzed and design improvements carried out by modifying the geometry of the individual components with an objective to reduce the stresses, total deformation, weight reduction and overcome failure. Improvements in the design of knee joint prosthesis have been carried out by Taguchi method for design optimization and L9 orthogonal array is used to develop new designs. The new designs of the knee joint prosthesis were studied by the finite element analysis and the optimized knee prosthesis design meeting all the requirements was recommended. The optimized design of the knee prosthesis is also subjected to the fatigue analysis by ANSYS to verify the performance compliance for cyclic strength testing as per ISO 10328.

3.11.1 Taguchi Method for Optimization

Optimization technique based on robust parameter design was developed by Dr. Genichi Taguchi. This is an engineering method for process or product design that focuses on minimizing variation and/or sensitivity to noise. Taguchi technique provides an efficient and powerful method for designing the products that operate consistently and optimally over a variety of conditions. In robust parameter design,

the main objective is to find the factor settings which minimize response variation, while adjusting or keeping the process on target. Engineering knowledge is used to guide the selection of factors and responses. A product designed with this goal will deliver more consistent performance regardless of the environment in which it is used. In Taguchi method, the orthogonal arrays are used to reduce the number of experimentations and thus the cost involved. Taguchi designs are balanced, and no factor is weighted more or less in an experiment and allows factors to be analyzed independently of each other.

The parameters for design improvement of knee joint prosthesis shall be identified based on the FEA results. Depending on the number of parameters and their levels, suitable orthogonal array is selected and the optimized design meeting the performance requirements of ISO 10328 is selected.

CHAPTER 4

MECHANICAL CHARACTERISATION AND TRIBOLOGY STUDY OF POLYMER MATERIAL AND COMPOSITES

CHAPTER 4

MECHANICAL CHARACTERISATION AND TRIBOLOGY STUDY OF POLYMER MATERIAL AND COMPOSITES

The experimental work is done as per the methods and procedures described in Chapter 3 and the results of mechanical and tribological properties of oil impregnated nylon material (Oilon), Nylon66 and composites of Nylon66 material are enumerated. The interpretation of results and comparison for various compositions is elaborated in detail. The SEM results of worn out surface of the specimens is also depicted. The optimal material selection by TOPSIS technique is also covered in detail.

4.1 Mechanical Characterisation

4.1.1 Mechanical Properties of Oil impregnated Nylon material (Oilon)

In order to understand the suitability of Oilon material, the mechanical properties of this material are investigated as per ASTM standards and procedure and the results obtained are as under:

Table 4.1: Mechanical properties of Oilon material

S. No.	Name of Test	Units	Test Methods	Value
01.	Density	gm/cc	ASTM D 792	1.14
02.	Tensile Strength	MPa	ASTM D 638	63
03.	Elongation	%	ASTM D 638	35
04.	Tensile Modulus	MPa	ASTM D 638	1143
05.	Izod Impact (Notched)	kJ/m^2	ASTM D256	5.9
06.	Flexural Strength	MPa	ASTM D 790	82
07.	Flexural Modulus	MPa	ASTM D 790	2600
08.	Compressive strength	N/mm^2	ASTM D 695	90
09.	Heat Deflection Temperature	^0C	ASTM D 648	57
10.	Rockwell Hardness	HRc	ASTM D 785	86

4.1.2 Mechanical Properties of Nylon 66 and Nylon 66-Alumina composites

The experimental results obtained for the mechanical properties of the Al_2O_3 - Nylon 66 composite material determined as per ASTM standard are given in the Table 4.2.

Table 4.2: Mechanical properties of Al_2O_3 filled Nylon66 composite material

S. No	Name of Test	Units	Test Methods	Nylon 66 with Al_2O_3				
				0%	2%	4%	6%	8%
01.	Density	gm/cc	ASTM D 792	1.14	1.15	1.16	1.17	1.18
03.	Tensile Strength	MPa	ASTM D 638	75.0	76.0	77.0	79.0	73.0
04.	Elongation	%	ASTM D 638	23	7.91	7.38	7.04	6.7
05.	Tensile Modulus	MPa	ASTM D 638	1200	1388	1408	1439	1313
06.	Izod Impact (Notched)	KJ/m^2	ASTM D256	5.10	5.24	5.96	6.02	5.88
07.	Flexural Strength	MPa	ASTM D 790	111	116	118	119	115
08.	Flexural Modulus	MPa	ASTM D 790	3000	3296	3311	3518	3423
09.	Compressive strength	N/mm^2	ASTM D 695	76	84	86	88	86
10.	Heat Deflection Temperature	^0C	ASTM D 648	66.2	66.8	68.0	69.4	71.9
11.	Rockwell Hardness	HRc	ASTM D 785	97	100	102	104	105

The variation in mechanical properties such as tensile strength, tensile modulus, flexural strength and modulus, impact strength, compressive strength, heat deflection temperature (HDT) and Rockwell hardness of different weight % Al_2O_3 filled Nylon66 composites is described below:

4.1.2.1 Tensile Strength of Al_2O_3 filled Nylon 66 composites

From the Figure 4.1, it can be noted that the tensile strength increases but only marginally with the increase in filler content upto 6 wt.% and therafter it reduces drastically. At 8 wt.% Al_2O_3, the tensile strength becomes less than that of pure Nylon 66. The improvement in tensile strength can be attributed to the high strength, homogenous distribution and good interfacial adhesion of the filler in the composite. The reduction in strength may be due to the conglomeration of filler

particles at higher loading resulting in stress concentration leading to failure. The tensile strength of all the four composites is more than that of Oilon material (63MPa). Kali Dass et al. [169] also reported the increase in tensile strength of Al_2O_3 –Epoxy composite from 5 to 10 wt.% and decrease at a filler content of 15 wt.%. whereas another study [170] reported the increase in tensile strength of nano composite of Al_2O_3 –monomer casting nylon upto 3wt.% but decrease in tensile strength with increase in particle size from nano to micro. Zhanhu Guo et al. [171] also observed the increase in tensile strength by 60% for 3 wt.% nano alumina vinyl ester composite. Thus the increase in tensile strength is in line with the findings of most of other researchers.

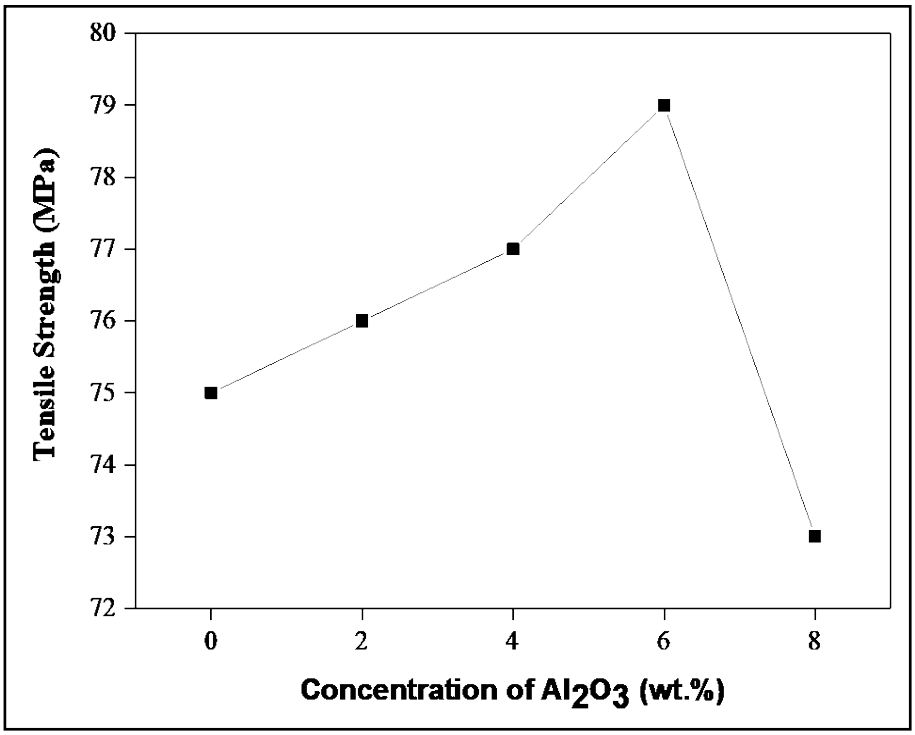

Figure 4.1: Tensile strength of Al_2O_3 - Nylon66 composites

4.1.2.2 Tensile Modulus of Al_2O_3 filled Nylon66 composites

The addition of any mineral filler to the polymer results in reduction in elongation and the increase in tensile strength, thus resulting in increase in tensile modulus. In this case from Figure 4.2 it can be noted that the value of tensile modulus first increases exponentially by 17% on addition of 2 wt.% micro alumina particles to Nylon 66, then it gradually increases upto 6 wt.% and thereafter it reduces at higher filler loading as reduction in tensile strength is noted.

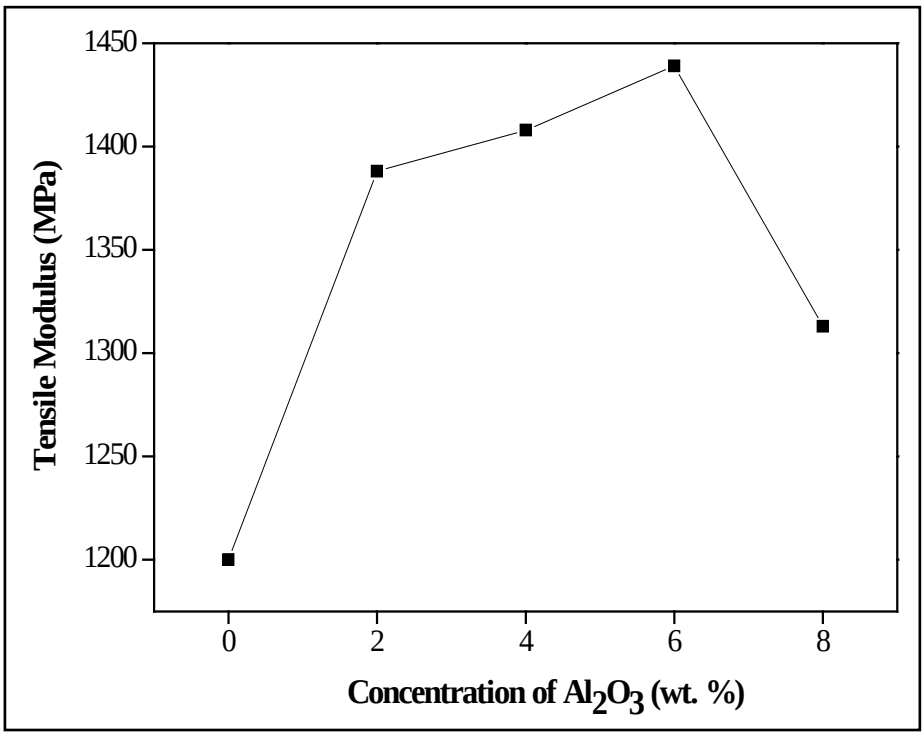

Figure 4.2: Tensile modulus of Al_2O_3 - Nylon66 composites

4.1.2.3 Flexural Strength and Modulus of Al_2O_3 filled Nylon66 composites

The flexural strength and modulus of Al_2O_3 - Nylon66 composites at various filler loadings are shown in Figures 4.3 & 4.4 respectively. It is noted that the flexural strength and modulus increases with the addition of micro alumina from 111 MPa at 0 % Al_2O_3 to 119 MPa at 6 wt % Al_2O_3 whereas flexural strength increased from 3000 MPa to 3516 MPa. Further, addition of micro alumina resulted in decrease in its values. The flexural strength of composites is more than that of Oilon material. The reported results are in agreement with the findings of other researches such as Abdollah Omrani et al. [172] who observed the increase in flexural properties at low loadings of upto 2% nano alumina to epoxy and when the level of loading was over 2%, the flexural modulus is decreased. It is believed that the aggregation of filler particles at higher concentration is responsible for the low value of flexural modulus. On similar lines Kali Dass et al. [169] reported the increase in flexural strength upto 10 wt.% micro alumina epoxy composite and reduction thereafter. Another study by Mahapatra et al. [173] also noticed that addition of 10 wt.% alumina to polyester resin improves the flexural strength but further addition causes reduction in strength.

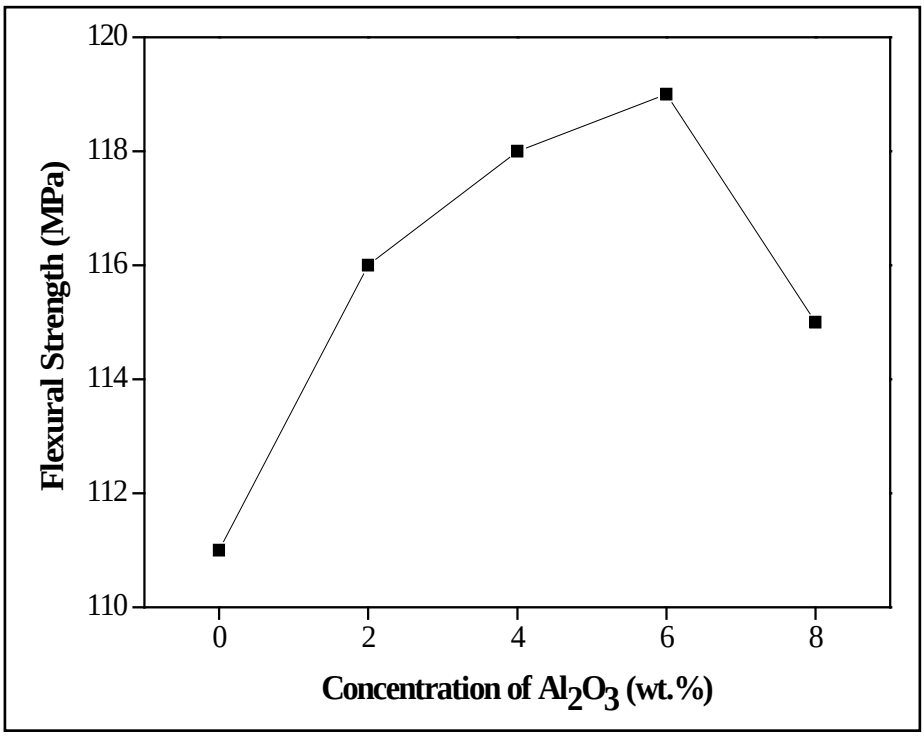

Figure 4.3: Flexural strength of Al_2O_3- Nylon66 composites

Flexural modulus of Al_2O_3 - Nylon66 composites

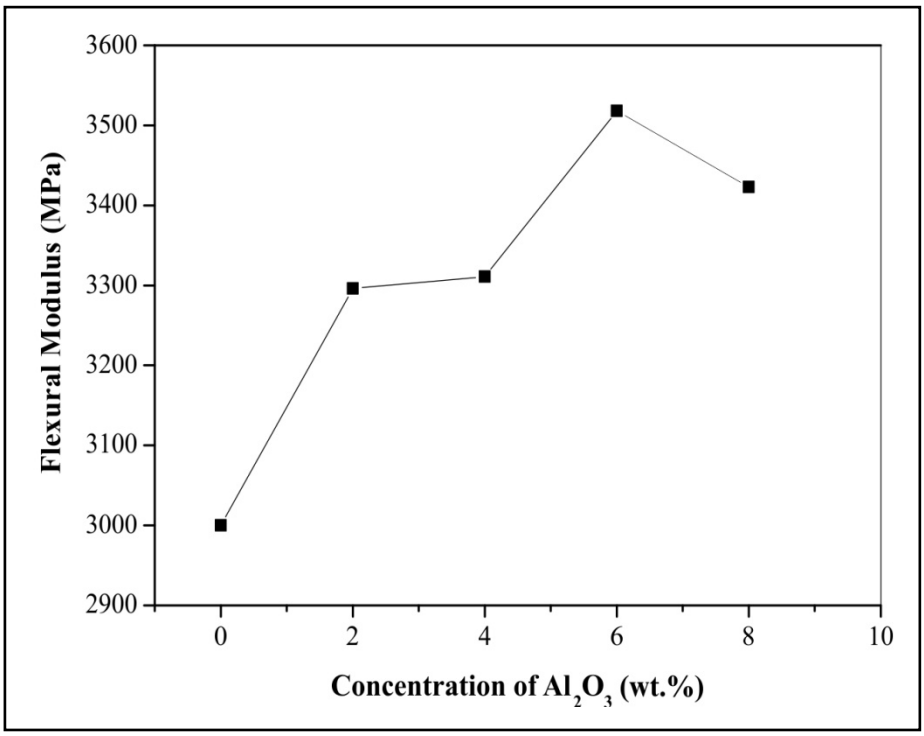

Figure 4.4: Flexural modulus of Al_2O_3 - Nylon66 composites

4.1.2.4 Impact Strength of Al_2O_3 filled Nylon66 composites

From the results of Figure 4.5 it is noted that the impact strength increases by about 18% upto 6 wt.% addition of the micro alumina particles to Nylon 66. The value increased more with the initial addition of 4% alumina and is marginally increased with further addition of filler upto 6 wt.% and the impact strength reduces at higher loading of alumina may be due to poor dispersion. S. S. Mahapatra & Amar Patnaik [173] reported that impact strength of unfilled glass fibre- polyester composite increases by about 10-15% with incorporation of alumina particles and also observed that impact strength marginally increases when wt% of fillers is increased from 10 to 20 %.

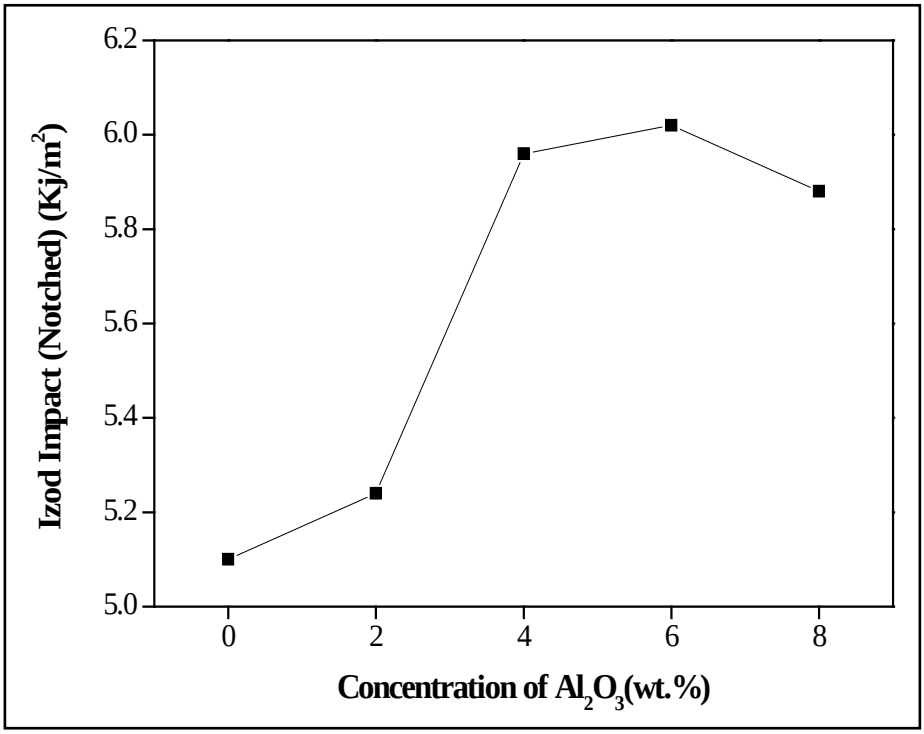

Figure 4.5: Izod impact strength of Al_2O_3- Nylon66 composites

4.1.2.5 Effect of Compressive Strength on Al_2O_3 filled Nylon66 composites

Figure 4.6 shows that the addition of micro alumina particles to Nylon66 resulted in increase of the compressive strength and the value increases from 76

N/mm^2 at 0% loading to 88 N/mm^2 at 6 wt. % of alumina and it reduces on further addition of filler and at 8 wt. % alumina it reaches to 86 N/mm^2 but still it is more than the value of plain Nylon66. The reduction in value of compressive strength at higher loading may be due to uneven distribution of filler particles in polymer matrix. Kali Dass et al. [169] also reported that the compressive strength of the m-cresol novalac epoxy composites increases with an increase in the filler content from 5 to 15 wt%.

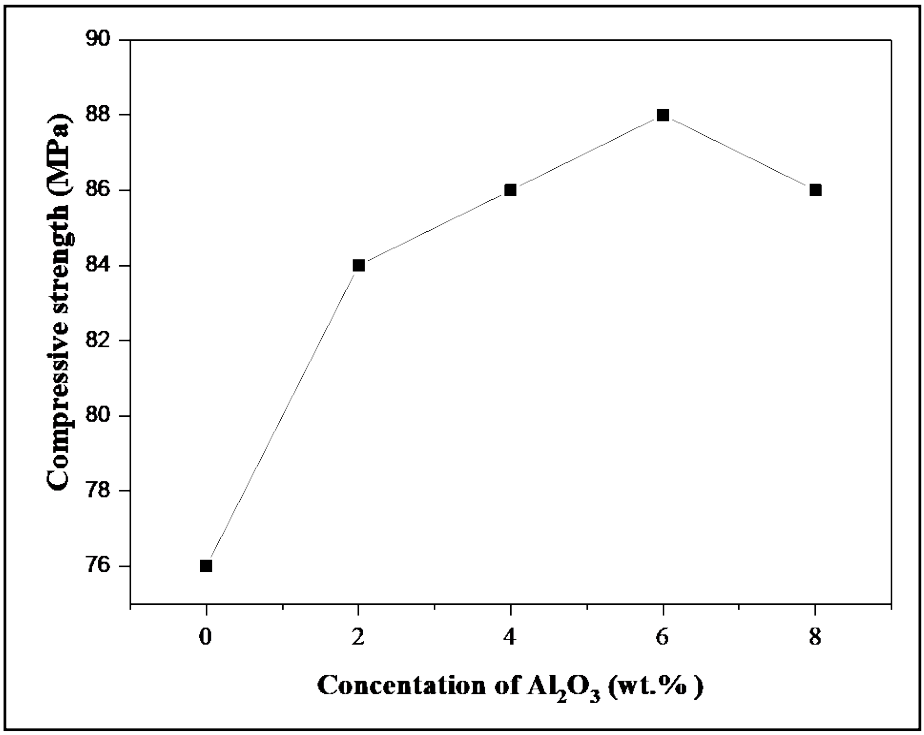

Figure 4.6: Compressive strength of Al_2O_3- Nylon66 composites

4.1.2.6 Heat Deflection Temperature (HDT) of Al_2O_3 filled Nylon66 composites

The Heat Deflection Temperature (HDT) of the composite is reported in Figure 4.7 and from that we note the increase in its value with the addition of alumina and it reaches to 71.9^0C at 8 wt.% from the value of 66.2 ^{0}C for pure Nylon 66. The addition of inorganic fillers to Nylon normally results in increasing the Heat deflection temperature and thus enhancing its applications at elevated temperatures.

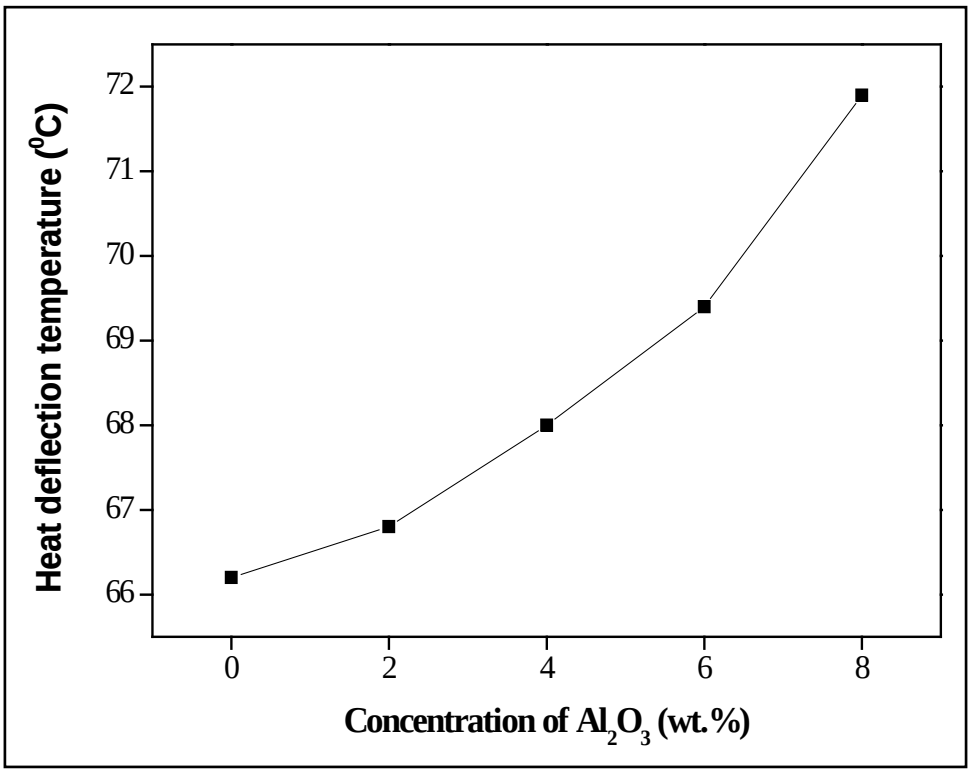

Figure 4.7: Heat Deflection Temperature (HDT) of Al_2O_3 filled Nylon66 composites

4.1.2.7 Rockwell Hardness of Al_2O_3 filled Nylon66 composites

Figure 4.8 shows the hardness variation with filler content for alumina filled Nylon 66 composites. It reveals that hardness increases with increment in alumina filler content in Nylon 66 matrix. This increase in hardness may be attributed to stiffer and more brittle nature of Al_2O_3 than the Nylon 66 material. According to investigation of Kumar et al., the alumina filler compacts the composite matrix and reinforcement arrangement, which results in improved packing and resistance to indentation [174-175].

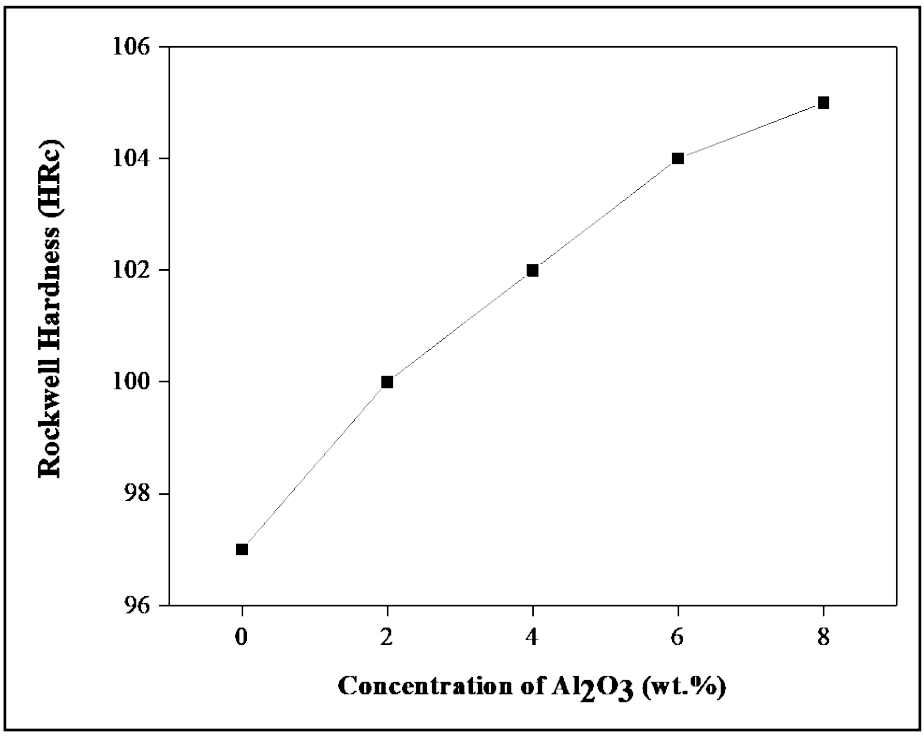

Figure 4.8: Rockwell Hardness of Al_2O_3 filled Nylon66 composites

4.1.3 Mechanical properties of TiO_2 filled Nylon66 composites

The experimental value of the mechanical properties of the TiO_2 – Nylon66 composite material determined as per ASTM standard is given in the Table 4.3

Table 4.3: Mechanical properties of TiO_2 – Nylon 66 composite material

S. No.	Name of Test	Units	Test Methods	Nylon 66 with TiO_2				
				0%	2%	4%	6%	8%
01.	Density	gm/cc	ASTM D 792	1.14	1.15	1.17	1.18	1.19
02.	Tensile Strength	MPa	ASTM D 638	75.0	76.0	78.0	82.0	78.0
03.	Elongation	%	ASTM D 638	23	23	22	22	7
04.	Tensile Modulus	MPa	ASTM D 638	1200	1261	1326	1489	1458
05.	Izod Impact (Notched)	KJ/m^2	ASTM D256	5.10	5.15	5.48	5.96	5.44
06.	Flexural Strength	MPa	ASTM D 790	111	114	116	119	115
07.	Flexural Modulus	MPa	ASTM D 790	3000	3045	3206	3436	3021
08.	Compressive Strength	N/mm^2	ASTM D 695	76	82	84	85	83
09.	Heat Deflection Temperature	^0C	ASTM D 648	66.2	67.1	68.3	69	71.6
10.	Rockwell Hardness	HRc	ASTM D 785	97	98	101	104	102

The variation in mechanical properties such as tensile strength, tensile modulus, flexural strength and modulus, impact strength, compressive strength, heat deflection temperature (HDT) and Rockwell hardness of different weight % TiO_2 filled Nylon66 composites is described below:

4.1.3.1 Tensile Strength of TiO_2 filled Nylon66 composites

From the Figure 4.9 we can see that the value of tensile strength increases almost linearly up to 4 wt % and it further increases gradually up to 6 wt %, before the value reduces at 8 wt % TiO_2. The tensile strength of Nylon66- TiO_2 composites is more than that of Oilon material. Bao jun found that the loading of TiO_2 was effective for improving the tensile strength of PA66 and inferred that nanosize TiO_2 as the reinforcing agent might effectively increase the load carrying capacity of PA66 nanocomposites [176]. The addition of TiO_2 to polystyrene also results in increase in the tensile strength linearly up to 15 wt.% and all the compositions showed a tensile strength higher than the virgin polymer [177].

The effect of differing particle sizes on the tensile strength was examined by various researchers and it is observed that PEEK reinforced with 15nm particles of TiO_2 improved the tensile strength starting from 86 MPa for neat PEEK up to 115 MPa at a filler content of 8.4 vol.%, whereas 300 nm particles decreased the tensile strength [178]. Thus, the increase in tensile strength is in line with the findings of other researchers [176-178].

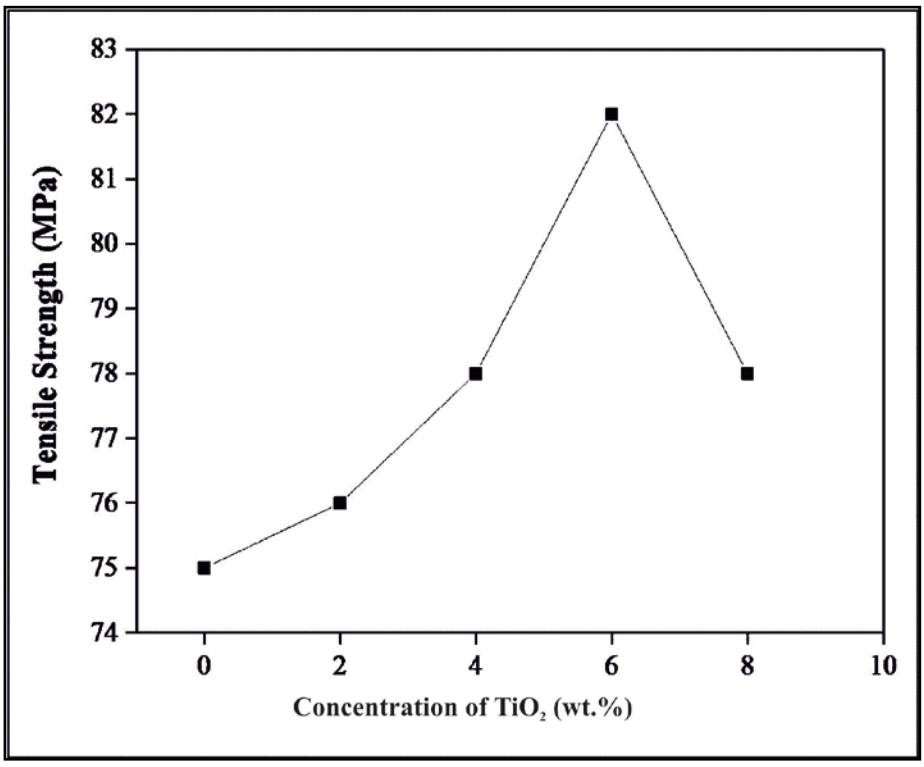

Figure 4.9: Tensile strength of TiO_2 filled Nylon66 composites

4.1.3.2 Tensile Modulus of TiO_2 filled Nylon66 composites

Tensile modulus is the ratio of the tensile stress to strain in the linear region of the stress- strain diagram and is known to increase on addition of any mineral filler to the polymer. Tensile modulus is increased by 23% on addition of 6 wt % micro TiO_2 to Nylon 66 and the increase in modulus happens due to the good reinforcement provided by the inorganic filler to the polymer matrix (Figure 4.10). Similarly, increase in the modulus was also reported by Jing-Lei-Yang et al. for PA66-21nm and 300nm TiO_2 composites [179]. The result of another research showed that PEEK filled with 15nm particles of TiO_2 exhibit higher modulus than the one filled with large 300nm particles. The nanocomposite filled with 8.4vol.% of 15nm particles is 39% enhanced in comparison to the neat PEEK matrix, whereas the compound owing 8.9vol.% of 300nm particles improves only about 30% [178]. The TiO_2 – Polystyrene composites also showed an increase in the tensile modulus up to 15wt. % of the filler and thereafter the value goes down [177].

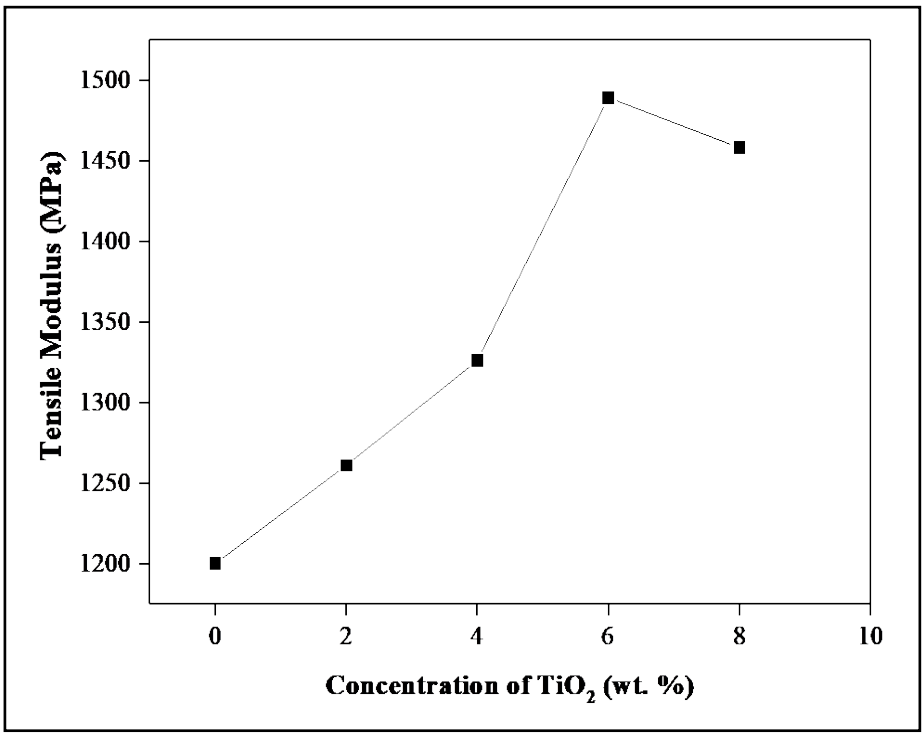

Figure 4.10: Tensile modulus of TiO_2 filled Nylon66 composites

4.1.3.3 Flexural Strength and Modulus of TiO_2 filled Nylon66 composites

Flexural properties of TiO_2- Nylon 66 composites at various filler loadings are shown in Figures 4.11 & 4.12 respectively. It is found that the flexural strength and modulus increases with the increase in TiO_2 up to 6 wt. % however the increase is not as much as in tensile properties. Flexural strength increased from 111 MPa at 0 % TiO_2 to 119 MPa at 6 wt. % TiO_2 whereas flexural strength increased from 3000 MPa to 3436 MPa. The effect of adding TiO_2 to polystyrene also reported an increase both in flexural strength and modulus up to 15 wt.% followed by a decrease at higher loading [177]. Another research reported the increase in flexural properties for Nylon 6-flyash microcomposites and observed that flexural strength attained maxima at lower filler concentration when smaller particle size flyash was used as compared to larger particle size flyash [180]. Generally the incorporation of mineral filler enhances the flexural properties as the interaction between filler and matrix makes the composite more stable and the values reduces at higher loading due to agglomeration of filler particles.

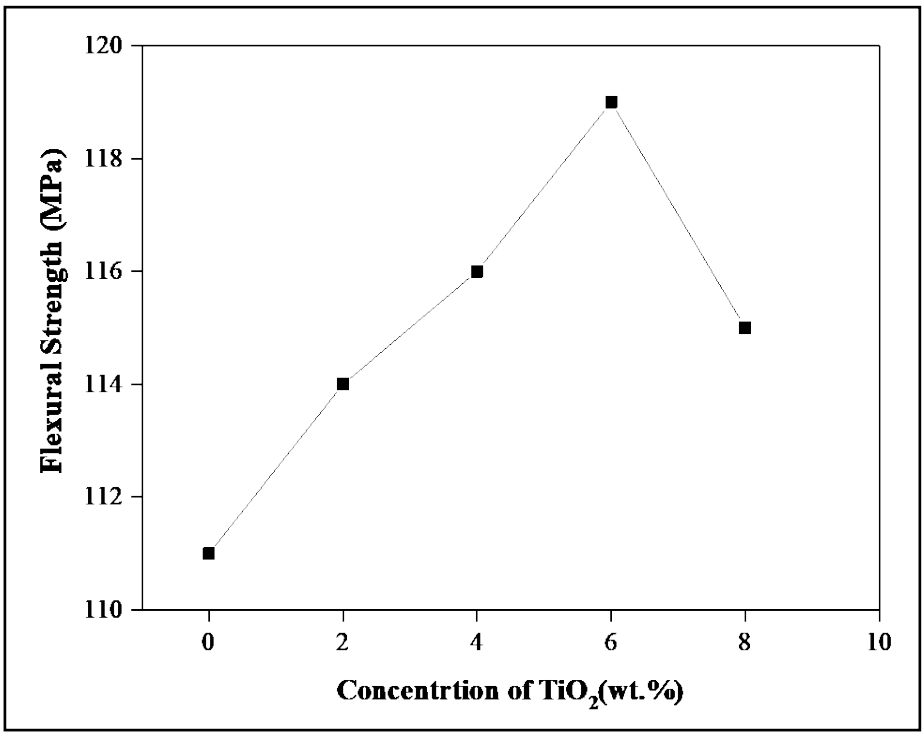

Figure 4.11: Flexural strength of TiO_2 filled Nylon66 composites

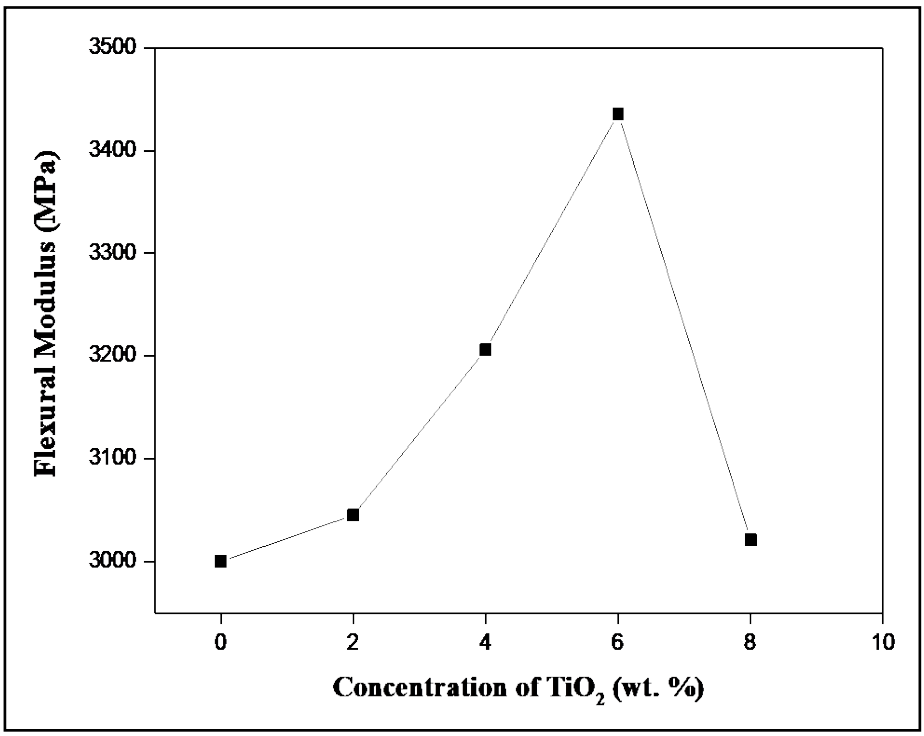

Figure 4.12: Flexural modulus of TiO_2 filled Nylon66 composites

4.1.3.4 Impact Strength of TiO_2 filled Nylon66 composites

An earlier study stated that filler can either decrease or increase the impact strength compared to the unfilled polymer [181]. The addition of flyash to Nylon 6 reported the reduction in impact strength [180] whereas Kaolin, talc mix resulted in increase and decrease at different proportion [182]. Study of PEEK -TiO_2 nanocomposites showed that the 15nm particles create high improvement in toughness, whereas the 300nm particles with increasing filler content cause a slight decrease in comparison to neat PEEK [178]. Impact strength showed a decrease with increase in filler in case of titanium dioxide filled polystyrene microcomposite as impact strength depends on the brittleness of the polymer matrix. The presence of coupling agent helps in better interfacial bonding between the matrix and the filler and improves the impact strength [177].

From Figure 4.13, we can note that addition of micro TiO_2 to Nylon66 resulted in substantial improvement in Izod Impact Strength by 17% at 6 wt.%. TiO_2 and reduces on further addition of filler as due to poor dispersion bigger agglomerates or particles lead to a reduction in impact energy and earlier failure because of stress induction.

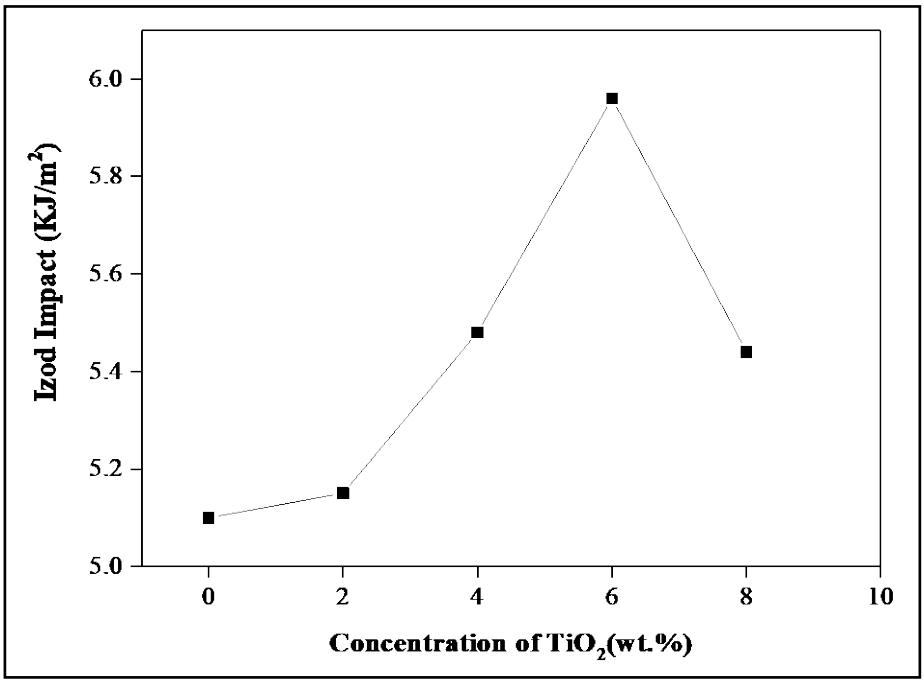

Figure 4.13: Izod impact strength of TiO_2 filled Nylon66 composites

4.1.3.5 Compressive Strength of TiO_2 filled Nylon66 composites

From Figure 4.14, it can be seen that the addition of micro TiO_2 to Nylon 66 resulted in increase of the compressive strength and the value increases from 76 N/mm^2 at 0wt. % loading to 85 N/ mm^2 at 6 wt. % of TiO_2 and it reduces to 83 N/ mm^2 at 8 wt. % but still it is more than the value of plain Nylon 66. V. L. Raja et al. studied the effect of adding silica fume to Nylon 66 and noticed the improvement in the compressive strength [183]. The results are in agreement with earlier studies that inorganic fillers and short fibres are used to increase the compressive strength of the polymer matrix system [184, 185].

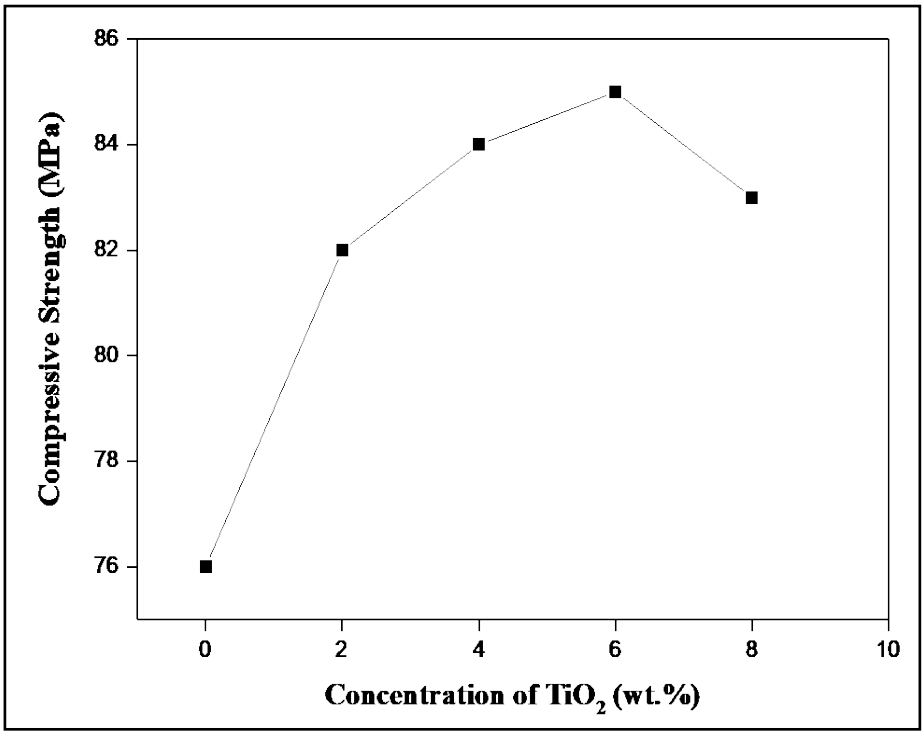

Figure 4.14: Compressive strength of TiO_2 filled Nylon66 composites

4.1.3.6 Heat Deflection Temperature (HDT) of TiO_2 filled Nylon66 composites

HDT is the temperature at which a beam of polymer deflects by a given amount under a specified load [181]. The addition of mineral fillers resulted in increase in HDT and from Figure 4.15 it is observed that with the increase in TiO_2 wt.% the HDT increases. Nylon 66 being semi crystalline, the crystalline regions help transfer stress to the filler under load. The test results of Nylon 66 – silica fume

composites confirmed the improvement in HDT properties [183]. Since the inorganic fillers are quite stable at elevated temperatures compared to polymers, their addition helps in enhancing the heat deflection properties of the composite.

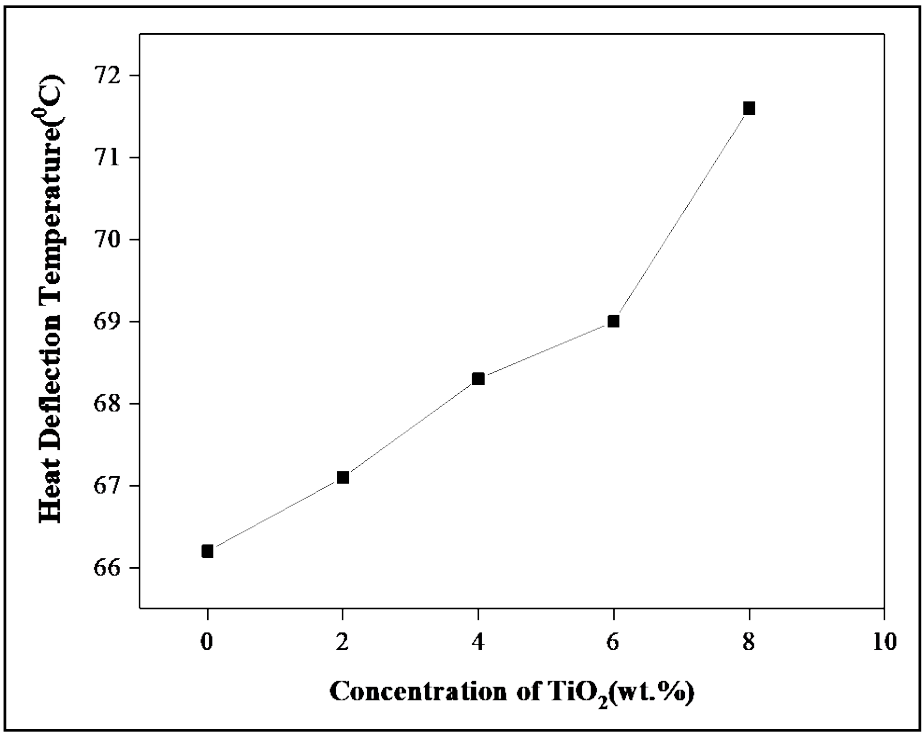

Figure 4.15: Heat Deflection Temperature of TiO_2 filled Nylon66 composites

4.1.3.7 Rockwell Hardness of TiO_2 filled Nylon66 composites

The Rockwell hardness variation for TiO_2 filled Nylon 66 composites are shown in Figure 4.16.It reveals that hardness increases with increase in TiO_2 filler content upto 6 wt.% in Nylon 66 matrix. This increase in hardness may be because of a more compact/rigid structure at the material's surface, which creates greater resistance to indentation resulting in the hardness of the composites showing higher values. At higher filler loading the hardness may not be increasing due to conglomeration and poor dispersion of the microparticulates.

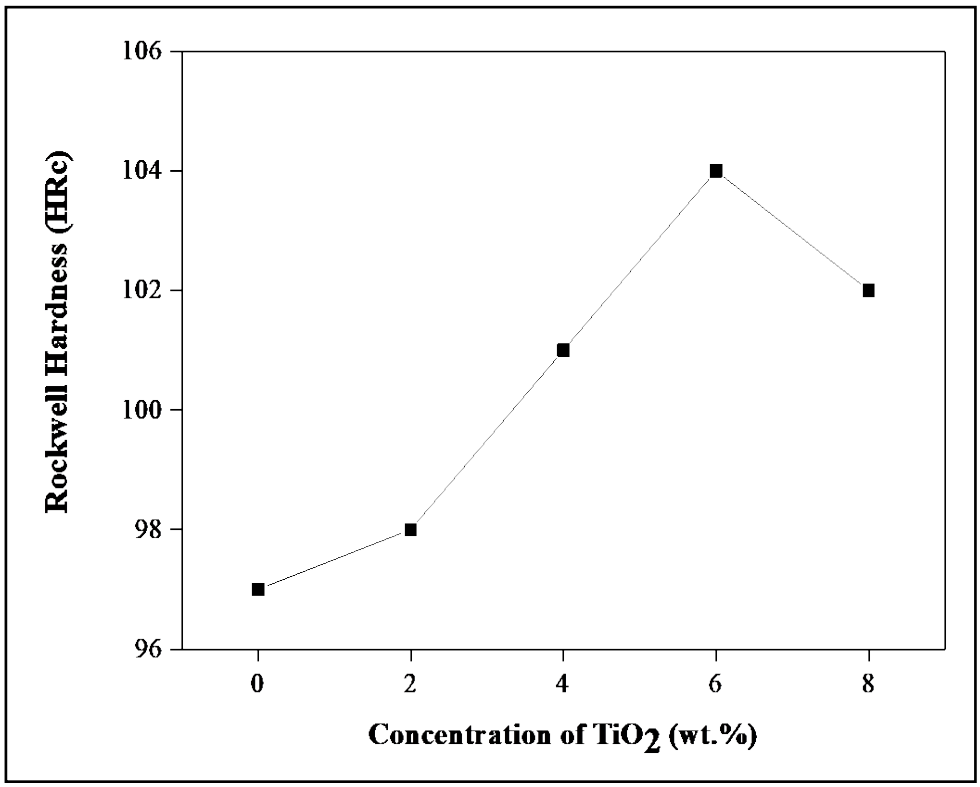

Figure 4.16: Rockwell hardness of TiO_2 filled Nylon66 composites

4.2 Tribological Properties

The wear rate and coefficient of friction of oil impregnated Nylon 66 (Oilon) material, Nylon 66 and composites of Nylon 66 with alumina and titanium dioxide are determined from the experiments conducted with pin on disc apparatus as per the procedure explained in Chapter 3.

4.2.1 Tribological Properties of oil impregnated Nylon 66 (Oilon) material

The experiment results for wear rate and coefficient of friction for oil impregnated Nylon 66 (Oilon) material are given in Table 4.4

Table 4.4: Tribological properties of oil impregnated Nylon 66 (Oilon) material

	Load(N)	**Wear Rate(mm^3)**	**Coefficient of Friction**
Sliding velocity: 6.5m/s, Sliding Distance: 2000 m	50	11.404	0.11
	60	23.684	0.26
	70	36.842	0.38
	80	51.754	0.51
	90	86.842	0.76
	100	278.947	0.91
	Sliding Velocity (m/s)		
Load: 100 N, Sliding Distance: 2000m	2.5	16.667	0.38
	3.5	34.21	0.51
	4.5	64.035	0.59
	5.5	139.474	0.67
	6.5	285.965	0.86
	Sliding Distance(m)		
Load :100N, Sliding Velocity : 6.5m/s	500	18.421	0.4
	1000	75.439	0.63
	1500	171.93	0.79
	2000	281.579	0.94

4.2.2 Tribological Properties of Al_2O_3 filled Nylon66 composites

4.2.2.1 Wear Rate of Al_2O_3 filled Nylon66 composites

The wear rate is calculated by measuring the wear volume in mm^3 for the experiments conducted for various wt.% micro alumina - Nylon 66 composites as a function of load, sliding velocity and sliding distance and the results are plotted in Figures 4.17-4.19 respectively. It is observed that the wear rate increases with the

increase in the applied normal load, sliding velocity and sliding distance for various wt.% composites with the increase in filler loading. However, the wear rate values were less than that of pure Nylon 66 for the micro composite of 4 wt.% alumina from Figure 4.17 and 6 wt.% alumina from Figures 4.18 & 4.19. The lowest wear rate is observed in case of 2 wt.% composite and the wear rate is linear upto load 90N, sliding velocity 6.5 m/s and distance 1500m and thereafter with increased slope. The decrease in the wear rate at lower filler loading can be attributed to the dispersion of micro alumina in the form of a single particle in the matrix and could give full advantage to the combination properties of the composite. The increase in wear rate at higher loading is because the micro Al_2O_3 tended to produce stress concentration due to its larger and harder particles where some particles were prone to disengage from the matrix due to poor adhesive strength [92].

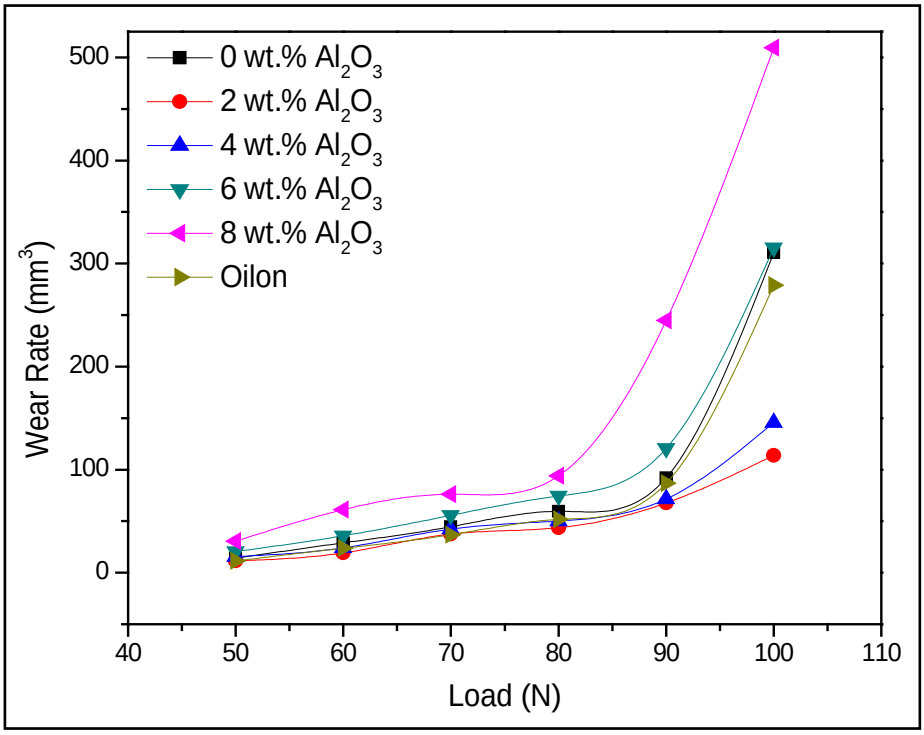

Figure 4.17: Relationship between wear rate and load on Al_2O_3 filled Nylon66 composites (Sliding Velocity: 6.5m/s, Sliding Distance: 2000 m)

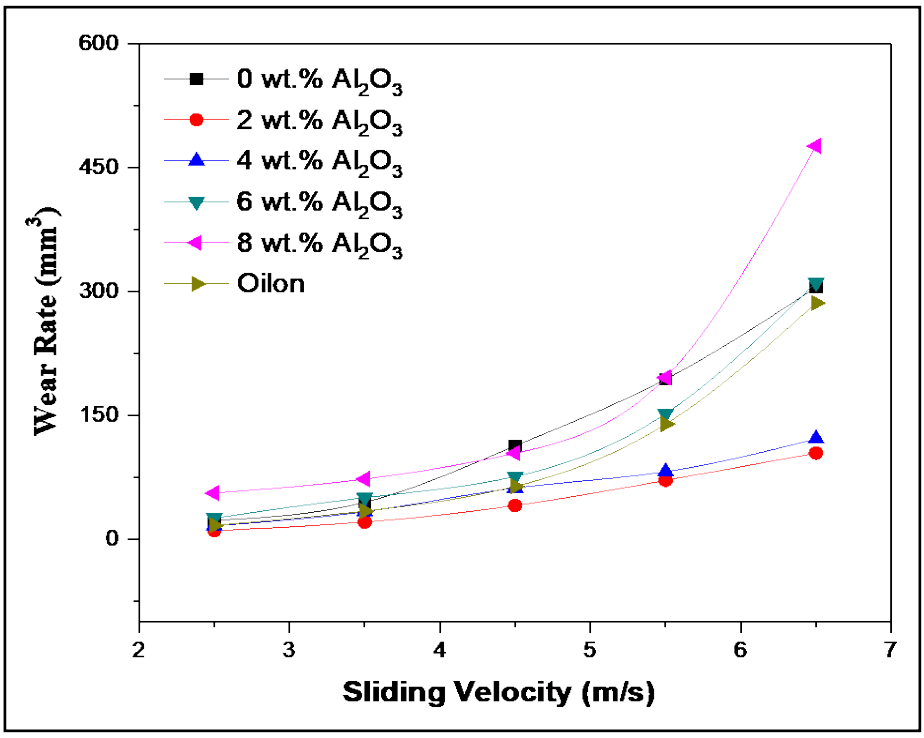

Figure 4.18: Relationship between wear rate and sliding velocity on Al_2O_3 filled Nylon66 composites (Load: 100 N, Sliding Distance: 2000 m)

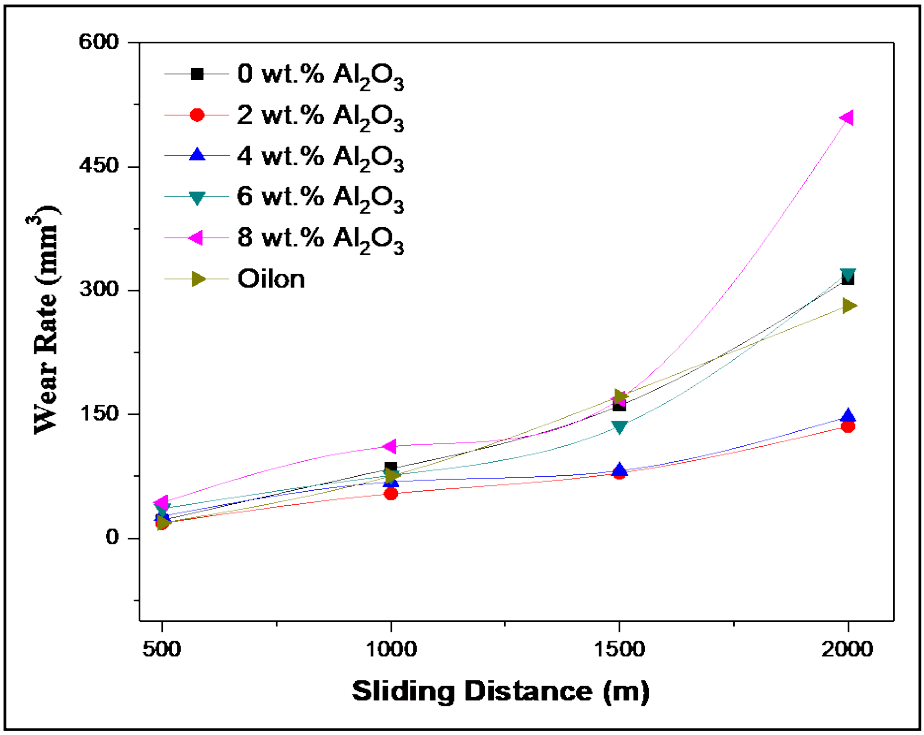

Figure 4.19: Relationship between wear rate and sliding distance on Al_2O_3 filled Nylon66 composites (Load: 100N, Sliding Velocity: 2000m)

4.2.2.2 Coefficient of Friction of Al_2O_3 filled Nylon66 composites

The effect on coefficient of friction of Nylon 66-Al_2O_3 composites with respect to load, sliding velocity and distance is shown in Figures 4.20-4.22. It is noted that the addition of small quantity of alumina reduces the coefficient of friction and lowest COF is for 2 wt.% Al_2O_3-Nylon 66 composite. The coefficient of friction of 2 wt.% Al_2O_3-Nylon 66 lies from 0.1 to 0.5 under various combinations of load, sliding velocity and sliding distance. COF increases with the percentage increase of alumina from 2 wt.% to 8 wt.% but remains less than that of pure Nylon 66. Friction coefficient increases linearly with varying load upto 80N and thereafter increases with increased slope. The sliding velocity also causes the friction coefficient to increase linearly for all ranges of sliding velocity from 2.5 m/s to 6.5 m/s and the friction coefficient increases linearly upto 1000m sliding distance and then with increased slope.

Cai et al. [96] investigated that the nanocomposites with mass fractions of Al_2O_3 below 4 wt.% give slightly decreased friction coefficients at both low and high sliding speeds compared to the bare Polyimide and inferred that the sliding surface temperature of PI/Al_2O_3 increased with sliding speed resulting in micro melting of the surface and the formation of a transfer film of the nanocomposite on the counterpart steel surface resulting in reduced friction. With the increase in wt.% of Al_2O_3 the transfer film gets damaged due to abrasion action of the agglomerated particulates in the wear debris thus increasing the friction. A study of micro and nanocomposite of PA6/Al_2O_3 at a velocity of 0.42 m/s for 1 hour under loads of 50 N to 250 N showed that friction coefficient reduced with increasing load and the friction coefficient of PA6/Al_2O_3 nanocomposite was slightly greater than that of the monomer casting PA6 and that of micron Al_2O_3 was the highest [92].

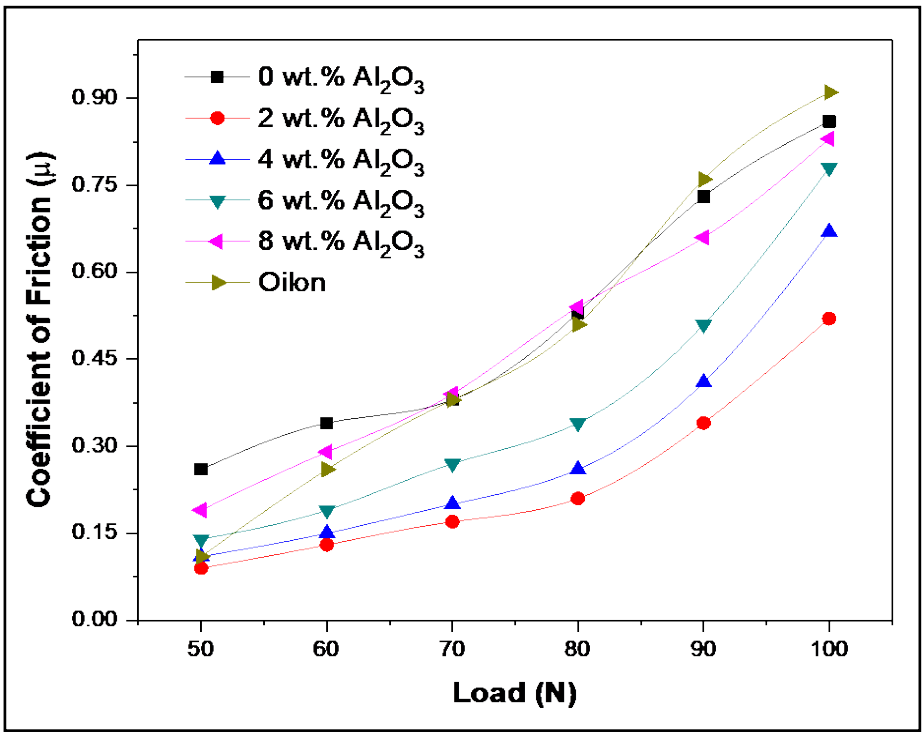

Figure 4.20: Relationship between coefficient of friction and load on Al_2O_3 filled Nylon66 composites (Sliding velocity: 6.5m/s, Sliding Distance: 2000 m)

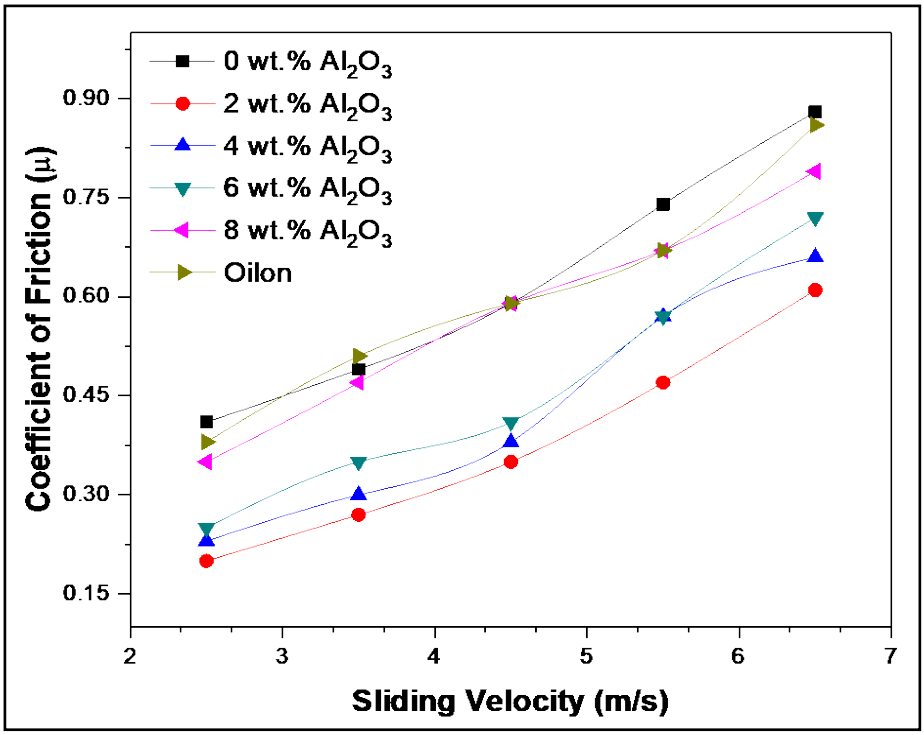

Figure 4.21: Relationship between coefficient of friction and sliding velocity on of Al_2O_3 filled Nylon66 composites (Load: 100 N, Sliding Distance: 2000 m)

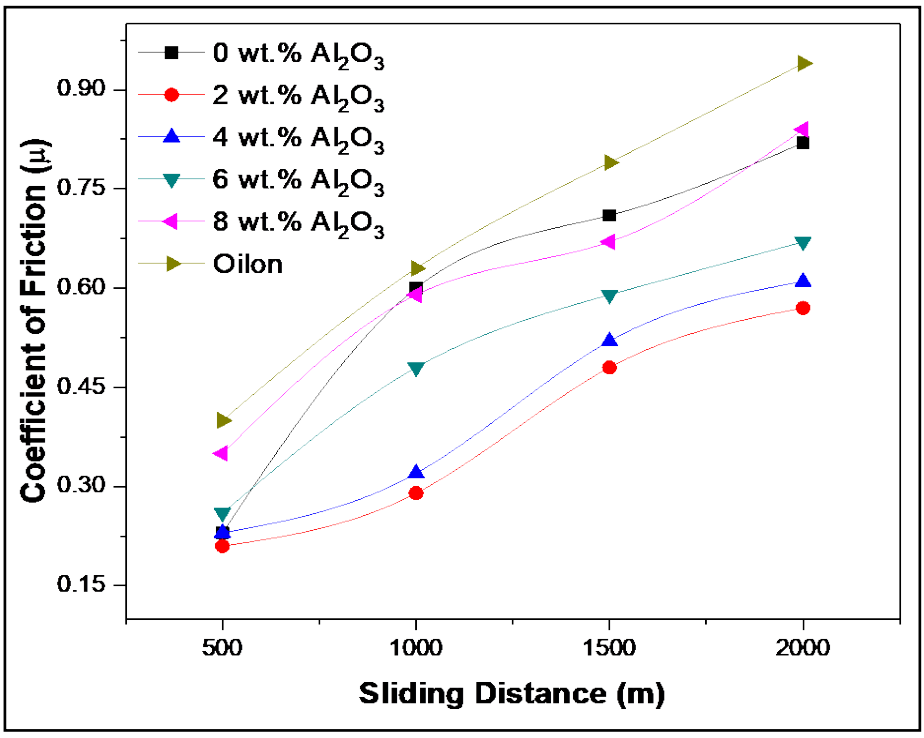

Figure 4.22: Relationship between coefficient of friction and sliding distance on Al_2O_3 filled Nylon66 composites (Load: 100N, Sliding Velocity: 2000m)

4.2.3 Tribological Properties of TiO_2 filled Nylon66 composites

4.2.3.1 Wear Rate of TiO_2 filled Nylon66 composites

Figures 4.23-4.25 display the wear rate of neat Nylon 66 and Nylon 66-TiO_2 composite as a function of load, sliding velocity and sliding distance respectively and it is observed that the wear rate increases with the increase in their values. It is noticed that the wear rate of 2, 4 & 6 wt. % TiO_2-Nylon 66 composites is less than the wear rate of pure Nylon 66, whereas the wear rate of 8 wt.% composite is more.

The lowest wear rate is observed in case of 2 wt. % composite and it is approximately one third of the wear rate of the pure Nylon 66. The wear rate of 2 and 4 wt. % composite is linear for all combinations of load, sliding velocity and distance. Further, it can be seen that the wear rate for 0, 6 and 8 wt. % is linear up to load 80N, sliding velocity 4.5 m/s and distance 1000 m and thereafter increases gradually. The increase in wear rate is due to the increase in the value of coefficient of friction due to the dislodged debris between contact surfaces. The contact surface

temperature increases resulting in the reduction of mechanical cohesion and eroding of the constituents.

Similar finding was reported by Bao jun [176] that Nano TiO_2 at 1vol.% was effective for improving the tribological properties of PA66 and noticed the increase in wear rate with increased load for TiO_2/PA66 composite and the wear rate of pure PA66 increased quickly. Another study concluded that the nano TiO_2 effectively reduces the wear rate of Nylon 66- TiO_2 composite especially under high pv conditions [186].

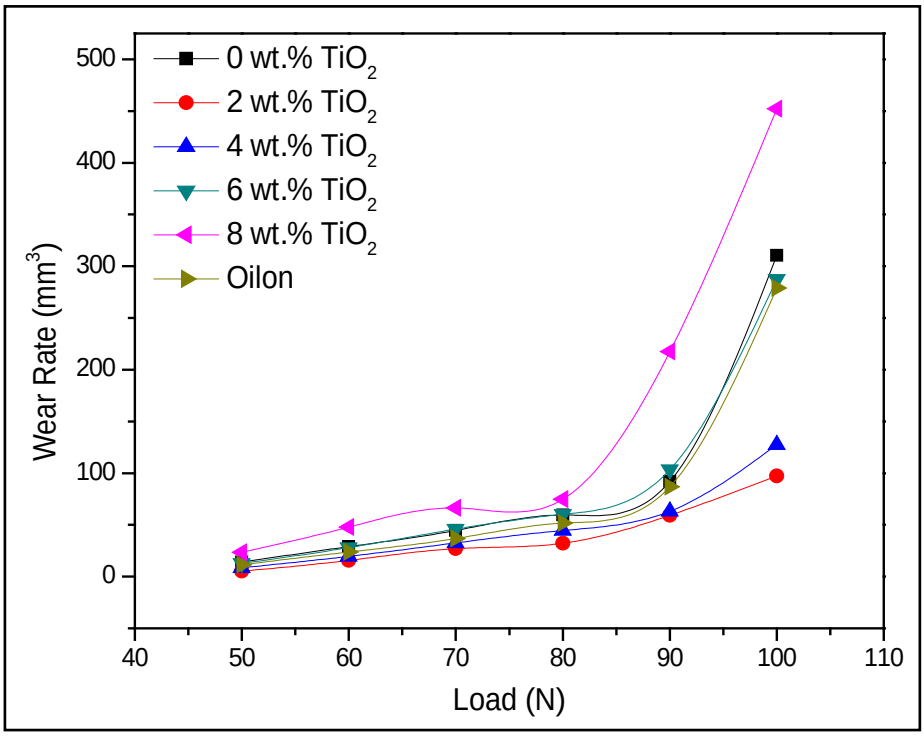

Figure 4.23: Relationship between wear and load on TiO_2 filled Nylon66 composites (Sliding velocity: 6.5m/s, Sliding Distance: 2000m)

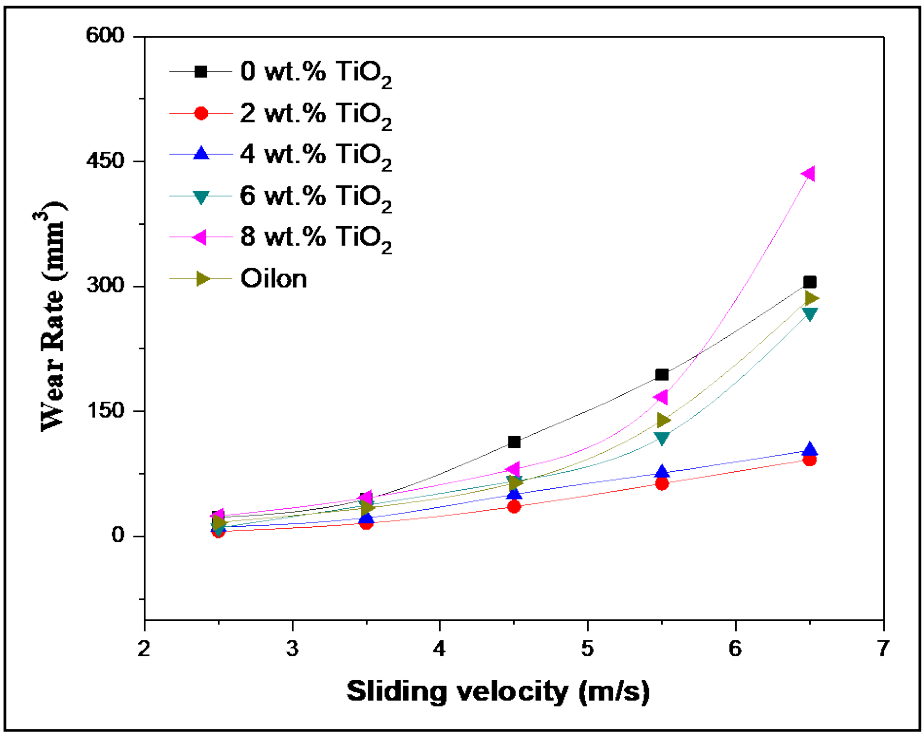

Figure 4.24: Relationship between wear and sliding velocity on TiO_2 filled Nylon66 composites (Load: 100N, Sliding Distance: 2000m)

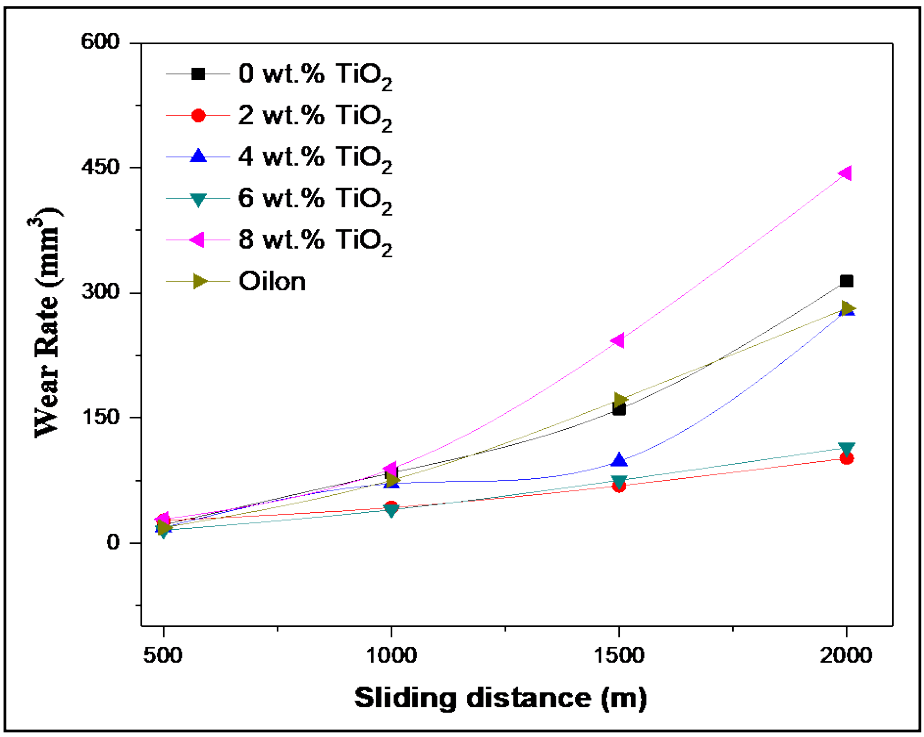

Figure 4.25: Relationship between wear and sliding distance on TiO_2 filled Nylon66 composites (Load: 100N, Sliding Velocity: 6.5m/s)

4.2.3.2 Coefficient of Friction of TiO_2 filled Nylon66 composites

Figures 4.26-4.28 show the coefficient of friction of Nylon 66 and Nylon 66-TiO_2 composites with respect to load, sliding velocity and distance. The friction coefficient decreases initially with the addition of TiO_2 and is lowest with 2 wt.% and increases gradually and becomes more than that of pure Nylon 66 beyond 6 wt.% filler loading. Increase in friction coefficient is noted with the increasing load, sliding velocity and sliding distance. From the results it is noted that sliding velocity is the maximum contributor to the increase in coefficient of friction. Earlier study also showed that the coefficient of friction of neat PA66 apparently increases during the initial wear stage probably due to the increase of contact area and contact temperature due to frictional heating [186]. Bao Jun studied the friction coefficients of monomer PA66 and TiO_2/PA66 composite as a function of load and noted that the friction coefficient of the materials was reduced with load in the test. The friction coefficient of 1vol% TiO_2/PA66 composite was the lowest and the friction coefficient of the pure PA66 was the highest [176].

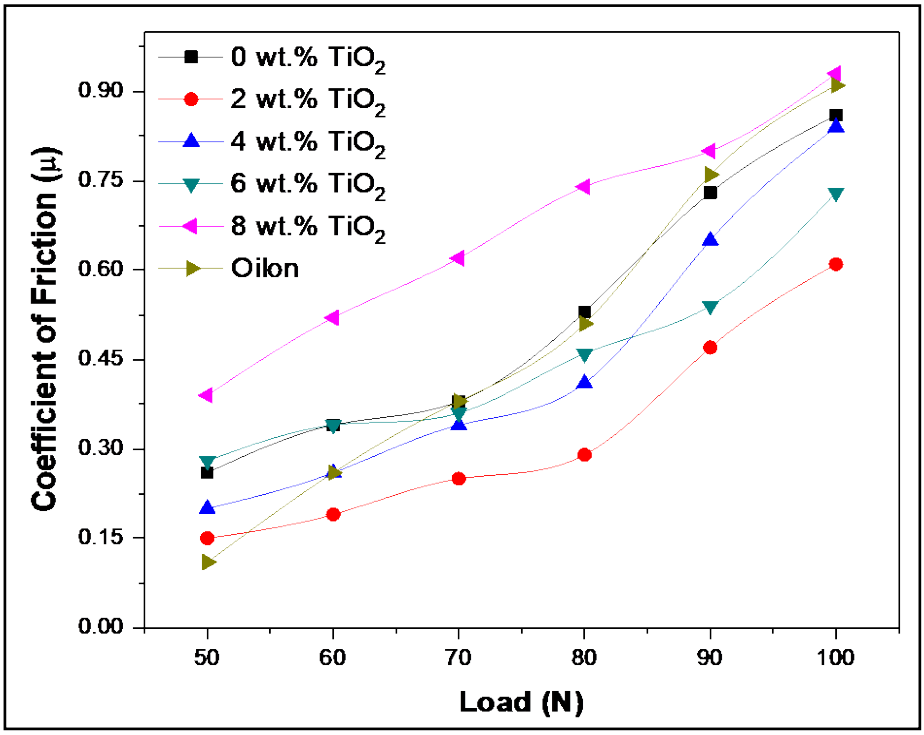

Figure 4.26: Relationship between coefficient of friction and load on TiO_2 filled Nylon66 composites (Sliding Velocity: 6.5m/s, Sliding Distance: 2000 m)

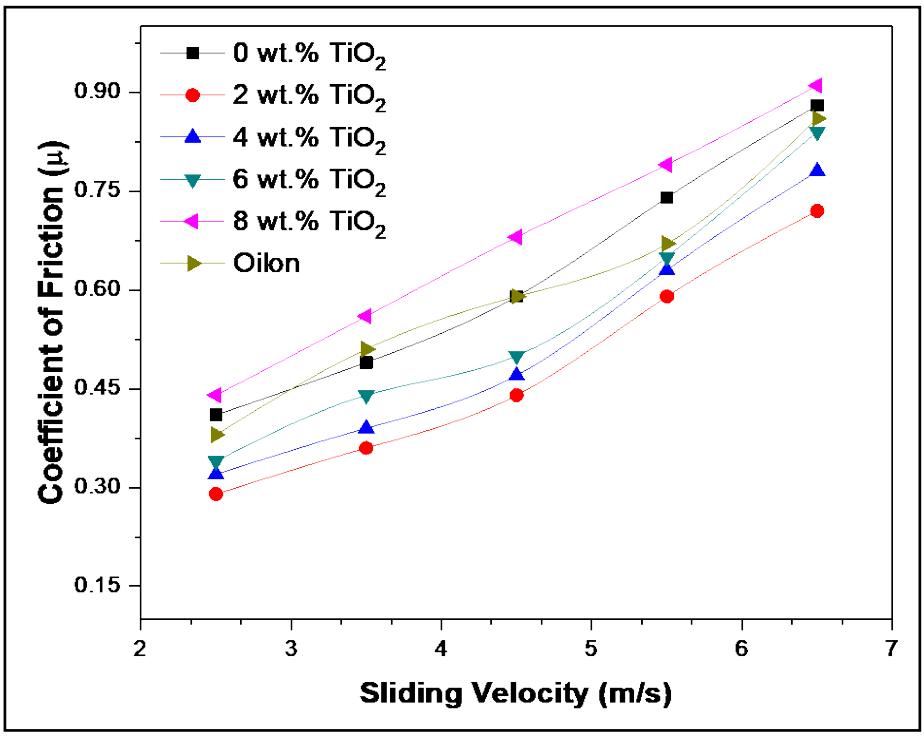

Figure 4.27: Relationship between coefficient of friction and sliding velocity on TiO_2 filled Nylon66 composites (Load: 100N, Sliding Distance: 2000 m)

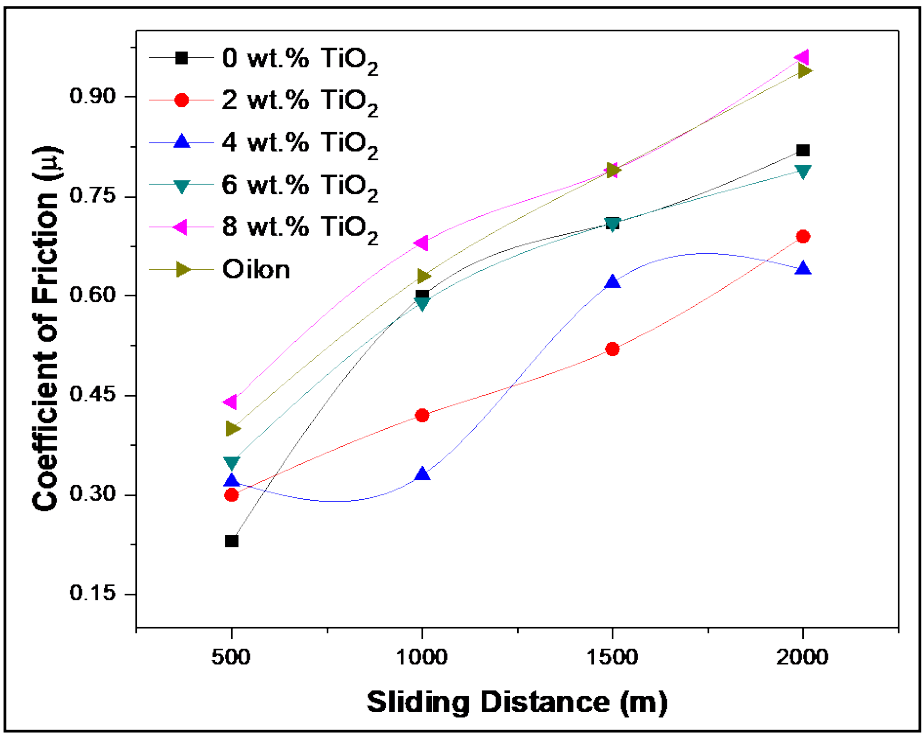

Figure 4.28: Relationship between coefficient of friction and sliding distance on TiO_2 filled Nylon66 composites (Load: 100N, Sliding Velocity: 6.5m/s)

4.3 Scanning Electron Microscopy

4.3.1 SEM of Oilon and Al_2O_3 filled Nylon 66 composites

The worn out surfaces of the composite specimens after the sliding wear test were subjected to Scanning Electron Microscopy [SEM] examination to understand the wear mechanism. The micrographs for Oilon and various compositions are shown in Figures 4.29 [a] to [f] from which it can be seen that wear grooves run parallel to the sliding direction and were present at all stages of the test. From figure 4.29[b], it is noted that for plain Nylon 66, deep wear grooves are observed which can be attributed to frictional heat generated due to the increase in coefficient of friction with increasing load and sliding velocity. Figure 4.29[c] shows that at 2 wt.% loading of alumina the wear is reduced as the state of dispersion was good and a suitable adhesion between alumina particles and the polymer matrix has been attained at low level of loading [172]. Figure 4.29[d] - 4.29[f] reveal that as the wt.% of alumina increases the wear and groove depth also increases. More scuffing, ploughing and plastic deformation marks appear on the worn surfaces at higher loading which indicates that higher mass fraction of Al_2O_3 experienced more severe plastic deformation and weakening of the molecular chain interaction which is related to the poorer wear resistance [96] as it can be observed from figure 4.22-4.24 that with increase in wt.% of Al_2O_3 the wear rate increases. Zhao et al. [92] also concluded that there was ploughing ditch on the worn surface and significant abrasive wear and because the friction force was larger, the worn surface showed micro cracking which was perpendicular to the sliding direction caused by the friction force and heat. Increase in wear at higher wt. % results in increase in friction coefficient.

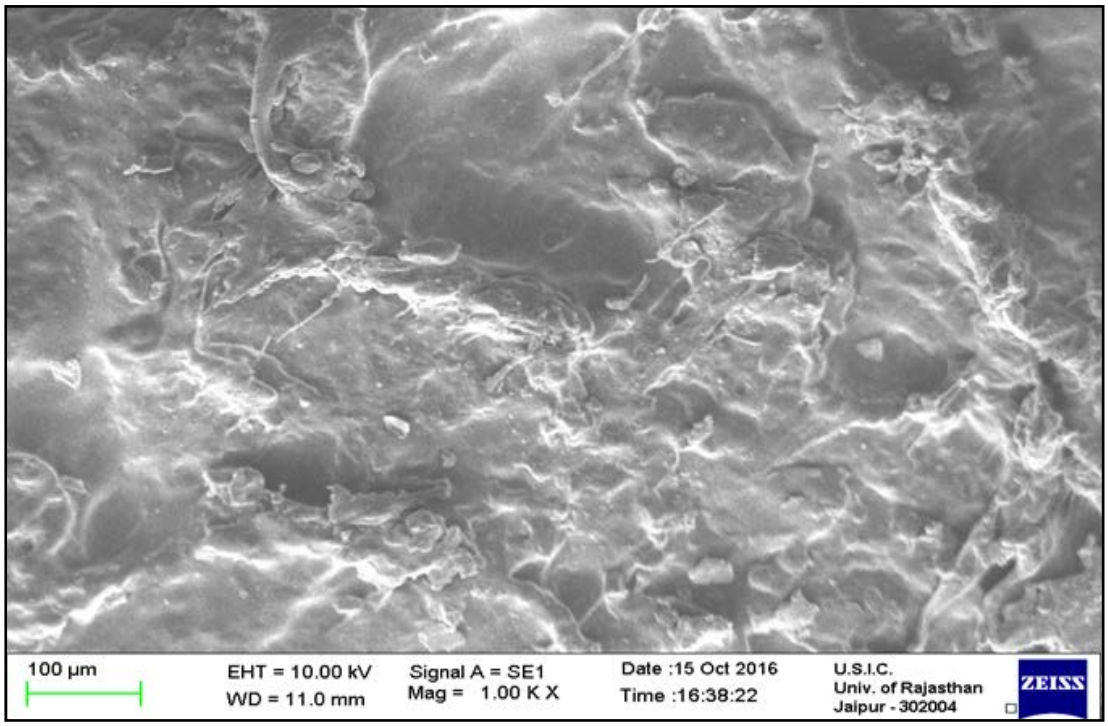

Figure 4.29[a]: Oilon (Oil impregnated Nylon)

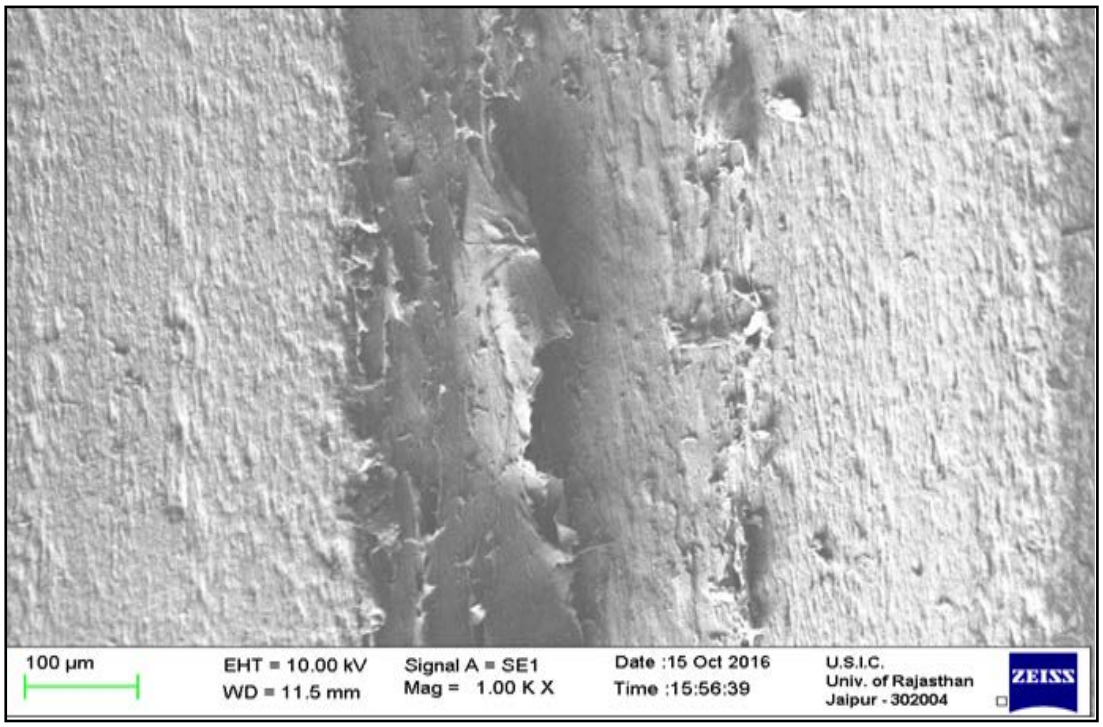

Figure 4.29[b]: Unfilled Nylon 66

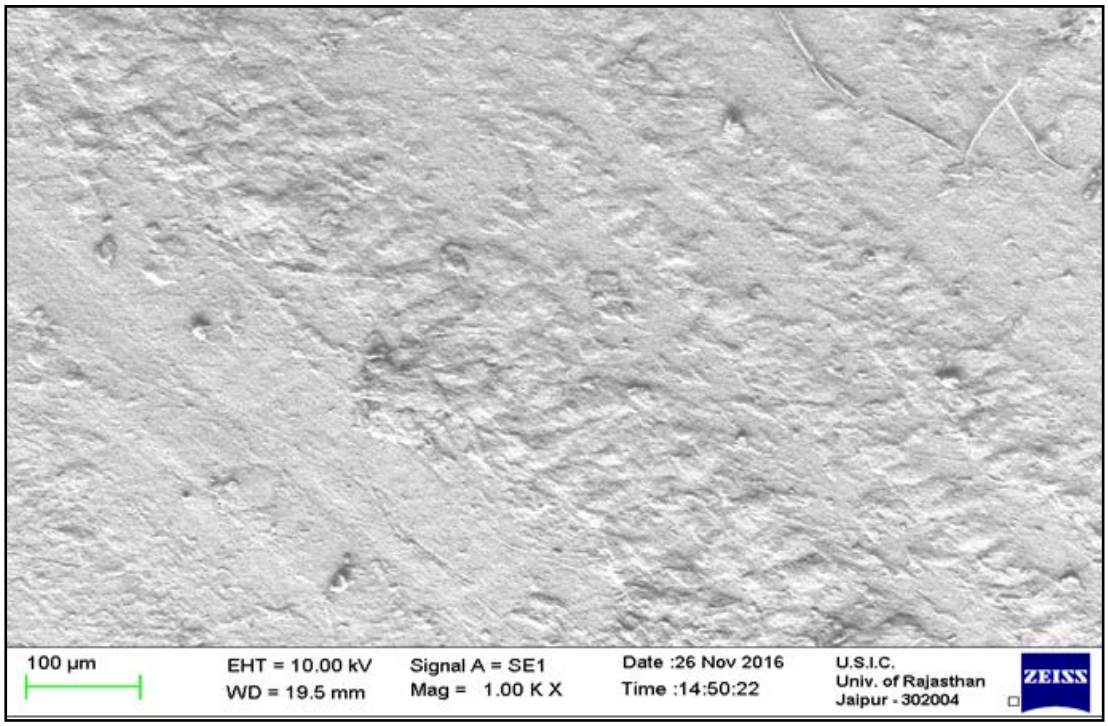

Figure 4.29[c]: Nylon 66+2wt.% Al_2O_3

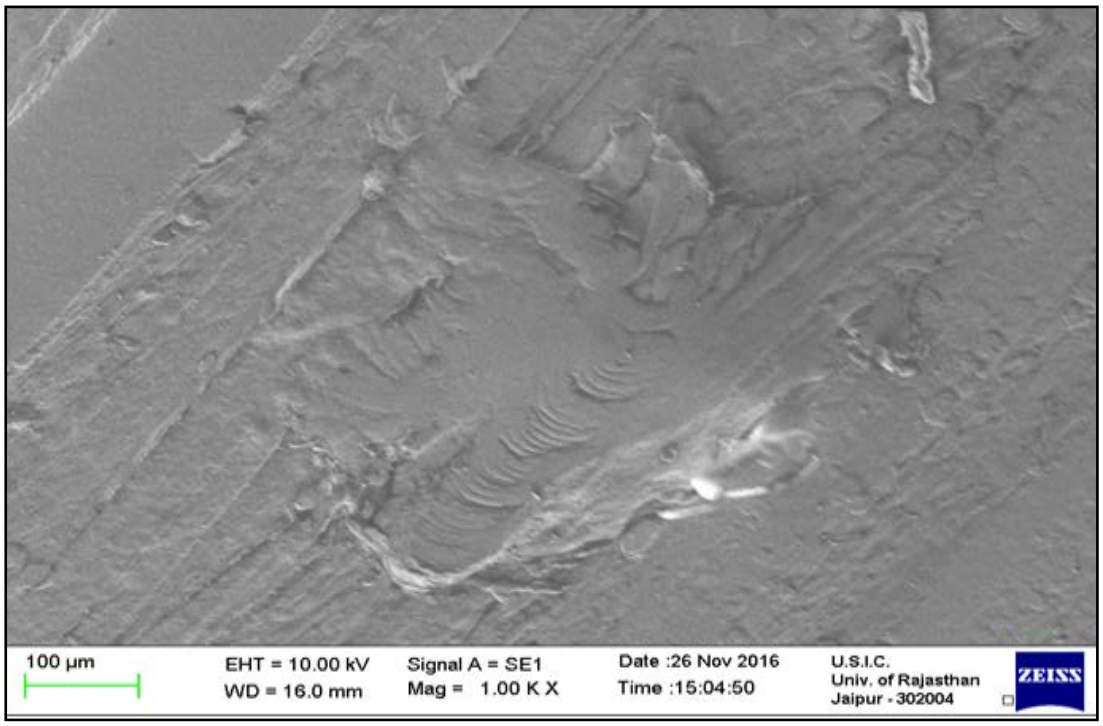

Figure 4.29[d]: Nylon 66+4wt.% Al_2O_3

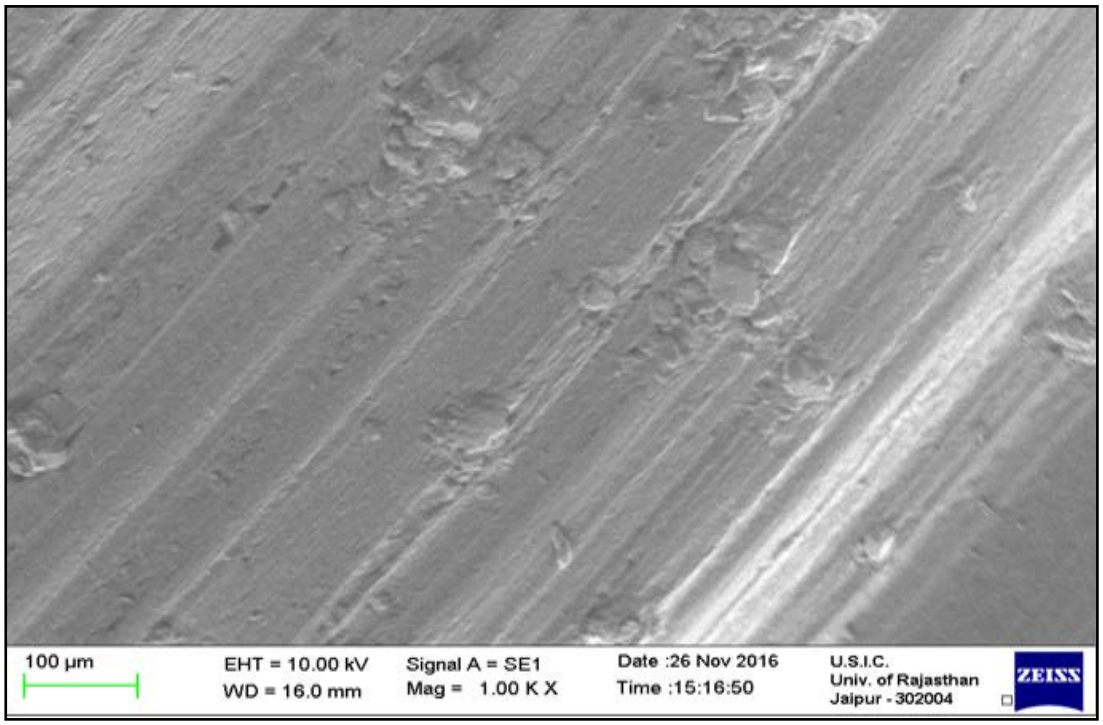

Figure 4.29 [e]: Nylon 66+6wt.% Al_2O_3

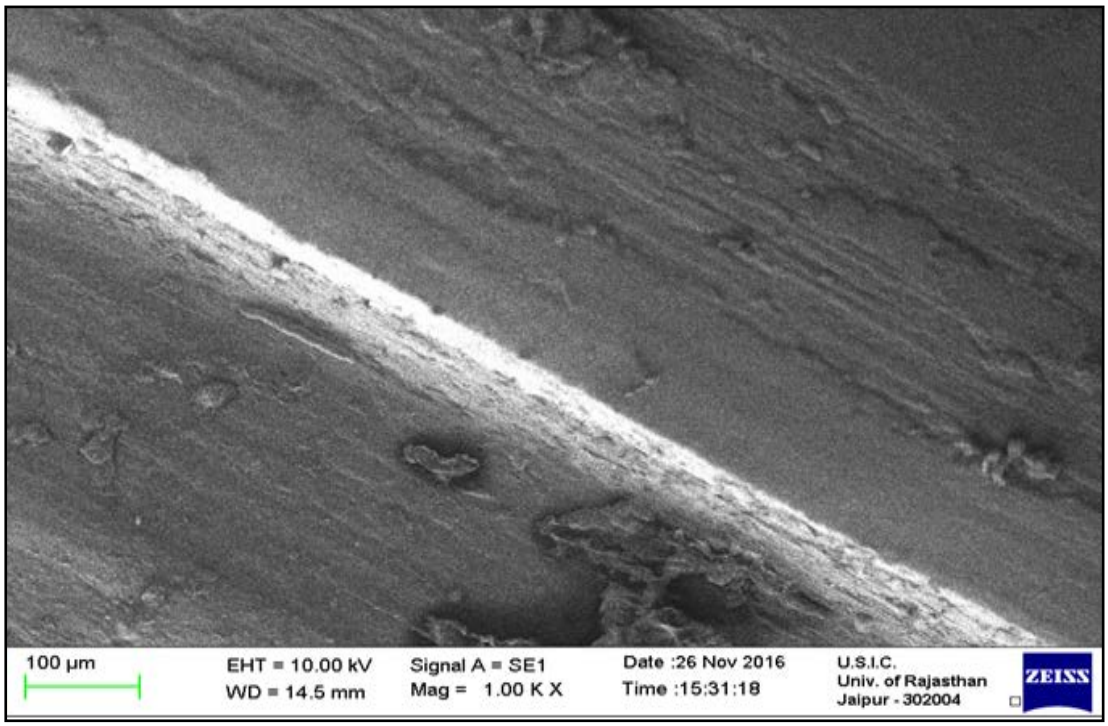

Figure 4.29[f]: Nylon 66+8wt.% Al_2O_3

Figure 4.29: Microstructure of Oilon and Al_2O_3 filled Nylon 66 composites

4.3.2 SEM of TiO_2 filled Nylon66 composites

The composite specimens are subjected to Scanning Electron Microscopy examination after the sliding wear test to understand the morphology of worn out surfaces. The representative micrographs are shown in Figures 4.30 [a] to [d]. It is noted that at lower loading, dispersion of filler in Nylon 66 matrix is good and agglomeration starts for filler e 6% and this accounts for decrease in mechanical properties. The worn surfaces mainly composed of longitudinal grooves whose width increases with the increase in filler content resulting in higher coefficient of friction. The wear is caused by micro- cutting and micro ploughing during the sliding action between the surfaces. Due to increase in the contact temperature during sliding, the Nylon 66 matrix softens resulting in increase in wear due to peeling off [186].

Figure 4.30 [a]: Nylon 66+2wt. % TiO_2

(Load: 100 N, Sliding Velocity: 6.5m/s, Sliding Distance: 2000m)

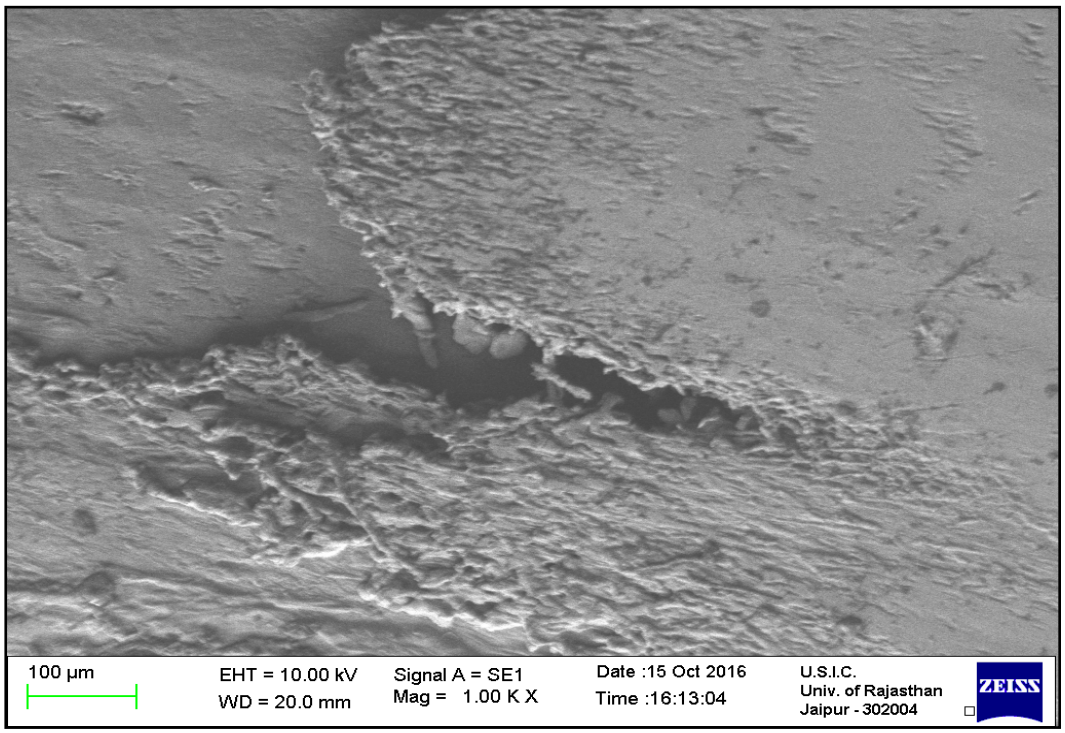

Figure 4.30[b]: Nylon 66+4wt. % TiO_2

(Load: 100 N, Sliding Velocity: 6.5m/s, Sliding Distance: 2000m)

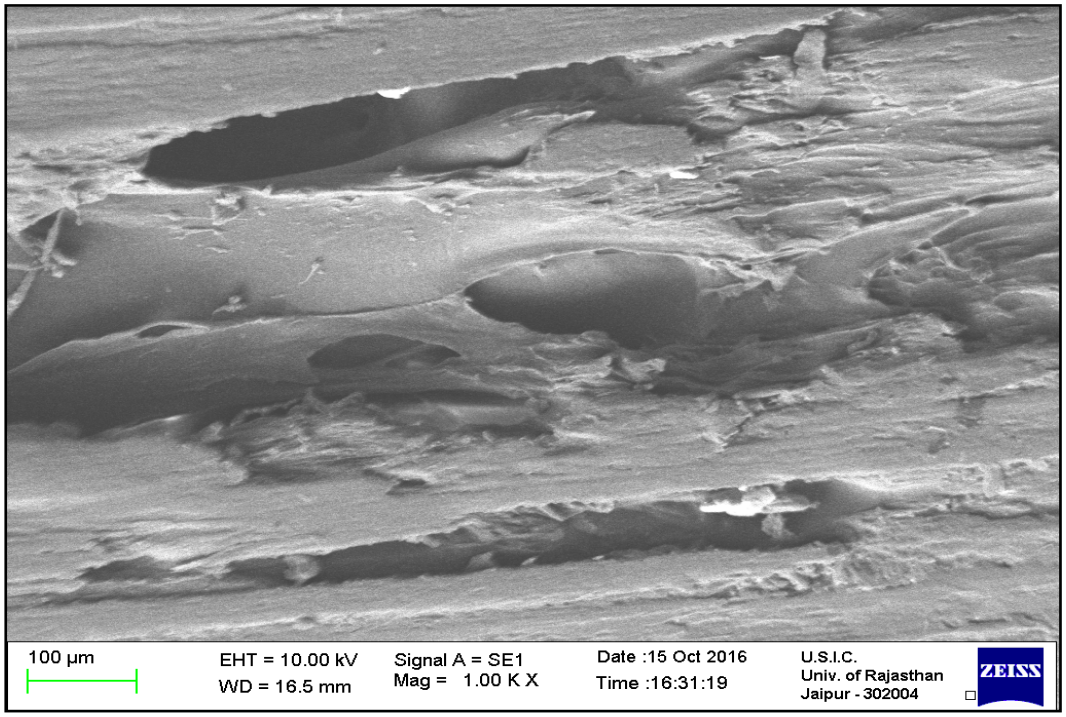

Figure 4.30[c]: Nylon 66+6wt. % TiO_2

(Load: 100 N, Sliding Velocity: 6.5m/s, Sliding Distance: 2000m)

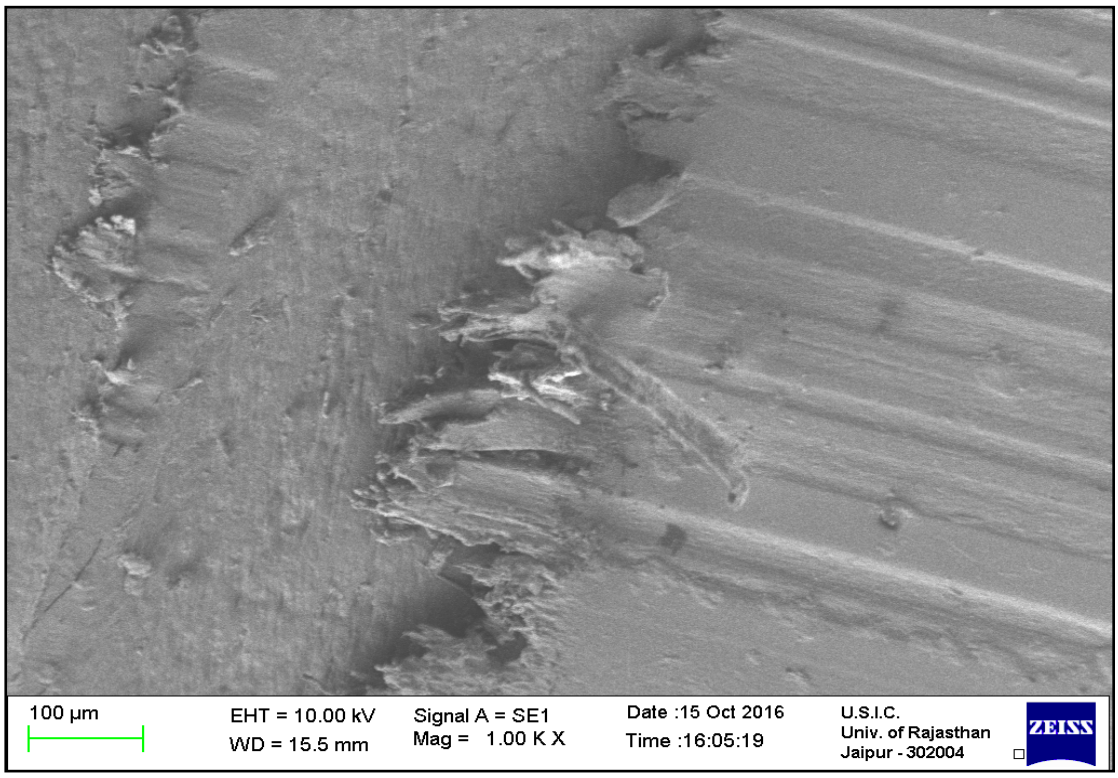

Figure 4.30[d]: Nylon 66+8wt. % TiO_2

(Load: 100 N, Sliding Velocity: 6.5m/s, Sliding Distance: 2000m)

Figure 4.30: SEM images of worn surfaces of TiO_2 filled Nylon66 composites

4.4 Material Selection by TOPSIS, Multi Criteria Design Analysis Technique

The decision matrix as shown in Table 4.5 is prepared by taking the experimental results of mechanical properties from Table 4.1-4.3.The values of wear and coefficient of friction are taken from Table 4.4 and Figures 4.17-4.28 for the experimental conditions of load 100N, sliding velocity 6.5 m/s and sliding distance 2000m. All the properties are given equal weightage.

In the next step the normalized decision matrix is prepared and the result is given in Table 4.6. The values are calculated as per the formula 3.1

Positive Ideal Solution and Negative Ideal Solution are calculated by the formulae 3.2. Example density, wear and coefficient of frictions are considered as cost factors whereas tensile strength, flexural strength, impact strength etc. are taken as benefit factors. The results of PIS and NIS are shown in Table 4.7.

The notations used in the tables are as below:

O-N	:	Oil Impregnated Nylon
N-66	:	Nylon 66
NA-2	:	Nylon 66 + 2% Al_2O_3
NA-4	:	Nylon 66 + 4% Al_2O_3
NA-6	:	Nylon 66 + 6% Al_2O_3
NA-8	:	Nylon 66 + 8% Al_2O_3
NT-2	:	Nylon 66 + 2% TiO_2
NT-4	:	Nylon 66 + 4% TiO_2
NT-6	:	Nylon 66 + 6% TiO_2
NT-8	:	Nylon 66 + 8% TiO_2
TS	:	Tensile Strength
TM	:	Tensile Modulus
II	:	Elongation
FS	:	Flexural Strength
FM	:	Flexural Modulus
CS	:	Compressive Strength
HDT	:	Heat Deflection Temperature
RH	:	Rockwell Hardness
WL	:	Wear at Load 100 N
WSV	:	Wear at Sliding Velocity 6.5 m/s
WSD	:	Wear at Sliding Distance 2000 m
COFL	:	Coefficient of Friction at Load 100 N
COFSV	:	Coefficient of Friction at Sliding Velocity 6.5 m/s
COFSD	:	Coefficient of Friction at Sliding Distance 2000 m

Table 4.5: Experimental data of mechanical and wear properties of various materials (Decision Matrix)

Samples	Density	TS	TM	II	FS	FM	CS	HDT	RH	WL	WSV	WSD	COFL	COFSV	COFSD
O-N	1.14	63	1143	5.9	82	2600	90	57	86	278.947	285.965	281.579	0.91	0.86	0.94
N-66	1.14	75	1200	5.1	111	3000	76	66.2	97	310.526	305.263	314.035	0.86	0.88	0.82
NA-2	1.15	76	1388	5.24	116	3296	84	66.8	100	113.913	104.348	135.652	0.52	0.61	0.57
NA-4	1.16	77	1408	5.96	118	3311	86	68	102	145.690	121.552	147.414	0.67	0.66	0.61
NA-6	1.17	79	1439	6.02	119	3518	88	69.4	104	315.385	311.111	321.368	0.78	0.72	0.67
NA-8	1.18	73	1313	5.88	115	3423	86	71.9	105	509.322	476.271	509.322	0.83	0.79	0.84
NT-2	1.15	76	1261	5.15	114	3045	82	67.1	98	97.391	92.174	101.739	0.61	0.72	0.69
NT-4	1.17	78	1326	5.48	116	3206	84	68.3	101	127.350	103.419	278.814	0.84	0.78	0.64
NT-6	1.18	82	1489	5.96	119	3436	85	69	104	287.288	268.644	114.530	0.73	0.84	0.79
NT-8	1.19	78	1458	5.46	115	3021	83	71.6	102	452.101	435.294	443.697	0.93	0.91	0.96

Table 4.6 Normalized decision matrix

Samples	Density	TS	TM	II	FS	FM	CS	HDT	RH	WL	WSV	WSD	COFL	COFSV	COFSD
O-N	0.3099	0.2626	0.2684	0.3316	0.2295	0.2572	0.3369	0.2665	0.2719	0.2974	0.3187	0.3004	0.3697	0.3475	0.3890
N-66	0.3099	0.3127	0.2817	0.2867	0.3107	0.2968	0.2845	0.3095	0.3066	0.3310	0.3402	0.3350	0.3494	0.3556	0.3394
NA-2	0.3127	0.3168	0.3259	0.2945	0.3247	0.3261	0.3144	0.3123	0.3161	0.1214	0.1163	0.1447	0.2112	0.2465	0.2359
NA-4	0.3154	0.3210	0.3306	0.3350	0.3303	0.3276	0.3219	0.3179	0.3224	0.1553	0.1355	0.1573	0.2722	0.2667	0.2524
NA-6	0.3181	0.3293	0.3379	0.3384	0.3331	0.3481	0.3294	0.3244	0.3288	0.3362	0.3467	0.3428	0.3169	0.2909	0.2773
NA-8	0.3208	0.3043	0.3083	0.3305	0.3219	0.3387	0.3219	0.3361	0.3319	0.5430	0.5308	0.5433	0.3372	0.3192	0.3476
NT-2	0.3127	0.3168	0.2961	0.2895	0.3191	0.3013	0.3070	0.3137	0.3098	0.1038	0.1027	0.1085	0.2478	0.2909	0.2856
NT-4	0.3181	0.3252	0.3113	0.3080	0.3247	0.3172	0.3144	0.3193	0.3193	0.1358	0.1153	0.2974	0.3412	0.3152	0.2649
NT-6	0.3208	0.3419	0.3496	0.3350	0.3331	0.3399	0.3182	0.3226	0.3288	0.3063	0.2994	0.1222	0.2965	0.3394	0.3269
NT-8	0.3235	0.3252	0.3423	0.3069	0.3219	0.2989	0.3107	0.3347	0.3224	0.4820	0.4851	0.4733	0.3778	0.3677	0.3973

Table 4.7: Positive Ideal Solution (PIS) and Negative Ideal Solution (NIS)

R^+	**0.3099**	**0.3419**	**0.3496**	**0.3384**	**0.3331**	**0.3481**	**0.3369**	**0.3361**	**0.3319**	**0.1038**	**0.1027**	**0.1085**	**0.2112**	**0.2465**	**0.2359**
R^-	**0.3235**	**0.2626**	**0.2684**	**0.2867**	**0.2295**	**0.2572**	**0.2845**	**0.2665**	**0.2719**	**0.5430**	**0.5308**	**0.5433**	**0.3778**	**0.3677**	**0.3973**

Finally, the euclidian distances between each of the alternatives and the positive ideal solution and the negative ideal solution are calculated as per formula 3.3 and the closeness index is calculated by the formula 3.4. The various materials are then ranked as per the result of closeness index. Higher the closeness index better is the rank of the material. The results are tabulated in Table 4.8.

Table 4.8: Closeness index and ranking of the alternatives

	D+	**D-**	**C.I.**	**RANK**
O-N	0.469054	0.412085	0.4677	**7**
N-66	0.465131	0.378185	0.4485	**8**
NA-2	0.08244	0.775915	0.904	**1**
NA-4	0.111369	0.727547	0.8672	**2**
NA-6	0.428765	0.424743	0.4976	**6**
NA-8	0.776201	0.191702	0.1981	**10**
NT-2	0.126271	0.78636	0.8616	**3**
NT-4	0.253011	0.667388	0.7251	**4**
NT-6	0.323715	0.582736	0.6429	**5**
NT-8	0.703984	0.196637	0.2183	**9**

From the results it is deduced that the composite of Nylon66 with 2 wt. % of aluminum oxide ranked first in the closeness index and it is recommended to chose this material due to its better mechanical and tribological properties for the application of knee joint for above knee prosthesis.

CHAPTER 5

FINITE ELEMENT ANALYSIS OF KNEE JOINT PROSTHESIS

CHAPTER 5

FINITE ELEMENT ANALYSIS OF KNEE JOINT PROSTHESIS

This chapter covers the finite element analysis of knee joint prosthesis. The test procedure of ISO 10328:2006 as explained in Chapter 3 is used to conduct static proof and ultimate stress analysis of the above knee prosthesis, used in developing country, by finite element method. The finite element analysis is performed with the material properties of oil impregnated nylon and the newly developed composite of Nylon66 prepared by adding 2 wt. % of aluminium oxide.

5.1 Three Dimensional CAD Model of Knee Prosthesis

The knee prosthesis individual components are measured with the help of measuring instruments - digital vernier calliper and three dimensional coordinate measuring machine of Electronica make (Model-Ruby CNC 564). Creo3.0 CAD modelling software is used to develop three dimensional solid model of the individual components and assembly of the knee prosthesis.

The knee prosthesis is a four bar linkage mechanism made of Oilon material (Nylon 6 impregnated with oil) which consists of upper block, lower block, middle link and two side links assembled with steel screws & hinges. The total weight of the knee joint components is 372 grams. The individual components are shown in Figure 5.1 and assembly is shown in Figure 5.2

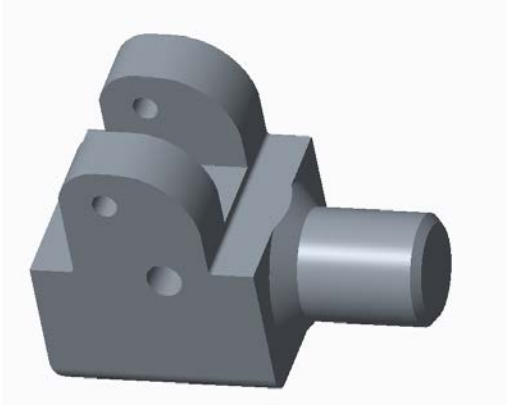

1. Upper Block

2. Side Link – 2 Nos.

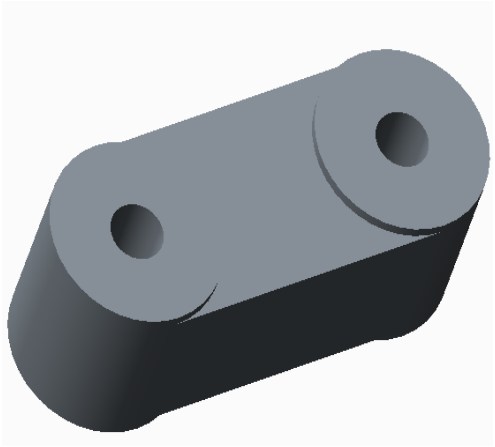

3. Middle Link

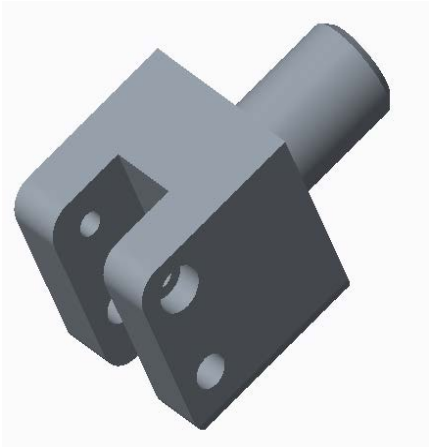

4. Lower Block

Figure 5.1: Components of knee prosthesis

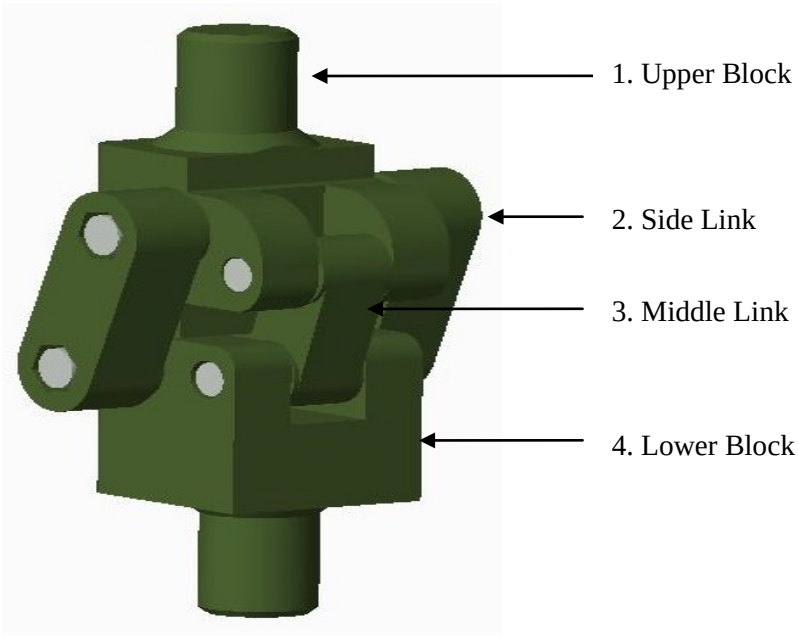

Figure 5.2 Assembly of knee prosthesis

5.2 Finite Element Analysis

ANSYS 16.0 software is used for the static and cyclic stress analysis of the knee joint prosthesis. For performing the analysis for the principal structural tests, the CAD model of the knee joint prosthesis is developed by adding end attachments, load application levers and non-prosthetic extension pieces. The total length of the assembly for test set-up is maintained to 650 mm as per the requirement of the ISO 10328 standard. The CAD model of the analysis set-up is shown in Figure 5.3

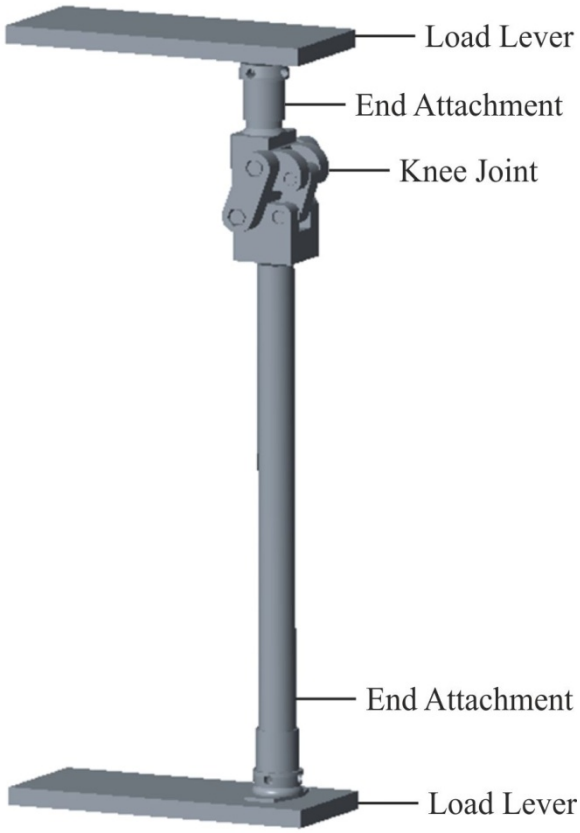

Figure 5.3: CAD model of knee prosthesis with end attachments and load lever

5.2.1 Loading Conditions and Load Line

According to the ISO 10328 standard, a single test force is applied through a specific line of load application and depending upon test conditions and load levels, the magnitude and direction of the test force are varied. As the knee prosthesis is widely utilized by people of developing countries, the loading values associated with level P5, corresponding to the amputee of 100kg weight, have been applied to the models to be analysed. For the complete structure analysis, both the test conditions, representing the peak loads exerting on the prosthesis at the beginning and end of the stance phase of walking, hereafter called condition I- Heel loading and condition II- Forefoot loading, respectively are done. Load conditions corresponding to the selected test load level P5 used for various simulations during this study are as per Table 5.1.

Table 5.1: Load conditions

Type of test	**Test load**	**Unit**	**Test loading level P5**	
			Heel loading	**Forefoot loading**
Static test	Proof test force	N	2240	2013
	Ultimate test force	N	3360	3019
Cyclic test	Min. test force	N	50	
	Max. test force	N	1330	1200
	Prescribed number of cycles	Nos.	$3x\ 10^6$	

The test load for P5 level for various finite element analyses as per Table 5.1 is applied along the load line passing through the reference planes as per the offset values given in Table 5.2 in accordance to the ISO 10328 standard.

Table 5.2 Loading offset values

Reference plane	**Direction and location**	**Offset in mm**	
		Test loading level P5	
		Loading Condition I	**Loading Condition II**
Top	f_T	82	55
	o_T	-79	-40
Knee	f_K	52	72
	o_K	-50	-35
Bottom	f_B	-48	129
	o_B	45	-19

The CAD model for the analysis set-up showing the load vector for loading condition I & II is depicted in Figure 5.4

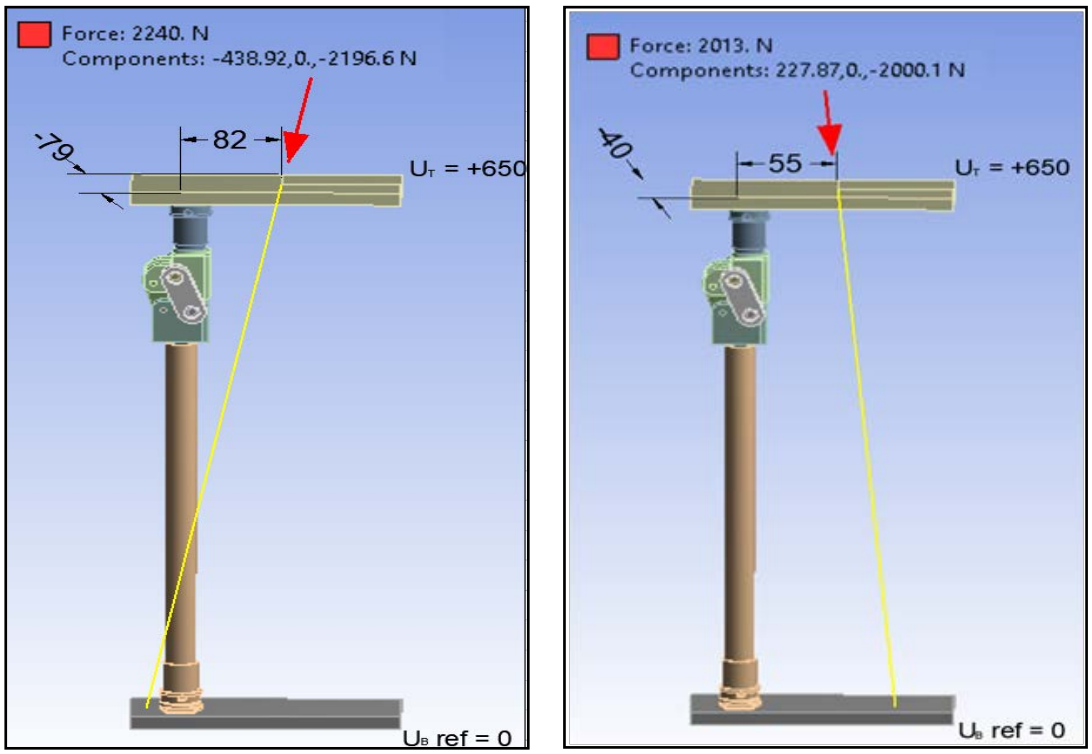

(a) Test loading condition I- Heel loading

(b) Test loading condition II- Fore foot loading

Figure 5.4: CAD model of analysis set-up showing the load vector

5.2.2 Material Properties

For performing the finite element analysis, the material properties are taken from Table 3.2 & 3.3 and are assigned to the CAD model as per Table 5.3. The CAD model from Creo 3.0 is imported to ANSYS software.

Table 5.3: Material Properties

Material	**Density (kg/m^3)**	**Yield Strength (MPa)**	**Poisson's Ratio**
Oilon (Nylon 6 impregnated with Oil)	1.14	63	0.39
Composite of Nylon 66 with 2 wt.% Al_2O_3	1.15	76	0.33
Steel	7850	300	0.30

5.2.3 Meshing

For the purpose of doing the finite element analysis, the solid model is divided into smaller elements called finite elements. The accuracy of any finite

element simulation depends to a large extent on the shape and size of the finite element. Smaller the size of the element, it needs more computational time and also the stress concentrations can lead to stress singularities where the maximum stress increases without limit as the element size is reduced.

Mesh convergence test was conducted before completing the meshing and stress level on assembly was tested for different size of elements as shown in Table 5.4 and Figure 5.5.

Table 5.4: Mesh convergence test

Element Size (mm)	No. of Elements	No. of Nodes	von Mises stress (MPa)
6.0	16678	31923	135.83
5.8	17194	32980	134.14
5.6	17548	33748	141.75
5.4	19171	37172	144.58
5.2	19865	39662	146.56
5.0	**22834**	**45342**	**146.24**
4.8	23448	46380	146.09

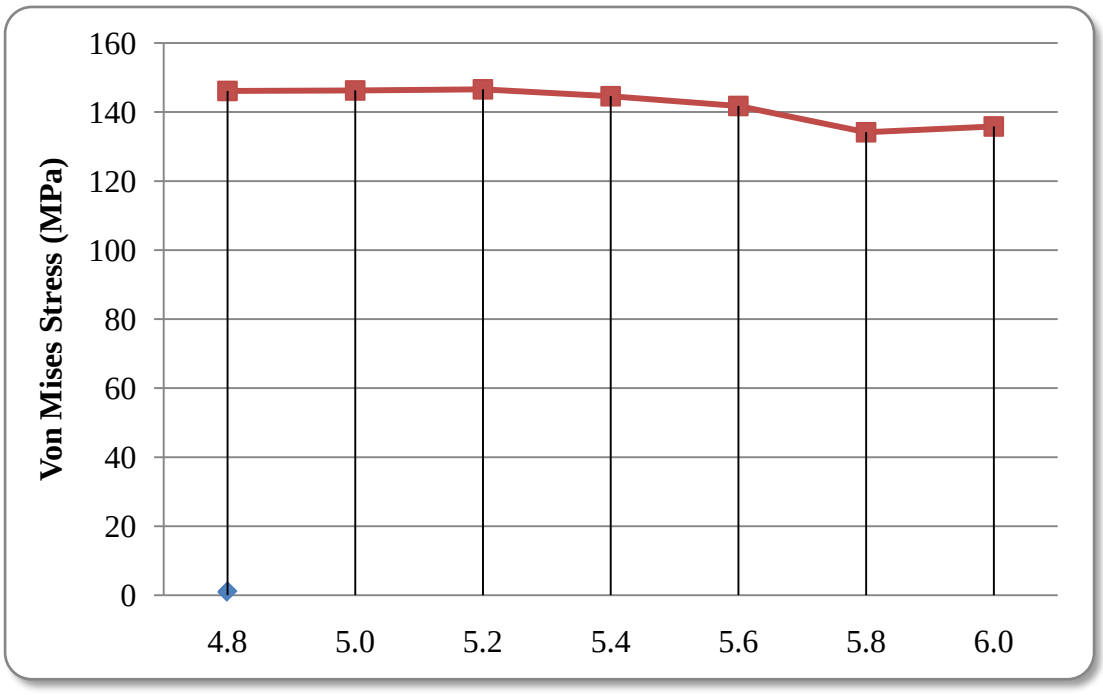

Figure 5.5 Mesh convergence test

The meshing of 3D CAD model of knee joint prosthesis was generated using Auto mode. In meshing with Auto mode, the element shape is selected automatically using computer algorithm. Automatic meshing refers to the automatic creation and numbering of nodes and elements based on a minimal amount of user supplied data. The Automatic mesh generation reduces errors, and saves a great deal of user time, therefore reducing the FEA cost.

The size of the mesh element equal to 5.0 mm is created by applying patch conformation method in Manual meshing mode. For the refinement of mesh, Advance size function and Curvature size function are used. The meshed model with tetrahedral mesh element of 5.00 mm containing 22834 elements with 45342 nodes is generated as shown in Figure 5.6

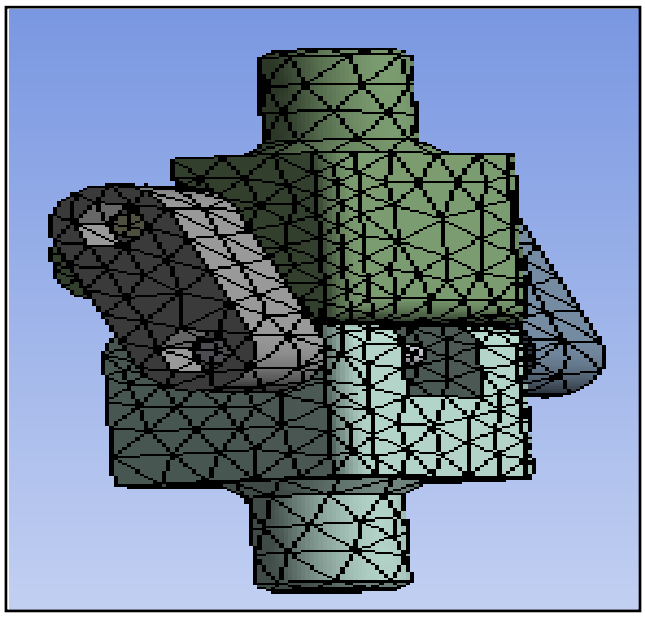

Figure 5.6: Meshed knee prosthesis CAD model

Tetrahedral elements are best suitable for 3 D complex geometries and can be used with adaptive mesh refinement. Also, less computational time is needed with this mesh element.

5.2.4 Defining Interfaces

In ANSYS 16.0 various types of interfaces are available and in this study Bonded type contact is considered at the assembly points. This is the default

configuration and applies to all contact regions (surfaces, solids, lines, faces, edges). If contact regions are bonded, then no sliding or separation between faces or edges is allowed. This type of contact allows for a linear solution since the contact length/ area will not change during the application of the load.

5.2.5 Boundary Conditions

The constant force as per the values mentioned in Table 5.1 is applied along the load line as per the load offset values mentioned in Table 5.2 from the top while keeping the bottom fixed.

5.3 Finite Element Analysis Results

Once the necessary prerequisite steps of assigning the material properties, meshing, defining interfaces and boundary condition is completed, the static structural analysis for proof and ultimate strength is performed, for both the loading conditions i.e. heel loading and forefoot loading as per the loads prescribed by ISO 10328 standard for P5 loading Table 5.1. The post processing of the ANSYS analysis results is taken in the form of von Mises stresses and the total deformation.

5.3.1 Static test for proof strength

5.3.1.1 Static test for proof strength; Loading condition I; Oilon material

Load of 2240 N is applied for conducting the above analysis with the material properties of Oilon material assigned to the CAD model. The results of von Mises stresses and total deformation on individual components and the assembly are given in Table 5.5 and Figure 5.7 & 5.8 respectively.

Table 5.5: Result for Static test (proof strength); loading condition I; Oilon material

Result	Upper Block	Lower Block	Side Link	Middle Link	Knee Prosthesis
Von Mises stress (MPa)	70.85	40.80	54.52	51.97	70.85
Total deformation (mm)	7.52	2.09	3.01	2.16	7.52

Upper Block

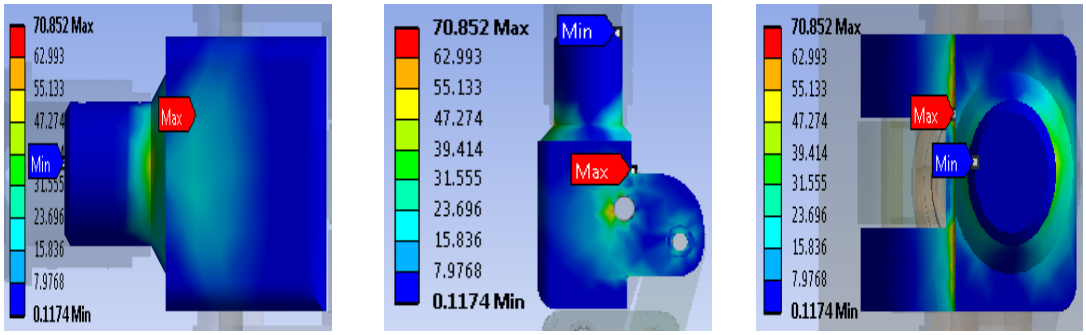

Lower Block

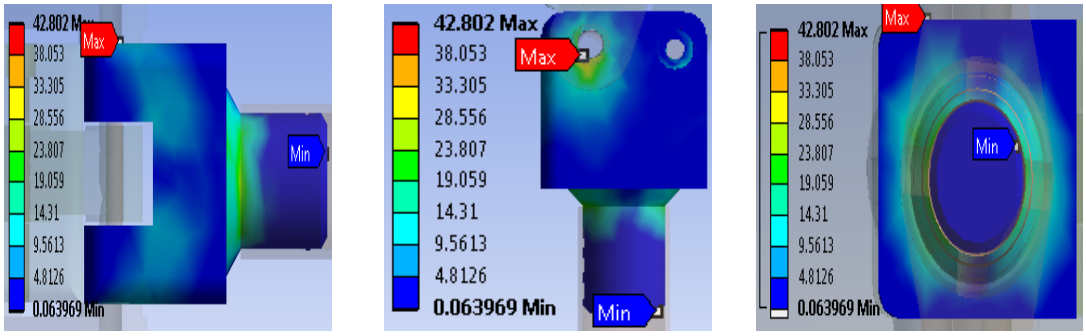

Side Link

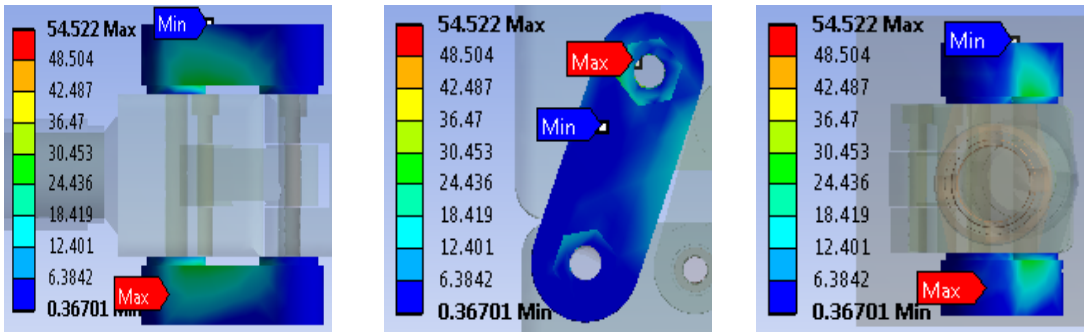

Middle Link

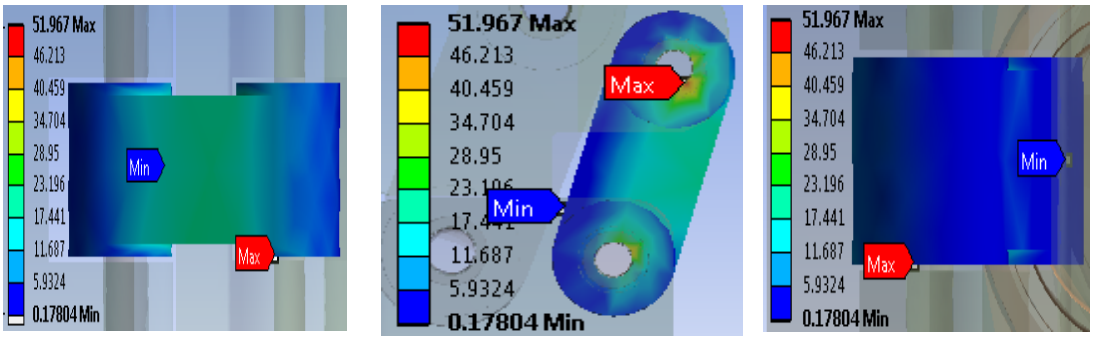

Figure 5.7: von Mises stress for Static test (proof strength); loading condition I; Oilon material

Upper Block

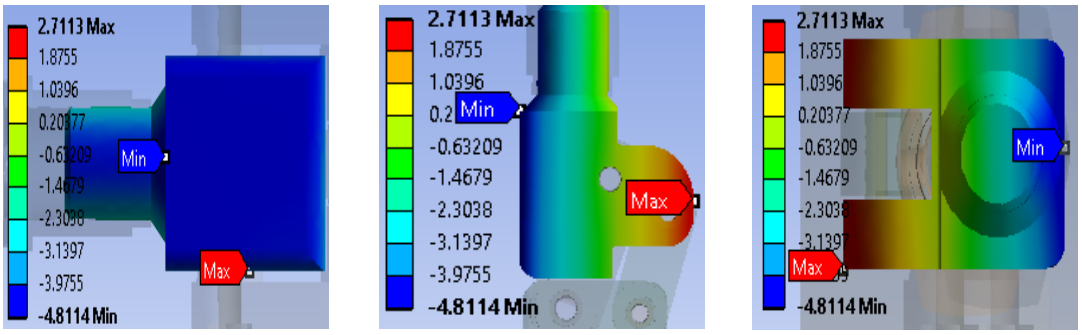

Lower Block

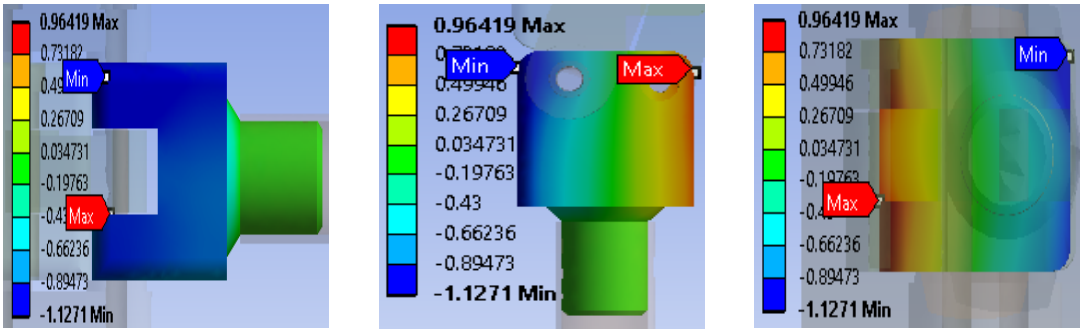

Side Link

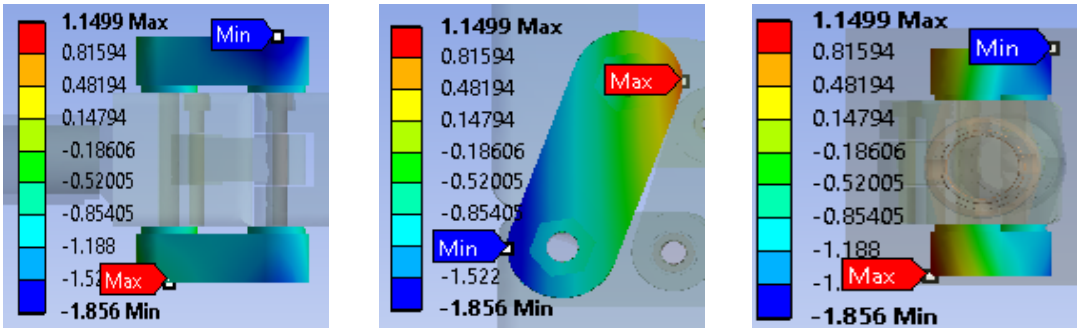

Middle Link

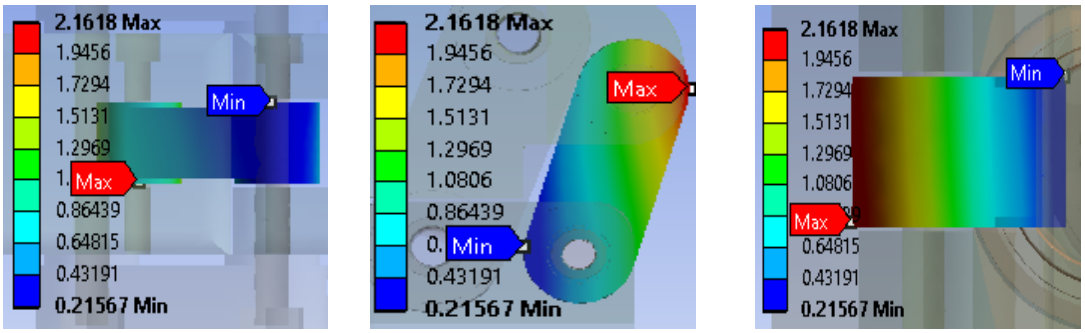

Figure 5.8 Total deformation for Static test (proof strength); loading condition I; Oilon material

From the finite element analysis results it is noted that the von Mises stresses are less than the yield strength of Oilon material of 63MPa for lower block, side link and middle link whereas maximum von Mises stresses in upper block is 70.852 MPa. Maximum stress concentration is noted in the assembly holes and sharp corners of the upper block. The total deformation is also more than the maximum permissible value of 5 mm. It can be construed that the upper block does not meet the criteria of ISO 10328 standard.

5.3.1.2 Static test for proof strength; Loading condition II; Oilon material

Load of 2013 N is applied for conducting the above analysis with the material properties of Oilon material assigned to the CAD model. The results of von Mises stresses and total deformation on individual components and the assembly are given in Table 5.6 and Figure 5.9 & 5.10 respectively.

Table 5.6: Result for static test (proof strength); loading condition II; Oilon material

Result	Upper Block	Lower Block	Side Link	Middle Link	Knee Prosthesis
Von Mises stress (MPa)	97.20	59.28	67.77	71.36	97.20
Total deformation (mm)	13.33	5.43	6.57	5.15	13.33

The results of finite element analysis shows that the von Mises stresses are less than the yield strength of Oilon material of 63MPa for lower block and more for upper block, side link and middle link. Maximum von Mises stresses are observed in upper block i.e. 97.204 MPa. Maximum stress concentration is noted in the assembly holes and sharp corners of the upper block. The total deformation is also on the higher side than the maximum permissible value of 5 mm and the assembly does not meet the criteria of ISO 10328 standard.

From Table 5.5 & 5.6, it is noted that, in load condition II forefoot loading (2013N), the stresses observed are more compared to the loading condition I (2240N) for static test (proof strength) for Oilon material.

Upper Block

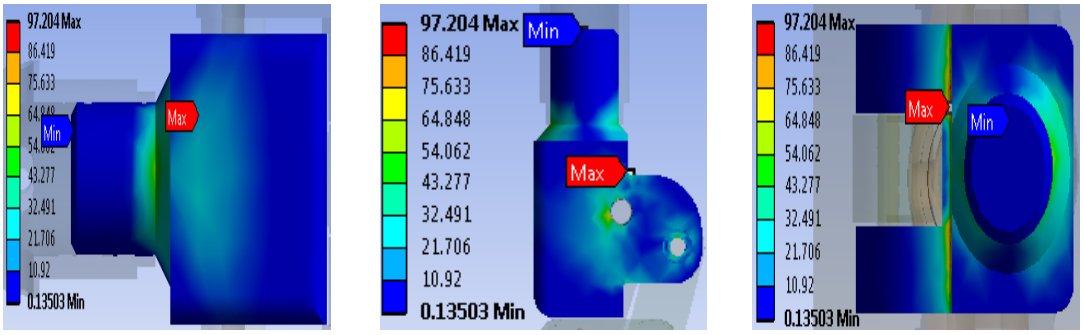

Lower Block

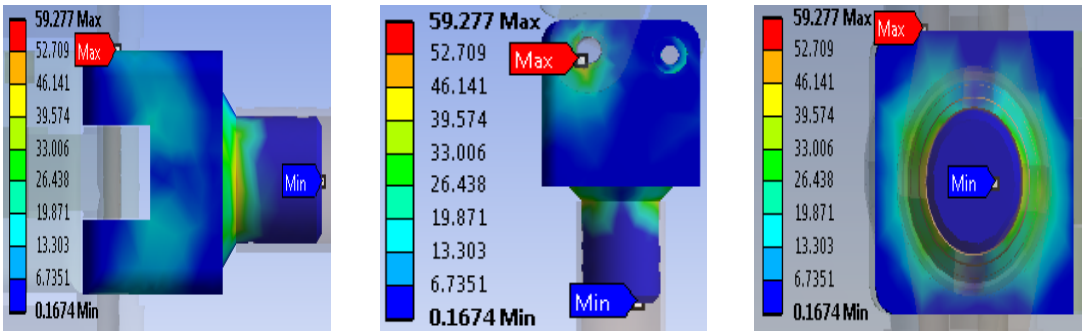

Side Link

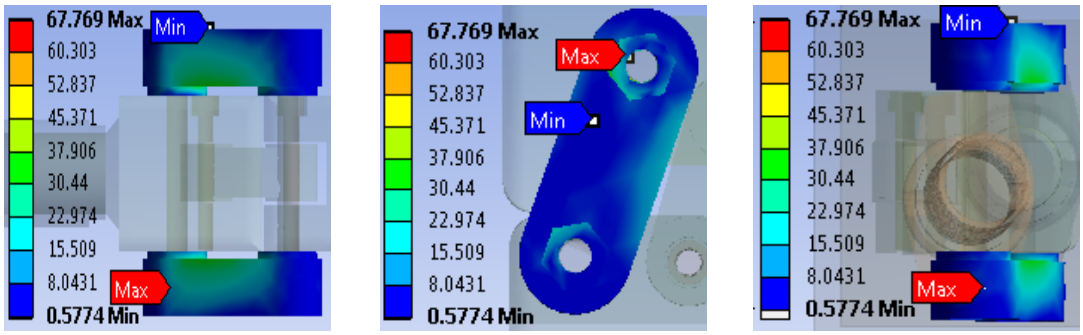

Middle Link

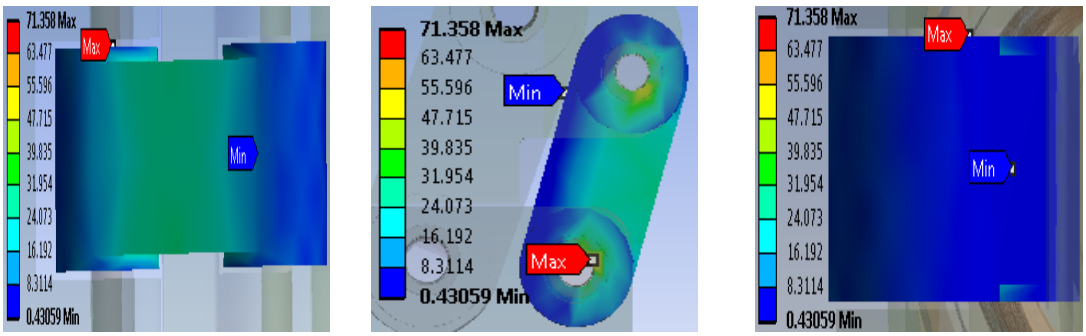

Figure: 5.9 von Mises stress for Static test (proof strength); loading condition II; Oilon material

Upper Block

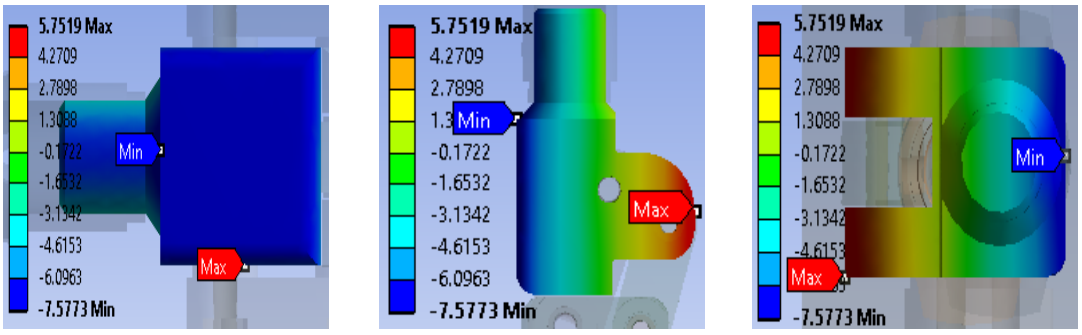

Lower Block

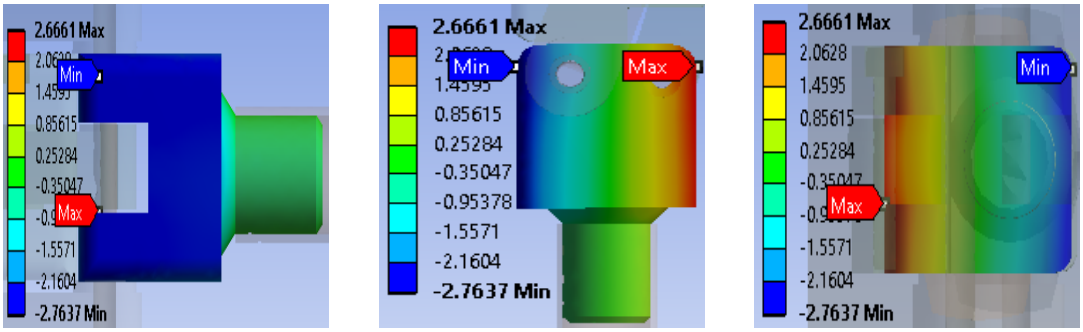

Side Link

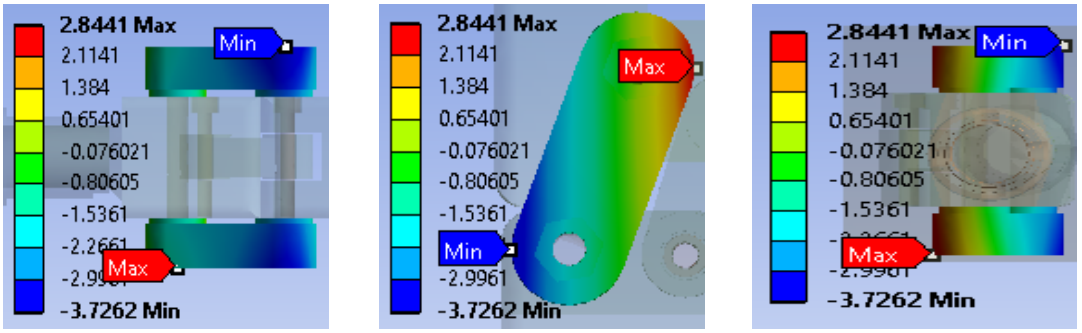

Middle Link

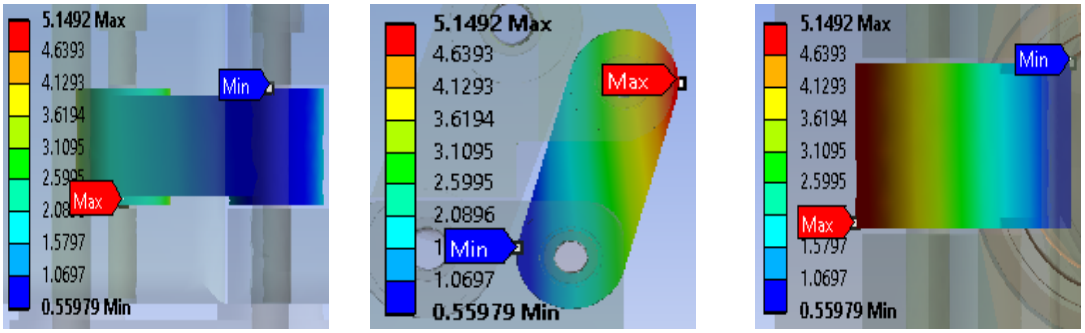

Figure 5.10 Total deformation for Static test (proof strength); loading condition II; Oilon material

5.3.1.3 Static test for proof strength; Loading condition I; Nylon 66 with 2 wt.% Al_2O_3 composite

The composite of Nylon66 with 2 wt.% of Al_2O_3 which is selected by the multi objective design criteria is analysed for its suitability and its mechanical properties are assigned to the CAD model of knee joint prosthesis in the ANSYS software. Load of 2240 N is applied for conducting the above analysis and the results of von Mises stresses and total deformation on individual components and the assembly are given in Table 5.7 and Figure 5.11 & 5.12 respectively.

Table 5.7 Result for Static test (proof strength); loading condition I; Nylon 66 with 2 wt.% Al_2O_3 composite

Result	Upper Block	Lower Block	Side Link	Middle Link	Knee Prosthesis
Von Mises stress (MPa)	71.29	42.31	52.64	51.52	71.29
Total deformation (mm)	7.40	1.91	2.78	1.20	7.40

The von Mises stress values observed in all the four components of the knee prosthesis are less than that of the yield strength of the developed composite of Nylon 66 with 2 wt.% Al_2O_3. Thus it meets the requirement of yield strength criterion; however the total deformation of upper block is more than the prescribed value of 5mm as per ISO 10328 standard.

Upper Block

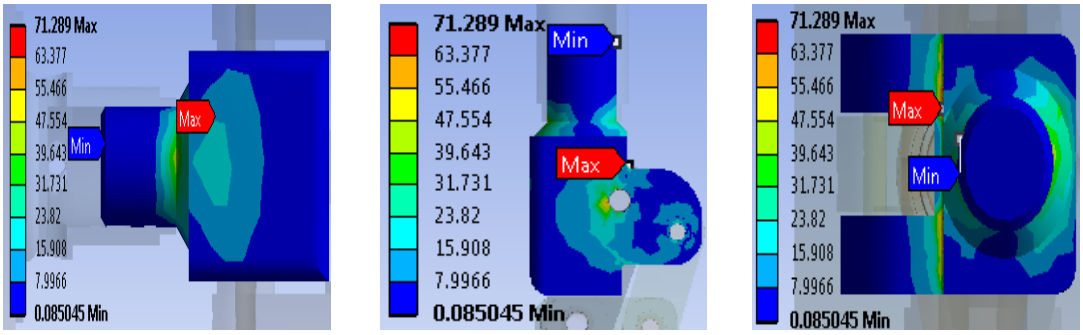

Lower Block

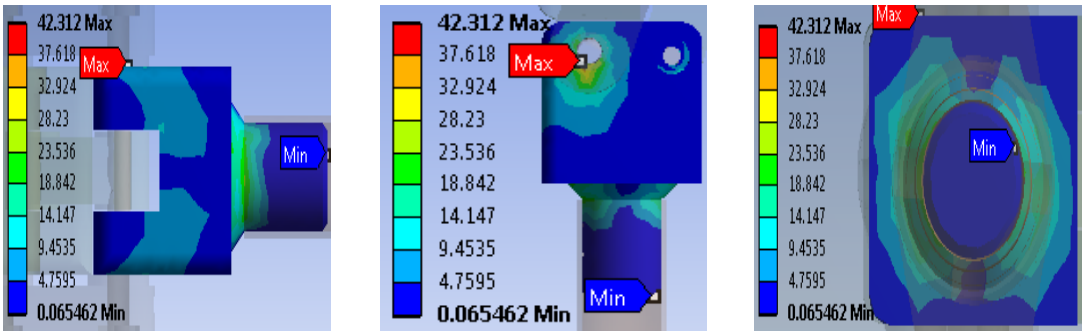

Side Link

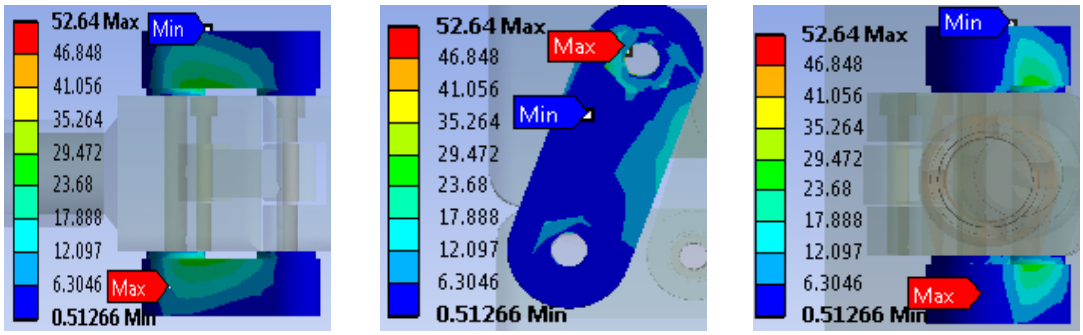

Middle Link

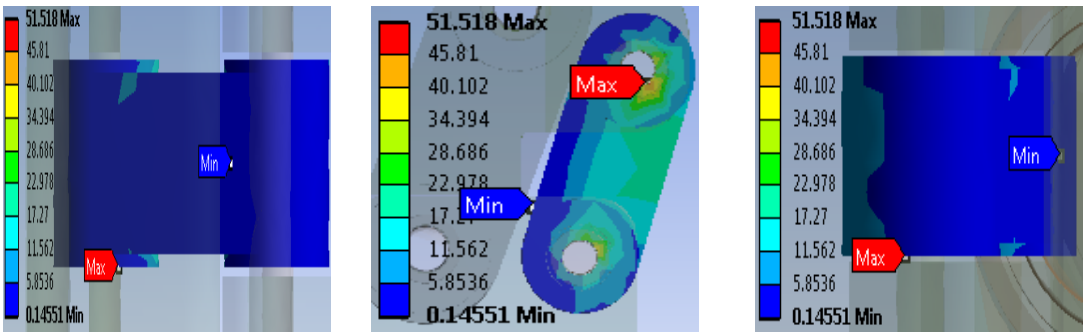

Figure 5.11: von Mises stress for Static test (proof strength); loading condition I; Nylon 66 with 2 wt. % Al_2O_3 composite

Upper Block

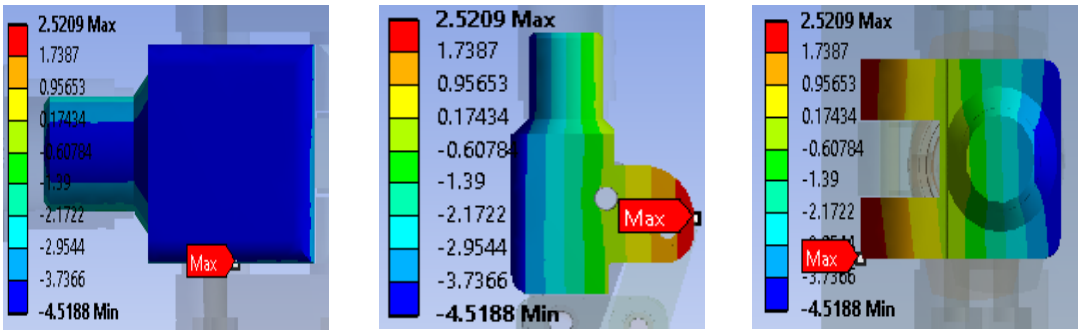

Lower Block

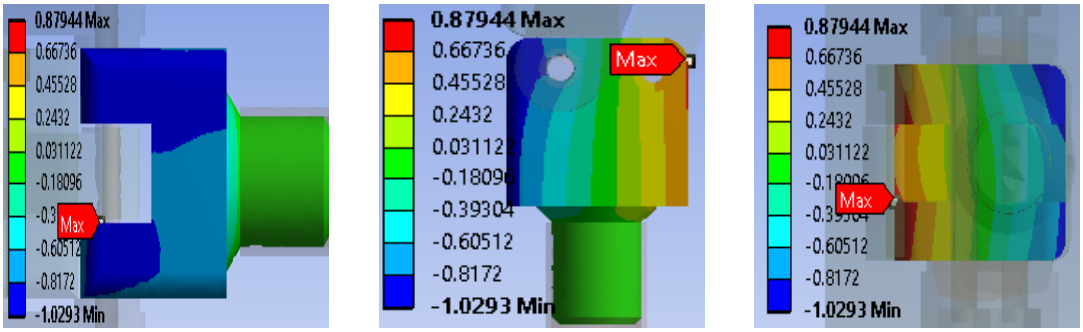

Side Link

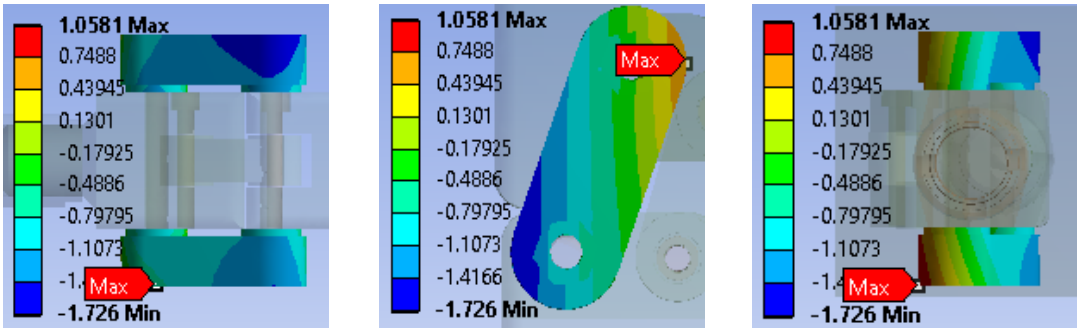

Middle Link

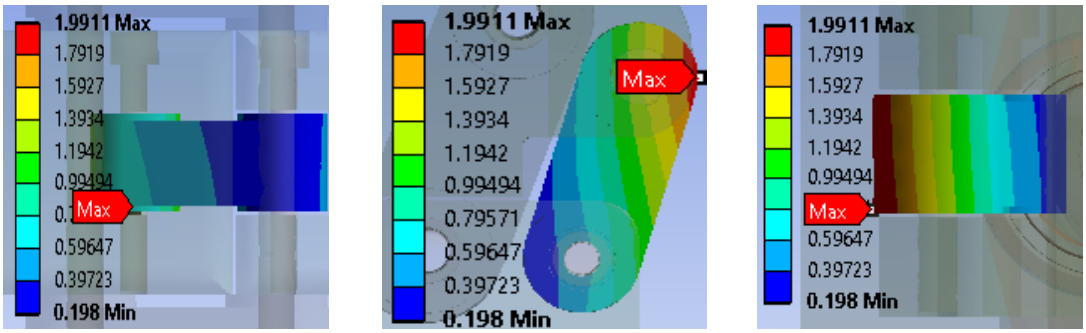

Figure 5.12: Total deformation for Static test (proof strength); loading condition I; Nylon 66 with 2 wt.% Al_2O_3 composite

5.3.1.4 Static test for proof strength; Loading condition II; Nylon 66 with 2 wt.% Al_2O_3 composite

Knee joint prosthesis with composite of Nylon66 with 2 wt.% Al_2O_3 is subjected to finite element analysis at a load of 2013N. The results of von Mises stresses and total deformation on individual components and the assembly are given in Table 5.8 and Figure 5.13 & 5.14 respectively.

Table 5.8: Result for Static test (proof strength); loading condition II; Nylon 66 with 2 wt.% Al_2O_3 composite

Result	Upper Block	Lower Block	Side Link	Middle Link	Knee Prosthesis
Von Mises stress (MPa)	97.72	58.66	65.39	69.49	97.72
Total deformation (mm)	12.57	5.09	6.18	4.83	12.57

From the finite element results, it is noted that the maximum von Mises stress of 97.722 MPa is in the upper block and which is more than the yield strength of the composite of Nylon 66 with 2 wt. % Al_2O_3. Also, the stresses are more severe in loading condition II. Further, the total deformation is more than the standard limits.

Upper Block

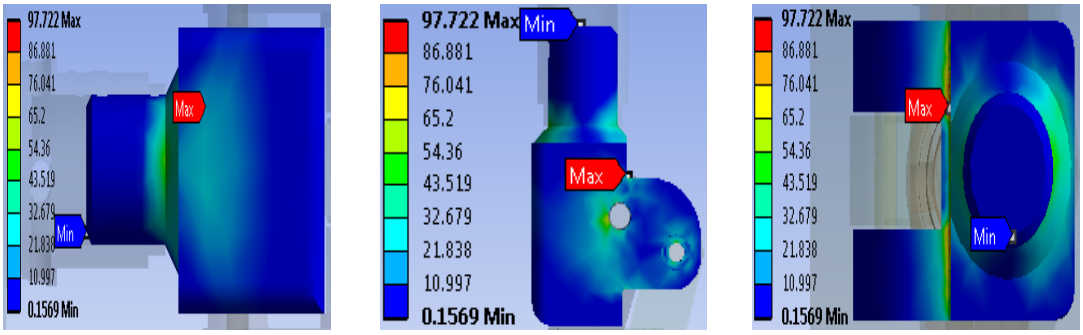

Lower Block

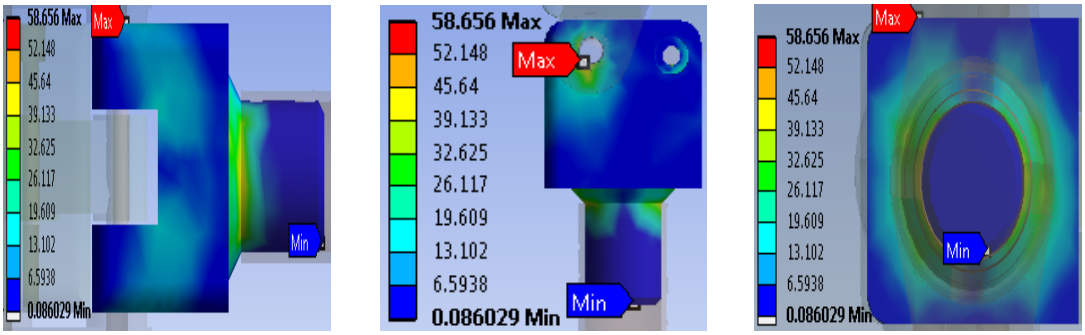

Side Link

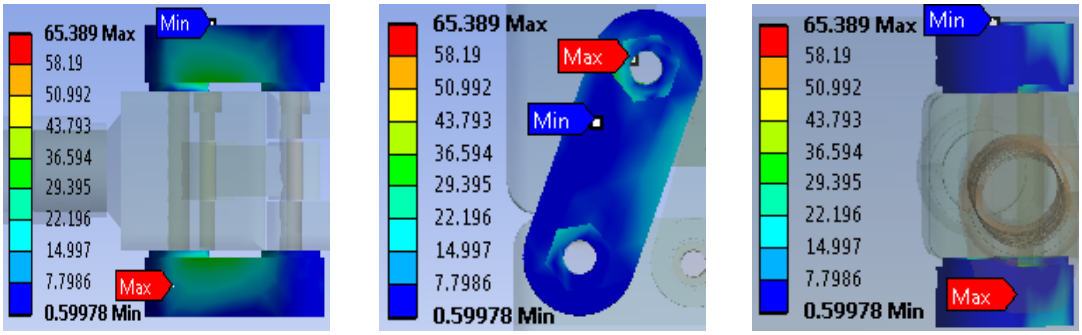

Middle Link

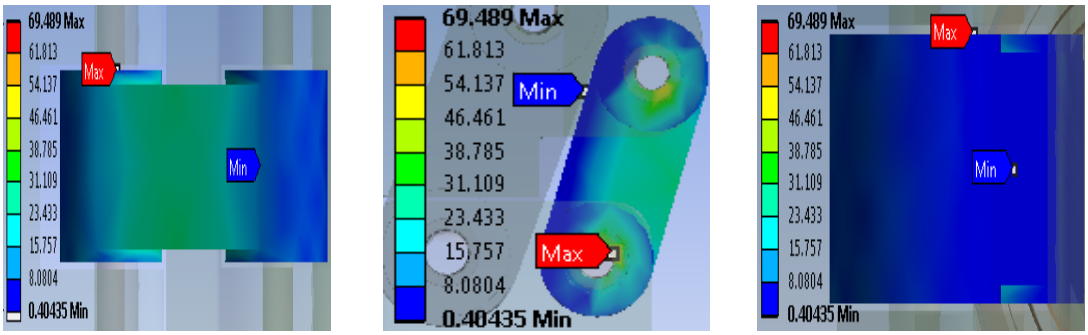

Figure 5.13: von Mises stress for Static test (proof strength); loading condition II; Nylon 66 with 2 wt.% Al_2O_3 composite

Upper Block

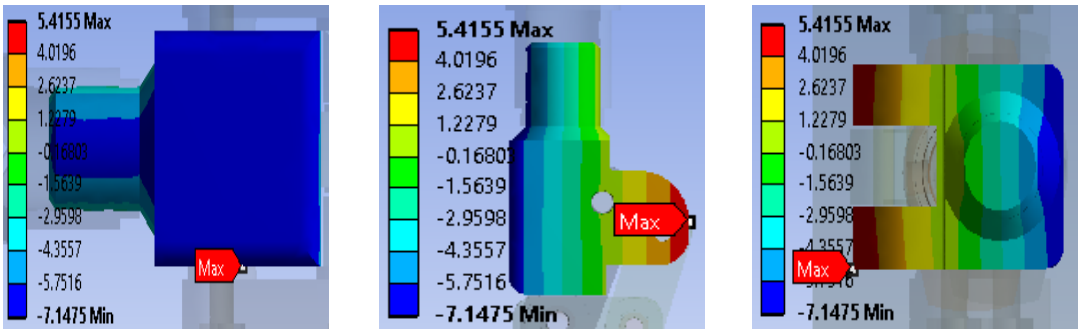

Lower Block

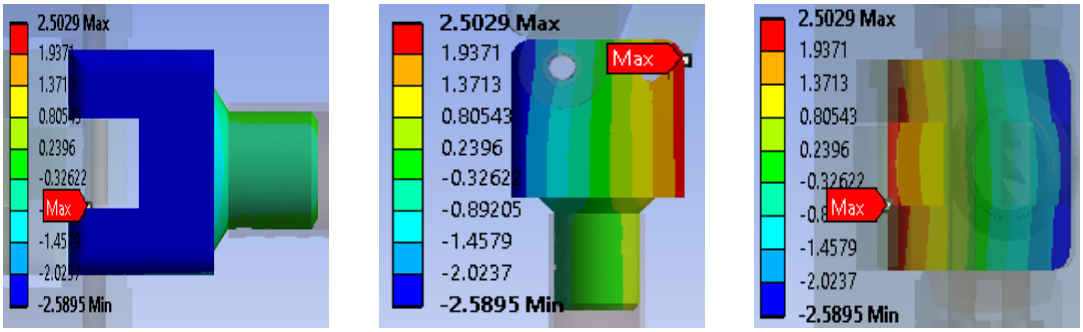

Side Link

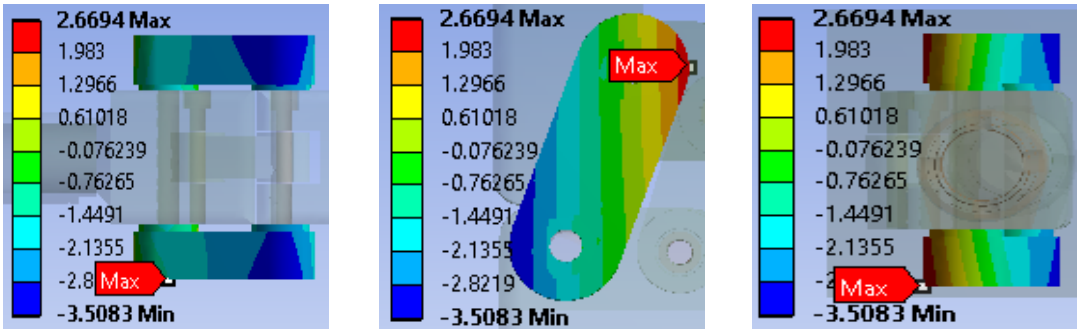

Middle Link

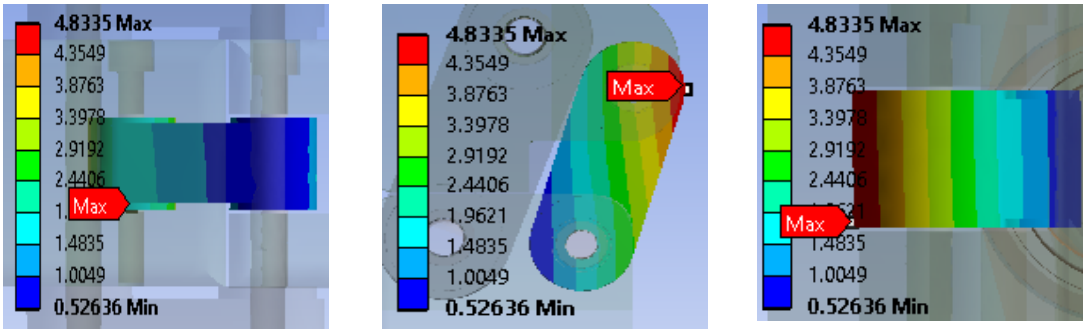

Figure 5.14: Total deformation for Static test (proof strength); loading condition II; Nylon 66 with 2 wt.% Al_2O_3 composite

5.3.2 Static test for ultimate strength

5.3.2.1 Static test for ultimate strength; Loading condition I; Oilon material

Load of 3360 N is applied for conducting the above analysis with the material properties of Oilon material assigned to the CAD model. The results of von Mises stresses and total deformation on individual components and the assembly are given in Table 5.9 and Figure 5.15 & 5.16 respectively.

Table 5.9: Result for Static test (ultimate strength); loading condition I; Oilon material

	Upper Block	**Lower Block**	**Side Link**	**Middle Link**	**Knee Prosthesis**
Von Mises stress (MPa)	106.28	64.20	81.78	77.95	106.28
Total deformation (mm)	11.29	3.14	4.50	3.24	11.29

From the results depicted in Table 5.9, it is observed that in all the components of the knee prosthesis, the von Mises stresses are more than the yield strength of Oilon material and thus does not fulfill the performance criteria. Also, the deformation in upper block, side link and middle link is more than the maximum allowable value of 5 mm as per ISO standard.

Upper Block

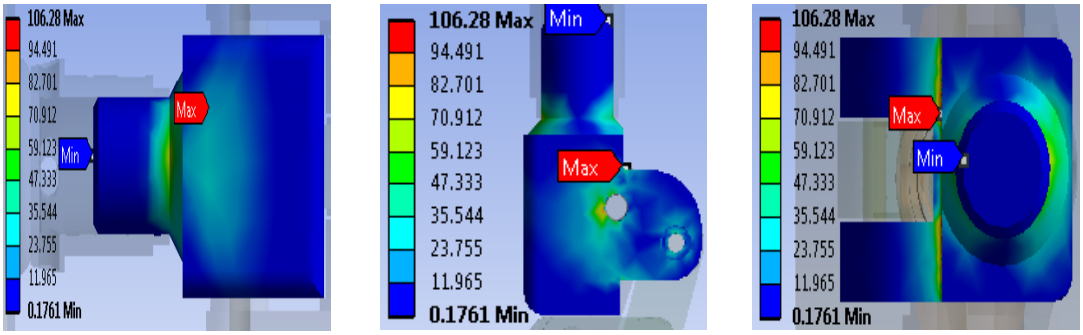

Lower Block

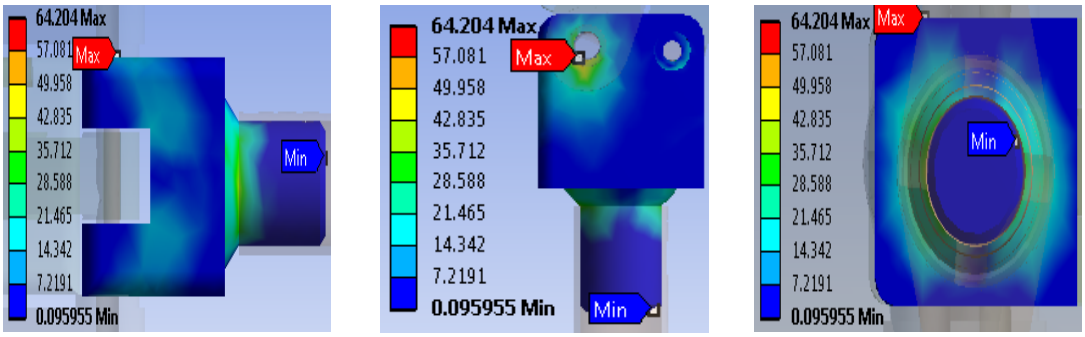

Side Link

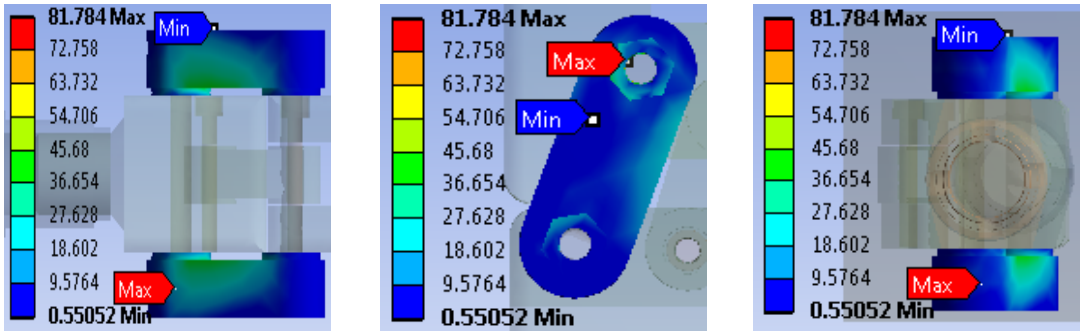

Middle Link

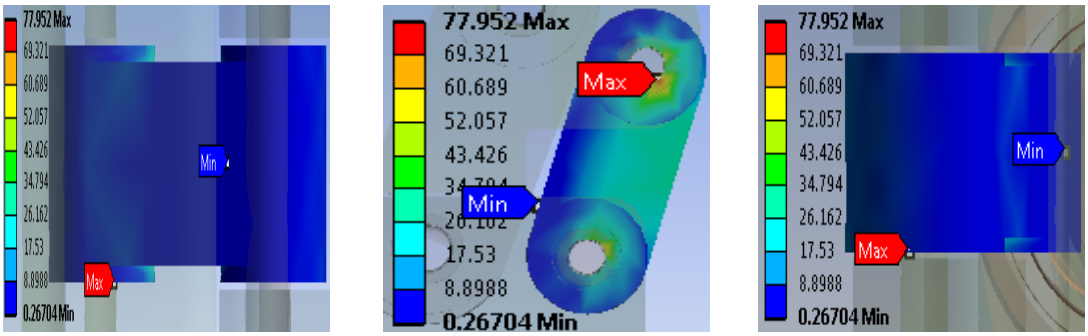

Figure 5.15: von Mises stress for Static test (ultimate strength); loading condition I; Oilon material

Upper Block

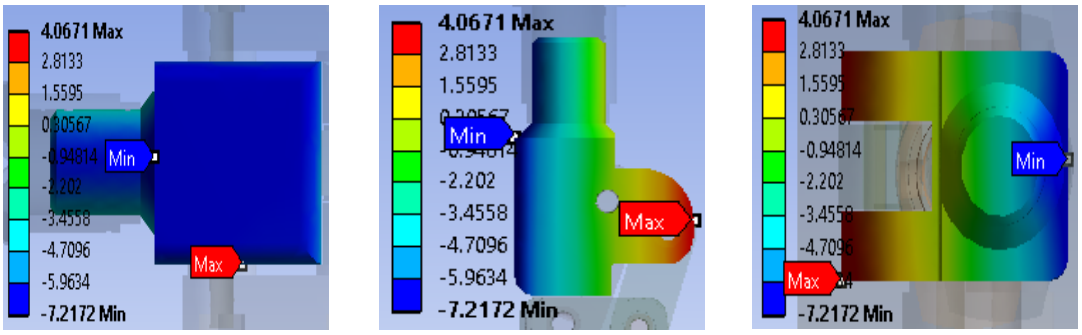

Lower Block

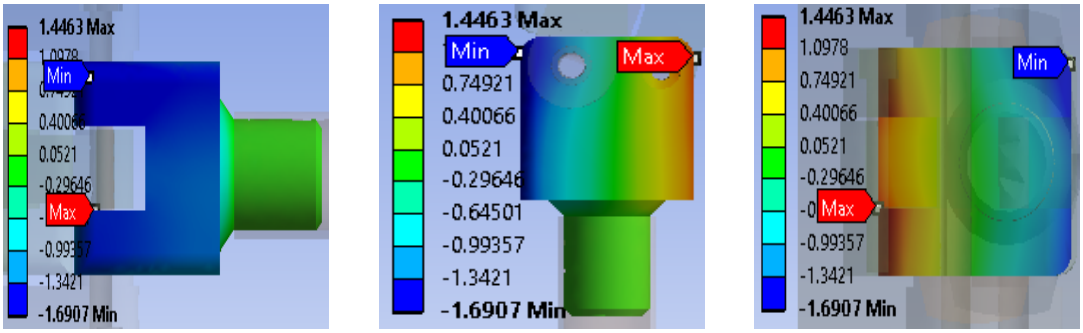

Side Link

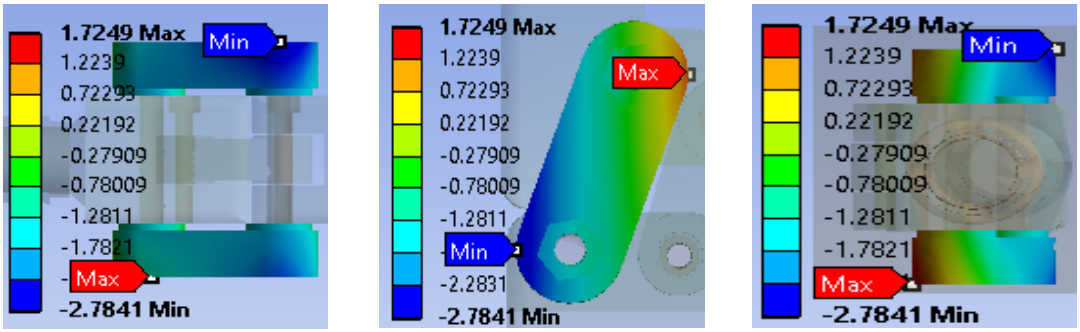

Middle Link

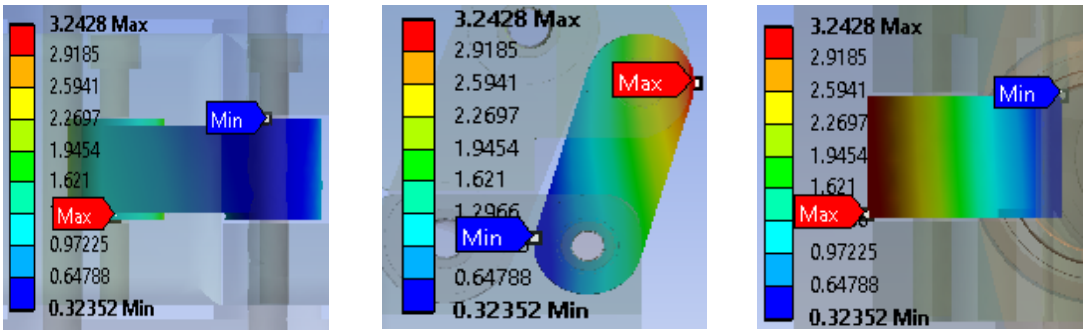

Figure 5.16: Total deformation for Static test (ultimate strength); loading condition I; Oilon material

5.3.2.2. Static test for ultimate strength; Loading condition II; Oilon material

The finite element analysis is performed under loading condition II; forefoot loading at 3019 N load with the material properties of Oilon material and the results are shown in Table 5.10, Figure 5.17 & 5.18.

Table 5.10: Result for Static test (ultimate strength); loading condition II; Oilon material

	Upper Block	Lower Block	Side Link	Middle Link	Knee Prosthesis
Von Mises stress (MPa)	145.78	88.90	101.64	107.02	145.78
Total deformation (mm)	19.99	8.14	9.86	7.72	19.99

From the results, it is observed that all the components of the knee prosthesis experiences von Mises stresses more than the yield strength of Oilon material and the stresses are much higher compared to the loading condition II. Further, the deformation is also much more than the maximum allowable value of 5 mm as per ISO standard.

Upper Block

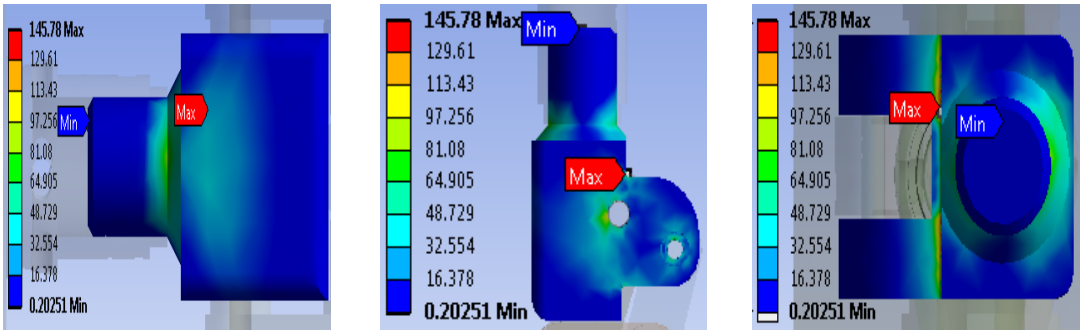

Lower Block

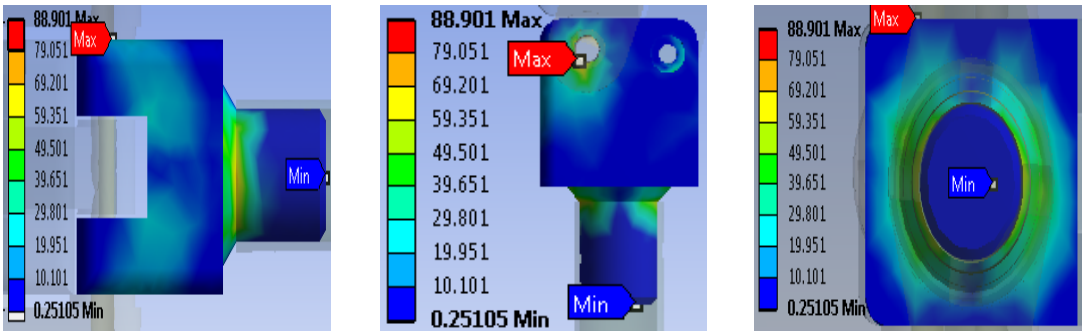

Side Link

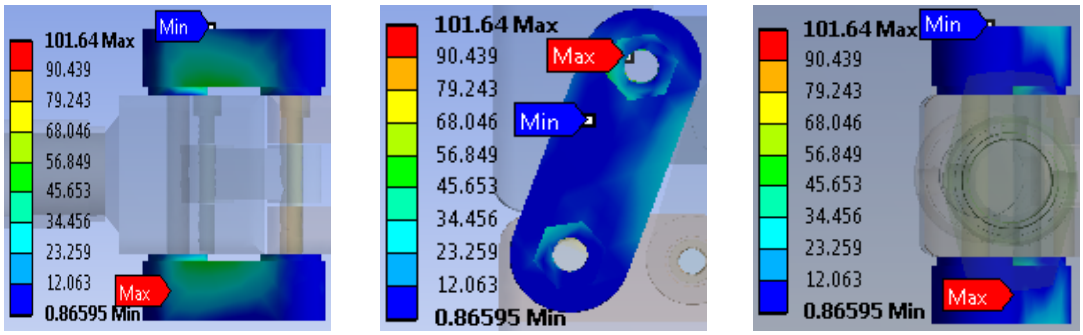

Middle Link

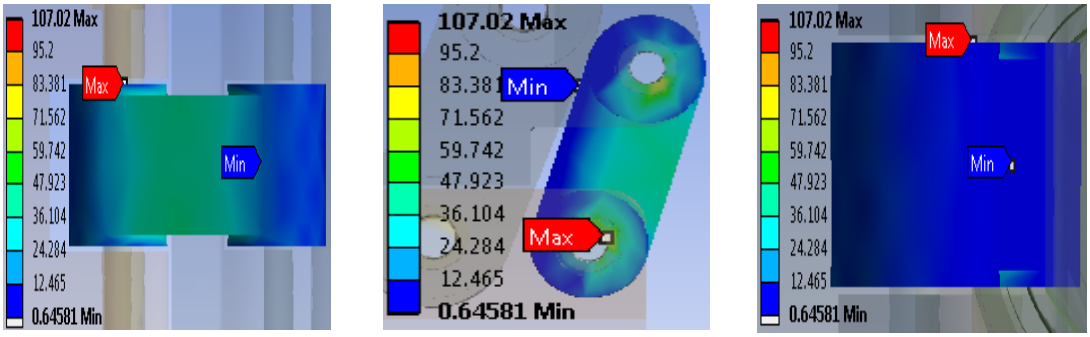

Figure 5.17: von Mises stress for Static test (ultimate strength); loading condition II; Oilon material

Upper Block

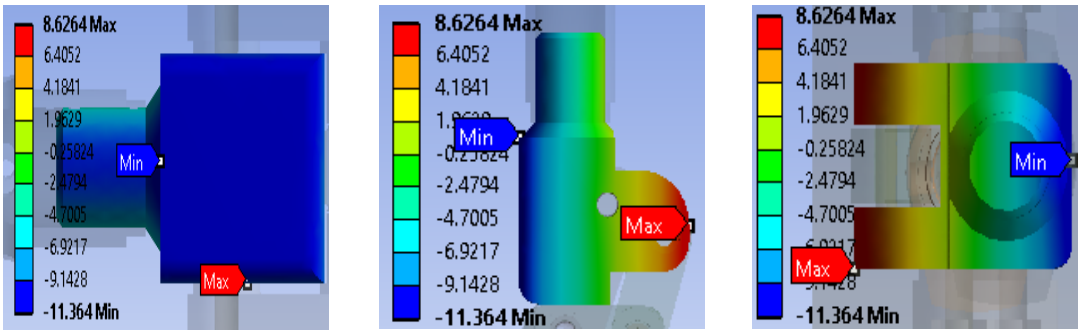

Lower Block

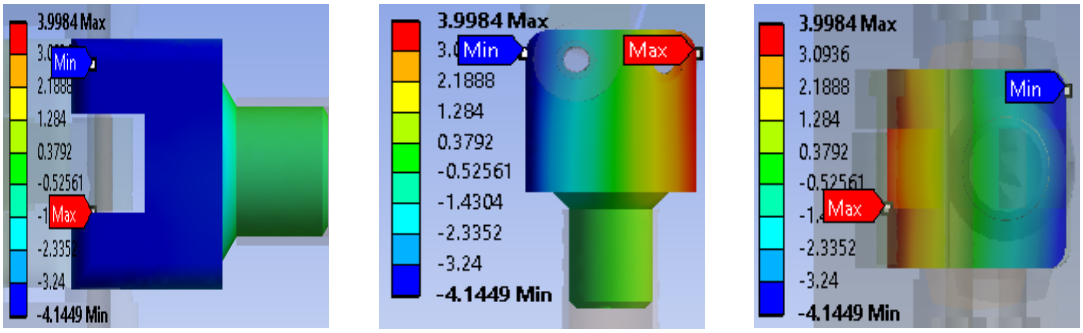

Side Link

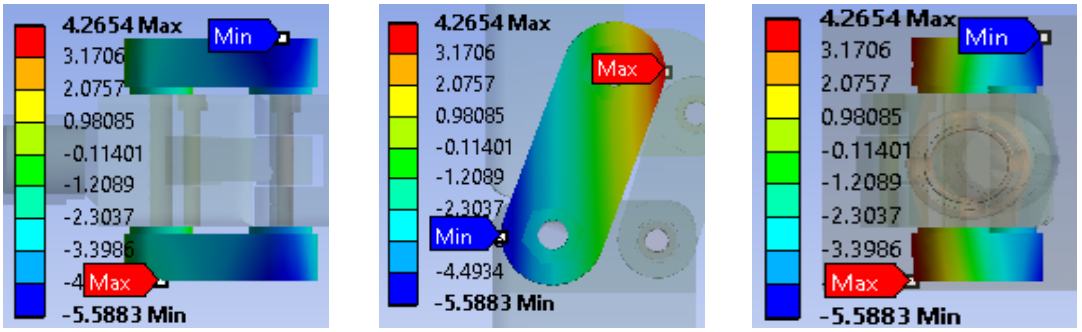

Middle Link

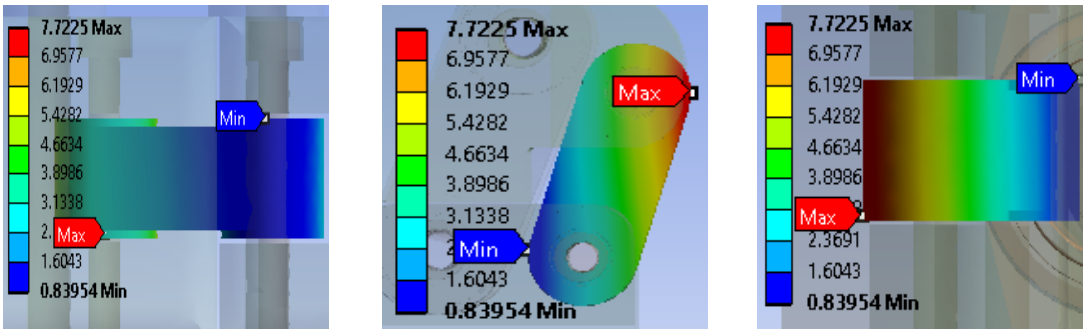

Figure 5.18: Total deformation for Static test (ultimate strength); loading condition II; Oilon material

5.3.2.3 Static test for ultimate strength; Loading condition I; Nylon 66 with 2 wt. % Al_2O_3 composite

To understand the areas of stress concentration and likely points of failure, the finite element analysis is performed at load of 3360 N for heel loading by assigning the mechanical properties of Nylon 66 with 2 wt. % Al_2O_3 composite. The result obtained by FEA is given in Table 5.11, Figures 5.19 & 5.20.

Table 5.11 Result for Static test (ultimate strength); loading condition I; Nylon 66 with 2 wt.% Al_2O_3 composite

	Upper Block	Lower Block	Side Link	Middle Link	Knee Prosthesis
Von Mises stress (MPa)	106.93	63.47	78.96	77.28	106.93
Total deformation (mm)	10.56	2.86	4.18	2.99	10.56

The von Mises stress is 106.93 MPa in upper block which is much more than the yield strength of 75 MPa pertaining to Nylon 66 with 2 wt.% Al_2O_3 composite. The stresses in side link and middle link are marginally higher than the yield strength of 75 MPa. The von Mises stresses is 63.467 MPa in the lower block.

Upper Block

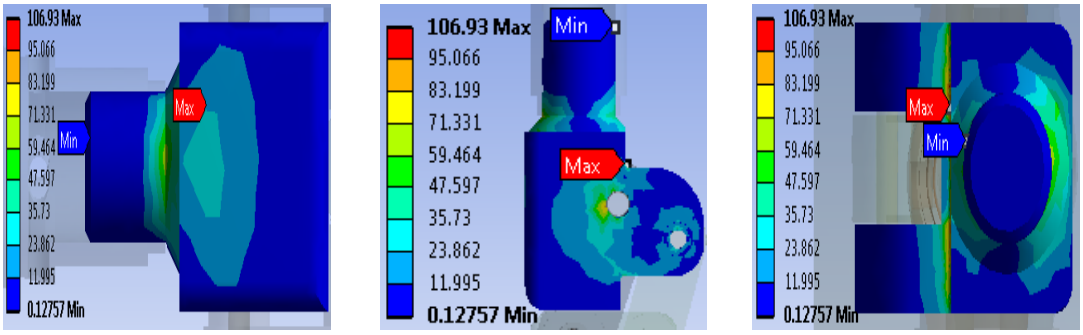

Lower Block

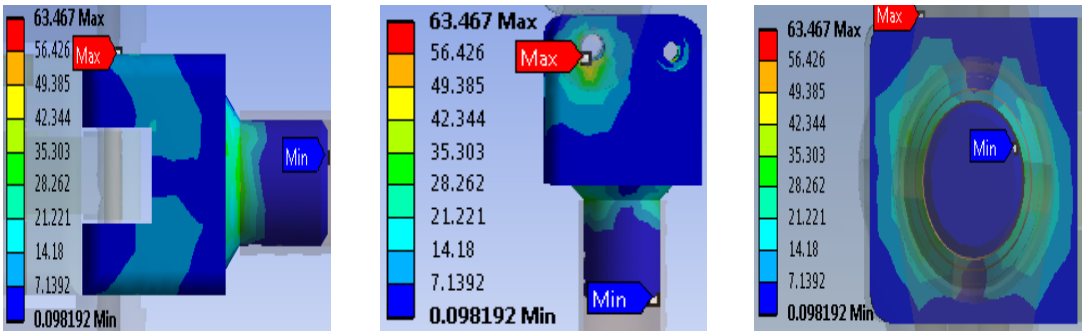

Side Link

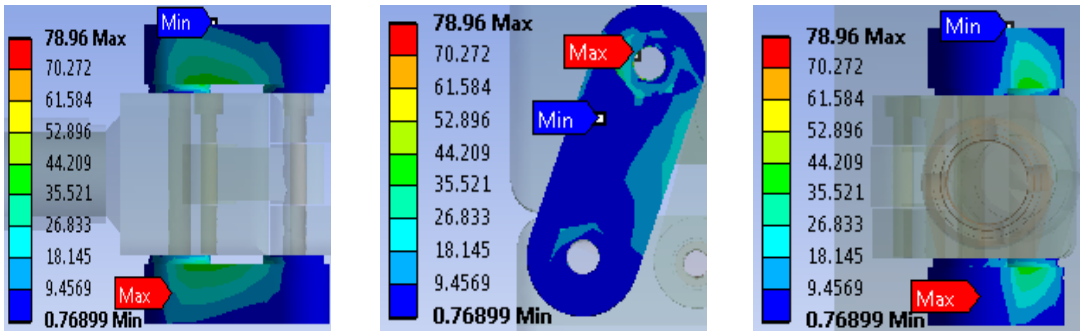

Middle Link

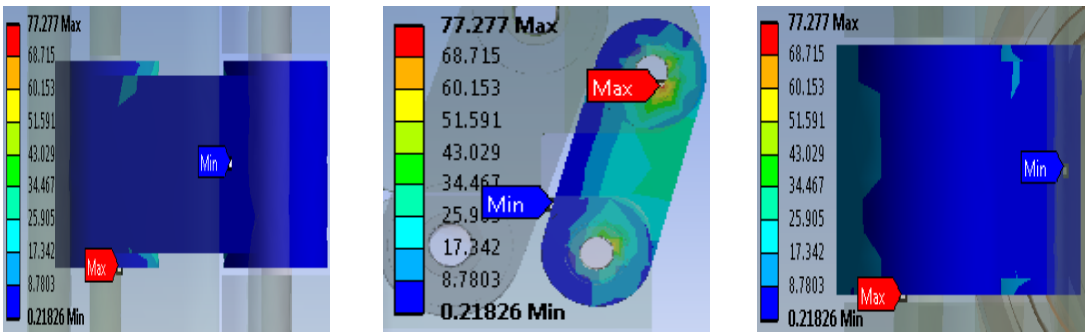

Figure 5.19: von Mises stress for Static test (ultimate strength); loading condition I; Nylon 66 with 2 wt.%Al_2O_3 composite

Upper Block

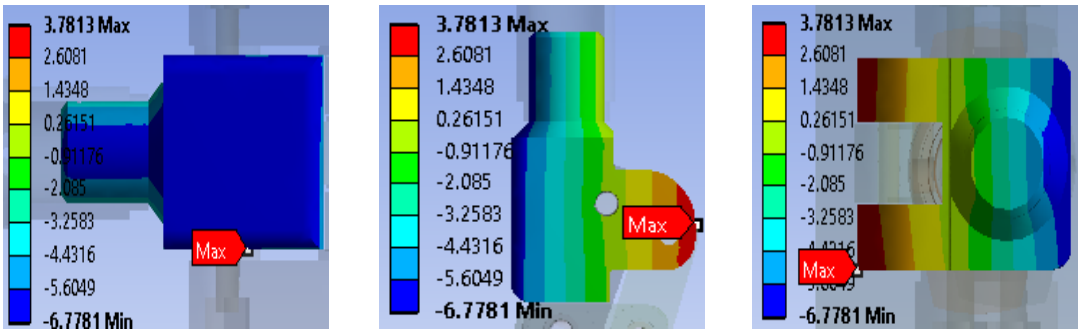

Lower Block

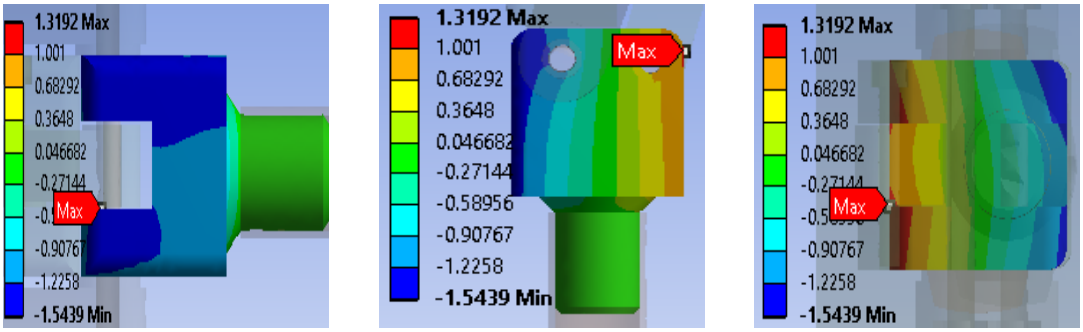

Side Link

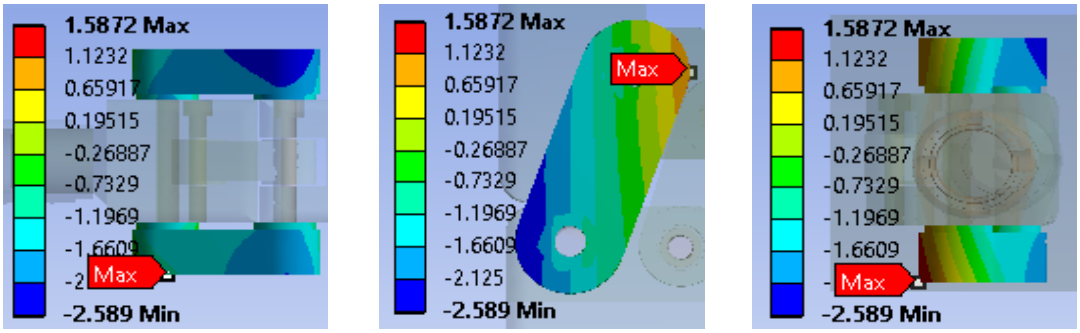

Middle Link

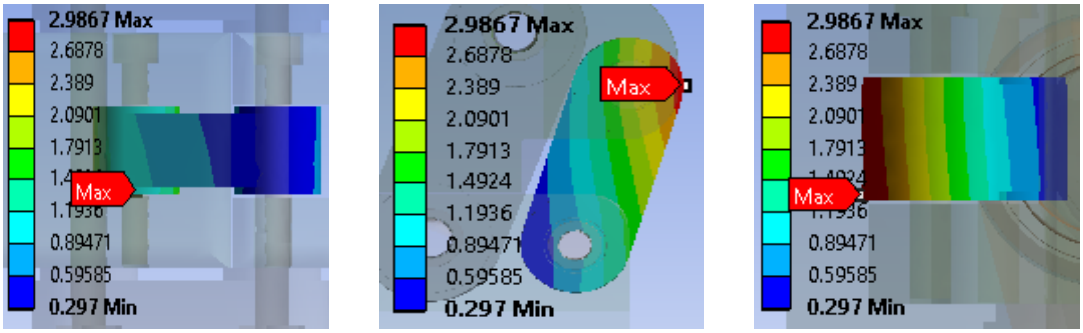

Figure 5.20: Total deformation for Static test (ultimate strength); loading condition I; Nylon 66 with 2 wt. % Al_2O_3composite

5.3.2.4 Static test for ultimate strength; Loading condition II; Nylon 66 with 2 wt. % Al_2O_3 composite

The load of 3019 N is applied for doing the finite element analysis of static test for ultimate strength for the forefoot loading. The analysis is performed for Nylon 66 with 2 wt.% Al_2O_3 composite to understand the stress distributions. The results of the analysis are given in Table 5.12 and the Figures 5.21 & 5.22 shows the von Mises stresses & total deformation.

Table 5.12: Result for Static test (ultimate strength); loading condition II; Nylon 66 with 2 wt.% Al_2O_3 composite

	Upper Block	Lower Block	Side Link	Middle Link	Knee Prosthesis
Von Mises stress (MPa)	146.56	87.97	98.07	104.22	146.56
Total deformation (mm)	18.84	7.36	9.26	7.25	18.84

It is observed that the von Mises stresses and total deformation for all the individual components is more than the permissible values and the knee prosthesis does not meet the requirements of ISO 10328 standard. From the results of heel loading and forefoot loading, it is concluded that the loading condition II generates more stresses in static test for ultimate strength. The results of FEA at various loading conditions for both the materials is summarized in Table 5.13

Table 5.13: von Mises stress and total deformation

Static test at Proof test force				Static test at ultimate test force			
Load Condition I 2240 N		Load Condition II 2013 N		Load Condition I 3360 N		Load Condition II 3019 N	
Oilon	Nylon66 with 2 wt.% Al_2O_3	Oilon	Nylon66 with 2 wt.% Al_2O_3	Oilon	Nylon66 with 2 wt.% Al_2O_3	Oilon	Nylon66 with 2 wt.% Al_2O_3
Von Mises Stress (MPa)							
70.85	71.29	97.20	97.72	106.28	106.93	145.78	146.56
Total Deformation (mm)							
7.52	7.40	13.33	12.57	11.29	10.56	19.99	18.84

Upper Block

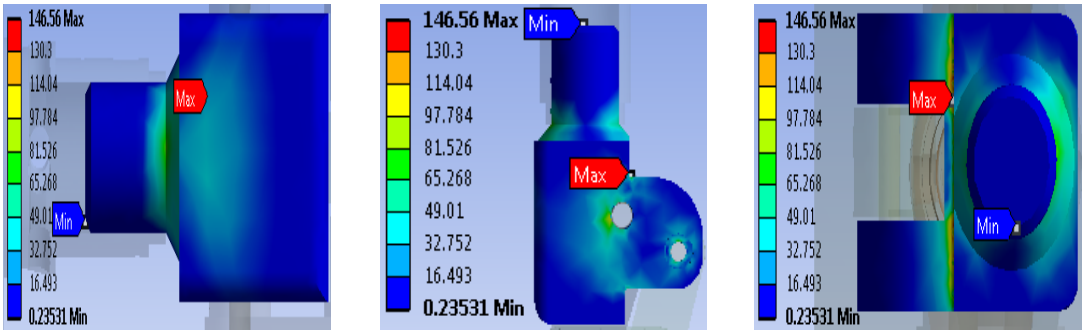

Lower Block

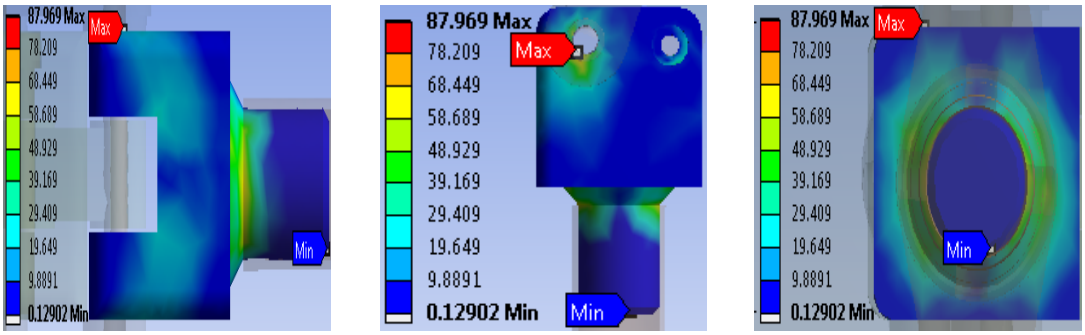

Side Link

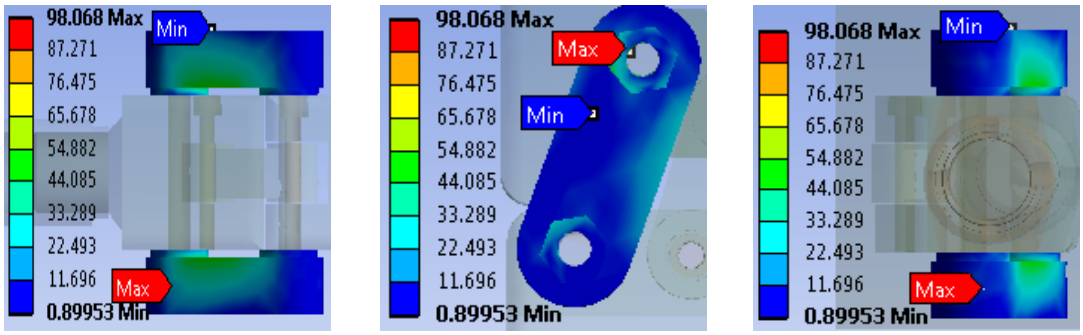

Middle Link

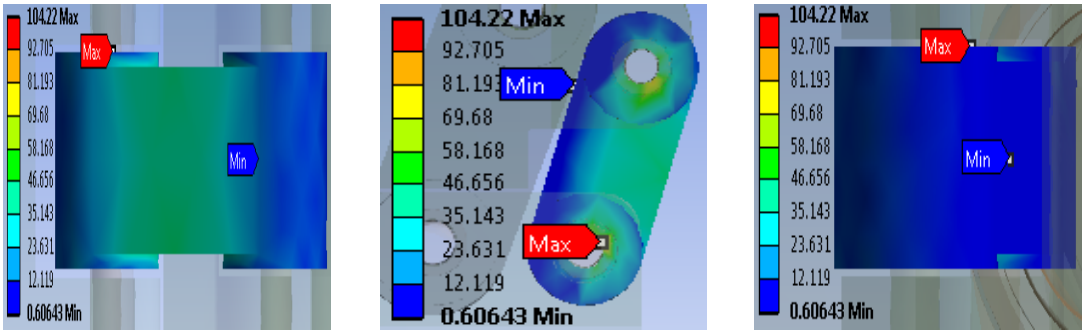

Figure 5.21: von Mises stresses for Static test (ultimate strength); loading condition II; Nylon 66 with 2 wt.% Al_2O_3 composite

Upper Block

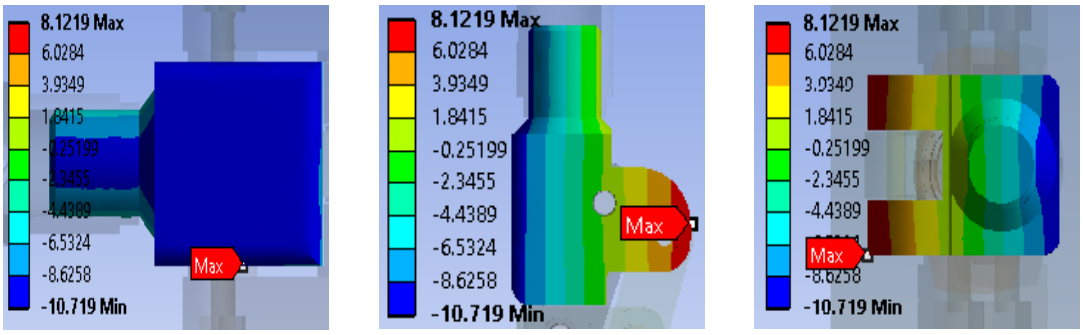

Lower Block

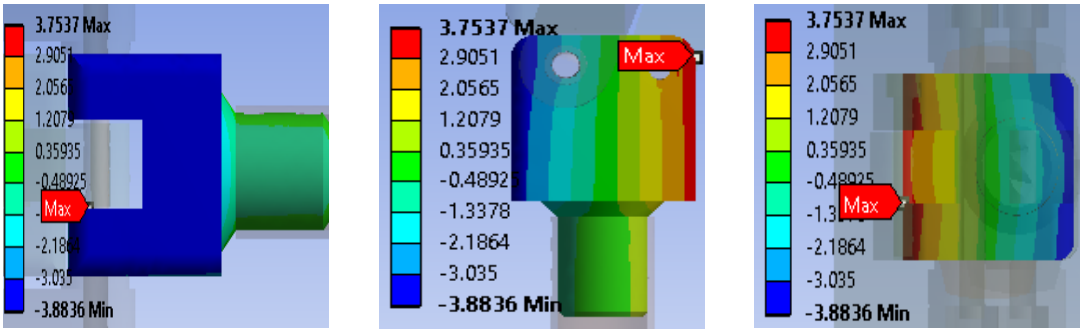

Side Link

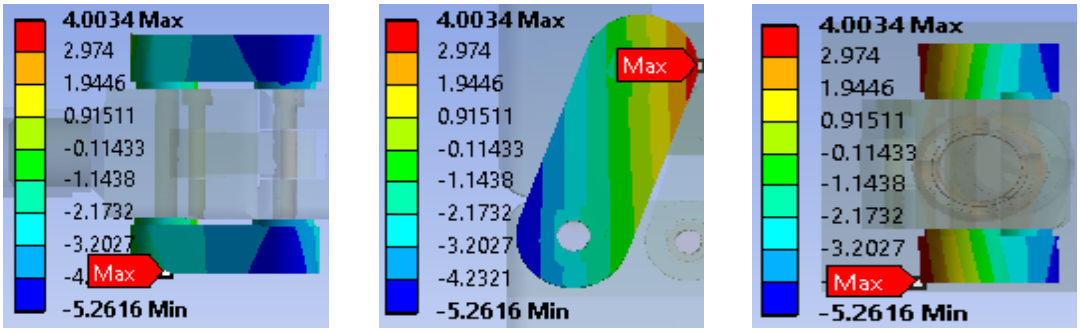

Middle Link

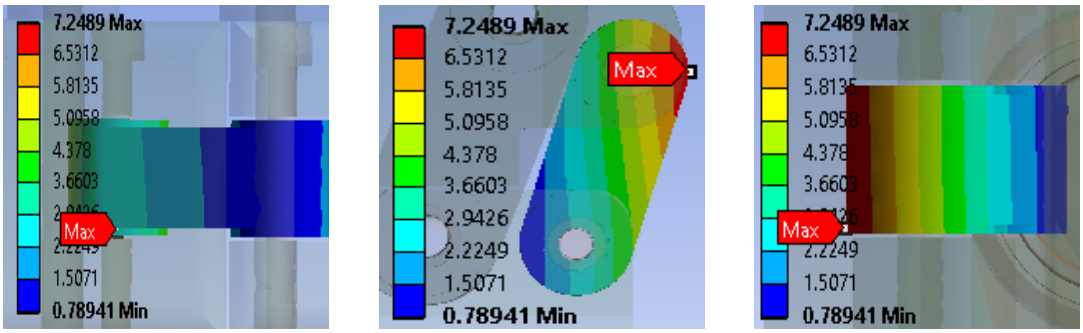

Figure 5.22: Total deformation for Static test (ultimate strength); loading condition II; Nylon 66 with 2 wt. % Al_2O_3 composite

CHAPTER 6

DESIGN MODIFICATIONS OF KNEE JOINT PROSTHESIS AND FINITE ELEMENT ANALYSIS

CHAPTER 6
DESIGN MODIFICATIONS OF KNEE JOINT PROSTHESISAND FINITE ELEMENT ANALYSIS

This chapter covers various designs developed for the knee joint prosthesis by modifying the geometry of the individual components with an objective to reduce the stresses, total deformation, weight reduction and overcome failure. The study of finite element analysis for static proof and ultimate strength of new designs as per the requirements of ISO 10328 standard is summarized. The fatigue testing of oil impregnated nylon and composite of Nylon66 with 2 wt.% of Al_2O_3 and S-N curve is explained. The fatigue life assessment of initial and new optimized design is also discussed.

6.1 Design of Knee Joint Prosthesis - Four Bar Mechanism

The knee joint prosthesis as shown in Figure 6.1 works on the principle of four bar mechanism.

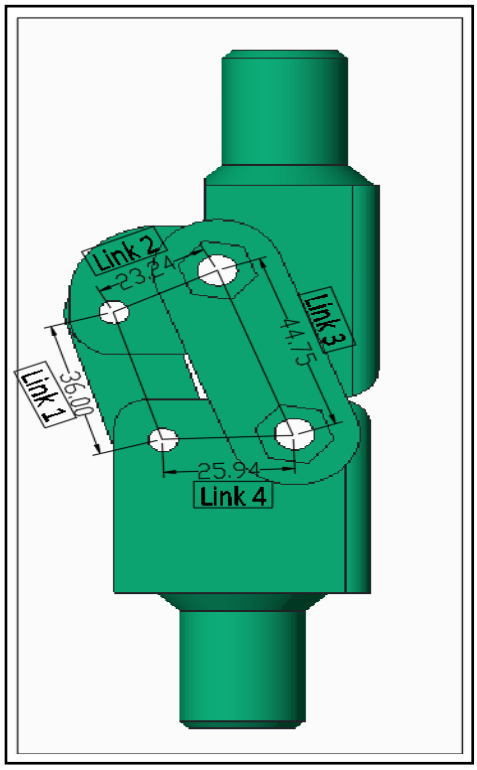

Figure 6.1: Knee Joint Prosthesis - Four-Bar Mechanism Design

The four bar links are shown as the connecting lines between the individual joints of the assembly. The socket component attaches to the upper block and pylon to the lower block.

This knee prosthesis was designed as a non-Grashof four bar linkage with the sum of its smallest and largest links being greater than the sum of the remaining two links.

$$L_{max} + L_{min} \text{ e } L_a + L_b \quad \text{..... (6.1)}$$

where L_{max} is the longest link, L_{min} is the shortest link, L_a and L_b are the remaining two links. In such a mechanism, the two side links are limited in rotational range of motion due to the geometries of the links combined with the frame and the coupler. This prosthesis is capable of having knee rotation from 0^0 to 158^0 where 0^0 refers to the fully extended knee prosthesis position.

The functioning of the prosthesis is controlled by Link 3 which gets its movement by hip moment through socket fitted to the residual limb. The instantaneous centre of rotation for Link 2 changes depending upon the configuration of four bar linkages. The centre of rotation of Link 2 is found by extending the line of Link 1 and Link 3 to their point of intersection. This centre of rotation (CoR) will define the axis about which links are rotating and is critical for the stability of knee [52].

The knee stability is dependent on the position of CoR relative to the load line for the ground reaction forces. The load line changes relative to the position of prosthetic foot i.e. forefoot or heel loading. When CoR is anterior to the knee and load line causes buckling and is unstable. For the stability, CoR shall be posterior to the knee, close to the knee joint. Stability of the knee prosthesis during various phases of gait is achieved by the translation of CoR with respect to load line. The voluntary control four bar knee is designed to give amputee ability to control knee stability at both heel contact, push-off and complete control over a limited range of knee flexion [11].

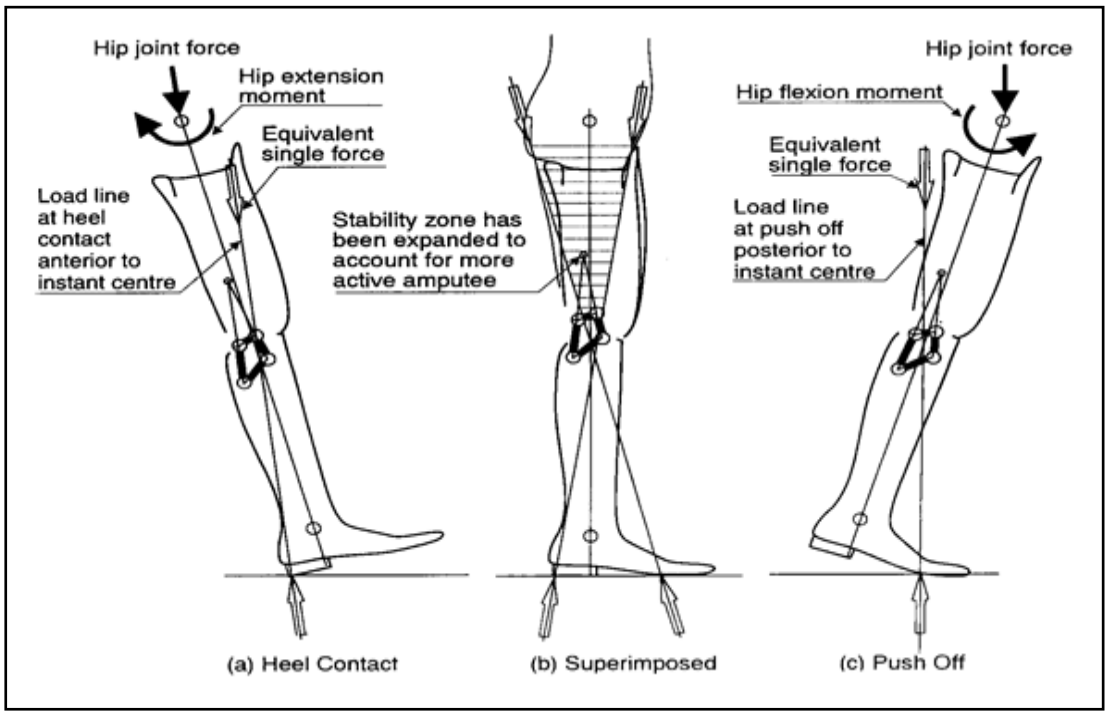

Figure 6.2: Knee stability diagram of voluntary control 4 bar mechanism

6.2 Design modifications of knee joint prosthesis

From the finite element analysis results given in Chapter 5, it is concluded that the present design with existing material (oil impregnated nylon) does not meet the performance criteria of ISO 10328 standard. The newly developed composite of Nylon66 with 2 wt. % of Al_2O_3 also does not fulfill all the needed requirements.

Design modification is proposed by the process of reverse engineering. The stress plots of existing design are studied for understanding the areas of failure. The stress pattern of different components reveals that maximum stresses are observed in the upper block and least in the lower block of the knee prosthesis. From the FEA plot of stresses of individual components, it is noted that the stress concentration is at the sharp corners and assembly holes. Design modifications are proposed by removing sharp corners, doing filleting, modifying the shape for smooth transition of stresses and stress distribution to meet the performance criteria and the objectives of this research work.

From the above inputs, it is proposed to do the design modifications by considering the below mentioned factors:

A- Modification in upper block

The geometry of the upper block is modified by providing the fillet and changing the shape of the profile. By the above changes, the weight of upper block will increase which shall help in reducing the stresses. It is proposed to do the analysis by considering three designs of upper block having different levels of weight. The drawing of upper block of existing design and the proposed modifications is shown in Figure 6.3.

B- Modification in lower block

In this case, the geometry is modified and fillet provided. The proposed changes are likely to reduce the weight and three designs of different weights are studied. The drawing of lower block of existing design and the proposed modifications is shown in Figure 6.4.

C- Making through hole in lower block

With an objective to redistribute the stresses and reduce weight, it is proposed to make through hole of different diameter in the lower block. Three conditions are studied i.e. without hole, hole of diameter 10mm and hole of diameter 14mm.

The three levels of the design factors A, B and C are tabulated as shown in Table 6.1

Table 6.1: Design factors and levels

Factor	Unit	Level 1	Level 2	Level 3
A	Kg	0.148	0.150	0.152
B	Kg	0.130	0.128	0.126
C	Mm	0	10	14

Existing Design of Upper Block	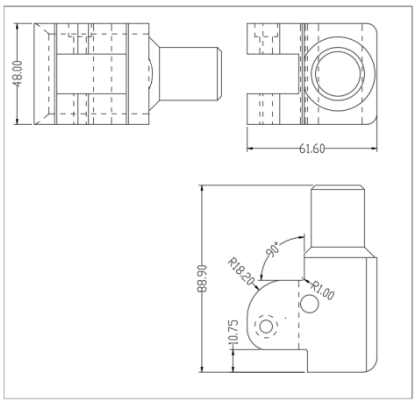
Modified Design Upper Block (Factor 1, Level 1)	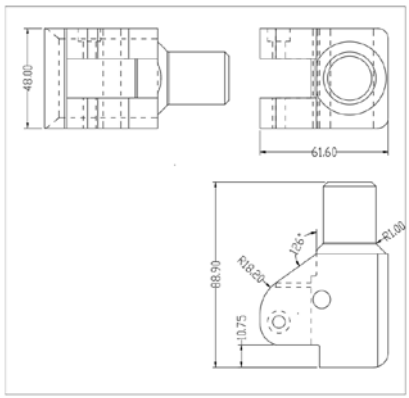
Modified Design Upper Block (Factor 1, Level 2)	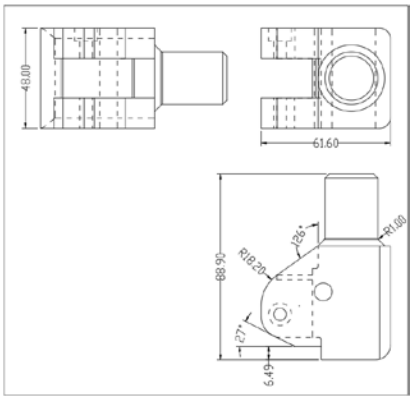
Modified Design Upper Block (Factor 1, Level 3)	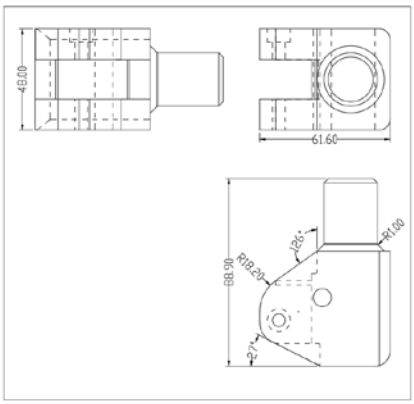

Figure 6.3: Existing and modified design of Upper Block

Existing Design Lower Block	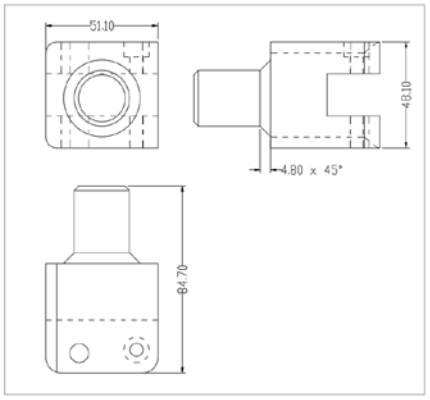
Modified Design Lower Block (Factor 2, Level 1)	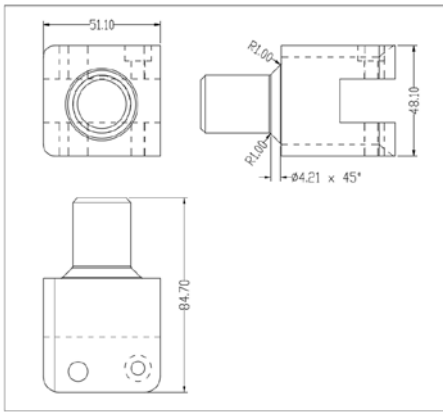
Modified Design Lower Block (Factor 2, Level 2)	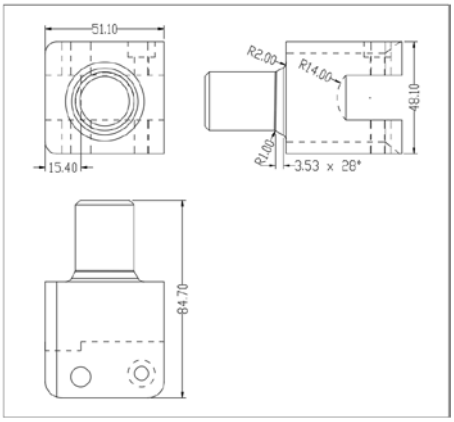
Modify Design Lower Block (Factor 2, Level 3)	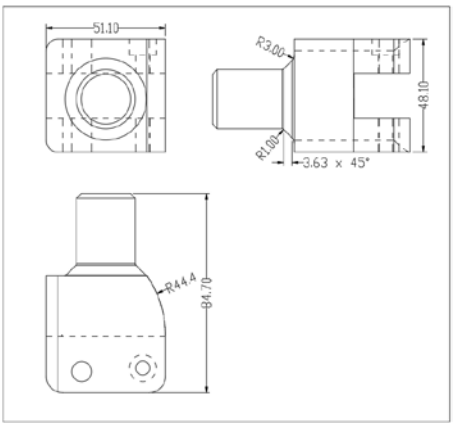

Figure 6.4: Existing and modified design of Lower Block

6.2.1 Taguchi technique

From the above proposed modifications, we understand that there are total 27(3^3) design possibilities and it will be very much time consuming and costly to do finite element analysis for all. Hence orthogonal array L9 is chosen as per Taguchi technique. The nine numbers of designs are prepared in accordance to the Table 6.2

Table 6.2: Orthogonal array L9

Design Sr. No.	A	B	C
1	1	1	1
2	1	2	2
3	1	3	3
4	2	1	2
5	2	2	3
6	2	3	1
7	3	1	3
8	3	2	1
9	3	3	2

The nine designs prepared by the combination of various factors and levels as per orthogonal array L9 Table 6.2 are shown in Figure 6.5.

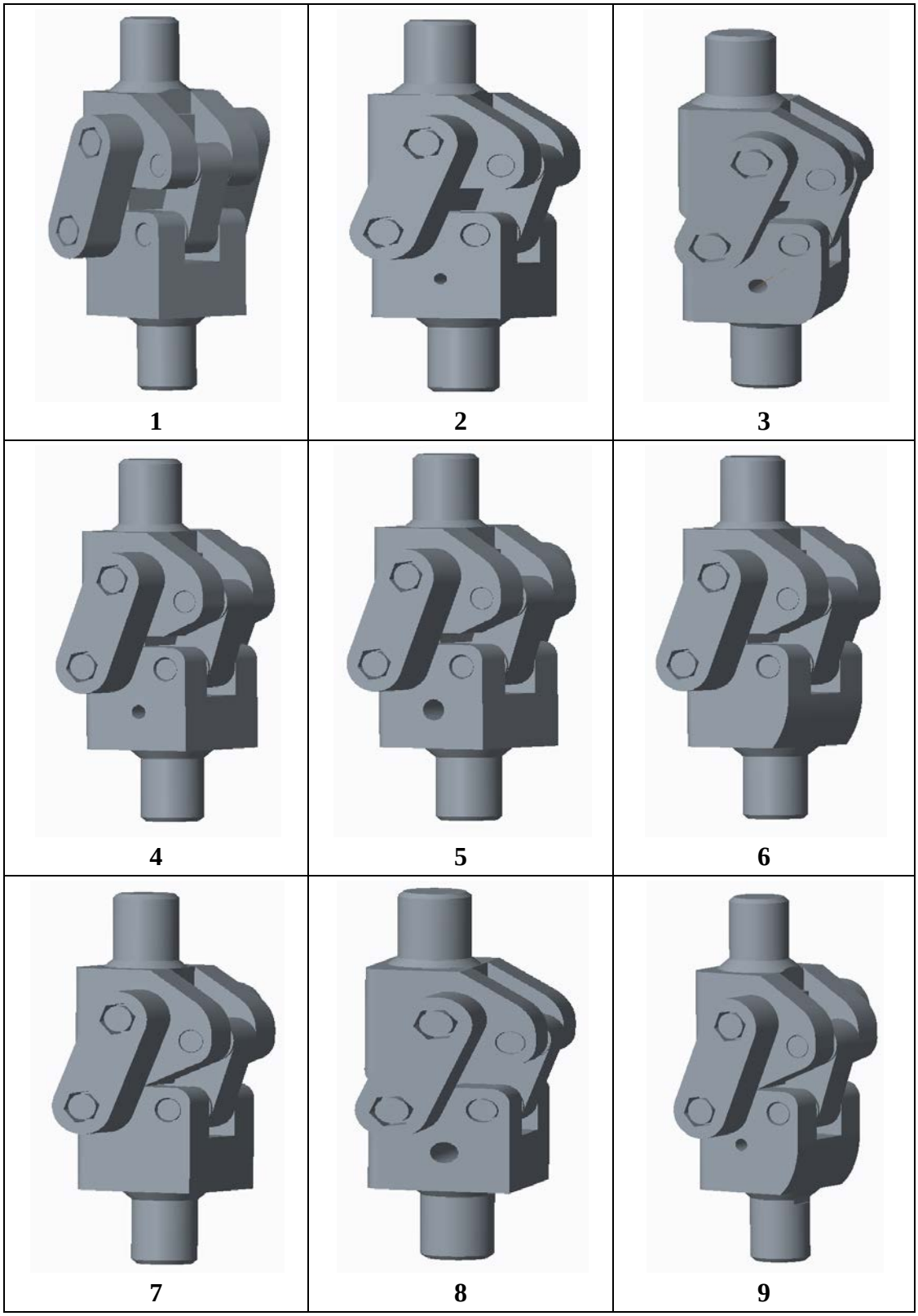

Figure 6.5: Modified design of knee prosthesis

6.3 Finite element analysis of modified designs

It is noted from the FEA results in Chapter 5 that the maximum stresses are occurring at static ultimate strength; loading condition II – forefoot loading, therefore the new designs are subjected to the finite element analysis, initially only for this condition. All the nine designs as shown in Figure 6.5 were analysed by ANSYS 16.0 software at 3019 N as per test load condition II for the Nylon 66 – 2 wt.% Al_2O_3 composite and the results for von Mises stresses and deformation are tabulated in Table 6.3.

Table 6.3: FEA results of modified design iterations

Ultimate test force static load condition II 3019 N; Nylon 6 – 2 wt.% Al_2O_3 composite					
Design No.	**Von Mises stresses (MPa)**				**Total deformation of knee joint (mm)**
	Upper Block	**Lower Block**	**Middle Link**	**Side Link**	
Initial	146.56	87.97	104.22	98.07	18.84
1	75.40	66.80	59.59	40.70	14.49
2	77.54	72.09	43.07	28.77	9.62
3	75.66	61.58	63.95	26.89	6.35
4	68.71	61.51	50.58	24.74	6.33
5	68.70	62.70	49.09	24.28	7.15
6	76.26	55.30	48.39	24.67	9.17
7	69.00	68.37	48.74	25.97	9.26
8	67.06	63.04	40.09	25.29	8.95
9	66.40	60.78	34.40	37.15	4.11

From the results of Table 6.3, it is noted that the Design number 9 meets the performance criteria for static ultimate strength for the load condition II- forefoot loading and the other eight designs are not fulfilling the criteria. The design number 9 is subjected to complete structural testing analysis for static proof and ultimate strength both for loading condition I & II for further analysis.

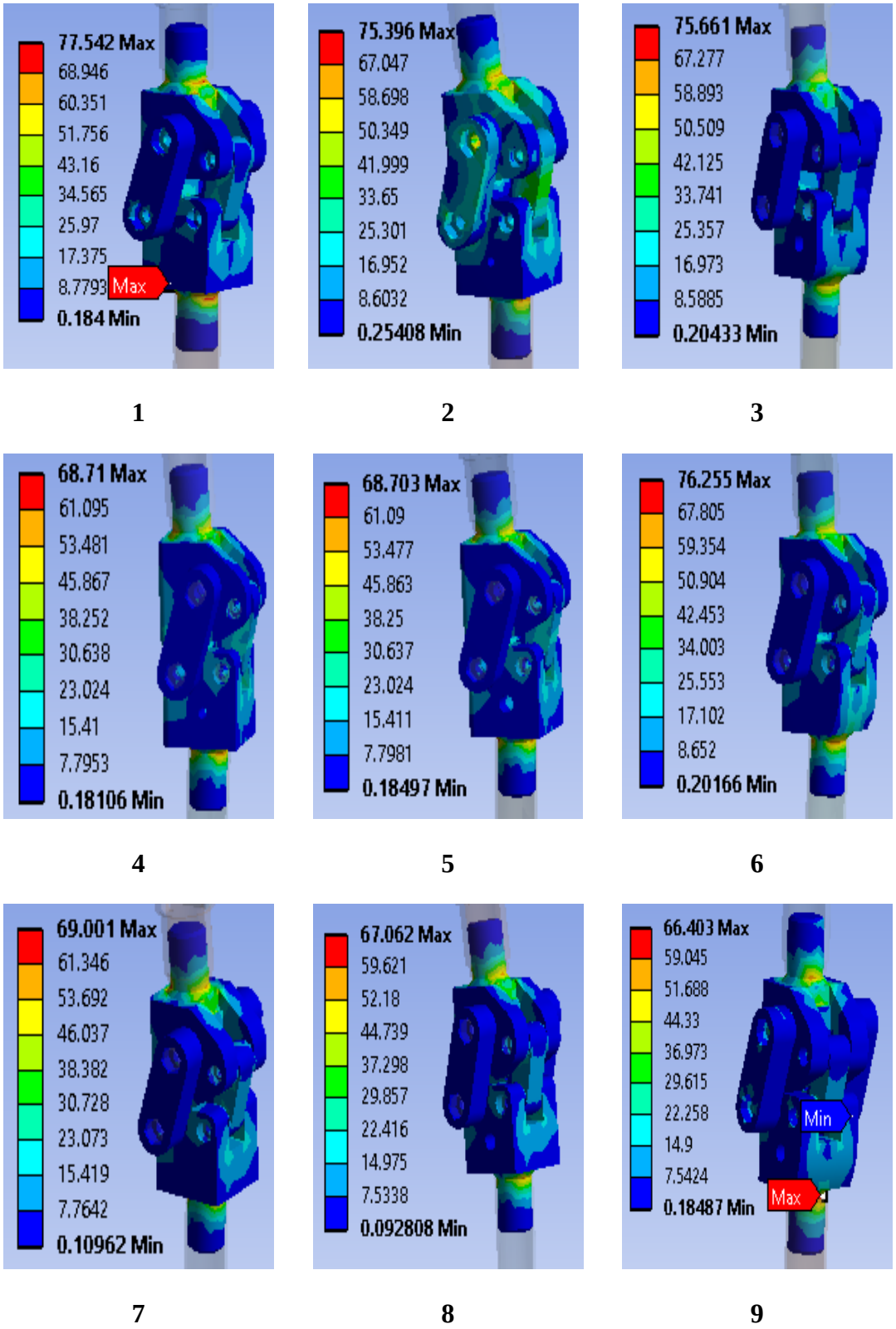

Figure 6.6: Von Mises stresses (MPa) for modified designs at ultimate test force static load condition II (3019 N); Nylon 6 – 2 wt. % Al_2O_3 composite

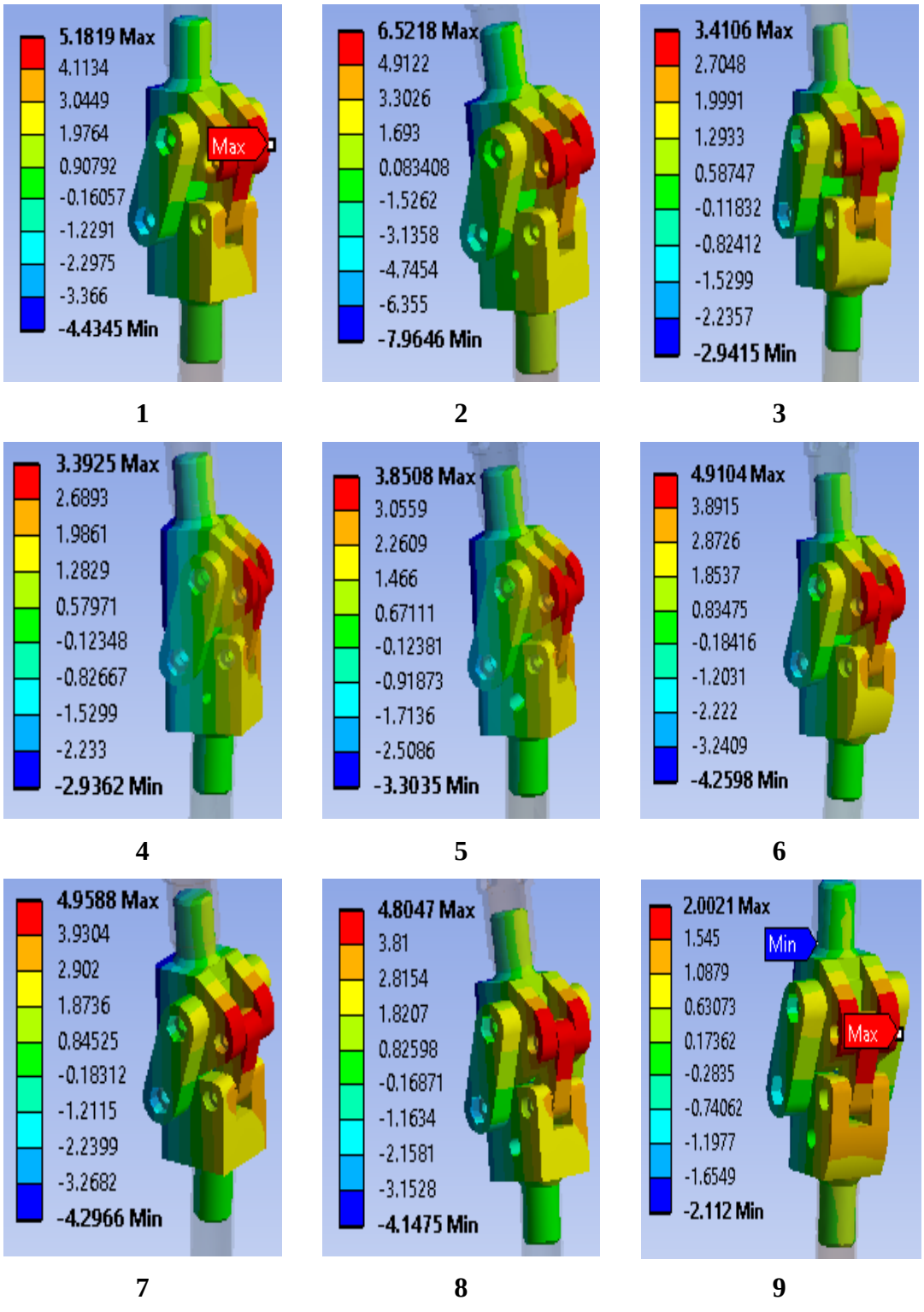

Figure 6.7: Total deformation of knee joint (mm) of modified designs at ultimate test force static load condition II (3019 N); Nylon 6 – 2 wt.% Al_2O_3 composite

6.3.1 Static test for proof strength; Loading condition I; Nylon 66 with 2 wt.% Al_2O_3 composite

Load of 2240 N is applied for conducting the above analysis with the material properties of Nylon66 with 2 wt. % of Al_2O_3composite assigned to the CAD model. The results of total deformation and von Mises stresses on individual components and the assembly are given in Table 6.4 and Figure 6.8 & 6.9 respectively.

Table 6.4: Result for Static test (proof strength); loading condition I; Nylon 66 with 2 wt.% Al_2O_3 composite

Result	Upper Block	Lower Block	Side Link	Middle Link	Knee Prosthesis
von Mises stress (MPa)	39.97	23.17	10.00	14.11	39.97
Total deformation (mm)	1.15				

The Von Mises stress values observed in all the four components of the knee prosthesis are less than that of the yield strength of the developed composite of Nylon 66 with 2 wt. % Al_2O_3. Thus it meets the requirement of yield strength criterion and the total deformation of the assembly is also less than the prescribed value of 5mm as per ISO 10328 standard.

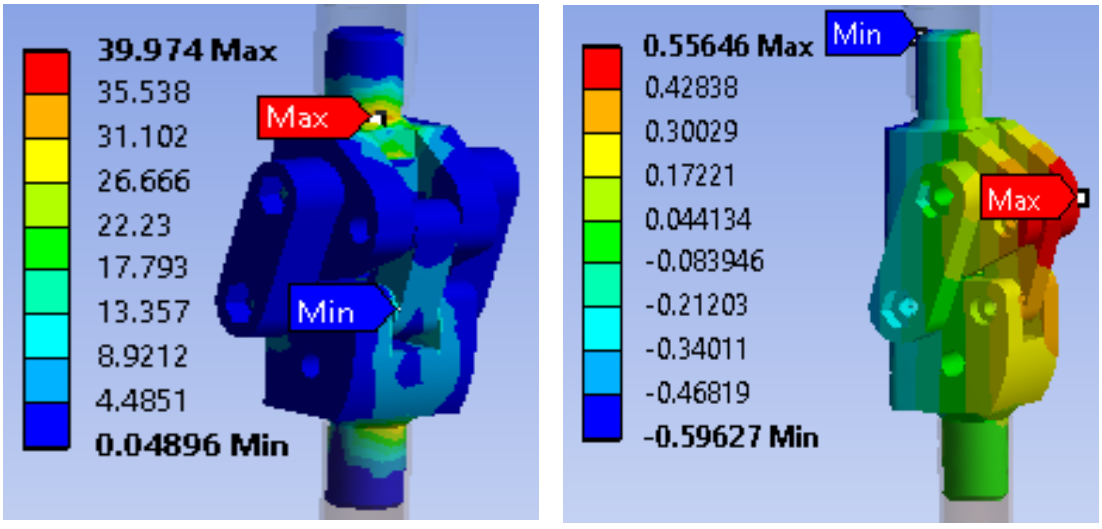

von Mises **Total deformation**

Figure 6.8: von Mises & Total deformation for Static test (proof strength); loading condition I; Nylon 66 with 2 wt. % Al_2O_3 composite

Upper Block

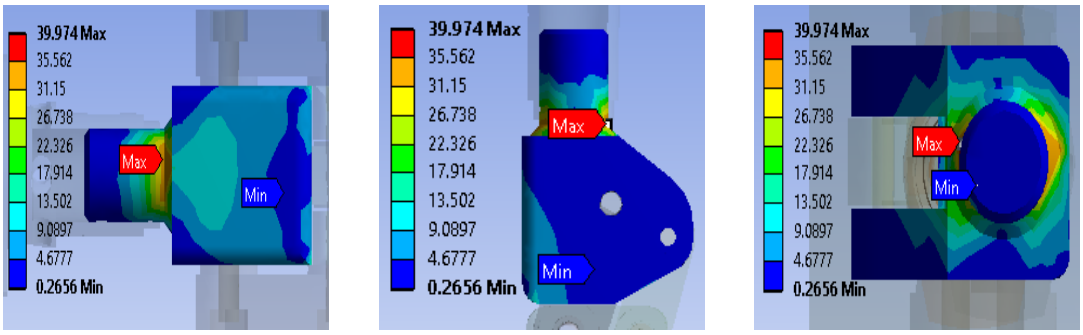

Lower Block

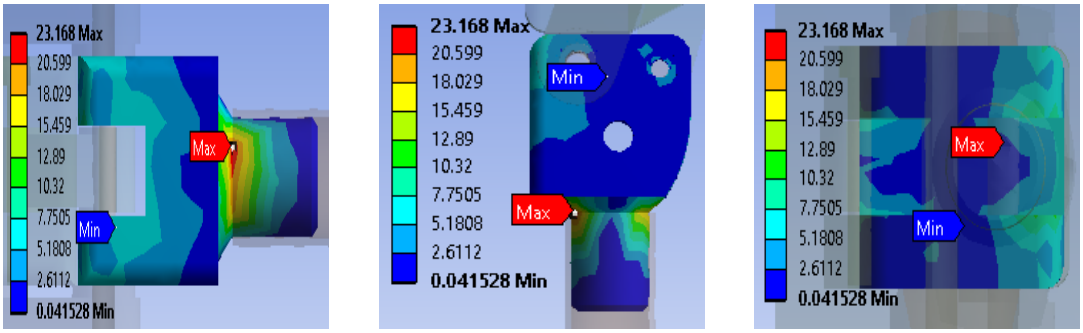

Side Link

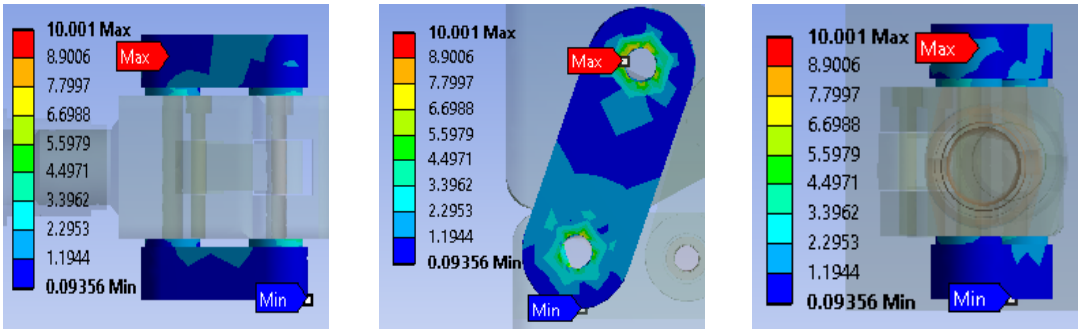

Middle Link

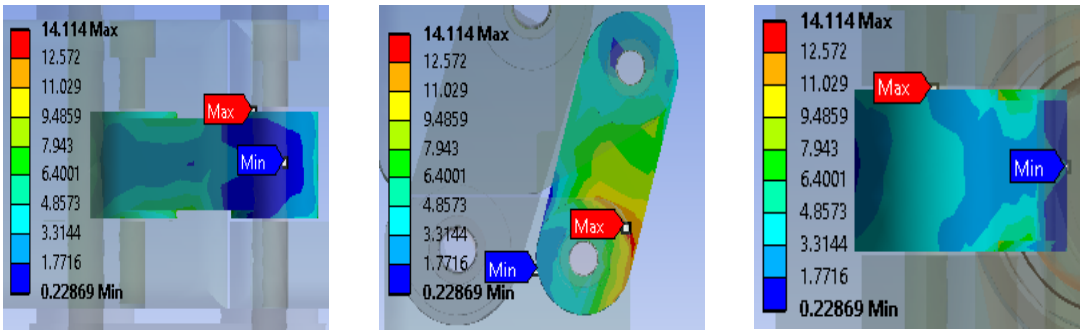

Figure 6.9: Von Mises stress for Static test (proof strength); loading condition I; Nylon 66 with 2 wt.% Al_2O_3 composite

6.3.2 Static test for proof strength; Loading condition II; Nylon 66 with 2 wt.% Al_2O_3 composite

Knee prosthesis design number 9 is subjected to finite element analysis at a load of 2013N. The results of total deformation and von Mises stresses on individual components and the assembly are given in Table 6.5 and Figure 6.10 & 6.11 respectively.

Table 6.5: Result for Static test (proof strength); loading condition II; Nylon 66 with 2 wt. % Al_2O_3 composite

Result	Upper Block	Lower Block	Side Link	Middle Link	Knee Prosthesis
Von Mises stress (MPa)	50.73	40.36	23.90	21.72	50.73
Total deformation (mm)	2.652				

From the finite element results, it is noted that the maximum von Mises stress in this condition are more than that of loading condition-I. The von Mises stresses are less than the yield strength of the composite of Nylon 66 with 2 wt.% Al_2O_3 and satisfies the performance criteria. Further, the total deformation is less than the permissible limits.

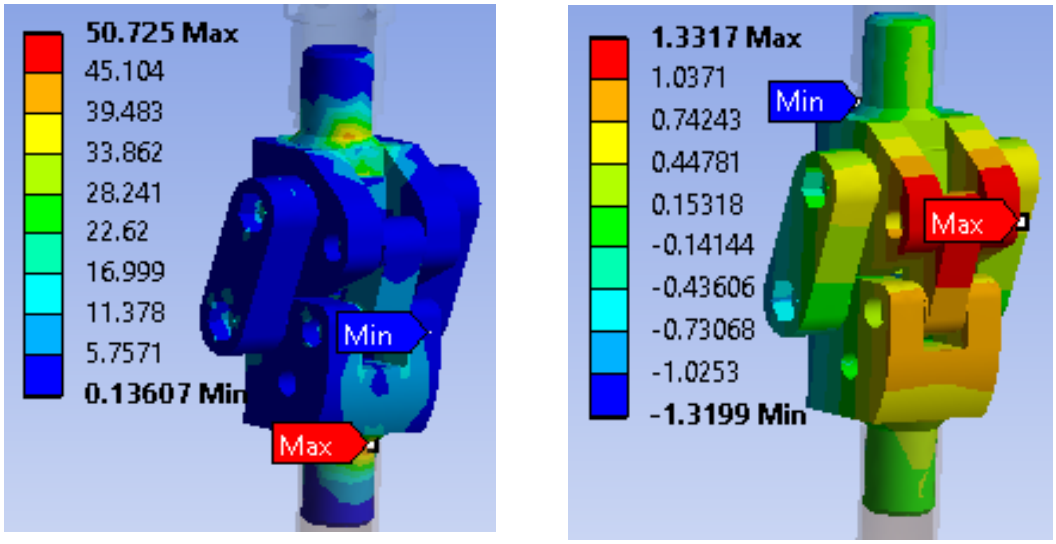

von Mises **Total deformation**

Figure 6.10: von Mises & Total deformation for Static test (proof strength); loading condition II; Nylon 66 with 2 wt. % Al_2O_3 composite

Upper Block

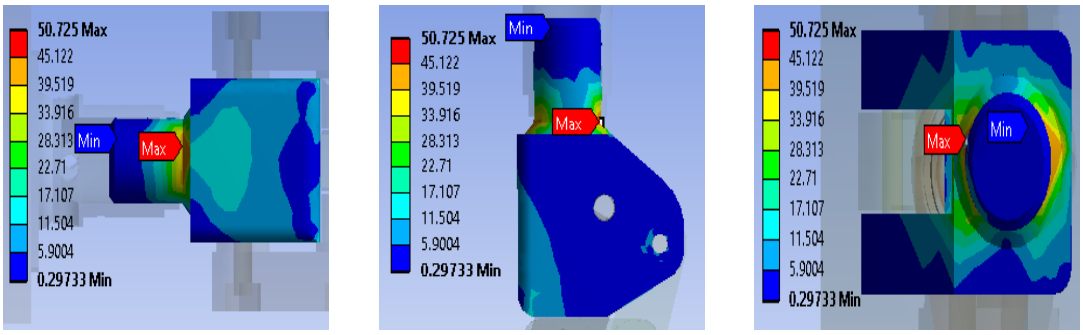

Lower Block

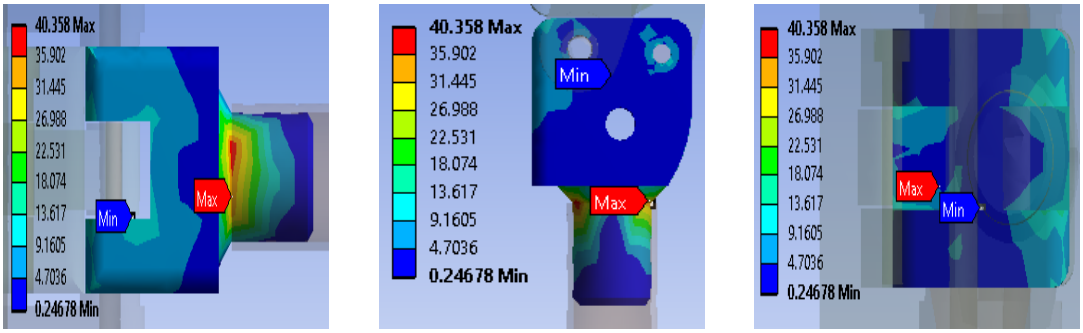

Side Link

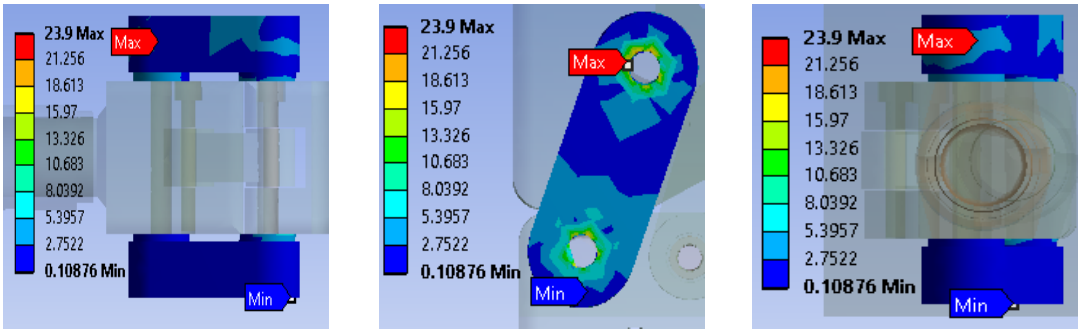

Middle Link

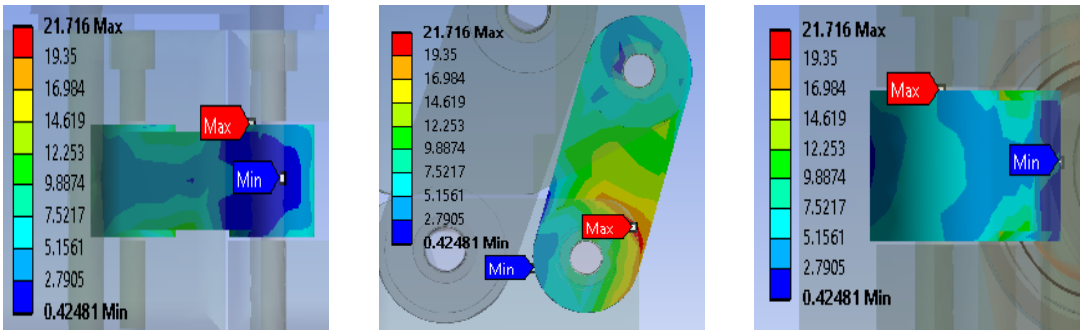

Figure 6.11: Von Mises stress for Static test (proof strength); loading condition II; Nylon 66 with 2 wt.% Al_2O_3 composite

6.3.3 Static test for ultimate strength; Loading condition I; Nylon 66 with 2 wt. % Al_2O_3 composite

The finite element analysis is performed at load of 3360 N for heel loading by assigning the mechanical properties of Nylon 66 with 2 wt. % Al_2O_3 composite. The result obtained by FEA are given in Table 6.6 and Figures 6.12 & 6.13

Table 6.6: Result for Static test (ultimate strength); loading condition I; Nylon 66 with 2 wt. % Al_2O_3 composite

	Upper Block	Lower Block	Side Link	Middle Link	Knee Prosthesis
Von Mises stress (MPa)	60.00	36.44	16.04	23.05	60.00
Total deformation (mm)	1.82				

The maximum von Mises stress is 60 MPa in upper block which is less than the yield strength of 75 MPa pertaining to Nylon 66 with 2 wt.% Al_2O_3 composite. The total deformation is also less than the allowable limit of 5 mm. Thus this new design is meeting the performance criteria of this loading condition.

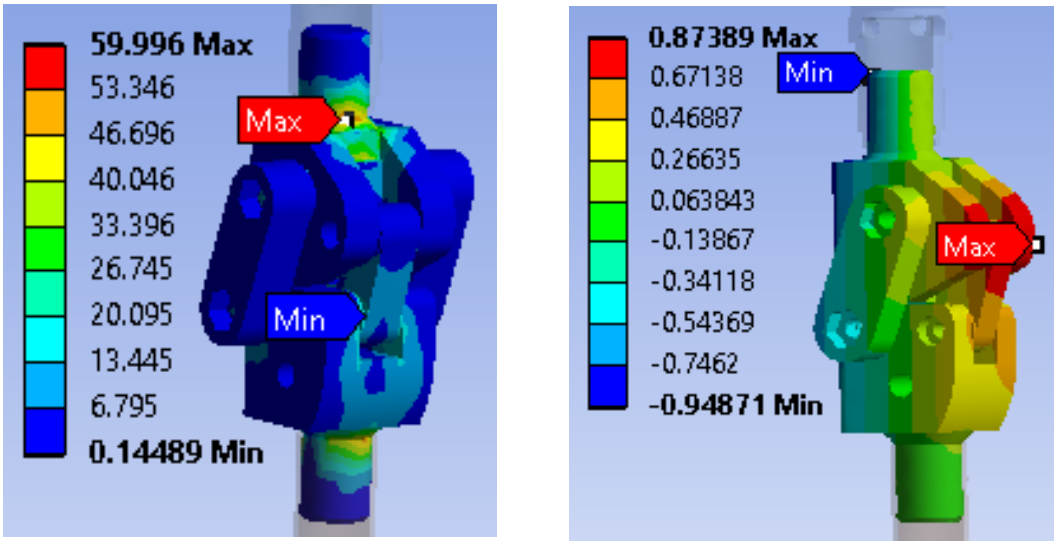

von Mises **Total deformation**

Figure 6.12: von Mises & Total deformation for Static test (ultimate strength); loading condition I; Nylon 66 with 2 wt.% Al_2O_3 composite

Upper Block

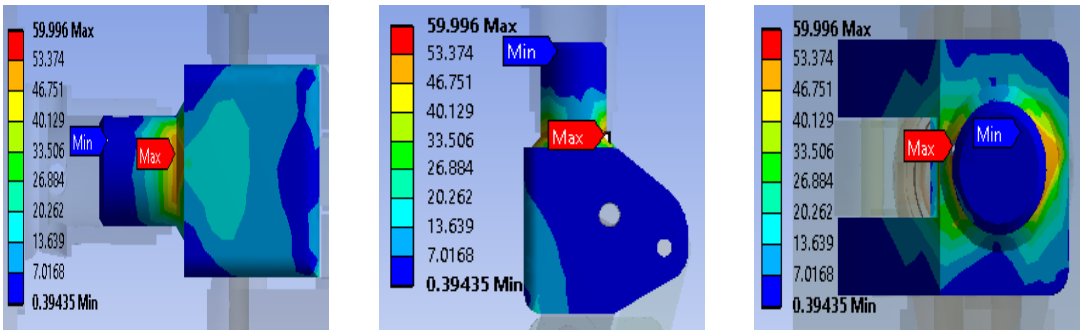

Lower Block

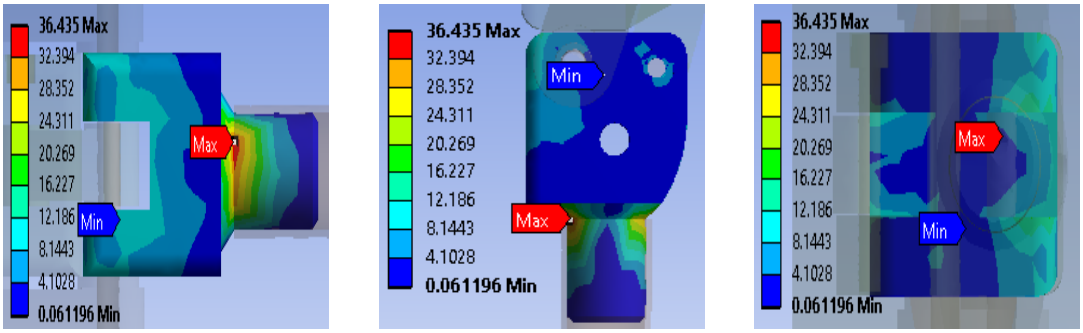

Side Link

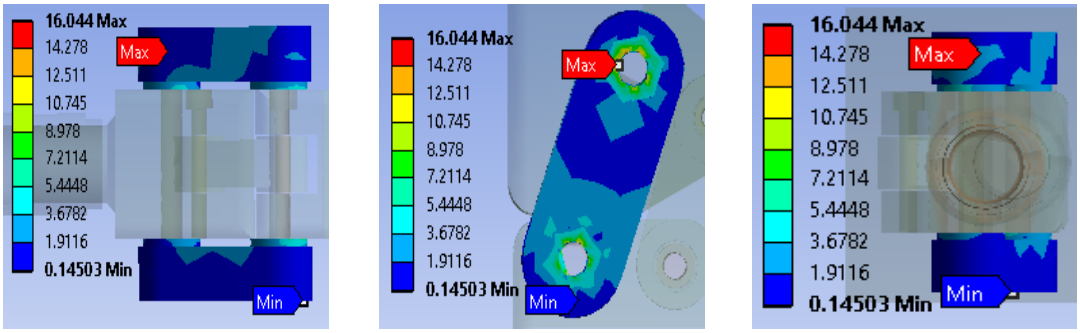

Middle Link

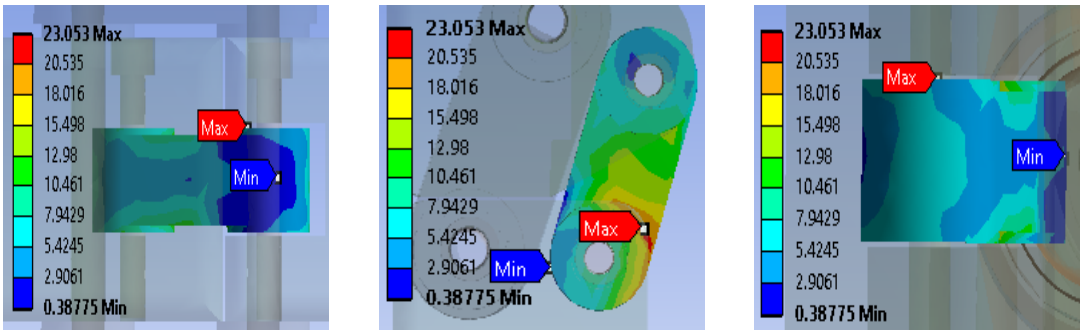

Figure 6.13: Von Mises stress for Static test (ultimate strength); loading condition I; Nylon 66 with 2 wt.% Al_2O_3 composite

6.3.4 Static test for ultimate strength; Loading condition II; Nylon 66 with 2 wt.% Al_2O_3 composite

The load of 3019 N is applied for doing the finite element analysis of static test for ultimate strength for the forefoot loading. The results of the analysis are given in Table 6.7 and the Figures 6.14 & 6.15 shows the total deformation & von Mises stresses.

Table 6.7: Result for Static test (ultimate strength); loading condition II; Nylon 66 with 2 wt.% Al_2O_3 composite

	Upper Block	Lower Block	Side Link	Middle Link	Knee Prosthesis
Von Mises stress (MPa)	66.40	60.78	37.15	34.40	66.40
Total deformation (mm)	4.11				

It is observed that the von Mises stresses and total deformation for all the individual components are less than the permissible values and the knee prosthesis design meets the requirements of ISO 10328 standard. From the results of heel loading and forefoot loading, it is concluded that the loading condition II generates more stresses in static test for ultimate strength.

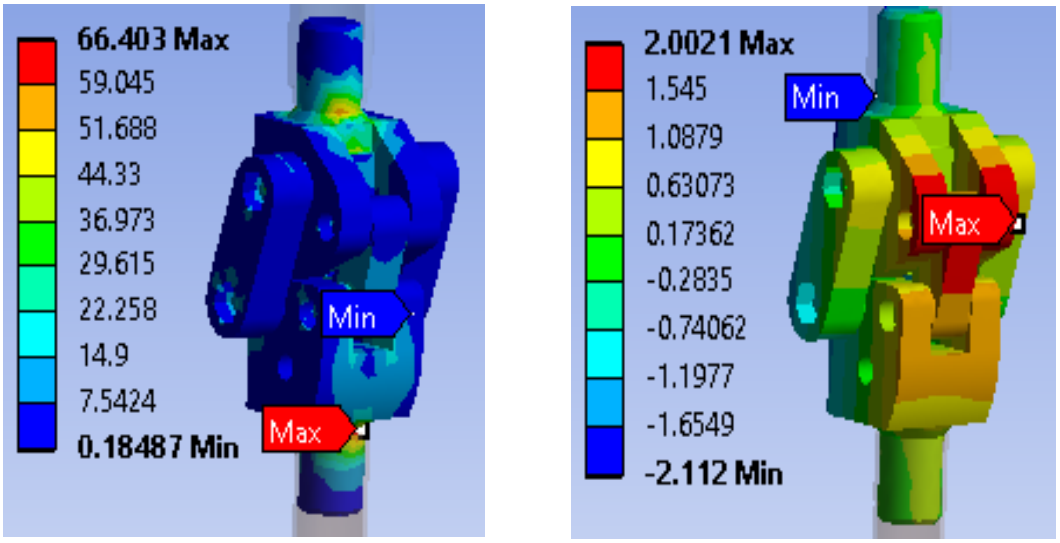

Figure 6.14: Total deformation for Static test (ultimate strength); loading condition II; Nylon 66 with 2 wt.% Al_2O_3 composite

Upper Block

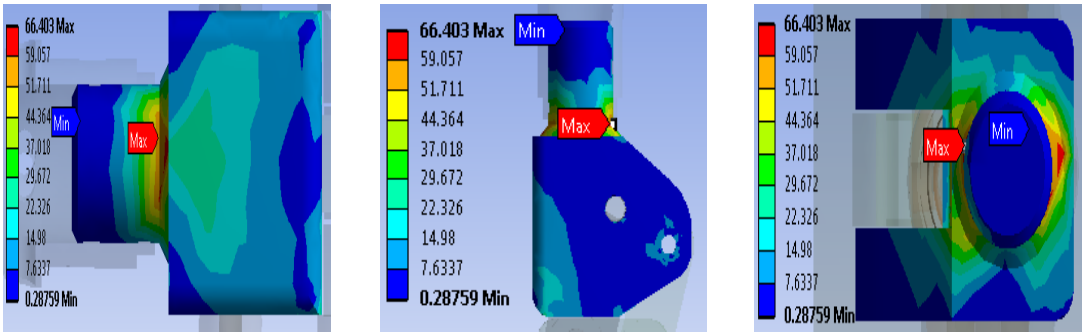

Lower Block

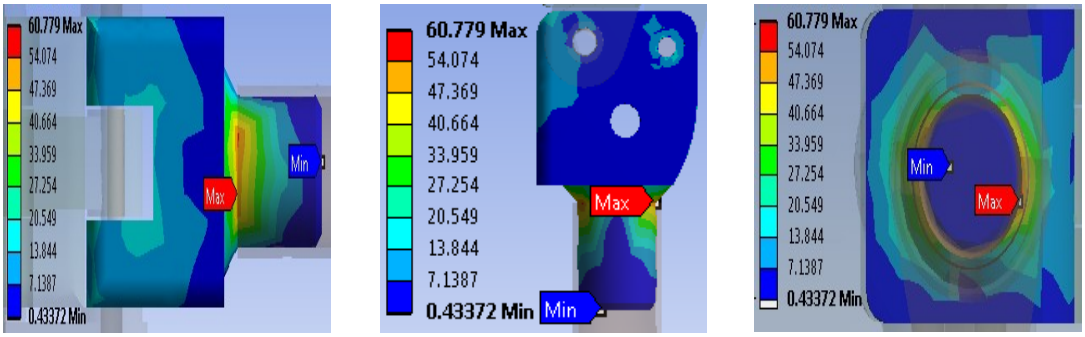

Side Link

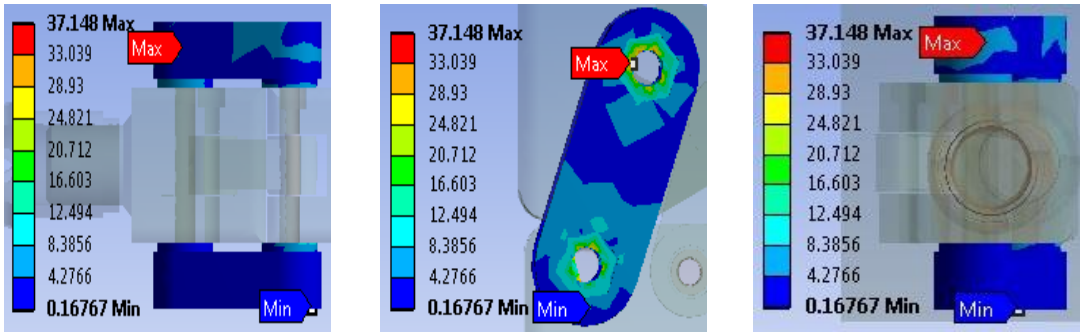

Middle Link

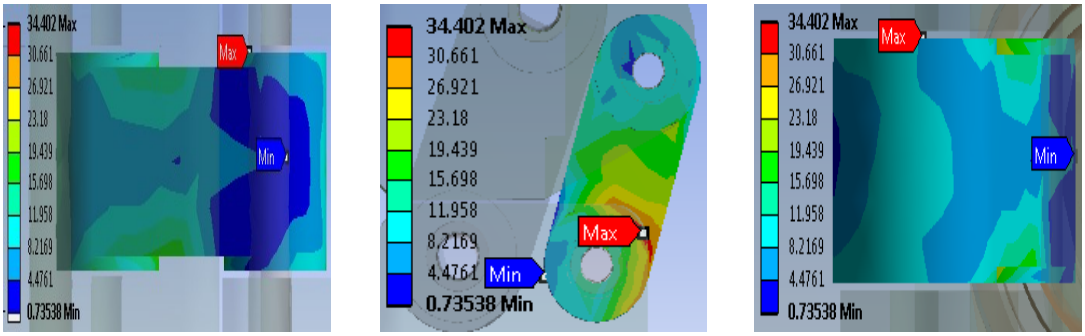

Figure 6.15: Von Mises stresses for Static test (ultimate strength); loading condition II; Nylon 66 with 2 wt. %Al_2O_3 composite

6.3.5 Contact Stresses

Contact stress causes deformation and the contact area may change depending on the magnitude of the contact stress. Thus, it is very important to calculate the actual stress at the point of contact, the so-called contact stress. The finite element analysis was also carried out to find out the contact stresses in all the assembly holes, both for the initial design and the optimized design. The nomenclature used for various holes of the knee joint is shown in Figure 6.16. The analysis were carried out at static ultimate test force of 3019 N for loading condition II and the results are tabulated in Table 6.8 and Figure 6.17.

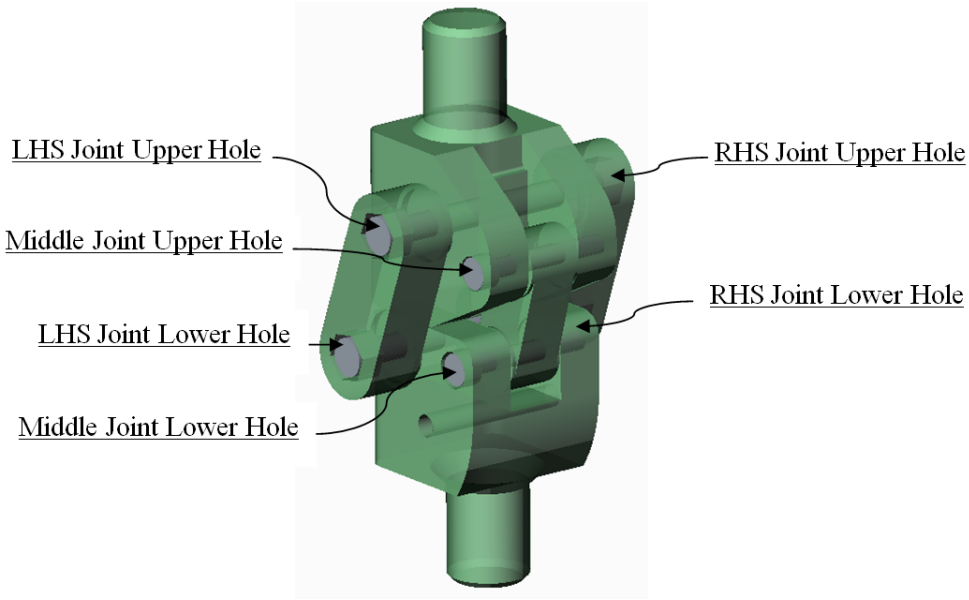

Figure 6.16: Knee joint holes nomenclature for contact stresses

Table 6.8: Contact stresses in assembly holes of knee joint

Assembly Holes	**Initial Design**	**Optimized Design**
	Contact Stresses (MPa)	
LHS Joint Upper Hole	90.62	18.68
LHS Joint Lower Hole	63.31	15.27
RHS Joint Upper Hole	79.82	28.92
RHS Joint Lower Hole	46.30	24.96
Middle Joint Upper Hole	78.42	19.14
Middle Joint Lower Hole	103.48	27.50

Assembly Holes	Initial Design	Optimized Design
	Contact Stresses (MPa)	
LHS Joint Upper Hole	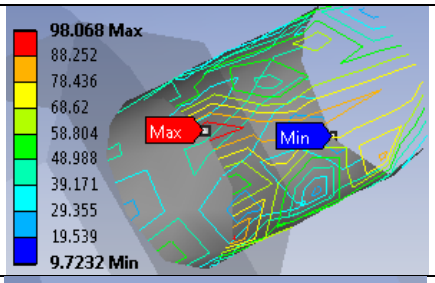	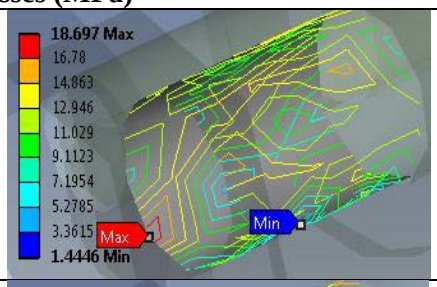
LHS Joint Lower Hole	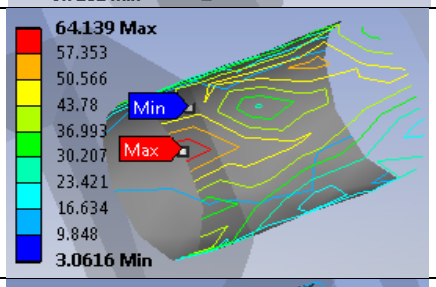	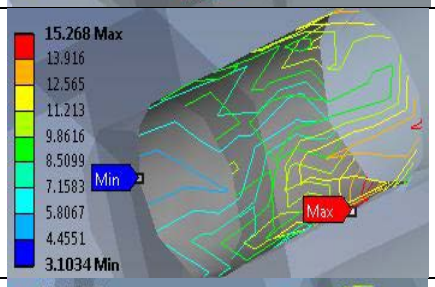
RHS Joint Upper Hole	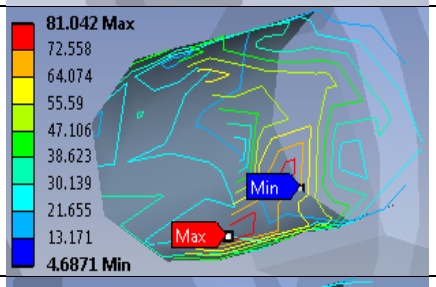	
RHS Joint Lower Hole	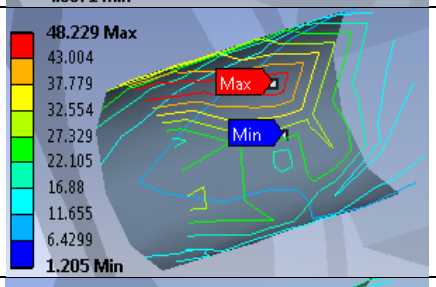	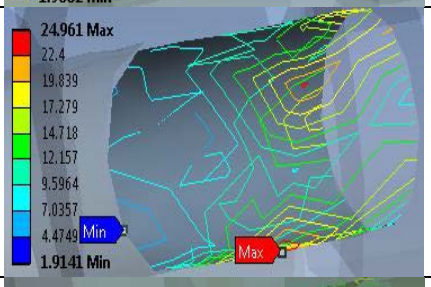
Middle Joint Upper Hole	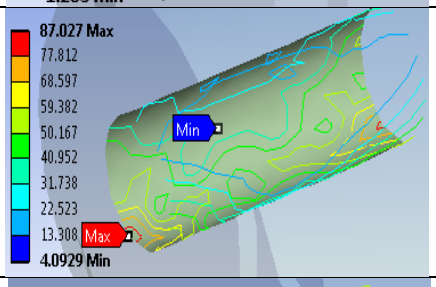	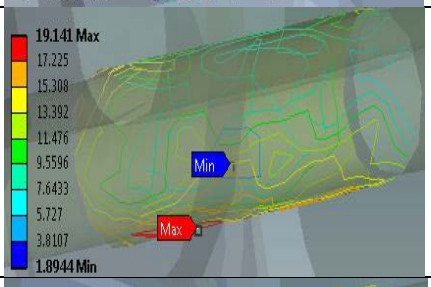
Middle Joint Lower Hole	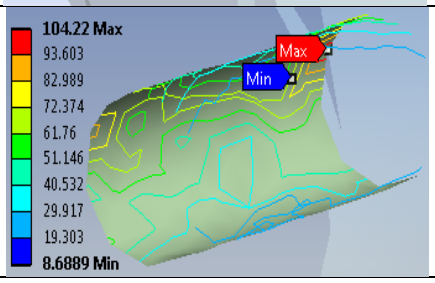	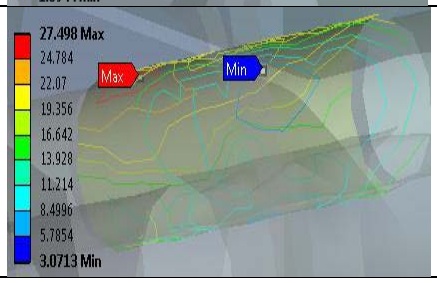

Figure 6.17: Contact stresses in the assembly holes of initial and optimized design

The finite element results revealed substantial reduction in the contact stresses in the optimized design. Thus, wear in the assembly holes will get reduced drastically enhancing the performance and the life of the knee prosthesis.

The optimized knee joint design as shown in Figure 6.18 & 6.19 is selected for further fatigue strength analysis by undertaking the cyclic test as per ISO 10328.

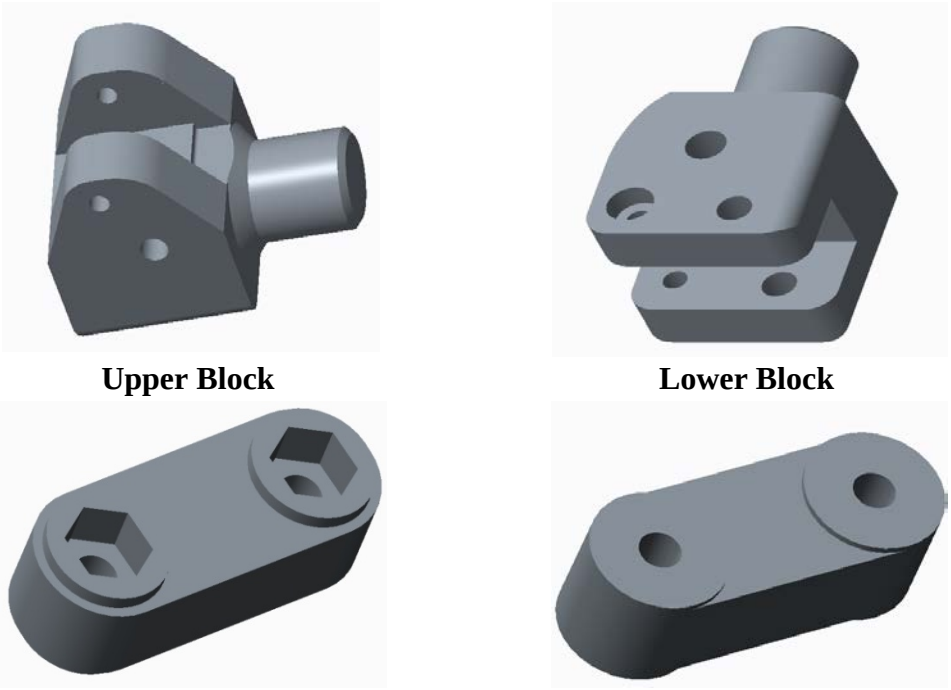

Upper Block **Lower Block**

Side Link- 2 nos. **Middle Link**

Figure 6.18: Optimized knee joint components

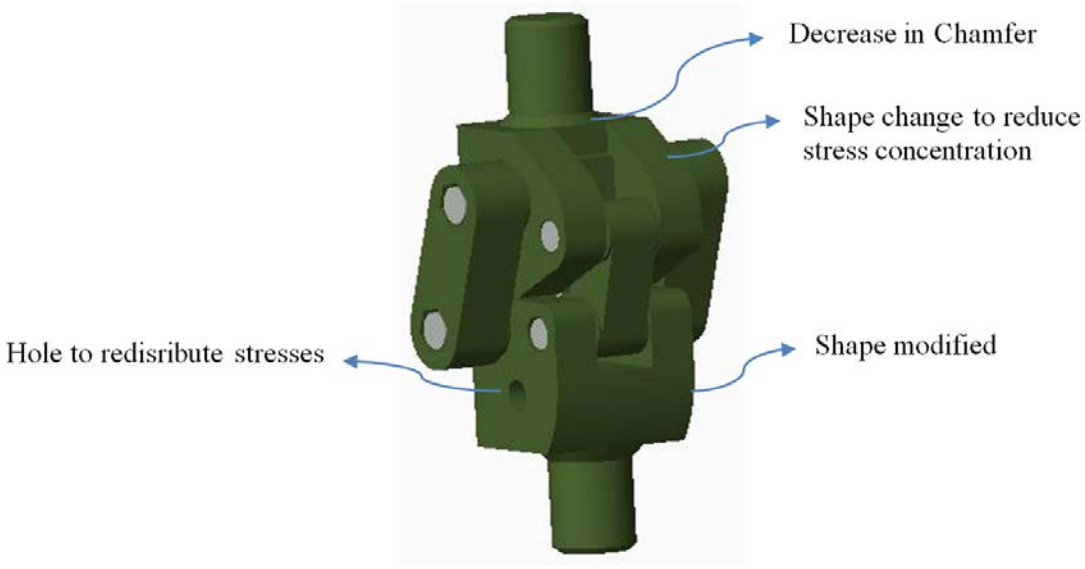

Figure 6.19: Optimized Knee Joint Prosthesis Model

6.4 Fatigue Testing

The failure of a mechanical component due to repeated loading which can occur at stress levels well below the tensile strength of a material is referred as fatigue. Fatigue testing as per ASTM D7791 was performed for Oilon and Nylon 66 – 2 wt. % Al_2O_3 composite. Tests were performed on Fatigue Tester Machine of Model 8874; INSTRON make of 25kN capacity. The test specimens were prepared as per ASTM D638 and test carried by applying sinusoidal loading with 5 Hz frequency. The tests were performed at four stress levels and from the experimental results S-N curves were drawn for Oilon and Nylon 66 – 2 wt. % Al_2O_3 composite as shown in Figure 6.20

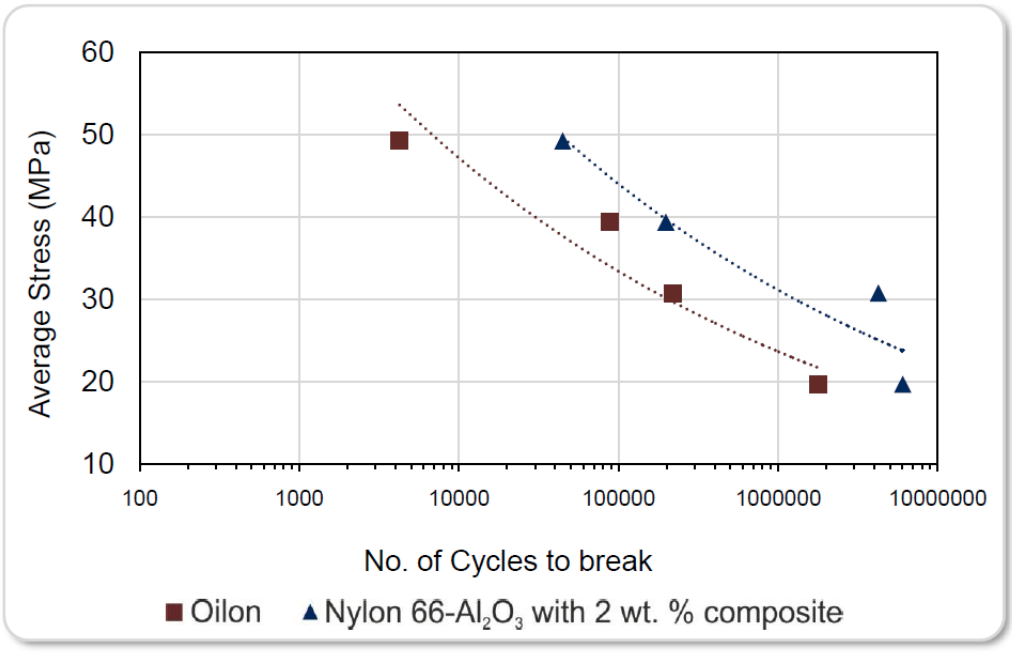

Figure 6.20: Experimental data of stress vs. number of cycles to failure for Oilon and Nylon 66 – 2 wt. % Al_2O_3 composite

6.5 Fatigue Life Assessment

The aim of the fatigue analysis is to characterize the capability of a material to survive the number of cyclic loading a product may experience during its lifetime before failure. As each cyclic test requires at least 35 days based on the loading frequency of 1 Hz, the cyclic strength tests were performed using FEM to save the development time and cost [19].

In ANSYS Fatigue module, the fatigue life assessment can be done by the methods based on Stress Life / Strain Life. Stress Life fatigue analysis is based on S-N curves (Stress – Cycle curves) and is suggested for applications where the product is subjected to relatively high numbers of cycles and therefore addresses High Cycle Fatigue (HCF), greater than 10^5 cycles. The Strain Life fatigue analysis is used for low cycle fatigue, when the numbers of cycles are less than 10^5.

The fatigue analysis based on Stress Life is done. The material parameters - Alternating Stress and Mean Stress obtained by fatigue testing experimentation are used for the simulation. Sinusoidal load as shown in Figure 3.15 and as per Table 5.1 of constant amplitude and proportional loading is applied for the analysis and simulation performed for fatigue life of 3×10^6 cycles. The results as shown in Figure 6.21, indicates that the fatigue life of initial design is 1.93×10^6 cycles and does not meet the criteria of ISO 10328 standard. From Figure 6.22, it is revealed that the optimized design may be able to exceed the specified number of 3×10^6 cycles and hence fulfills the requirements of ISO 10328 standard.

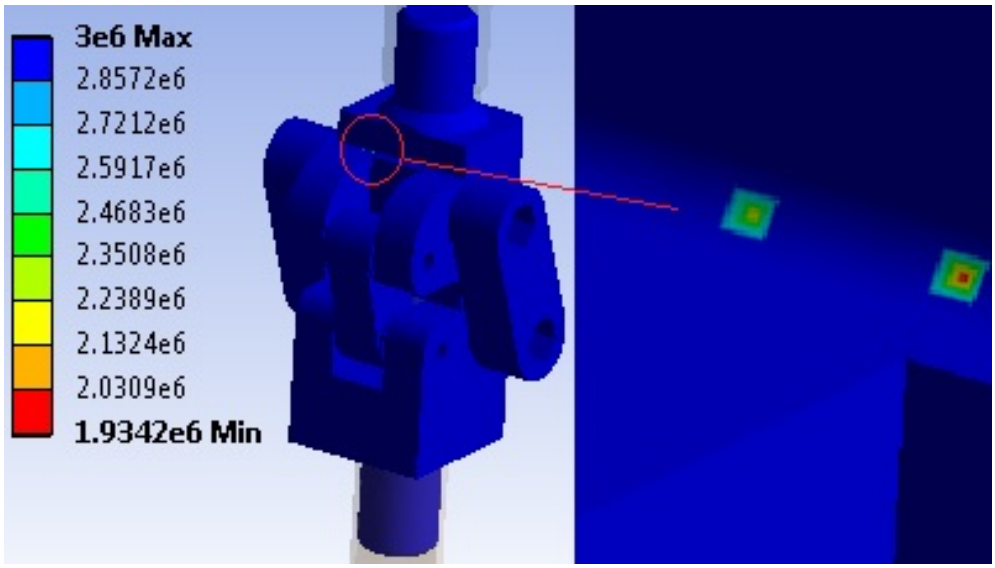

Fig 6.21: Fatigue life of initial design of above knee prosthesis

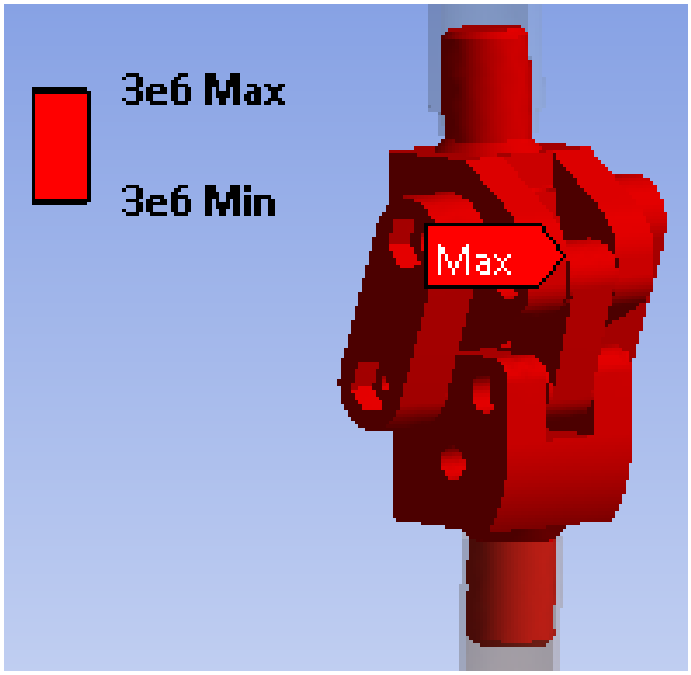

Fig 6.22: Fatigue life of optimized knee prosthesis

Thus the modified design number 9 meets all the performance requirements of the ISO 10328 standard requirements and meets the research objectives. The optimized design of the above knee prosthesis meets the static and cyclic strength criteria and the weight of optimized above knee prosthesis is reduced to 356 grams compared to the existing design of 372 grams.

*****

CHAPTER 7

SUMMARY, CONCLUSIONS AND SCOPE FOR FUTURE WORK

CHAPTER 7
SUMMARY, CONCLUSIONS AND SCOPE FOR FUTURE WORK

This chapter contains the summary of the work done along with objectives and analysis of experimental results. The conclusions based on the research work are presented systematically in this chapter followed by the scope for future work in this field.

7.1 Background to the research work

The work in this thesis is initiated with an objective to develop new material with better mechanical and tribological properties for knee prosthesis and select the optimal material using TOPSIS technique. To perform finite element analysis on the initial design of knee prosthesis as per ISO 10328 standard and to develop optimized design for knee prosthesis meeting its performance criteria including fatigue life assessment.

To develop new material, reinforcement of micro sized filler of aluminium oxide and titanium dioxide is made to Nylon66 material and following eight types of composites were developed:

1. Composites of Nylon66 by adding 2 wt.%, 4 wt.%, 6 wt.% and 8 wt.% of microparticulates of aluminium oxide.
2. Composites of Nylon66 by adding 2 wt.%, 4 wt.%, 6 wt.% and 8 wt.% of microparticulates of titanium dioxide.

The above eight types of Nylon66 composites were prepared under identical processing conditions and were studied for the following properties alongwith Nylon66 and oil impregnated nylon. The experimental results were used to select the optimal material:

- Mechanical and thermo-mechanical properties (Chapter 4)
- Tribological properties (Chapter 4)
- Morphological properties (Chapter 4)

The finite element analysis of the initial design of knee prosthesis is performed with the material properties of oil impregnated Nylon and composite of Nylon66 with 2 wt. % of aluminium oxide. (Chapter 5)

The knee prosthesis design is modified and nine designs were prepared by using orthogonal array L9 and the optimized design selected. (Chapter 6)

7.2 Conclusions of the research work

Following salient conclusions are drawn based on the experimental studies and research work during the course of this thesis.

Composites of Nylon66 and aluminum oxide

1. The results show that wear rate reduces with addition of alumina microparticles to Nylon66 and lowest wear is exhibited by 2 wt.% Al_2O_3-Nylon 66 composite. The lowest friction coefficient is also observed for 2 wt.% Al_2O_3-Nylon 66 composite and the value increases with increasing load, sliding velocity and sliding distance.
2. The coefficient of friction of 2 wt.% Al2O3-Nylon 66 lies between 0.1 to 0.5 under various combinations of load, sliding velocity and sliding distance. COF increases with the percentage increase of alumina from 2 wt.% to 8 wt.% but remains less than that of pure Nylon 66 and oilon material.
3. The mechanical properties such as tensile strength, tensile modulus, flexural strength, flexural modulus, compressive strength and impact strength increases with the increase in wt.% of micro alumina upto 6 wt.% and thereafter reduces.
4. The heat deflection temperature of the microcomposite increased with increasing wt.% of alumina.
5. Thus the study concluded that the addition of micro alumina particles to Nylon 66 resulted in improving the mechanical and tribological properties more effectively at lower filler loading.

Composites of Nylon66 and titanium dioxide

6. Addition of titanium dioxide has positive effect on the mechanical properties such as tensile strength, tensile modulus, flexural strength, flexural modulus, compressive strength and impact strength increases with the increase in wt.% of titanium dioxide up to 6 wt.% and thereafter reduces.
7. The heat deflection temperature increases almost linearly with the addition of titanium dioxide.
8. The tribological properties, sliding wear and COF were systematically studied on pin- on-disk equipment under different sliding condition of load, velocity and distance. It is found that addition of micro TiO_2 to Nylon66 reduces the wear and COF up to 6 wt.% and beyond that the values increases and become more than that of plain Nylon66 and oil impregnated nylon.
9. The lowest wear and COF were observed at 2 wt% loading of TiO_2 and with the increase in filler, wear and COF keep on increasing. Higher filler content increases the COF due to more particles coming in contact and thus resulting in increase of wear.
10. The worn surfaces were examined by SEM and studies indicated that at lower loading TiO_2 is well dispersed in Nylon 66 but at higher wt.% TiO_2 agglomerates resulting in higher COF and wear.
11. The best results for mechanical properties are observed at 6 wt.% and for tribological properties at 2 wt.%. Thus suitable composite can be selected based on the end application.

Selection of Material

12. The results of Closeness Index obtained by the application of TOPSIS reveals that the composite of Nylon66 with 2 wt.% of aluminum oxide ranks first followed by Nylon66 with 4 wt.% of aluminum oxide and Nylon66 with 2 wt.% of titanium dioxide thereafter.
13. The composites of Nylon66 with 8 wt.% of aluminum oxide and Nylon66 with 8 wt.% of titanium dioxide ranks lower than that of plain Nylon66 and oil impregnated nylon and thus not recommended.

14. The composite of Nylon66 with 2 wt.% of aluminum oxide which ranked first in Closeness Index is chosen as the optimal material for knee joint prosthesis.

Finite Element Analysis

15. The finite element analysis results reveal that the stresses are more severe in forefoot loading in comparison to heel loading both for static proof and static ultimate strength loading as per ISO 10328.
16. The finite element analysis performed for the static test at loading level P5 suitable for person of 100 kg weight and test loading conditions I & II reveals that the design is not complying the requirements of ISO 10328 standard as the von Mises stresses are more than the yield strength of the Oilon and composite of Nylon 66 filled with 2 wt. % of aluminum oxide material.
17. The modified design number 9 meets the static structural requirements of the ISO 10328 standard as the maximum von Mises stresses are less than that of Nylon66 with 2 wt.% aluminum oxide and the total deformation is also less than 5mm.
18. The fatigue life assessment of the modified design predicts the fatigue life of more than $3x10^6$ cycles and meets the performance criteria of ISO 10328 whereas, the initial design predicts the fatigue life of 1.93×10^6 cycles which is less than the requirement.
19. FEA results shows that the optimized design of the knee joint prosthesis meets the structural strength criteria for static and cyclic loading for P5 level as per ISO 10328 standard.
20. The weight of optimized knee joint prosthesis is reduced to 356 grams from the initial design of 372 grams thus reducing the weight by 4.3%.

7.3 Scope for future work

Because of time limit, the research work accomplished in this project is still in initial stage. Following aspects could not be addressed in this thesis work and hence may be taken up in the future work.

1. The studies are mainly focused on development of new composite material with Nylon66 as the matrix; however the scope with other engineering materials may be explored in future.
2. The present studies can be extended in future by conducting the dynamic analysis and field testing of the new proposed design.
3. Design optimization of the initial design can be extended further by modifying the side and middle links to further reduce the weight.

*****

REFERENCES

REFERENCES

1. Disabled Persons in India A statistical profile, 2016; Social Statistics Division, Ministry of Statistics and Programme Implementation, Government of India; http://www.mospi.gov.in
2. Gottschalk, F. (1992). *Atlas of Limb Prosthetics: Surgical, Prosthetic, and Rehabilitation Principles - Transfemoral Amputation: Surgical Procedures*. Mosby; 20:2.
3. Smith, D. (2004). *The Transfemoral Amputation Level*. Motion; 14:2.
4. Sugarbaker, P. et al. (2001). *Musculoskeletal cancer surgery*; Chapter 22-Above-knee Amputation.
5. Michael, J. W., & Bowker, J. H. (Eds.). (2004). *Atlas of amputations and limb deficiencies: surgical, prosthetic, and rehabilitation principles.* American Academy of Orthopaedic Surgeons.
6. Chakravarthy Y. K., Suneel & Lingaraju D. (2011). Alternate materials for Modeling and Analysis of Prosthetic Knee joint. *International Journal of Science and Advanced Technology*, 1(5), 262-266.
7. Anand, T. S., & Sujatha, S. (2017). A method for performance comparison of polycentric knees and its application to the design of a knee for developing countries. *Prosthetics and orthotics international*, *41*(4), 402-411.
8. Gard, S. A., Childress, D. S., & Uellendahl, J. E. (1996). The influence of four-bar linkage knees on prosthetic swing-phase floor clearance. *JPO: Journal of Prosthetics and Orthotics*, *8*(2), 34-40.
9. Greene, M. P. (1983). Four bar linkage knee analysis. *Orthot Prosthet*, *37*(1), 15-24.
10. Hobson, D.A. & Torfason, L.E. (1975). Computer Optimization of Polycentric Prosthetic Knee Mechanisms. *Bulletin of prosthetics research*, 10(23), 187-201.

11. Radcliffe, C. W. (1994). Four-bar linkage prosthetic knee mechanisms: kinematics, alignment and prescription criteria. *Prosthetics and orthotics international*, *18*(3), 159-173.

12. Bneakey, J. W., & Marquette, S. H. (1998). Beyond the four-bar knee. *JPO: Journal of Prosthetics and Orthotics*, *10*(3), 77-80.

13. Sancisi, N., Caminati, R., & Parenti-Castelli, V. (2009, September). Optimal four-bar linkage for the stability and the motion of the human knee prostheses. In *Atti del XIX CONGRESSO dell' Associazione Italiana di Meccanica Teorica e Applicata. Ancona,* 1-10

14. Scholz, M. S., Blanchfield, J. P., Bloom, L. D., Coburn, B. H., Elkington, M., Fuller, J. D.,... & Trevarthen, J. A. (2011). The use of composite materials in modern orthopaedic medicine and prosthetic devices: A review. *Composites Science and Technology*, *71*(16), 1791-1803.

15. Lu, J., & Chen, Y. (2013). Topology optimisation and customisation of a prosthetic knee joint design. *International Journal of Computer Integrated Manufacturing*, *26*(10), 968-976.

16. Magnissalis, E. A., Solomonidis, S. E., Spence, W. D., Paul, J. P., & Zahedi, S. (1999). Prosthetic loading during kneeling of persons with transfemoral amputation. *Journal of rehabilitation research and development*, *36*(3), 164-172.

17. "Prosthetics—Structural testing of lower limb prostheses—Requirements and test methods", International *Standard ISO 10328*, First edition 2006-10-01.

18. Phanphet, S., Dechjarern, S., & Jomjanyong, S. (2017). Above-knee prosthesis design based on fatigue life using finite element method and design of experiment. *Medical engineering & physics*, *43*, 86-91.

19. Lapapong, S., Sucharitpwatskul, S., Pitaksapsin, N., Srisurangkul, C., Lerspalungsanti, S., Naewngerndee, R., ... & Pipitpukdee, J. (2014). Finite element modeling and validation of a four-bar linkage prosthetic knee under static and cyclic strength tests. *Journal of Assistive, Rehabilitative & Therapeutic Technologies*, *2*(1), 23211.

20. Thurston, A. J. (2007). Paré and prosthetics: the early history of artificial limbs. *ANZ journal of surgery*, *77*(12), 1114-1119.

21. Norton, K. (2007). A brief history of prosthetics. *InMotion*, *17*(7), 11-13.

22. Childress, D. S. (1985). Historical aspects of powered limb prostheses. *Clin Prosthet Orthot*, *9*(1), 2-13.

23. Wells, R. P. (1981). The projection of the ground reaction force as a predictor of internal joint moments. *Bulletin of prosthetics research*, *10*, 15-19.

24. Mensch, G., & Ellis, P. M. (1986). *Physical therapy management of lower extremity amputations*. Rockville, MD: Aspen Publishers.

25. Boonstra, A. M., Rijnders, L. J. M., Groothoff, J. W., & Eisma, W. H. (2000). Children with congenital deficiencies or acquired amputations of the lower limbs: functional aspects. *Prosthetics and orthotics international*, *24*(1), 19-27.

26. Krebs, D. E., & Fishman, S. (1984). Characteristics of the child amputee population. *Journal of pediatric orthopedics*, *4*(1), 89-95.

27. Bossert, J.L. (1991). Quality Function Deployment. Milwaukee, WI: ASQC

28. Jacques, G. E., Ryan, S., Naumann, S., Milner, M., & Cleghorn, W. L. (1994). Application of quality function deployment in rehabilitation engineering. *IEEE Transactions on Rehabilitation Engineering*, *2*(3), 158-164.

29. Shurr, Donald G., John, W. Michael & Thomas Michael Cook. (2002). Prosthetics and orthotics. Prentice Hall.

30. Highsmith, M. J., Kahle, J. T., Bongiorni, D. R., Sutton, B. S., Groer, S., & Kaufman, K. R. (2010). Safety, energy efficiency, and cost efficacy of the C-Leg for transfemoral amputees: a review of the literature. *Prosthetics and orthotics international*, *34*(4), 362-377.

31. Highsmith, M. J., Kahle, J. T., Carey, S. L., Lura, D. J., Dubey, R. V., Csavina, K. R., & Quillen, W. S. (2011). Kinetic asymmetry in transfemoral amputees while performing sit to stand and stand to sit movements. *Gait & posture*, *34*(1), 86-91.

32. Highsmith, M. J., Schulz, B. W., Hart-Hughes, S., Latlief, G. A., & Phillips, S. L. (2010). Differences in the spatiotemporal parameters of transtibial and transfemoral amputee gait. *JPO: Journal of Prosthetics and Orthotics*, *22*(1), 26-30.

33. Sadler, David Greig (2009). "A $20 prosthetic knee to bring relief to disadvantaged amputees" *April 22*, *PDT*.

34. Baumgartner, R. F. (1979). Knee disarticulation versus above-knee amputation. *Prosthetics and Orthotics International*, *3*(1), 15-19.

35. Unal, R., Carloni, R., Hekman, E. E., Stramigioli, S., & Koopman, H. F. (2010, October). Conceptual design of an energy efficient transfemoral prosthesis. *IEEE/RSJ International Conference on Intelligent Robots and Systems*, 343-348.

36. Christensen, B., Ellegaard, B., Bretler, U., & Østrup, E. L. (1995). The effect of prosthetic rehabilitation in lower limb amputees. *Prosthetics and orthotics international*, *19*(1), 46-52.

37. Sushko, J., Honeycutt, C., & Reed, K. B. (2012, June). Prosthesis design based on an asymmetric passive dynamic walker. *4th IEEE RAS/EMBS International Conference on Biomedical Robotics and Biomechatronics (BioRob)*, 1116-1121.

38. Andrysek, J., Klejman, S., Torres-Moreno, R., Heim, W., Steinnagel, B., & Glasford, S. (2011). Mobility function of a prosthetic knee joint with an automatic stance phase lock. *Prosthetics and orthotics international*, *35*(2), 163-170.

39. Michael, J. W. (1999). Modern prosthetic knee mechanisms. *Clinical Orthopaedics and Related Research®*, *361*, 39-47.

40. Andrysek, J. (2010). Lower-limb prosthetic technologies in the developing world: A review of literature from 1994–2010. *Prosthetics and orthotics international*, *34*(4), 378-398.

41. Mukul, P., Sadler, J., & Thorsell, E. (2010, May). Stanford–jaipur knee joint for trans femoral amputees. *Proceedings of the 13th world congress of the International Society for Prosthetics and Orthotics, Leipzig, Germany*, 10-15.

42. Radcliffe, C. W. (1977). Above-knee prosthetics. *Prosthetics and Orthotics International*, *1*(3), 146-160.

43. Highsmith, M. J., Kahle, J. T., Lura, D. J., Lewandowski, A. L., Quillen, W. S., & Kim, S. H. (2014). Stair ascent and ramp gait training with the Genium knee. *Technology & Innovation*, *15*(4), 349-358.

44. Sup, F., Bohara, A., & Goldfarb, M. (2008). Design and control of a powered transfemoral prosthesis. *The International journal of robotics research*, *27*(2), 263-273.

45. Sup, F., Varol, H. A., Mitchell, J., Withrow, T. J., & Goldfarb, M. (2009, June). Self-contained powered knee and ankle prosthesis: Initial evaluation on a transfemoral amputee. *IEEE 11th International Conference on Rehabilitation Robotics*, 638-644.

46. Zlatnik, D., Steiner, B., & Schweitzer, G. (2002). Finite-state control of a trans-femoral (TF) prosthesis. *IEEE Transactions on Control Systems Technology*, *10*(3), 408-420.

47. Yokogushi, K., Narita, H., Uchiyama, E., Chiba, S., Nosaka, T., & Yamakoshi, K. I. (2004). Biomechanical and clinical evaluation of a newly designed polycentric knee of transfemoral prosthesis. *Journal of Rehabilitation Research & Development*, *41*(5), 675-682.

48. Martinez-Villalpando, E. C., & Herr, H. (2009). Agonist-antagonist active knee prosthesis: a preliminary study in level-ground walking. *Journal of Rehabilitation Research & Development*, *46*(3), 361-373.

49. Berger, N. (1992). *Atlas of Limb Prosthetics: Surgical, Prosthetic, and Rehabilitation Principles*; Chapter 14 - Analysis of Amputee Gait. Mosby

50. Hagberg, K., & Brånemark, R. (2001). Consequences of non-vascular trans-femoral amputation: a survey of quality of life, prosthetic use and problems. *Prosthetics and orthotics international*, *25*(3), 186-194.

51. Dudek, N. L., Marks, M. B., Marshall, S. C., & Chardon, J. P. (2005). Dermatologic conditions associated with use of alower-extremity prosthesis. *Archives of physical medicine and rehabilitation*, *86*(4), 659-663.

52. De Vries, J. (1995). Conventional 4-bar linkage knee mechanisms: a strength-weakness analysis. *Journal of rehabilitation research and development*, *32*(1), 36-42.

53. Strait, E. (2006). Prosthetics in developing countries. *Prosthetic Resident*, 1-40.

54. Argun_ah Bayram, H. (2015). Recent Developments in Above-Knee Prosthetics and the Importance of Energy Recovery in Transfemoral Amputee Gait, *Physical Medicine and Rehabilitation*,2, 61-68.

55. Unal, R., Behrens, S. M., Carloni, R., Hekman, E. E. G., Stramigioli, S., & Koopman, H. F. J. M. (2010, September). Prototype design and realization of an innovative energy efficient transfemoral prosthesis. *3rd IEEE RAS/EMBS International Conference on Biomedical Robotics and Biomechatronics*, 191-196.

56. Radcliffe, C. W., & Lamoreux, L. W. (1968). *UC-BL Pneumatic swing-control unit for above-knee prostheses: Design, adjustment and installation*. *Bulletin of Prosthetics Research*, 73-89.

57. Hansen, A. H., Childress, D. S., & Knox, E. H. (2000). Prosthetic foot rollover shapes with implications for alignment of transtibial prostheses. *Prosthetics and Orthotics International*, *24*(3), 205-215.

58. Steven A. Gard. "The Influence of Four-Bar Linkage Knees on Prosthetic Swing-Phase Floor Clearance". *JPO, 1996 Vol. 8, Num. 2 , pp. 34-40*.

59. Jin, D., Zhang, R., Dimo, H. O., Wang, R., & Zhang, J. (2003). Kinematic and dynamic performance of prosthetic knee joint using six-bar mechanism. *Journal of rehabilitation research and development*, *40*(1), 39-48.

60. Michael, J. W. (1994). Prosthetic knee mechanisms. *Physical Medicine and Rehabilitation: State of the Art Reviews*, *8*, 147-164.

61. James, W., & Stuart, H. (1998). Technical note: Beyond the four-bar knee. *Journal of prosthetics and orthotics*, *10*(3), 77-80.

62. Chakraborty, J. K., & Patil, K. M. (1994). A new modular six-bar linkage trans-femoral prosthesis for walking and squatting. *Prosthetics and Orthotics International*, *18*(2), 98-108.

63. Van de Veen, P. G. (1994). Principles of multiple-bar linkage mechanisms for prosthetics knee joints. In *Abstract of the 8th World Congress, ISPO,* 2-7.

64. Mangera, T., Kienhöfer, F., Carlson, K. J., Conning, M., Brown, A., & Govender, G. (2018). Optimal material selection for the construction of a paediatric prosthetic knee. *Proceedings of the Institution of Mechanical Engineers, Part L: Journal of Materials: Design and Applications*, *232*(2), 137-147.

65. Gutfleisch, O. (2003). Peg legs andbionic limbs: the development of lower extremity prosthetics. *Interdisciplinary Science Reviews*, *28*(2), 139-148.

66. Klasson, B. L. (1995). Carbon fibre and fibre lamination in prosthetics and orthotics: some basic theory and practical advice for the practitioner. *Prosthetics and Orthotics International*, *19*(2), 74-91.

67. Sherry Metzger. “Materials science: Producing lighter, more cosmetically appealing o&p devices”. The O & P EDGE. August 2006

68. Hanson, B. H. (1986). Present and future uses of titanium in engineering. *Materials & Design*, *7*(6), 301-307.

69. Coombes, A. G., Greenwood, C. D., & Shorter, J. J. (1996). Plastic materials for external prostheses and orthoses. *Human biomaterials applications*. Humana Press, Totowa, NJ, 11, 215-255.

70. Coombes, A. G. A., & MacCoughlan, J. (1988). Development and testing of thermoplastic structural components for modular prostheses. *Prosthetics and orthotics international*, *12*(1), 19-40.

71. Oberg, K. (1991). Cost-benefits in orthopaedic technology by using thermoplastics in developing countries. *Prosthetics and orthotics international*, *15*(1), 18-22.

72. Oberg, K. “Report on Orthopaedic Technology in Major Centres in Thailand, India and Jordan (1988)”. *A report commissioned by WHO RHBl HQ. - Geneva*.

73. Quigley, M. J., Irons, G., & Donaldson, N. R. (1977). *The Rancho Ultralight Below Knee Prosthesis*. Rehabilitation Engineering Center at Rancho Los Amigos Hospital, County of Los Angeles, University of Southern California.

74. Convery, P., Hughes, J., Jones, D., & Whitefield, G. (1986). A Clinical-Evaluation of An Ultralight weight Polypropylene Below-Knee Prosthesis. *Orthotics and Prosthetics*, *40*(3), 30-37.

75. Day, H. J. B. (1996). A review of the consensus conference on appropriate prosthetic technology in developing countries. *Prosthetics and orthotics international*, *20*(1), 15-23.

76. Baena, J. C., Wu, J., & Peng, Z. (2015). Wear performance of UHMWPE and reinforced UHMWPE composites in arthroplasty applications: a review. *Lubricants*, *3*(2), 413-436.

77. Bono, J. V., & Scott, R. D. (2005). *Revision total knee arthroplasty* (Vol. 113). New York: Springer.

78. Faulkner, V., Field, M., Egan, J. W., & Gall, N. G. (1987). Evaluation of high strength materials for prostheses. *Orthot Prosthet*, *40*(4), 44-58.

79. Najeeb, S., Zafar, M. S., Khurshid, Z., & Siddiqui, F. (2016). Applications of polyetheretherketone (PEEK) in oral implantology and prosthodontics. *Journal of prosthodontic research*, *60*(1), 12-19.

80. Toth, J. M., Wang, M., Estes, B. T., Scifert, J. L., Seim III, H. B., & Turner, A. S. (2006). Polyetheretherketone as a biomaterial for spinal applications. *Biomaterials*, *27*(3), 324-334.

81. Skinner, H. B. (1988). Composite technology for total hip arthroplasty. *Clinical orthopaedics and related Research*, (235), 224-236.

82. Plastic Prosthetics for the Developing World. *(2014), Plastics Makes It Possible.*

83. Agarwal, B. D., Broutman, L. J., & Chandrashekhara, K. (2017). *Analysis and performance of fiber composites*. John Wiley & Sons.

84. Leong, Y. W., Bakar, M. A., Ishak, Z. M., & Ariffin, A. (2004). Characterization of talc/calcium carbonate filled polypropylene hybrid composites weathered in a natural environment. *Polymer Degradation and Stability*, *83*(3), 411-422.

85. Chisholm, N., Mahfuz, H., Rangari, V. K., Ashfaq, A., & Jeelani, S. (2005). Fabrication and mechanical characterization of carbon/SiC-epoxy nanocomposites. *Composite structures*, *67*(1), 115-124.

86. Zimmerman, S., Hawkes, W. G., Hudson, J. I., Magaziner, J., Hebel, J. R., Towheed, T., ... & Kenzora, J. E. (2002). Outcomes of surgical management of total HIP replacement in patients aged 65 years and older: cemented versus cementless femoral components and lateral or anterolateral versus posterior anatomical approach. *Journal of orthopaedic research*, *20*(2), 182-191.

87. Marrs, B., Andrews, R., & Pienkowski, D. (2007). Multiwall carbon nanotubes enhance the fatigue performance of physiologically maintained methyl methacrylate–styrene copolymer. *Carbon*, *45*(10), 2098-2104.

88. Carotenuto, G., Nicolais, L., Kuang, X., & Zhu, Z. (1996). A method for the preparation of PMMA-SiO_2 nanocomposites with high homogeneity. *Applied Composite Materials*, *2*(6), 385-393.

89. De Santis, R., Ambrogi, V., Carfagna, C., Ambrosio, L., & Nicolais, L. (2006). Effect of microencapsulated phase change materials on the thermo-mechanical properties of poly (methyl-methacrylate) based biomaterials. *Journal of Materials Science: Materials in Medicine*, *17*(12), 1219-1226.

90. Maiti, S. N., & Lopez, B. H. (1992). Tensile properties of polypropylene/ kaolin composites. *Journal of applied polymer science*, *44*(2), 353-360.

91. Kohan, M. I. (Ed.). (1973). *Nylon plastics*. Wiley.

92. Zhao, L. X., Zheng, L. Y., & Zhao, S. G. (2006). Tribological performance of nano-Al_2O_3 reinforced polyamide 6 composites. *Materials Letters*, *60*(21-22), 2590-2593.

93. Mahfuz, H., Rangari, V. K., Islam, M. S., & Jeelani, S. (2004). Fabrication, synthesis and mechanical characterization of nanoparticles infused polyurethane foams. *Composites Part A: Applied Science and Manufacturing*, *35*(4), 453-460.

94. Chen, G., Luo, G., Yang, X., Sun, Y., & Wang, J. (2004). Anatase-TiO_2 nano-particle preparation with a micro-mixing technique and its photocatalytic performance. *Materials Science and Engineering: A*, *380*(1-2), 320-325.

95. Bose, S., & Mahanwar, P. A. (2004). Effect of particle size of filler on properties of nylon-6. *Journal of Minerals and Materials Characterization and Engineering*, *3*(01), 23.

96. Cai, H., Yan, F., Xue, Q., & Liu, W. (2003). Investigation of tribological properties of Al_2O_3-polyimide nanocomposites. *Polymer Testing*, *22*(8), 875-882.

97. Zhao, Y. J., Huang, X. M., Dai, R. R., Zhang, W., Wu, Y. C., Shu, X., & Xu, P. (2013). Study on properties of epoxy resin/Al_2O_3 composites. In *Advanced Materials Research* (Vol. 652, pp. 116-120). Trans Tech Publications.

98. Cho, J., Joshi, M. S., & Sun, C. T. (2006). Effect of inclusion size on mechanical properties of polymeric composites with micro and nano particles. *Composites Science and Technology*, *66*(13), 1941-1952.

99. Bhimaraj, P., Burris, D. L., Action, J., Sawyer, W. G., Toney, C. G., Siegel, R. W., & Schadler, L. S. (2005). Effect of matrix morphology on the wear and friction behavior of alumina nanoparticle/poly (ethylene) terephthalate composites. *Wear*, *258*(9), 1437-1443.

100. Schwartz, C. J., & Bahadur, S. (2000). Studies on the tribological behavior and transfer film–counterface bond strength for polyphenylene sulfide filled with nanoscale alumina particles. *Wear*, *237*(2), 261-273.

101. Zhao, L. X., Zheng, L. Y., & Zhao, S. G. (2006). Tribological performance of nano-Al_2O_3 reinforced polyamide 6 composites. *Materials Letters*, *60*(21-22), 2590-2593.

102. Solomon, D. H., & Hawthorne, D. G. (1983). *Chemistry of pigments and fillers* (p. 309). New York: Wiley.

103. Ng, C. B., Schadler, L. S., & Siegel, R. W. (1999). Synthesis and mechanical properties of TiO_2-epoxy nanocomposites. *Nanostructured Materials*, *12*(1-4), 507-510.

104. Ali, N. A., Al-Ajaj, I. A., & Noori, F. T. M. (2014). Effect of nano SiO2 on some mechanical properties of biodegradable polylactic acid. *Int. J. Mech. Eng. Technol*, *5*(2), 1-7.

105. Wacharawichanant, S., Thongyai, S., Siripattanasak, T., & Tipsri, T. (2009). Effect of mixing conditions and particle sizes of titanium dioxide on mechanical and morphological properties of polypropylene/titanium dioxide composites, *Iranian Polymer Journal*, 18 (8), 607-616.

106. Sudeepan, J., Kumar, K., Barman, T. K., & Sahoo, P. (2014). Tribological behavior of ABS/TiO_2 polymer composite using Taguchi statistical analysis. *Procedia Materials Science*, *5*, 41-49.

107. Sahibata Kei, Yamaguchi Takeshi, Kishi Moeko, Hokkirigawa Kazuo, "Friction and wear Behaviour of polyamide 66Composites", Filled with Rice Bran Ceramics under a wide range of Pv Values **10,2,** 213-219 (2015).

108. Yang, J. L., Zhang, Z., & Zhang, H. (2005). The essential work of fracture of polyamide 66 filled with TiO_2 nanoparticles. *Composites Science and Technology*, *65*(15-16), 2374-2379.

109. Karana, E., Hekkert, P., & Kandachar, P. (2008). Material considerations in product design: A survey on crucial material aspects used by product designers. *Materials & Design*, *29*(6), 1081-1089.

110. Chiner, M. (1988). Planning of expert systems for materials selection. *Materials & Design*, *9*(4), 195-203.

111. Farag, M. M. (2002). Quantitative methods of materials selection. *Handbook of materials selection*, 1-24.

112. Rao, R. V., & Davim, J. P. (2008). A decision-making framework model for material selection using a combined multiple attribute decision-making method. *The International Journal of Advanced Manufacturing Technology*, *35*(7-8), 751-760.

113. Ashby, M. F., Brechet, Y. J. M., Cebon, D., & Salvo, L. (2004). Selection strategies for materials and processes. *Materials & Design*, *25*(1), 51-67.

114. Giachetti, R. E. (1998). A decision support system for material and manufacturing process selection. *Journal of Intelligent Manufacturing*, *9*(3), 265-276.

115. Hwang, C. L., & Yoon, K. (1981). Methods for multiple attribute decision making. *Multiple attribute decision making.* Springer, Berlin, Heidelberg, 58-191.

116. Wang, M. J. J., & Chang, T. C. (1995). Tool steel materials selection under fuzzy environment. *Fuzzy Sets and Systems*, *72*(3), 263-270.

117. Liao, T. W. (1996). A fuzzy multicriteria decision-making method for material selection. *Journal of manufacturing systems*, *15*(1), 1.

118. Yoon, K. (1987). A reconciliation among discrete compromise solutions. *Journal of the Operational Research Society*, *38*(3), 277-286.

119. Hwang, C. L., Lai, Y. J., & Liu, T. Y. (1993). A new approach for multiple objective decision making. *Computers & operations research*, *20*(8), 889-899.

120. Assari, A., Mahesh, T. M., & Assari, E. (2012). Role of public participation in sustainability of historical city: usage of TOPSIS method. *Indian Journal of Science and Technology*, *5*(3), 2289-2294.

121. Yoon, K. P., & Hwang, C. L. (1995). *Multiple attribute decision making: An Introduction* (Vol. 104). SAGE Publications.

122. Zavadskas, E. K., Zakarevicius, A., & Antucheviciene, J. (2006). Evaluation of ranking accuracy in multi-criteria decisions. *Informatica*, *17*(4), 601-618.

123. Greene, R., Devillers, R., Luther, J. E., & Eddy, B. G. (2011). GIS•based multiple•criteria decision analysis. *Geography Compass*, *5*(6), 412-432.

124. Weaver, P. M., Ashby, M. F., Burgess, S., & Shibaike, N. (1996). Selection of materials to reduce environmental impact: a case study on refrigerator insulation. *Materials and Design*, *17*(1), 11-18.

125. Roth, R., Field, F., & Clark, J. (1994). Materials selection and multi-attribute utility analysis. *Journal of Computer-Aided Materials Design*, *1*(3), 325-342.

126. Sirisalee, P., Ashby, M. F., Parks, G. T., & Clarkson, P. J. (2004). Multi• criteria material selection in engineering design. *Advanced Engineering Materials*, *6*(1•2), 84-92.

127. Goldsberry, C. (2006). Computer modeling and how it helps drive material selection. *Modern plastics worldwide*, *83*(6), 150-152.

128. Aceves, C. M., Skordos, A. A., & Sutcliffe, M. P. (2008). Design selection methodology for composite structures. *Materials & Design*, *29*(2), 418-426.

129. Prendergast, P. J., Monaghan, J., & Taylor, D. (1989). Materials selection in the artificial hip joint using finite element stress analysis. *Clinical Materials*, *4*(4), 361-376.

130. Farag, M. M. (1997). *Materials selection for engineering design*. Prentice Hall.

131. Quigley, F. P., Buggy, M., & Birkinshaw, C. (2002). Selection of elastomeric materials for compliant-layered total hip arthroplasty. *Proceedings of the Institution of Mechanical Engineers, Part H: Journal of Engineering in Medicine*, *216*(1), 77-83.

132. Cicek, K., Celik, M., & Topcu, Y. I. (2010). An integrated decision aid extension to material selection problem. *Materials & Design*, *31*(9), 4398-4402.

133. Bahraminasab, M., & Jahan, A. (2011). Material selection for femoral component of total knee replacement using comprehensive VIKOR. *Materials & Design*, *32*(8-9), 4471-4477.

134. Mangera, T., Kienhöfer, F., Carlson, K. J., Conning, M., Brown, A., & Govender, G. (2018). Optimal material selection for the construction of a paediatric prosthetic knee. *Proceedings of the Institution of Mechanical Engineers, Part L: Journal of Materials: Design and Applications*, *232*(2), 137-147.

135. Kabir, G., & Lizu, A. (2016). Material selection for femoral component of total knee replacement integrating fuzzy AHP with PROMETHEE. Journal of Intelligent & Fuzzy Systems, 30(6), 3481-3493.

136. Radcliffe, C. W. (1955). Functional considerations in the fitting of above-knee prostheses. *Artificial Limbs*, 2(1),35-60.

137. Brenner, S., & Scott, R. (2007). The mathematical theory of finite element methods (Vol. 15). Springer Science & Business Media.

138. Saad, H., Abdullah, M. Q., & Wasmi, H. R. (2017). The Modeling and Effect of FEM on Prosthetic limb, International Journal of Cell Science and Biotechnology, 7(3), 892-895.

139. Reggiani, B., Leardini, A., Corazza, F., & Taylor, M. (2006). Finite element analysis of a total ankle replacement during the stance phase of gait. *Journal of biomechanics*, 39(8), 1435-1443.

140. Mihradi, S., Abdiwijaya, C. Z., Dirgantara, T., & Mahyuddin, A. I. (2015). Design of Above-Knee Prosthesis: A Finite Element Stress Analysis. *In Advanced Materials Research* (Vol. 1125, pp. 432-436).

141. Kumbhalkar, M. A., Nawghare, U., Ghode, R., Deshmukh, Y., & Armarkar, B. (2013). Modeling and finite element analysis of knee prosthesis with and without implant. *Universal Journal of Computational Mathematics*, 1(2), 56-66.

142. Samadhiya, S., Yadav, A., & Rawal, B. R. (2014). Biomechanical analysis of different knee prosthesis biomaterials using fem. IOSR Journal of Mechanical and *Civil Engineering (IOSR-JMCE)*, *11*, 120-128p.

143. Nautiyal, A. N., Nain, P. K. S., & Kumar, P. (2014). Study of knee-joint mechanism before implanting a knee prosthesis by modeling and finite element analysis of knee-joint bones. *International Journal of Advanced Mechanical Engineering*, *4*, 721-727p.

144. Mallesh, G., & Sanjay, S. J. (2012). Finite element modeling and analysis of prosthetic knee joint. *International Journal of Emerging Technology and Advanced Engineering*, *2*(8), 264-69.

145. ISO 10328: 2006. Prosthetics—structural testing of lower limb prostheses—requirements and test methods.

146. Colombo, C., Marchesin, E. G., Vergani, L., Boccafogli, E., & Verni, G. (2011). Study of an ankle prosthesis for children: adaptation of ISO 10328 and experimental tests. *Procedia Engineering*, *10*, 3510-3517.

147. Belkys T. Amador, Carmen M. Müller-Karger, Euro Casanova, Rafael R. Torrealba. (2013, August) "Structural analysis during the design of polycentric Prosthetic knee". *24th Congress of the International Society of Biomechanics. DOI: 10.13140/RG.2.1.1079.3124.*

148. Rosa, J. L., Robin, A., Silva, M. B., Baldan, C. A., & Peres, M. P. (2009). Electrodeposition of copper on titanium wires: Taguchi experimental design approach. *Journal of Materials Processing Technology*, *209*(3), 1181-1188.

149. Rao, R. S., Prakasham, R. S., Prasad, K. K., Rajesham, S. S. P. N., Sarma, P. N., & Rao, L. V. (2004). Xylitol production by Candida sp.: parameter optimization using Taguchi approach. *Process Biochemistry*, *39*(8), 951-956.

150. Rao, R. S., Kumar, C. G., Prakasham, R. S., & Hobbs, P. J. (2008). The Taguchi methodology as a statistical tool for biotechnological applications: a critical appraisal. *Biotechnology Journal: Healthcare Nutrition Technology*, *3*(4), 510-523.

151. Jaquess, J. F. (1997). Sales Process Engineering: A Personal Workshop. *Quality Progress*, *30*(9), 129.

152. Taguchi, G. (1978, October). Off-line and on-line quality control systems. *Proceedings of International Conference on Quality Control*.

153. Byrne D. M., S. Taguchi. "The Taguchi approach to parameter design". *Quality Progress, vol. 20 (12), pp. 19-26, (1987).*

154. Phadke, M. S. (1995). *Quality engineering using robust design*. Prentice Hall PTR.

155. Ross., P.J.: "Taguchi Techniques for Quality Engineering: Loss Function, Orthogonal Experiments, Parameter and Tolerance Design - 2nd ed.", *New York, NY: McGraw-Hill, (1996).*

156. Taguchi, G., Clausing, D., & Watanabe, L. T. (1987). *System of experimental design: engineering methods to optimize quality and minimize costs* (Vol. 2). White Plains, NY: UNIPUB/Kraus International Publications.

157. Taguchi, G.: "Taguchi on Robust technology development methods". *ASME Press, New York, 1- 40, (1993).*

158. Ealey Lance A. "Quality by design Taguchi methods and US industry". *2nd ed. Sidney: Irwin professional publishing and ASI Press, 189–207, (1994).*

159. Kamaruddin, S., Khan, Z. A., & Foong, S. H. (2010). Application of Taguchi method in the optimization of injection moulding parameters for manufacturing products from plastic blend. *International Journal of Engineering and technology*, *2*(6), 574-580.

160. Chen, H. J., Chang, S. N., & Tang, C. W. (2017). Application of the Taguchi method for optimizing the process parameters of producing lightweight aggregates by incorporating tile grinding sludge with reservoir sediments. *Materials*, *10*(11), 1294.

161. Lee, W. C., & Zhang, M. (2005). Design of monolimb using finite element modelling and statistics-based Taguchi method. *Clinical biomechanics*, *20*(7), 759-766.

162. Unal, H., & Mimaroglu, A. (2004). Influence of filler addition on the mechanical properties of nylon-6 polymer. *Journal of reinforced plastics and composites*, *23*(5), 461-469.

163. Alsharif, S. O., Akil, H. B. M., El-Aziz, N. A. A., & Ahmad, Z. A. B. (2014). Effect of alumina particles loading on the mechanical properties of light-cured dental resin composites. *Materials & Design (1980-2015)*, *54*, 430-435.

164. Díez-Pascual, A. M., & Naffakh, M. (2013). Mechanical and thermal behaviour of isotactic polypropylene reinforced with inorganic fullerene-like WS2 nanoparticles: Effect of filler loading and temperature. *Materials Chemistry and Physics*, *141*(2-3), 979-989.

165. Pérez, E., Alvarez, V., Pérez, C. J., & Bernal, C. (2013). A comparative study of the effect of different rigid fillers on the fracture and failure behavior of polypropylene based composites. *Composites Part B: Engineering*, *52*, 72-83.

166. Zapata, P. A., Zenteno, A., Amigó, N., Rabagliati, F. M., Sepúlveda, F., Catalina, F., & Corrales, T. (2016). Study on the photodegradation of nanocomposites based on polypropylene and TiO_2 nanotubes. *Polymer Degradation and Stability*, *133*, 101-107.

167. Cao, S., Liu, T., Tsang, Y., & Chen, C. (2016). Role of hydroxylation modification on the structure and property of reduced graphene oxide/TiO_2 hybrids. *Applied Surface Science*, *382*, 225-238.

168. Yesgat, A. L., & Kitey, R. (2016). Effect of filler geometry on fracture mechanisms in glass particle filled epoxy composites. *Engineering Fracture Mechanics*, *160*, 22-41.

169. Dass, K., Chauhan, S. R., & Gaur, B. (2014). Study on mechanical and dry sliding wear characteristics of meta-cresol novalac epoxy composites filled with silicon carbide, aluminum oxide, and zinc oxide particulates. *Tribology Transactions*, *57*(2), 157-172.

170. Zheng, L. Y., Lau, K. T., Zhao, L. X., Zhang, Y. Q., & Hui, D. (2009). Mechanical and thermal properties of nano-Al_2O_3/nylon 6 composites. *Chemical Engineering Communications*, *197*(3), 343-351.

171. Guo, Z., Pereira, T., Choi, O., Wang, Y., & Hahn, H. T. (2006). Surface functionalized alumina nanoparticle filled polymeric nanocomposites with enhanced mechanical properties. *Journal of Materials Chemistry*, *16*(27), 2800-2808.

172. Omrani, A., Simon, L. C., & Rostami, A. A. (2009). The effects of alumina nanoparticle on the properties of an epoxy resin system. *Materials Chemistry and Physics*, *114*(1), 145-150.

173. Mahapatra, S. S., & Patnaik, A. (2009). Study on mechanical and erosion wear behavior of hybrid composites using Taguchi experimental design. *Materials & Design*, *30*(8), 2791-2801.

174. Kumar, S. R., Bhat, I. K., & Patnaik, A. (2017). Novel dental composite material reinforced with silane functionalized microsized gypsum filler particles. *Polymer Composites*, *38*(2), 404-415.

175. Kumar, S. R., Patnaik, A., & Bhat, I. K. (2016). Analysis of polymerization shrinkage and thermo-mechanical characterizations of resin-based dental composite reinforced with silane modified nanosilica filler particle. *Proceedings of the Institution of Mechanical Engineers, Part L: Journal of Materials: Design and Applications*, *230*(2), 492-503.

176. Bao, J. (2011). The effect of TiO_2 on the mechanical and tribological properties of PA66 nanocomposites. *Advanced Materials Research*, 284, 513-516.

177. Selvin, T. P., Kuruvilla, J., & Sabu, T. (2004). Mechanical properties of titanium dioxide-filled polystyrene microcomposites. *Materials Letters*, *58*(3-4), 281-289.

178. Knör, N., Walter, R. O. L. F., & Haupert, F. (2011). Mechanical and thermal properties of nano-titanium dioxide-reinforced polyetheretherketone produced by optimized twin screw extrusion. *Journal of Thermoplastic Composite Materials*, *24*(2), 185-205.

179. Yang, J. L., Zhang, Z., Schlarb, A. K., & Friedrich, K. (2006). On the characterization of tensile creep resistance of polyamide 66 nanocomposites. Part I. Experimental results and general discussions. *Polymer*, *47*(8), 2791-2801.

180. Bose, S., & Mahanwar, P. A. (2004). Effect of flyash on the mechanical, thermal, dielectric, rheological and morphological properties of filled nylon 6. *Journal of Minerals & Materials Characterization & Engineering*, *3*(2), 65-89.

181. Rothon R. N. (2003).Particulated-Filled Polymer Composites. Shrewsbury, Shropshire, SY4 4NR, UK: 2nd Edition, Rapra Technology Limited.

182. Unal, H., Fındık, F., & Mimaroglu, A. (2003). Mechanical behavior of nylon composites containing talc and kaolin. *Journal of Applied Polymer Science*, *88*(7), 1694-1697.

183. Raja, V. L., & Kumaravel, A. (2015). Studies on physical and mechanical properties of silica fume-filled nylon 66 polymer composites for mechanical components. *Polymers & Polymer Composites*, *23*(6), 427-433.

184. Friedrich, K., Zhang, Z., & Schlarb, A. K. (2005). Effects of various fillers on the sliding wear of polymer composites. *Composites Science and Technology*, *65*(15-16), 2329-2343.

185. Chang, L., Zhang, Z., Ye, L., & Friedrich, K. (2007). Tribological properties of high temperature resistant polymer composites with fine particles. *Tribology International*, *40*(7), 1170-1178.

186. Chang, L., Zhang, Z., Zhang, H., & Schlarb, A. K. (2006). On the sliding wear of nanoparticle filled polyamide 66 composites. *Composites Science and Technology*, *66*(16), 3188-3198.

187. Prabu S.S., Prathiba S., Sharma A. et al.(2014). Investigation on adhesive wear behaviour of industrial crystalline and semi-crystalline polymers against steel counterface. *International Journal of ChemTech Research*, 6, 3422–3430.

188. Villa T, Migliavacca F, Gastaldi D, Colombo M & Pietrabissa R. (2004). Contact stresses and fatigue life in a knee prosthesis: comparison between in vitro measurements and computational simulations. *Journal of Biomechanics*, 37(1), 45-53.

189. Rawal B.R., Yadav Amit & Pare Vinod. (2016). Life estimation of knee joint prosthesis by combined effect of fatigue and wear. *Procedia Technology*, 23, 60-67.

APPENDICES

List of Publications out of this research work

Publications in Journal

1. Guglani L and Gupta T.C. Wear and mechanical properties of Nylon 66-Al_2O_3 microcomposite. *Journal of Reinforced Plastics and Composites* 2017; 36; 17: 1254 -1262. (**Sci Indexed**, SAGE Publishers).
2. Guglani L and Gupta T. C. Study of mechanical and tribological properties of nylon 66-titanium dioxide microcomposite. *Polymers Advanced Technologies* 2018; 29; 2: 906–913. (**Sci Indexed**, Wiley Publishers).

Research paper communicated to Journal

1. Guglani L and Gupta TC. Design improvement of above knee prosthesis using finite element analysis. (*Medical Engineering and Physics*).

Brief Bio-Data of the Author

The author Lalit Guglani, graduated in Mechanical Engineering from Government Engineering College, Kota (University of Rajasthan, Jaipur) in the year 1990. He did his Masters in the Mechanical engineering with the specialization - Manufacturing System Engineering from Malaviya National Institute of Technology (MNIT), Jaipur, in the year 2012. He is the Director & Head of CIPET- Jaipur, a Government of India organisation engaged in academic and technical activities in the field of plastics engineering, design and tooling. He has 27 years of teaching and technical experience and delivered invited lectures at various forums. Author had attended various training programmes on ISO, 5S, Six Sigma, Lean Manufacturing etc. in India and also participated in International exhibitions and training in Switzerland, Japan, Sharjah, Mexico and Germany.

He has published three research papers in International Journals. Since 2012, he has been engaged in his Doctoral Research in the area of development of new polymer composites and characterization, study and design improvements in the knee joint prosthesis at MNIT, Jaipur. His areas of interest are above knee joint prosthesis, FEA, polymer composites, mechanical characterization, tribology, plastic injection moulding and optimization.